Pyrethroid resistance in *Varroa destructor:*

Investigating the role of mutations in the voltage-gated sodium channel

Anabel Millán Leiva

Doctorat en Biomedicina i Biotecnologia
Director: Joel González Cabrera
Universitat de València

PhD Thesis

2022

Facultat de Ciències Biològiques

PhD Thesis

Ana Isabel Millán Leiva

May 2022

Pyrethroid resistance in *Varroa destructor*: Investigating the role of mutations in the voltage-gated sodium channel

Supervisor   **Dr. Joel González Cabrera**

Professor titular

Departament de Genètica

Institut de Biotecnologia i Biomedicina

Universitat de València

Programa de Doctorat en

Biomedicina i Biotecnologia

Dr. Joel González Cabrera

Instituto BIOTECMED. Departmento de Genética
Fac. Ciencias Biológicas. Universitat de València
c/Dr. Moliner, 50. Burjassot-46100.
Valencia, España.
E-mail: joel.gonzalez@uv.es
Tel: +34 96 354 3122
http://cbp.uv.es/research/pesticide-resistance/

Informa:

Que la Sra. Ana Isabel Millán Leiva, Licenciada en Ciencias Biológicas, ha realizado bajo mi dirección el trabajo de investigación recogido en la tesis doctoral que tiene por título: "Pyrethroid resistance in Varroa destructor: Investigating the role of mutations in the voltage-gated sodium channel", presentada para optar por el grado de doctora por la Universidad de Valencia.

Y para que conste, de acuerdo con la legislación vigente, firmo la presente en Burjassot a 31 de enero de 2022.

Fdo. Dr. Joel González Cabrera
Director de tesis

Agraïments

Hacer una tesis doctoral no es fácil, pero si se sabe aprovechar, puede ser una etapa muy enriquecedora. En mi etapa como estudiante de doctorado he aprendido infinidad de cosas, pero la lección más importante que he extraído es que en el mundo científico no basta con valerse por sí mismo, sino que se necesita una buena dirección y mejores compañeros. Y me siento muy afortunado de haber encontrado ambas cosas.

He tenido la suerte de tener un gran director de tesis que me ha enseñado a ser mejor científica y a trabajar con honestidad. Por todo ello, gracias, Joel, por haberme dado la oportunidad de realizar este trabajo y demostrar que puedo hacerlo.

A Salva y Agata, ya que si no fuera por vosotros yo no estaría aquí ahora.

Gracias a todos mis compañeros y amigos de grupo CBP (y GenBqBt), a los que están y a los que estuvieron. Por todos los momentos que han hecho más llevaderas las largas jornadas en el laboratorio. Las comidas apretujados en la mesa del 'comedor', los cafés en las escaleras, las cervecitas de después, … Pero sobre todo por vuestra contagiosa alegría y sentido del humor. No me olvido de los compañeros de GT, y de las fiestas en el departamento.

I would like to thank Prof. Ian L. Mellor for allowing me to be in his lab and for teaching me such a complex and new subject to me in a simple way. Like he once said to me, we will always be learning something new. I would also like to thank the people I met in Nottingham for making my stay there so much more pleasant.

A la gente que me acompaño en Málaga y me ayudaron cuando más lo necesitaba.

A la família Castelló-Abad, qui foren com una la segona família duran anys.

A mis amigas y amigos que son capaces de hacer que me ría de mis problemas. Aunque algunos estéis lejos, yo os siento al lado. Os quiero.

A mi familia, que siempre me apoyaron en todas mis decisiones e intentaron ayudarme en todo lo que estaba a su alcance; aunque algunas veces no entendían muy bien lo que estaba haciendo. A mis padres que nunca dejaron de esforzarse y me enseñaron que ante todo hay que ser honrado para poder estar orgulloso de lo haces, pero también a mantener los pies en el suelo. A mis hermanos, Lucía y Javier, que han sacado la fuerza, bondad y ganas de luchar de mis padres.

A Dani, porque contigo es todo más fácil.

A toda la gente que me he cruzado desde que comencé mi carrera científica, que habéis influido en mayor o menor medida a formar a la persona que soy hoy en día.

Gracias a todos.

Cover design by Daniel Pinos.

A mi madre.

A mis hermanos, Lucía y Javier.

A mi padre.

ACRONYMS AND ABBREVIATIONS

bp: base pair
CDS: Coding sequence
cRNA: complementari RNA
DI-DIV: Domains I to IV
DMSO: dimethyl sulphoxide
DNA: Deoxyribonucleic acid
dNTPs: Deoxynucleosides triphosphate
IPM: Integrated Pest Management
kb: kilobases
kdr :- knockdown resistance
mtDNA: mitochondrial DNA
Na^+: sodium ions
P: probability
para: *paralytic gene* (encodes VGSC in *D. melanogaster*)
PCR: polymerase chain reaction
PCR-RFLP: *polymerase chain reaction*-restriction fragment length polymorphism

R: resistant allele
S.O.B.: super optimal broth
S: susceptible allele
S1-S6: transmembrane segments
SEM: standard error of the mean
SNPs: single nucleotide polymorphisms
spp: species
UK: United Kingdom
USA: United Stated of America
*Vd*VGSC: VGSC of *Varroa destructor*
VGSC: voltage-gated sodium channel
wt: wild-type
2x: concentrated 2 times

International System of Units

$\times g$: g-force or relative centrifugal force (RCF)
µg: microgram
µL: microliters
µM: micromolar
cm: centimetre
Hz: Hertz
kV: kilovolts
M: Molar
min: minutes
mL: mililiter
mM: milimolar

MOhm: megaohm
mV: millivolts
nA: nanoAmp
ng: nanograms
nos.: numbers
ºC: degrees celsius
pH: potential of Hidrogen scale
s: seconds; ms: milliseconds
w/v: weight/volume
µF: microfaraday
Ω: Ohm

Amino acids (aa), one and three letters code

Alanine	-	Ala	- A	Leucine	- Leu	- L
Arginine	-	Arg	- R	Lysine	- Lys	- K
Asparagine	-	Asn	- N	Methionine	- Met	- M
Aspartic Acid	-	Asp	- D	Phenylalanine	- Phe	- F
Cysteine	-	Cys	- C	Proline	- Pro	- P
Glutaminc acid	-	Glu	- E	Serine	- Ser	- S
Glutamine	-	Gln	- Q	Threonine	- Thr	- T
Glycine	-	Gly	- G	Tryptophan	- Trp	- W
Histidine	-	His	- H	Tyrosine	- Tyr	- Y
Isoleucine	-	Iso	- I	Valine	- Val	- V

Missense mutation annotation: e.g. L925V denotes that aa Leucine is changed by Valine at position 925

Abbreviations for TEVC

a: amplitude of the exponential

Amp: amplifier

EC_{50}: half maximal effective concentration

G: conductance

G_{max}: maximal conductance

G_{norm}: Conductance normalized

I: current flow of charged ions

I_m: membrane current

I_{peak}: peak amplitude of ion inward current

M: modified VGSC

M_I: integral modification

RF: resistant factor

t: time

tau (**τ**): time constant of the exponential.

V: voltage

V_{50}: voltage for half maximal current activation

V_m: transmembrane potential

V_{rev}: is the Reversal potential

V_T: Test voltage, or membrane potential tested

V_{cmd}: voltage commanded

V_1: voltage-sensing microelectrode

V_2: bath electrode or reference electrode

V_i: current injection microelectrode

INDEX OF CONTENTS

INDEX OF FIGURES

CHAPTER 2.

CHAPTER 3.

CHAPTER 4.

INDEX OF TABLES

RESUM ESTÈS

Entre les majors amenaces de l'apicultura contemporània es troba el parasitisme de *Varroa destructor*, Anderson & Trueman (Acari: *Varroidae*), també conegut simplement com la *Varroa* pels apicultors. Aquest àcar ectoparàsit altament especialitzat s'alimenta directament de les pupes i els adults de l'abella mel·lífera europea, *Apis mellifera* L. (Hymenoptera: *Apidae*), la qual cosa debilita greument a les abelles i les indueix una immunosupressió que desemboca en brots d'infeccions preexistents o vectorizades pels àcars que comprometen la viabilitat de les colònies.

Originalment, la distribució de *V. destructor* estava restringida a algunes regions d'Àsia oriental, on es trobava parasitant al seu hoste natural, la abella asiàtica *Apis cerana* Fabricius (Hymenoptera: *Apidae*). No obstant, amb el seu hoste natural manté una relació parasitaria més o menys equilibrada, ja que *A. cerana* mostra certa tolerància a *Varroa* i pot mantindré la població d'aquests àcars controlada en els seus ruscos. Per tant, el número de infestacions crítiques que provoca el parasitisme de *V. destructor* en les seues colònies es baix. D'altra banda, la relació amb el nou hoste, l'abella mel·lífera europea, és evolutivament parlant molt recent, menys d'un segle, per el que aquest no ha tingut l'ocasió de desenvolupat mecanismes de defensa per a contrarestar els efectes d'aquest paràsit. El salt de *V. destructor* al nou hoste, *A. mellifera*, es va produir quan les dos especies d'abelles van entrar en simpatria; poc després de la introducció de l'abella mel·lífera europea a Àsia amb motius comercials y de producció. Poc després del pas al nou hoste, *V. destructor* es va estendre ràpidament a altres regions geogràfiques, amb l'ajuda del transport mediat per l'esser humà, convertint-se en una amenaça per a l'apicultura arreu del món. Actualment, l'àcar *Varroa* és un problema mundial i el principal factor causant de pèrdues de colònies d'abella mel·lífera, amb un cost econòmic estimat en milions de dòlars a l'any.

Per evitar les pèrdues desproporcionades que causa el parasitisme de *Varroa* es necessari el control regular d'aquest àcar als ruscos. Aquest control s'aconsegueix principalment mitjançant l'aplicació d'acaricides. Avui en dia existeixen un reduït número de principis actius permesos i efectius per fer front a *V. destructor*. Entre estos, els piretroides acaricides han sigut un dels tractaments més comuns per fer front a *V. destructor*, fortament utilitzats al llarg de moltes generacions, fins i tot després que la aparició de resistència a mitjan dels anys 90. El seu gran ús es deu a la baixa toxicitat que presenta per a les abelles, la baixa residualitat que deixen en els productes comercials del rusc, la seua alta eficàcia quan no hi ha resistència, però sobretot per l'escàs número de

tractaments disponibles i efectius. Els piretroides sintètics són una de les principals classes de plaguicides àmpliament utilitzats per al control de plagues i vectors de malalties. Alguns tipus de piretroides tenen un ampli espectre d'espècies diana (molt eficaços front a insectes o artròpodes en general), mentre que uns altres són més selectius front als àcars (àcars i paparres). Els piretroides amb selectivitat acaricida són especialment útils en situacions en les quals és necessari atacar una plaga específica que cohabita amb insectes beneficiosos, com és el cas de la Varroosis (malaltia de les abelles mel·líferes causada per la infestació de *Varroa*). En l'actualitat, el *tau*-fluvalinat (Apistan®) i la flumetrina (Bayvarol®, Polyvar®) són els dos únics piretroides permesos i disponibles per a controlar els àcars paràsits als ruscos sense danyar significativament a les abelles.

Desgraciadament, igual que amb molts altres pesticides, l'ús intensiu de piretroides acaricides ha favorit l'aparició de resistències en poblacions d'àcars de tot el món. En *V. destructor*, igual que en altres artròpodes, el mecanisme més comú implicat en la pèrdua de sensibilitat als piretroides és la substitució de certs aminoàcids en la seua proteïna diana, el canal de sodi depenent de voltatge (VGSC, de les seues segles en anglès *Voltage-Gated Sodium Channel*). El VGSC és una proteïna canal transmembrana gran que es troba en els axons neuronals i que te un paper essencial en la propagació de l'impuls nerviós a través d'ells. Aquestes mutacions puntuals, sovint denominades mutacions de tipus *kdr* (per les segles en anglès del nom assignat al seu fenotip, *knockdown resistance*), es localitzen principalment en les hèlixs transmembrana del domini II i III (hèlixs IIS5, IIS6 i III6) i en la regió d'enllaç entre IIS4-S5 del VGSC. Mitjançant estudis de modelització de l'estructura de la proteïna es va predir que aquestes regions es plegarien formant una butxaca hidrofòbica, lloc on interaccionarien el piretroides amb la proteïna canal. Mentre que en algunes espècies d'artròpodes s'han trobat varies mutacions del tipus *kdr* responsables de la resistència, soles o en combinació, en *V. destructor* només es va descriure el canvi de la posició 925 (numerada segons l'homologia amb els residus de la proteïna VGSC de la mosca domèstica, *Musca domestica*) associat amb una reducció de la susceptibilitat als piretroides. No obstant això, es van descriure tres mutacions diferents per a aquesta posició, a partir de la substitució de la Leucina de tipus salvatge per Valina (L925V), Isoleucina (L925I) i Metionina (L925M). Un aspecte destacable es la marcada distribució geogràfica que mostren aquests al·lels, havent-se detectat la mutació L925V en poblacions d'àcars europees i la substitució L925I i L925M en ruscos dels Estat Units

d'Amèrica. No obstant això, Durant la realitzció de la present tesi, s'han notificat ocasionalment les mutació L925I i L925M en àcars fora del territori estatunidenc, com Creta, el Japó o Turquia.

En el present treball ens hem centrat en les mutacions de tipus *kdr* en la posició 925 del VGSC de *V. destructor*, que s'han associat amb àcars de diverses localitats que sobrevisqueren a tractaments basats en el *tau*-fluvalinat i la flumetrina. La intenció d'aquest estudi d'investigació es contribuir al coneixement sobre les implicacions d'aquestes mutacions en la resistència als piretroides, la seua relació evolutiva i la incidència actual. Tot açò amb el propòsit final d'establir algunes claus bàsiques per a desenvolupar un programa eficaç basat en la Gestió Integrada de Plagues (GIP) front al problema de la *Varroa*. Aquest treball s'emmarca en un projecte més ampli destinat a esclarir les bases moleculars subjacents que confereixen el fenotip resistent a les substàncies químiques actives autoritzades per al control de *V. destructor*.

En el capítol 1, mitjançant tècniques d'electrofisiologia i assajos farmacològics hem demostrat que la susceptibilitat als piretroides es redueix en els VGSC de *V. destructor* que tenen la posició 925 mutada. Les implicacions d'aquestes mutacions en el mecanisme de resistència s'han estudiat a través de la caracterització funcional i farmacològica d'aquests canals, mitjançant la seua expressió heteròloga en oòcits de *Xenopus laevis*. Aquesta metodologia permet estudiar l'efecte que produeixen els piretroides en els canals de sodi de *V. destructor* de forma aïllada, i en conseqüència, si aquestes mutacions tenen un paper en la resistència. En primer lloc, es va clonar la seqüència completa que codifica per al VGSC de tipus salvatge (l'al·lel L925, susceptible a piretroides) de *V. destructor* en un vector plasmídic que contenia tots els elements necessaris per a la transcripció i expressió del ARN complementari (ARNc) en oòcits de *Xenopus* spp. Utilitzant aquest plasmid com a motlle, hem generat els tres canals mutants per a la posició 925 mitjançant mutagènesis dirigida, obtenint variacions del VGSC de *V. destructor* que només difereixen en el residu de l'aminoàcid 925. Utilitzant els VGSC clonats com a motlle, es van sintetitzar *in vitro* els transcrits de ARNc de les quatre variants del canal de sodi (tipus salvatge i les tres mutacions), i posteriorment aquests es microinjectaren separadament en oòcits de *X. laevis* en fase V-VI per a la seua expressió heteròloga. Les característiques funcionals i farmacològiques que les modificacions en la posició 925 confereixen al VGSC de *V. destructor* es van examinar en els oòcits que expressaven el canal corresponent mitjançant el mètode de *Two-Electrode Voltage Clamp* (TEVC). Els oòcits

que expressaren els canals van ser exposar a concentracions creixents de deltametrina (un potent piretroide d'ampli espectre front a artròpodes), *tau*-fluvalinat i flumetrina (ambdós són piretroides selectius per als àcars, i els que s'utilitzen per al control de *Varroa*) per a avaluar els efectes en els VGSC de tipus salvatge i mutant de *V. destructor*.

En comparació amb el VGSC de tipus salvatge, la sensibilitat als piretroides es va veure significativament reduïda en els canals de sodi mutats. En contrast amb el canal de tipus salvatge, els canals de sodi mutats L925I i L925V no van provocar cap resposta de corrent de cua (típic efecte de la interacció del canal de sodi amb piretroides) quan es van exposar a tots tres piretroides (deltametrina, flumetrina i *tau*-fluvalinat). En un nivell intermedi, la mutació L925M va mostrar més susceptibilitat als piretroides que la L925I i la L925V, però l'efecte en resposta va ser significativament menor que el del canal de tipus salvatge. Els nostres resultats recolzen que la substitució puntual del residu 925 en el VGSC influeix en la interacció dels piretroides amb el canal, per la qual cosa l'aminoàcid 925 juga un paper rellevant en el lloc receptor de piretroides de tipus II en els canals de sodi dels àcars, de manera similar al que ocorre en els insectes. En els canals mutats, la interacció amb els piretroides es veu molt probablement dificultada per la cadena lateral alternativa del residu modificat en la posició 925, la qual cosa dificulta la correcta inserció del piretroide al seu lloc d'unió en la butxaca hidrofòbica.

A més, vam observar que en absència de compostos piretroides, les tres mutacions del residu 925 modifiquen les propietats cinètiques i fisiològiques del canal de sodi dels àcars; açò es una característica que també s'observa en els canals mutats de tipus *kdr* dels insectes. Els tres canals mutats mostren un desplaçament de la corba l'activació ($V_{50,act}$) cap a voltatges més positius, però aquesta diferència és major per als canals mutats L925I i L925V. A banda, el canal L925M també s'inactiva més ràpidament que el de tipus salvatge. En resum, els canals mutats L925V i L925I són menys propensos a obrir-se que els de tipus salvatge, mentre que el L925M, a més, passa a l'estat tancat més ràpidament. Aquesta característica podria ser un factor que contribueix a la resistència, però al mateix temps podria tindre un impacte potencialment negatiu per als àcars portadors en absència de piretroides. Els piretroides tenen major afinitat i s'uneixen preferentment al VGSC en el seu estat obert. La formació de contactes d'unió entre el piretroide i els diferents residus del canal a través de la cavitat d'unió podria estabilitzar el canal en l'estat obert, prolongant així el flux de sodi i originant els corrents de cua. En passar el canal a l'estat tancat, el reposicionament del connector S4-S5 del domini II conduiria a la pertorbació dels

contactes d'unió del canal amb el piretroide i el conseqüent alliberament d'aquest. Segons aquest model, la reduïda disponibilitat del canal mutat a l'estat obert i la transició més ràpida cap a l'estat tancat poden ser també factors que contraresten l'acció dels piretroides, que a més es sumarien a la reduïda interacció dels piretroides amb els canals mutants degut a la modificació del lloc de interacció, contribuint així a la resistència.

Les mutacions detectades en els àcars en la posició 925 (Valina, Metionina i Isoleucina) no comprometen la funcionalitat del VGSC. No obstant això, i tenint en compte el paper clau en la transmissió de l'impuls nerviós que exerceix el VGSC, és molt probable que aquestes tres substitucions impliquen un cert impacte en l'aptitud biològica dels àcars portadors. En comparació amb el canal de tipus salvatge, la modificació de la cinètica d'activació dels canals mutants pot ser avantatjosa en contrarestar la interacció dels piretroides, com em vist abans, però en absència de piretroides, aquesta condició podria ser desavantatjosa. Aquests canals requereixen una despolarització de membrana més forta per a activar-se que el canal de tipus salvatge, per la qual cosa aquests canals mutants són essencialment canals menys excitables que el de tipus salvatge. En conseqüència, en absència de la forta pressió selectiva exercida pels piretroides, els àcars individuals amb neurones menys excitables estarien en desavantatge en comparació amb els àcars que requereixen un potencial d'excitació menor. Diversos estudis ja han assenyalat el possible cost biològic que la mutació L925V pot tindre quan cessa la pressió selectiva dels piretroides. Els nostres resultats ací proporcionen una explicació possible per a aquest fet basada en les característiques biofísiques dels canals mutats i dels de tipus salvatge. A més, si la nostra hipòtesi és certa, donades les característiques biofísiques dels canals mutats, s'esperaria un cost biològic comparable per als àcars portadors de la mutació L925I. Generalment, les pressions adaptatives que actuen sobre els al·lels resistents són més intenses per a les mutacions que afecten llocs d'una proteïna que son clau per a la seua funció, com es el cas de les mutacions de tipus *kdr*. En rares ocasions, aquests al·lels es veuen afavorits quan la pressió de selecció està absent, per la qual cosa aquests individus resistents es troben en desavantatge en comparació amb els de tipus salvatge (susceptibles als piretroides). En conseqüència, la prevalença dels al·lels resistents en una població es veu compromesa si no es restableix la pressió selectiva, que en aquest cas seria el tractament amb piretroides. El nostre treball, entre altres estudis, planteja la hipòtesi que aquests al·lels en *V. destructor* comporten un major cost biològic en absència de la pressió exercida pels piretroides. Encara que es necessiten estudis

addicionals per a confirmar esta hipòtesi, aquest fet podria obrir una via d'actuació que possibilite contrarestar la prevalença d'aquests al·lels resistents en les poblacions de *V. destructor*. Amb un programa adequat de gestió de la resistència que considere el major cost biològic del al·lels mutants per a la posició 925 del VGSC es podria revertir la freqüència d'àcars resistents en una colònia o rusc de forma controlada, simplement deixant actuar a les forces selectives.

Un altre aspecte especialment destacable es l'efecte contrari que els piretroides indueixen en la cinètica d'activació dels canals de sodi de *V. destructor* i dels insectes. En el canal de sodi de insectes, la interacció amb els piretroides sol promoure l'estat actiu en desplaçar el potencial d'activació ($V_{50,act}$) a valors més negatius. Els canals es tornen més fàcilment excitables, la qual cosa condueix a un estat d'obertura accelerat i prolongat i, en conseqüència, a una major exposició del lloc d'unió als piretroides. De manera oposada, la interacció de la deltametrina, el *tau*-fluvalinat i la flumetrina amb els canals de sodi de *V. destructor* provoquen un desplaçament del potencial de activació ($V_{50,act}$) cap a voltatges més positius, la qual cosa podria disminuir la capacitat d'unió dels piretroides. La diferent influència en l'activació pot ser un dels factors subjacents a que els canals de sodi de *V. destructor* presenten una menor sensibilitat als piretroides que els canals d'insectes.

En el capítol 2 hem estudiat la relació filogenètica entre els al·lels de resistència per a la posició 925 del VGSC en *V. destructor*. Els tres al·lels resistents diferents per a aquesta posició s'han trobat en diferents poblacions d'àcars d'arreu del món. La mutació L925V es distribueix en gran part a Europa, mentre que L925M i L925I s'han trobat sobretot als Estats Units. En discernir la relació filogenètica entre els al·lels de resistència, podem identificar els esdeveniments de mutació passats que han donat lloc a la distribució actual dels àcars resistents. Així també podem saber si aquestes mutacions es van originar a partir d'esdeveniments de mutació únics o múltiples. Entendre la història evolutiva dels al·lels resistents és un pas clau per a comprendre la pressió de selecció a la qual estan sotmesos aquests variant del VGSC amb els residus en posició 925 modificats, i així es podríen predir la freqüència de possibles esdeveniments futurs d'aparició de resistència, i per tant, contribuir a dissenyar estratègies de gestió més afinades.

Amb la finalitat d'estudiar la relació evolutiva de les mutacions resistents a piretroides en *V. destructor*, vam recol·lectar mostres de *V. destructor* procedent de

diverses localitat arreu del món en les quals s'havia registrat resistència a Apistan® (*tau*-fluvalinat). Es va extraure el material genètic d'aquests àcars, i mitjançant PCR amb primers específics es va amplificar la regió del gen per al VGSC que conté l'exó complet que codifica per a la posició 925 de la seqüencia proteica del canal i els fragments parcials dels introns que el flanquegen aigües amunt i aigües avall, i es van genotipar per seqüenciació.

Les seqüències d'ADN van revelar, a més de les tres mutacions esperades, la presència de la mutació de tipus *kdr* M918L en els àcars recollits en la Comunitat Valenciana (Espanya) per als anys 2018 i 2019. La mutació M918L no havia estat detectada en *V. destructor* abans, i en el nostre treball la vam trobar en co-ocurrència amb la mutacions L925V; es a dir, en àcars que portaven ambdues mutacions. Tots dos residus M918 i L925 estan localitzats respectivament en la regió d'unió IIS4-S5 i en el IIS5 del canal. Com s'ha descrit abans, es prediu que aquestes regions, juntament amb IIIS6, es pleguen en forma de butxaca hidròfobica; proposat com al lloc d'interacció dels piretroides en el canal. Per tant, i segons aquest model, qualsevol substitució en els aminoàcids que recobreixen la butxaca hidròfobica interferiria amb l'allotjament del piretroide, fent que el canal siga menys sensible a aquests productes químics. Encara que l'efecte de la mutació M918L no s'ha caracteritzat en *V. destructor*, en altres artròpodes s'ha demostrat que les substitucions del residu M918 disminueixen significativament la susceptibilitat del canal als piretroides. A més, la co-ocurrència de més d'una mutació de tipus *kdr* sol produir un major nivell de resistència que les mutacions individuals. En conseqüència, podem proposar la hipòtesi que la combinació de M918L i L925V donaria lloc a una major desestabilització en la unió dels piretroides al canal que la produïda per L925V o M918L per separat.

Els anàlisis filogenètics de la regió del gen vinculada a la posició 925 del VGSC de *V. destructor* revelaren un origen únic per a cada mutació de tipus *kdr*. A més, els resultats suggereixen dos orígens diferents i paral·lels per a les mutacions, amb una clara relació filogenètica entre les mutacions L925M i L925I d'una banda, i L925V i M918L per una altra banda. La distribució geogràfica dels al·lels resistents es correlaciona bé amb els resultats obtinguts per la reconstrucció filogenètica, i per tant també dona suport a la proposta d'un únic esdeveniment de mutació per a cada substitució d'aminoàcids relacionada amb la resistència. La reconstrucció filogenètica suggereix que L925M i L925I són el resultat d'un procés seqüencial, sent la mutació L925M l'ancestre de la

mutació L925I, que hauria sorgit en un segon esdeveniment de mutació paral·lel (Leu →
Met → Ile). Els nostres resultats van mostrar, a més, l'estreta relació entre els al·lels L925I
i L925M trobats a Grècia i Canàries (Espanya), respectivament, amb els trobats als Estats
Units, la qual cosa suggereix que comparteixen un origen comú. Per tant, es més probable
que la presència d'aquestes mutacions en les colònies de fora d'Amèrica siga conseqüència
d'un moviment facilitat per l'ésser humà que d'un esdeveniment de mutació independent.
L'origen múltiple d'al·lels resistents és un reflex de l'heterogeneïtat genètica dins d'una
espècie. En altres artròpodes, per exemple, l'ús intensiu de pesticides piretroides ha
conduït a la selecció independent de varies mutacions idèntiques del tipus *kdr* en regions
geogràficament distants. Tanmateix, la variabilitat genètica global dels àcars de *V.
destructor* que parasiten a *A. mellifera* és extremadament baixa, i les poblacions es
consideren quasi clonals. Aquesta baixa variabilitat genètica s'atribueix als múltiples
esdeveniments de coll d'ampolla que va experimentar durant el canvi d'hoste, juntament
amb la ràpida propagació per tot el món, la determinació sexual per haplodiploïdia i
l'aparellament predominantment entre germans.

En el capítol 3, estudiem la distribució de les mutacions de tipus *kdr* en la posició
925 en el territori dels Estats Units d'Amèrica. Abans d'aquest estudi, la detecció
d'aquestes mutacions es limitava a uns pocs ruscs del sud-est dels Estats Units. Conèixer
el nivell de propagació i la incidència d'aquestes mutacions en tot el país permetrà
comprendre l'escenari real que afronten els apicultors estatunidencs, i permetrà també
abordar la situació del seu control d'una manera més eficaç. Utilitzant la metodologia de
TaqMan® múltiplex, un assaig de discriminació al·lèlica per a més de dos al·lels diferents
basat en la TaqMan®, vam genotipar femelles adultes de *V. destructor* recollides en
apiaris dels Estats Units durant la campanya de 2016 i 2017. Aquesta metodologia és
capaç de discriminar genotips d'àcars individuals comparant la intensitat de la senyal de
fluorescència que emeten unes sondes específiques per a cada al·lel en cada cicle del
procés d'amplificació de la PCR. Els nostres resultats evidenciaren que les mutacions de
tipus *kdr* L925M i L925I estan àmpliament distribuïdes en les poblacions de *V. destructor*
de tot el país, però amb una gran variabilitat d'incidència entre apiaris. En aquest estudi
no es va trobar la mutació L925V en els àcars analitzats.

Prenent en conjunt els resultats dels capítols 2 i 3, podem plantejar la hipòtesi de
que l'àmplia distribució d'aquests dos al·lels en tot el territori dels Estats Units és el
resultat de la distribució posterior dels àcars portadors d'aquests al·lels després de que

ocorregueren els esdeveniments de mutació que els van originar. A nivell nacional, l'al·lel de tipus salvatge L925 va ser el predominant, amb una freqüència del 54,7% en tots dos anys; seguit de L925I (25,1% i 28,7% en 2016 i 2017, respectivament) i L925M (20,2% i 16,6% en 2016 i 2017, respectivament). A partir de les freqüències per Estat, vam generar un mapa de distribució d'al·lels de resistència a piretroides en *V. destructor* per a 2016 i 2017. Mentre que a nivell nacional la proporció global de genotips i fenotips va ser relativament estable al llarg dels dos anys estudiats, a nivell d'Estat i de apiaris es van observar canvis considerables per al mateix any i entre els dos anys d'estudi. L'alta variabilitat trobada entre apiaris suggereix que les freqüències d'aquests al·lels esta fortament influenciades per factors externs, com són les aplicacions recents de acaricides front a *V. destructor*, l'acumulació de productes pesticides agrícoles en les matrius de les colònies, la biologia reproductiva de *V. destructor* i l'apicultura migratòria.

En tot el país, l'al·lel 925M es va trobar amb una incidència menor en comparació amb l'al·lel 925I; a més d'una disminució significativa de l'al·lel 925M entre els dos anys mostrejats. Aquests resultats no serien els que cabrien esperar si totes dues substitucions tingueren una aptitud biològica equivalent, i sent que la mutació L925M va sorgir abans com a precursora de la L925I, com suggereixen els nostres resultats filogenètics. És possible plantejar la hipòtesi que el VGSC amb la mutació L925M comporta un major cost biològic sobre els àcars en comparació amb la L925I. En el capítol 1, els anàlisis farmacològics van revelar que el canal mutat L925M es més sensible als piretroides assajats (deltametrina, flumetrina i *tau*-fluvalinat) que les mutacions L925I i L925V. La nostra hipòtesi és que la mutació L925M, fins i tot conferint resistència, és un pas intermedi cap a l'al·lel resistent més estable L925I. No obstant això, es necessiten estudis addicionals sobre la prevalença i el cost biològic associat a aquestes mutacions per a validar o rebutjar aquesta hipòtesi.

Els nostres resultats també demostren que els informes persistents sobre el baix èxit dels tractaments amb *tau*-fluvalinat als Estats Units poden atribuir-se a l'alta incidència d'aquestes mutacions en els apiaris. Al voltant del 40% dels àcars analitzats van ser fenotipats com a àcars resistents. Això, juntament amb el fet de que menys del 10% dels apiaris mostrejats contenien una població àcars totalment susceptibles planteja seriosos dubtes sobre la sostenibilitat del tractament a base de piretroides a llarg termini als Estats Units. L'escenari actual és especialment preocupant pel fet que un nombre molt baix de compostos han demostrat ser eficaços en el control de *V. destructor*, i sense un control

periòdic eficient, les colònies d'abelles poden aplegar a col·lapsar en un curt període de dos anys. Un panorama similar pot extrapolar-se amb l'al·lel L925V a Europa, on diversos estudis han informat de l'àmplia distribució d'aquest per diversos països, en ocasions en altes freqüències.

De la mateixa manera, els nostres resultats van revelar una prevalença considerablement alta dels al·lels resistents, tenint en compte la baixa taxa d'ús de *tau*-fluvalinat reportada entre els apicultors estatunidencs en l'enquesta de pràctiques apícoles d'abril de 2013 a març de 2017. Conseqüentment, és concebible que puga haver-hi altres fonts de pressió selectiva que mantinguen els al·lels resistents en freqüències altes en la població de *V. destructor* dels Estats Units; com pot ser l'acumulació de productes acaricides en les matrius dels ruscos. Paral·lelament, s'ha documentat una alta incidència d'àcars resistents en els apiaris europeus malgrat l'escàs ús de piretroides. Així doncs, l'ús "general" del *tau*-fluvalinat o d'altres tractaments a base de piretroides està certament amenaçat en un futur pròxim si no es prenen mesures per a fer front a la situació de resistència. En la situació actual, amb molt pocs tractaments efectius per a controlar a *V. destructor*, i un número creixent d'informes de resistència a la majoria d'ells, destaquem la rellevància d'implementar el seguiment dels al·lels resistents en els programes de gestió de plagues per al parasitisme de *V. destructor*.

Ara com ara, evitar el parasitisme de *V. destructor* és pràcticament inviable, per la qual cosa l'única solució és minimitzar les pèrdues i els danys econòmics. Si la població d'àcars es manté a ratlla, també ho estarien les malalties víriques, i les abelles mel·líferes poden romandre sanes. És quan la població de *V. destructor* es descontrola quan la colònia s'emmalalteix greument i existeix un alt risc de col·lapse. L'ús de qualsevol acaricida en l'apicultura pretén protegir les abelles, però al mateix temps imposa pressions de selecció que poden donar lloc al desenvolupament de resistències. Malauradament, els informes de resistència als tres ingredients sintètics actius continuen creixent. No obstant això, aquests productes podrien tindre utilitat en el futur si s'incloguerer en una estratègia de gestió de plagues que vigilés la freqüència dels àcars resistents i combinés els tractaments disponibles (piretroides, cumafós, amitraz, àcids orgànics i olis essencials) juntament amb tècniques de gestió y prevenció correctes.

La gestió integrada de plagues (GIP) és considerada per els experts com l'enfocament més exitós i respectuós amb el medi ambient per a fer front a les plagues

d'artròpodes. En aquesta gestió s'integra l'ús de plaguicides químics i biològics en combinació amb el control biològic i millores tècniques culturals, minimitzant l'impacte de la gestió en el medi ambient. Dins d'una aproximació GIP, els tractaments amb plaguicides només s'aplicaran quan els danys causats per la plaga suposen una pèrdua econòmica per a l'apicultor, i seguint un pla de tractament per fases segons les necessitats, on els tractaments químics serien l'última opció. Es a dir, es necessari que els acaricides químics es mantinguen efectius, ja que aquests tractaments s'utilitzaran quan no siga possible controlar la població de *V. destructor* d'altra manera. En conseqüència, els mètodes de control de *V. destructor* han d'incorporar estratègies per a minimitzar el desenvolupament de resistències i preservar la utilitat dels tractaments a llarg termini; però sobretot, evitar l'aparició de poblacions de *V. destructor* multiresistents.

Abordar el control de resistència als plaguicides és un component important en la gestió sostenible de la plaga, que allargarà la vida útil dels pocs acaricides autoritzats per al control de la *V. destructor*. Com s'ha esmentat abans, la hipòtesi plantejada sobre un major cost biològic d'aquestes mutacions de tipus *kdr* en l'absència de la pressió exercida pels piretroides pot ser un factor que ens ajudi a disminuir la incidència d'àcars resistent en una colònia. Tanmateix, es necessari conèixer l'estat de resistència d'una colònia per a poder actuar de manera més adequada, segons les circumstàncies donades i el moment (p. ex. establir períodes d'absència de piretroides). Per això, es essencial establir un seguiment de la resistència en els apiaris que tinguen o hagin tingut problemes d'efectivitat amb tractaments basats en piretroides.

El seguiment de les freqüències d'al·lels resistents en les poblacions d'àcars és un dels pilars fonamentals en la gestió de la resistència als plaguicides. En el cas particular dels piretroides, les proves basades en les freqüències al·lèliques són especialment útils per a la detecció precoç de resistències, fins i tot quan els àcars resistents es troben encara en freqüències baixes en la població. En una perspectiva a curt termini, la detecció d'aquestes mutacions abans del tractament permetria predir la seua eficàcia i aconsellar la selecció de la forma més convenient de tractar a l'àcar. En el capítol 3, hem utilitzat un assaig TaqMan® multiplex, que ha resultar ser molt eficient en la discriminació del al·lels de tipus *kdr* per a la posició 925 del VGSC. No obstant això, els assajos TaqMan® requereixen de recursos determinats, com a sondes d'ADN marcades amb fluorescència i dispositius de detecció, que augmenten el cost de l'assaig i el fan inassequible per a laboratoris amb pocs recursos. Amb l'objectiu de que la detecció d'àcars resistents siga

accessible a qualsevol laboratori estàndard, en el capítol 4 hem dissenyat una metodologia senzilla basada en la PCR-RFLP (reacció en cadena de la polimerasa - polimorfisme de longitud de fragments de restricció). En el VGSC de *V. destructor*, quan el codó 925 codifica una Leucina (sensible als piretroides), es forma una diana en l'ADN per a l'enzim de restricció *Sac*I. Aquesta diana de restricció desapareix quan aquest codó canvia a un dels tres al·lels resistents, L925V, L925I i L925M. En conseqüència, després de l'amplificació dels fragments d'ADN per PCR i la restricció amb *Sac*I, és possible diferenciar cadascun dels tres fenotips possibles; SS: homozigot per a l'al·lel susceptible L925; SR: heterozigot que porta un al·lel susceptible L925 i un al·lel resistent (V925, M925 o I925); i RR: àcar que porta dos al·lels resistents (V925, M925 o I925), ja siga en homozigosis o en heterozigosis. La resistència de tipus *kdr* s'hereta com un tret recessiu, per la qual cosa els àcars que tenen almenys un al·lel susceptible (SS i SR) són sensibles al tractament amb piretroides. La metodologia PCR-RFLP no és tan precisa com la seqüenciació directa o els assajos TaqMan® per a assignar un genotip a una determinada mostra, però és molt més senzill discriminar si una mostra procedeix d'un àcar resistent o no. Així mateix, és significativament més barat i accessible a tots els laboratoris que treballen en biologia molecular, a més de ser bastant versàtil i adaptable als recursos del laboratori que executa el protocol.

Les metodologies de mostreig utilitzades en aquesta tesi han demostrat ser senzilles de realitzar, robustes, fiables i ràpides per a genotipar un gran nombre d'àcars de manera individual, podent així determinar la incidència d'àcars resistents i susceptibles als piretroides en un determinat apiari. A més, funcionen bé amb els àcars recol·lectats i conservats sense requisits especials, i poden enviar-se a temperatura ambient, la qual cosa facilita la manipulació i recol·lecció de mostres per part dels apicultors. S'ha provat que totes dues metodologies emprades en aquesta tesi poden aplicar-se com a assaig de rutina en un laboratori i, per tant, són adequades per als programes de gestió i control a la resistència als plaguicides. Encara que de moment la detecció de resistències només és aplicable als piretroides, creiem que pot ser ben acollit per part dels apicultors. Ells són conscients que els piretroides com el *tau*-fluvalinat o la flumetrina són molt efectius per a eliminar els àcars dels ruscos quan no hi ha resistència. Per tant, el conèixer prèviament el nivell de resistència als piretroides de la població de *V. destructor* dels seus apiaris por ser una gran ajuda a l'hora de decidir si tractar amb aquest productes serà l'elecció correcta o no. En el cas de trobar una freqüència alta d'al·lels resistents, caldrà establir la rotació

amb altres acaricides i tècniques de prevenció disponibles, per a que no es seleccionen els àcars resistents i mantindre els al·lels de resistència en la menor freqüència possible; la qual cosa permetrà un control efectiu del paràsit a llarg termini. Conèixer l'eficàcia esperada d'un producte abans de aplicar-lo milloraria sens dubte el resultat en el control de *V. destructor* en els ruscos a curt termini. De la mateixa manera, disposar d'aquesta informació reduiria els tractaments acaricides innecessaris. Al mateix temps, es minimitzaria la seua acumulació en les matrius dels ruscos, i també es disminuiria la probabilitat de que es desenvolupessin noves mutacions resistents en una població d'àcars. A més, un seguiment regular permetrà detectar les fluctuacions dels al·lels resistents i actuar en conseqüència, per exemple, programant un període sense piretroides quan aquests no vagin a ser eficaços. La detecció precisa dels àcars resistents abans del tractament obri una finestra per a una estratègia de gestió de la resistència, dirigida a aconseguir un control suficient de l'àcar; al mateix temps que es protegeix l'eficàcia dels piretroides durant el màxim temps possible.

Un dels majors canvis als quals s'enfronten els apicultors hui en dia és el control dels àcars *V. destructor*; un problema agreujat pel limitat número de productes de control disponibles i l'evolució de la resistència a aquests en les poblacions d'àcars. Encara que es disposa de tractaments alternatius no sintètics, la seua eficàcia és variable, ja que els resultats es veuen afectats per factors externs, com les condicions climàtiques, les del rusc i l'aplicació del producte. El desenvolupament d'acaricides sintètics basats en nous ingredients actius és cada vegada més difícil i costós, per la qual cosa sembla poc probable que es puguen comercialitzar nous acaricides eficaços front a *V. destructor* en un futur pròxim. Per tant, ara cal centrar-se en mantindre l'eficàcia dels acaricides actuals durant el major temps possible; però això es veu amenaçat per l'evolució de la resistència. Per a desenvolupar mesures eficaces de gestió de la resistència a aquests productes, és essencial comprendre el mecanisme molecular subjacent a la resistència en *V. destructor*, així com els factors dinàmics que influeixen en la incidència dels al·lels de resistència en les poblacions. D'aquesta manera, es pot abordar la amenaça del parasitisme de *V. destructor* en el context específic del moment, evitant el fracàs del tractament i minimitzant l'aparició de futurs esdeveniments de resistència.

En aquesta tesi, hem evidenciat la implicació de les mutacions en la posició 925 del canal de sodi de *V. destructor* en la resistència als piretroides (capítol 1). Els resultats del nostre seguiment han revelat que, encara que amb una incidència variable, tant els al·lels

resistents L925I com L925M estan molt estesos per tot els Estats Units d'Amèrica, sent la causa més probable de la baixa eficàcia del tractament amb piretroides al país (capítol 3). A més, hem trobat per primera vegada la substitució M918L en els àcars *V. destructor*, associada també amb resistència als piretroides en altres espècies (capítol 2). Els anàlisis filogenètiques donen suport a l'origen únic de cada mutació de tipus *kdr* en el VGSC de *V. destructor*, a més d'una estreta relació entre els al·lels L925M i L925I (capítol 2). També hem desenvolupat un mètode de detecció dels al·lels mutants per a la posició 925 del VGSC senzill i assequible basat en una PCR-RFLP que pot adaptar-se com a assaig de rutina en qualsevol laboratori (capítol 4).

SUMMARY

One of the major concerns in contemporaneous apiculture is the parasitism of *Varroa destructor* Anderson & Trueman (Acari: *Varroidae*). This highly specialised obligate ectoparasite feeds directly on pupae and adults of *Apis mellifera* L. (Hymenoptera: *Apidae*), inducing immunosuppression in bees that leads to the outbreak of pre-existing or mite-vectored infections that compromise colony viability. *Varroa destructor* distribution was limited to some regions of East Asia while parasitizing its natural host, *Apis cerana* Fabricius (Hymenoptera: Apidae), with which it keeps a balanced parasitic relationship, causing a low level of damaging infestations (*A. cerana* shows some tolerance to *Varroa* mites). But it rapidly spread out after shifting to *A. mellifera* less than a century ago, becoming a threat to global apiculture. Today, the *Varroa* mite is a worldwide concern with an estimated economic toll of millions of US dollars per year. Regular control of the mite is necessary to prevent huge colony losses, and this control is mainly achieved by the application of acaricides. Pyrethroid compounds have been among the most common treatments for controlling *Varroa*, strongly used over many generations, even after resistance evolved in the mid-1990s, due to their low toxicity against bees, low pesticide residue, and high efficacy when there is no resistance, but mostly because of the very low number of available and effective treatments.

Synthetic pyrethroids are a major class of pesticides widely used for controlling pests and disease vectors. Some types of pyrethroids have a broad spectrum of target species (highly effective against insects), whereas others are more selective against acari (mites and ticks). Pyrethroids with acaricidal selectivity are particularly useful in situations where it is needed to attack one specific pest cohabitating with beneficial insects, as is the case with Varroosis (the honey bee disease caused by *Varroa* infestation). Currently, *tau*-fluvalinate (Apistan®) and flumethrin (Bayvarol®, Polyvar®) are the only two pyrethroids available for managing parasitic mites inside honeybee colonies without significantly harming the bees. Unfortunately, as happened with many other pesticides, the intensive use of varroacide pyrethroids has led to the development of resistance in many mite populations around the globe. In *Varroa,* as in arthropods, the most common mechanism involved in the loss of pyrethroid sensitivity is the substitution of certain amino acids in their target protein, the voltage-gated sodium channel (VGSC). The VGSC is a large transmembrane protein found in the axon membranes of neurons that is essential for the propagation of nerve impulses across neuronal axons. These point mutations, often

referred to as *kdr*-type mutations (*knockdown* resistance), are mostly located in domain II and III transmembrane helices (IIS5, IIS6 and III6) and the linker IIS4-S5. Modeling studies of protein structure predicted that these regions would be shaped into a hydrophobic pocket wherein pyrethroids would bind. While several mutations that trigger resistance have been found in some arthropod species, either alone or in combination, only a change in position 925 (numbered after the housefly *para*-type sodium channel protein) has been described as associated with pyrethroid susceptibility in *V. destructor*. Nevertheless, three different resistant mutations have been described for this position following the replacement of the wild-type Leucine by Valine (L925V), Isoleucine (L925I) and Methionine (L925M). These alleles have a distinct geographical distribution, with the mutation L925V found in European mite populations and the L925I and L925M substitutions found in North American hives. However, during the course of the present thesis, there were occasional reports of the L925I and L925M mutations in mites from outside the USA territory, such as Crete, Japan, or Turkey.

In the present work, we have focused on *kdr*-type mutations at position 925 of the *V. destructor* VGSC, which have been associated with mites from many locations surviving treatments based on *tau*-fluvalinate and flumethrin. The intention of this research study was to shed light on the implications of these mutations on pyrethroid resistance, their evolutive relations, and present status, with the eventual purpose of establishing some basic keystones to develop an effective Integrated Pest Management (IPM) approach. This work is framed within a larger project aimed at elucidating the molecular basis behind the resistant phenotype to the active chemicals authorised for *Varroa* control.

In Chapter 1, by electrophysiological and pharmacological assays, we have demonstrated that pyrethroid susceptibility is reduced in *Varroa*'s 925-mutated VGSC. The implications of these mutations in the mechanism of resistance have been studied through the functional and pharmacological characterization of these channels by their expression in *Xenopus spp.* oocytes. Firstly, the complete coding sequence of the *para*-type (the L925 allele, also known as wild-type or susceptible) VGSC of *V. destructor* (*Vd*VGSC) was cloned in a plasmid vector containing all the necessary elements for cRNA (complementary RNA) transcription and expression in *Xenopus spp.* oocytes. Using this plasmid as a template, we have generated the three 925 position mutant channels by site-directed mutagenesis, obtaining variations of the *Vd*VGSC that only

differ in the 925 aminoacid residue. The cRNA transcripts of either the wild-type or mutant channels were synthesised *in vitro* using the cloned VGSCs as a template, and subsequently microinjected into V-VI stage oocytes of *Xenopus spp*. for their heterologous expression. The functional and pharmacological characteristics that modifications at position 925 confer on the *Vd*VGSC were examined in the oocytes that expressed the channel by the Two Electrode Voltage Clamp method. Those were exposed to increasing concentrations of deltamethrin (a potent generalist pyrethroid against arthropods), *tau-fluvalinate,* and flumethrin (both are mite-selective pyrethroids) to assess the effects on wild-type and mutated *Vd*VGSCs.

Compared to the wild-type *Vd*VGSC, the sensitivity to pyrethroids was found to be significantly reduced when mutated *Vd*VGSC were expressed in *Xenopus spp.* oocytes. In contrast to the wild-type channel, L925I and L925V mutated sodium channels did not elicit any tail current response when exposed to all tested pyrethroids (deltamethrin, flumethrin, and *tau*-fluvalinate). At an intermediate level, the L925M mutation showed more susceptibility to pyrethroids than the L925I and L925V but displayed a lower response effect than the wild-type channel. Our results support that the point substitution of residue 925 at the *Vd*VGSC influences the interaction of pyrethroids with the channel, so clearly the 925 amino acid plays a relevant role in the type II pyrethroid receptor site in mite sodium channels, similarly to that in insects. In mutated channels, pyrethroid interaction is most probably hindered by the alternative side chain of the modified residue at position 925, preventing the proper attachment of the pyrethroid to their binding pocket site.

Besides, in the absence of pyrethroid compounds, the three mutations at residue 925 modify the physiological kinetics properties of the mite sodium channel, also observed in insect *kdr*-mutated channels. All three mutated channels exhibit a shift of activation ($V_{50,act}$) towards a more positive voltage, but the difference is higher for the L925I and L925V mutated channels. Moreover, the L925M channel also inactivates more rapidly than the wild type. In short, the mutated L925V and L925I channels are less likely to open than the wild type, while L925M will switch to the closed state more quickly. This characteristic could contribute to resistance, but it could also have a potentially negative impact in the absence of pyrethroids. Pyrethroids have higher affinity and preferentially target the channel in their open state. The formation of bonding contacts between the pyrethroid and different channel residues across the predicted binding cavity could

stabilise the VGSC in the open state, prolonging sodium tail currents. Upon return to the closed state, repositioning of the domain II S4-S5 linker would lead to disturbance of the pyrethroid-binding contacts and release of pyrethroids. According to this model, the reduced availability of the mutated VdVGSC in the open state and the faster transition towards the closed states may also be factors counteracting the action of pyrethroids, thus contributing to resistance.

The mutations detected in mites at position 925 (Valine, Methionine, and Isoleucine) do not compromise the functionality of the VdVGSC. However, they entail an alteration of the gating kinetics of the sodium channel over the wild-type channel. Considering the key role in the transmission of the nerve impulse played by the VGSC, it is very probable that these three substitutions have a certain impact on the fitness of the mites. In the characterization of the L925 mutant VdVGSC, our results showed a shift towards positive voltages in the channel activation potential ($V_{50,act}$) for the three mutant channels to a higher or lower degree. Compared to the wild-type, this kinetic modification can be advantageous by counteracting the pyrethroid interaction since these channels are less likely to open, and pyrethroids bind preferentially to the channel in their open state. Notwithstanding, in the absence of pyrethroids, this condition could be disadvantageous. These channels require stronger membrane depolarization to activate than the wild-type channel. Thus, these mutant channels are essentially less excitable than the wild-type. Accordingly, in the absence of the strong selective pressure exerted by pyrethroids, individual mites with less excitable neurons would be at a disadvantage when compared to mites that require a lower excitatory potential. Several studies point out the possible fitness penalty that the L925V mutation could have when the selective pressure of pyrethroids is absent. Our results here provide a plausible explanation for this fact based on the biophysical characteristics of the mutated and wild-type VdVGSC. In turn, if our hypothesis is correct, given the biophysical characteristics of the mutated VdVGSC, a comparable fitness cost would be expected for mites carrying the L925I mutation.

Particularly remarkable is the opposite effect that pyrethroids induce on the activation kinetics of $V. destructor$ and insect sodium channels. In the insect sodium channel, interaction with pyrethroids often enhances the activation state by shifting $V_{50,act}$ to more negative values. The channels become more easily excitable, leading to a hastened and prolonged open state and, consequently, to a higher exposure of the pyrethroid binding site. However, the interaction of deltamethrin, tau-fluvalinate, and

flumethrin alters the channel kinetics of *V. destructor* channels by shifting the $V_{50,act}$ to more positive voltages, which could diminish the binding potential of pyrethroids. The dissimilar influence on activation may be one of the factors underlying the lower sensitivity of *V. destructor* sodium channels than insect sodium channels to pyrethroids.

In Chapter 2, we studied the phylogenetic relationship between the resistance alleles at position 925 of the VGSC in *V. destructor*. The three different resistant alleles for this position have been found in different mite populations around the world. The mutation L925V is distributed largely in Europe, while L925M and L925I are found mostly across the USA. By unravelling the phylogenetic relationship between the resistance alleles, we can identify past mutation events that have resulted in the present distribution of resistance mites and know whether the evolutive origin of the different mutations in mite populations has originated from single or multiple mutation events. Understanding the evolutionary history of the resistant alleles is a key step to understanding the selection pressure these *kdr*-type residues are under, thus predicting future events of emerging resistance and contributing to designing more finely tuned management strategies.

In order to assess the evolution of resistant mutations in *V. destructor*, we amplified and genotyped the region of the VGSC containing the complete exon codifying for 925 residue and partial fragments of the upstream and downstream flanking introns from *V. destructor* samples collected worldwide, from a diverse number of locations where mites resistant to Apistan® (*tau*-fluvalinate) have been reported. Sequences revealed the presence of the *kdr*-type mutation M918L in mites collected from the Comunitat Valenciana (Spain). The mutation M918L was not reported in *V. destructor* up to date, and we found it in co-occurrence with L925V mutations. Both M918 and L925 residues are located in the IIS4-S5 linker and the IIS5 of the VGSC, respectively. It is predicted that these regions, together with IIIS6, fold into a hydrophobic pocket, proposed to be the interaction site of pyrethroids in the channel. According to this model, any substitution in the amino acids lining the hydrophobic pocket would interfere with the accommodation of the pyrethroid, making the channel less sensitive to these chemicals. Although the effect of the mutation M918L has not been characterised on *Varroa*, in other arthropods it has been demonstrated that substitutions of M918 significantly reduce the susceptibility of the channel to pyrethroids. Moreover, the co-occurrence of more than one *kdr*-type mutation often leads to a greater resistance level than the individual mutations.

31

Accordingly, we can hypothesise that the combination of M918L and L925V would trigger a higher destabilisation than that produced by L925V or M918L alone.

Phylogenetic analyses of the gene region linked to position 925 of the *V. destructor* VGSC revealed a single origin for each *kdr*-type mutation. Furthermore, it suggests two different parallel origins for the mutations, with a clear phylogenetic relationship between mutations L925M and L925I, on one hand, and L925V and M918L on the other. The geographical distribution of the resistant alleles correlates well with the results obtained by phylogenetic reconstruction, and therefore also supports the proposal of a single mutation event for each resistance-related amino acid substitution. The phylogenetic reconstruction suggests that L925M and L925I are the results of a sequential process, with the L925M mutation being an ancestor of the Isoleucine mutation, which would have arisen in a second parallel mutation event (Leu → Met → Ile). Our analyses also showed the close relationship between the L925I and L925M alleles found in Greece and the Canary Islands (Spain), respectively, with those found in the USA, suggesting that they share a common origin. Hence, the presence of these mutations in colonies outside America is more likely to be a consequence of human-facilitated movement than of an independent mutation event.

Multiple origins of resistant alleles reflect genetic heterogeneity within a species. In many other arthropods, the intensive use of pyrethroid pesticides has led to the multiple selection of identical *kdr*-type mutations around the globe. In *V. destructor*, the global genetic variability of mites parasitizing *A. mellifera* is extremely low, with populations considered to be almost clonal. This is attributed to several bottleneck events, together with rapid spread around the world, haplodiploidy, and predominantly sibling mating. Our findings have a significant implication in the control of *V. destructor*, revealing that the movement of honey bees has a stronger influence on the current distribution of *kdr*-type alleles than new mutation events. Indeed, given these results, it is possible to hypothesise that the rapid expansion of resistant mites bearing these mutations could have been in part facilitated by human and honey bees-mediated transport, coupled with the intensive treatment schemes based only on pyrethroid acaricides for many years in a row.

In Chapter 3, we studied the distribution of the *kdr*-type mutations at position 925 in the USA territory. Prior to this study, the detection of these mutations was limited to a few South-eastern apiaries in the USA. Knowing the spread and incidence of these

mutations throughout the country will allow us to comprehend the current scenario for USA beekeepers, and will allow us to address the situation more effectively. Using a TaqMan® multiplex assay, a high-throughput allelic discrimination assay based on TaqMan®, we genotyped adult *Varroa* females collected from USA apiaries in 2016 and 2017 as part of the US National Honey Bee Disease Survey (NHBDS). This methodology is capable of discriminating between individual mite genotypes by comparing the intensity of fluorescence signals emitted by specific probes during each cycle of the PCR amplification process. Our results demonstrate that the L925M and L925I *kdr*-type mutations are widely distributed in *V. destructor* populations across the country, showing high variability among apiaries. We did not find the L925V mutation in the apiaries tested. Taking together the results of chapters 2 and 3, we can hypothesise that the broad distribution of these two alleles across the USA territory is the outcome of the subsequent distribution of mites carrying these alleles after the mutation events. Nationally, the wild-type allele L925 was the predominant, with a frequency of 54.7% in both years, followed by L925I (25.1% and 28.7% in 2016 and 2017, respectively) and L925M (20.2% and 16.6% in 2016 and 2017, respectively). Based on the frequencies by state, we have generated a distribution map of pyrethroid resistance alleles in *V. destructor* for the situation in 2016 and 2017. While nationally, the overall proportion of genotypes and phenotypes was relatively stable across years, considerable changes were noted at the State and apiary level within and between years. The high variability among apiaries suggests that allele frequencies are strongly influenced by external factors, such as recent varroacide applications, the accumulation of pesticide products in colony matrices, *Varroa*'s reproductive biology, and migratory beekeeping.

Across the country, the 925M allele was found at a lower incidence when compared to the 925I allele, with a significant decrease of 925M between the two years sampled. These results would not be an expected outcome if both substitutions had an equivalent fitness cost, and the L925M mutation had arisen before as the precursor of L925I, as our phylogenetic results show. It is possible to hypothesise that L925M allele is posing a higher fitness cost to the mites when compared to L925I. Our pharmacological analyses revealed that the L925M mutated *Vd*VGSC was more sensible to the tested pyrethroids (deltamethrin, flumethrin and *tau*-fluvalinate) than the L925I and L925V mutations (Chapter 1). We propose that L925M, even conferring resistance, would be an intermediate through the more stable resistant allele L925I. Nevertheless, further studies

on the prevalence and fitness cost associated with these mutations are needed to validate or reject this hypothesis.

Our results also prove that the persistent reports of *tau*-fluvalinate treatment failures across the USA can be attributed to the high incidence of these mutations in apiaries. Around 40% of mites tested were genotyped as resistant mites. This, together with the fact that only less than 10% of the apiaries sampled contained fully resistant mites, poses serious questions about the sustainability of pyrethroid-based treatment for the long term in the USA. The current scenario is especially worrying due to the fact that very low compounds have been proven to be effective in controlling *V. destructor*, and without periodic control, honeybee colonies can collapse in a short period of two years. A similar scenario can be extrapolated to the L925V allele in Europe, where its wide distribution across countries, sometimes at high frequencies, has been reported by several studies.

In the same way, our results revealed a considerable high prevalence of the resistant alleles, considering the very low rate of *tau*-fluvalinate use reported among USA beekeepers in the beekeeping practises survey from April 2013 to March 2017. It is conceivable that there might be other sources of selection pressure keeping resistant alleles at high frequencies in the USA *V. destructor* population, such as the accumulation of acaricide products in colony matrices. Similarly, a high incidence of resistant mites has been documented in European apiaries despite the low use of pyrethroid. So, the "general" use of *tau*-fluvalinate or other pyrethroid-based products is certainly threatened in the near future if no action is taken to address the situation. In the current situation, with very few effective treatments to control *V. destructor* parasitism and many reports of resistance to most of them, we highlight the relevance of implementing the monitoring of resistant alleles in pest management programmes for varroosis.

For now, avoiding *V. destructor* parasitism is virtually impossible, and the only solution is to minimise the losses and the economic damage. If the population of mites were kept in check, so too would be the viral diseases, and honey bees could remain healthy. It is when the *V. destructor* population gets out of control that the colony becomes seriously sick and there is a high risk of collapse. The use of any miticide in apiculture is intended to protect bees but imposes selection pressures that can result in the development of resistance. Worryingly, reports of resistance to the three synthetic active ingredients are on the rise. These products, however, could have utility if they were included in a pest

management strategy that monitors the frequency of resistant mites and combines the available treatments (pyrethroids, coumaphos, amitraz, organic acids, or essential oils) along with correct management approaches. Integrated Pest Management (IPM) is considered by experts to be the most successful and environmentally friendly approach to dealing with arthropod pests. It integrates the use of chemical pesticides in combination with better cultural and biological techniques, minimising the management impact on the environment. In an IPM approach, pesticide treatments should only be applied when pest damage implies an economic loss for the beekeeper, following a phased treatment plan according to need. Consequently, *Varroa* control methods must incorporate strategies to minimise resistance development and preserve the utility of the treatments for the long term, but above all, prevent the emergence of multi-resistant *V. destructor* strains or populations.

Managing the development of pesticide resistance is an important component of sustainable pest management that will prolong the lifespan of the few acaricides authorised for *Varroa* control. The monitoring of resistant allele frequencies in mite populations is one of the fundamental pillars in pesticide resistance management. In the particular case of pyrethroids, allelic frequency-based tests are particularly useful for early detection of resistance, even when resistant mites are still present in low numbers in the population. In a short-term perspective, detecting these mutations prior to the treatment would allow us to predict its efficacy and provide advice for selecting the most convenient way to deal with the mite. In Chapter 3, we used a TaqMan® multiplex assay, which was found to be highly efficient for 925-allelic discrimination. However, TaqMan® assays require certain resources, such as fluorescently labelled DNA probes and detection devices, which increase the cost of the assay and make them unaffordable for low-resourced laboratories. With the aim of making the detection of resistant mites accessible to any standard laboratory, in Chapter 4, we have designed a simple methodology based on PCR-RFLP (polymerase chain reaction - restriction fragment length polymorphism). In the *V. destructor* VGSC, when codon 925 encodes a Leucine (pyrethroid-sensitive), a target for the *Sac*I restriction enzyme is formed. This restriction target disappears when this codon changes to one of the three resistant alleles, L925V, L925I, or L925M. Consequently, after DNA amplification fragments by PCR and restriction with *Sac*I, it is possible to differentiate each of the three possible phenotypes: SS: homozygous for the susceptible allele L925; SR: heterozygous that carries a

susceptible allele L925 and a resistant allele (V925, M925, or I925); and RR: mite carrying two resistant alleles (V925, M925, or I925), either in homozygosis or heterozygosis. The *kdr*-type resistance is inherited as a recessive trait, hence, mites having at least one susceptible allele (SS and SR) are susceptible to pyrethroid treatment. The PCR-RFLP methodology is not as accurate as direct sequencing or TaqMan® assays to assign a genotype to a given sample, but it is far more straightforward in determining whether a sample is coming from a resistant mite or not. Besides, it is significantly cheaper and accessible to all laboratories working in molecular biology, as well as being quite versatile and adaptable to the resources of the laboratory running the protocol.

The screening methodologies used in this thesis have been demonstrated to be simple to perform, robust, reliable, and fast for genotyping large numbers of mites individually, thereby allowing us to determine the incidence of pyrethroid-resistant and susceptible mites in a given apiary. In addition, they work well with mites collected and preserved without special requirements, which can be shipped at room temperature, making it easy to handle for beekeepers. Both methodologies have been proven to be capable of being implemented as a routine assay in a laboratory and therefore suitable for pesticide resistance management programmes. Although this is only applicable to pyrethroids at the moment, we believe that it will be very attractive to beekeepers. They are aware that pyrethroids such as *tau*-fluvalinate or flumethrin are very effective at removing mites from the colonies when there is no resistance. Thus, previous knowledge of pyrethroid resistance status in their apiaries will help in deciding whether they will be the right choice or not. Accurate pre-treatment detection of resistant mites opens a window for a resistance management strategy aimed at achieving sufficient control of the mite while protecting the efficacy of pyrethroids for the longest possible time. Knowing the expected efficacy of a product beforehand would undoubtedly improve the outcome of *Varroa* control in the short term. In the same way, having such information would cut down on unnecessary acaricide treatments. Therefore, they minimise their accumulation in hive matrixes, and also reduce the likelihood of new resistant mutations developing in a mite population. In addition, regular monitoring will allow the detection of fluctuations in resistant alleles and allow us to act accordingly, e.g., by scheduling a pyrethroid-free period when pyrethroids become less effective. Further rotation with other available acaricides and management approaches will need to be implemented to keep resistance

alleles at the lowest possible frequency, contributing to successful long-term control of the parasite.

One of the largest challenges facing beekeepers today is controlling *Varroa* mites, a problem exacerbated by the limited number of control products available and the evolution of resistance in mite populations. Although alternative non-synthetic based treatments are available, their efficacy is variable as outcomes are dependent on external factors such as climatic, in-hive conditions, and product application. The development of synthetic miticides based on new active ingredients is becoming harder and more costly, so it seems unlikely that new effective varroacides will be available on the market in the near future. Therefore, the focus now must be on keeping current acaricides effective for the longest time possible, but this is threatened by the evolution of resistance. To develop effective resistance management measures, it is essential to understand the molecular mechanism underlying resistance in *V. destructor* as well as the dynamic factors influencing the incidence of the resistance alleles in the populations. Therefore, the challenge of *Varroa* parasitism can be addressed within the specific context of the moment, preventing treatment failure and minimising the occurrence of future resistance events.

In this thesis, we have evidenced the implication of the mutations at position 925 of the VGSC in the resistance of pyrethroids in *V. destructor* (Chapter 1). Our monitoring results have revealed that, although with varying incidence, both L925I and L925M resistant alleles are widespread throughout the USA, being the most plausible cause of pyrethroid treatment failure in the country (Chapter 3). Moreover, we found for the first time in *V. destructor* the substitution M918L, associated with pyrethroid resistance in other species (Chapter 2). The phylogenetic analyses support the single origin for each *kdr*-type mutation on the *V. destructor* VGSC and a close relationship between the L925M and L925I alleles (Chapter 2). We also developed a simple and affordable detection method of 925-mutant alleles based on PCR-RFLP that can be adapted as a routine assay in any laboratory (Chapter 4).

GENERAL INTRODUCTION

i.1. Introduction to *Varroa destructor*

i.1.1. The western honey bee

The Western honey bee, *Apis mellifera* L. (Hymenoptera: *Apidae*), is the most common domesticated bee species worldwide. Originally kept for honey production, they have become the flagship species for pollination in large-scale agriculture (Abrol, 2012; Rucker et al., 2012; Voorhies et al., 1933) and are a highly valued resource around the world. They constitute a fundamental agricultural commodity for human well-being since they can produce two different kinds of benefits, measured on the basis of the products that come from them, directly or indirectly (Gallai et al., 2009; Hung et al., 2018; Potts et al., 2016). In the first case, they can produce six hive products used for nutritional and medicinal purposes: honey, pollen, royal jelly, beeswax, propolis, and venom (Cornara et al., 2017; Mizrahi and Lensky, 2013; Schmidt, 1997). In the second case, and more important, the greatest value of honey bees to human well-being is through their indirect work as plant pollinators (Abrol, 2012; Potts et al., 2016). Honey bee pollination is both, an ecosystem service and a production practice used extensively by farmers all over the world for crop production (Klein et al., 2007). In fact, approximately one-third of our total diet is dependent, directly or indirectly, on insect-pollinated plants (McGregor, 1976), where honey bees represent by far the most important group of pollinators (Boecking and Veromann, 2020; Calderone, 2012).

It is estimated that around 70% of the 107 global crops used directly for human food are dependent on pollinators, and that more than 90% of the flowers are visited by bees (Klein et al., 2007; Potts et al., 2016; Southwick and Southwick, 1992). This applies to all kinds of fruits and vegetables, almost all oilseeds, and also pastures, such as clovers. Similarly, seed production of fodder crops and vegetables requires bee pollination. For some crops, such as almonds, the reliance is almost absolute and very little fruit would set without honeybee pollination (Degrandi-Hoffman et al., 2019). Besides, for other agricultural plants, such as apples, flower pollination is not completely dependent on bees; however, the quality and yield are significantly higher when pollinated by them. In such cases, fruit setting can be inadequate when it is not pollinated by bees, which essentially results in impaired development and/or smaller fruit size (Klatt et al., 2014; Samnegård et al., 2019).

INTRODUCTION

Honey bees have become a management tool, purchased or rented by farmers in many countries to supplement the local pollinator fauna (Free, 1993; Gallai et al., 2009; McGregor, 1976). Of the about 12 managed bee species commonly used commercially for crop pollination, the Western honey bee is the most exploited for pollination services around the globe. Its characteristics as a generalist pollinator and the wide range of climate tolerance makes this bee highly versatile and adaptable to a wide variety of agricultural and horticultural environments all around the world (Boecking and Veromann, 2020; Degrandi-Hoffman et al., 2019; Wallberg et al., 2014). Furthermore, its status as a social insect and well-established management practises make it easy to handle, with high flexibility for matching the magnitude of service requirements, particularly when large-scale services are required, as well as the ability to move colonies where the service is required (McGregor, 1976; Potts et al., 2016; Seeley, 1989). Its elevated crop pollinating efficiency is also linked to its larger colony population than other social bees, such as the Eastern honey bee (*Apis cerana* Fabr.), another species of domesticated bee. A typical size colony for *A. mellifera* ranges from 10,000 to 100,000 bees, depending on season, weather, and food availability, whereas other honey bees establish less populous and thus less productive colonies.

Demand for pollination services has increased in recent decades, gaining economic significance. Changes in agriculture to more intensive practises, especially since the 1950s, have led to a sharp loss of habitat and food diversity for insects. As a result of the decline in wild bees and pollination insects, farmers and producers rely heavily on managed honey bees for crop pollination; as well as on wild plant reproduction needs for the maintenance of biodiversity in ecosystems (Breeze et al., 2014; Deguines et al., 2014; Klein et al., 2007; Kremen et al., 2002).

i.1.2. The introduction of *A. mellifera* in Asia.
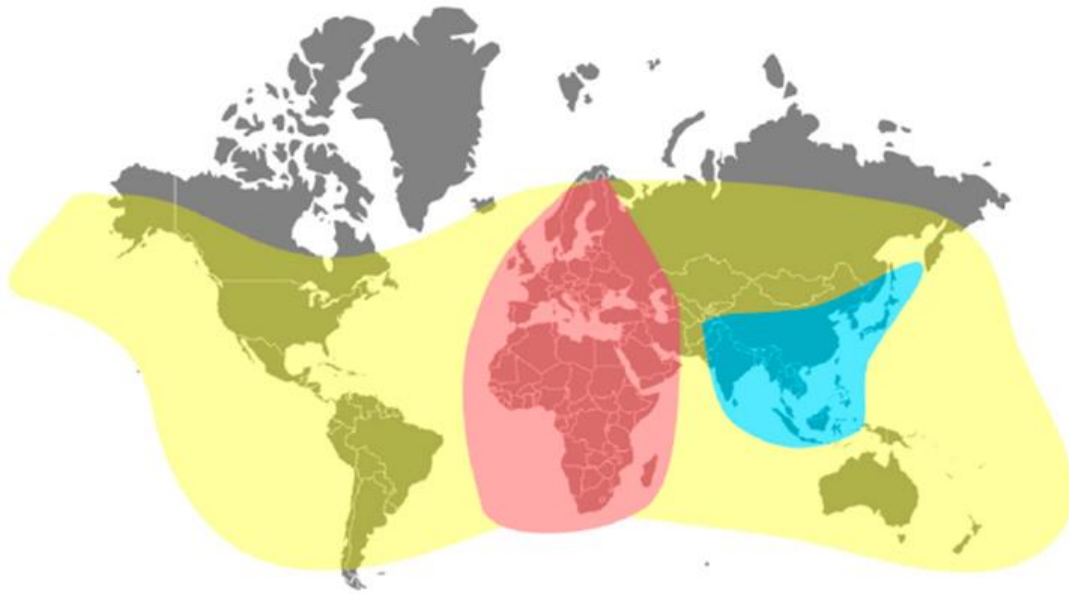
Figure i.1. Geographical distribution of *A. mellifera* and *A. cerana* domesticated honey bees. *A. mellifera* native (red) and current (yellow) distributions, as well as *A. cerana* native distribution (blue). Adapted from Beaurepaire et al. (2020).

The western honeybee, *Apis mellifera* L. (see Supplementary Figure Si.1 for taxonomic classification, p. 239), originally occurred only in Europe, the Middle East, and Africa (Fig. i.1). Nevertheless, the greater potential for profitability of *A. mellifera* compared to other native species of managed honey bees, such as *A. cerana* in Asia, led to its wide importation from Europe to North America (from around 1621), eastern Russia (in the late 1700s), followed by Japan (1877), India, and Indonesia (late 1800s), South America (1839), Australia (1810), New Zealand (1839), New Guinea, and the Pacific Islands (1857) (Chantawannakul et al., 2016; Crane, 1999). By the 1980s, nearly every country in America and Asia had accommodated *A. mellifera* (Chantawannakul et al., 2016; Crane, 1999).

Honey bees have naturally occurring parasites and pathogens which usually have evolved in sympatry and do not destroy the bees colonies (Sammataro et al., 2000). The development of long-distance travel among human beings initiated a global trade in plants and animals, introducing new species and diseases to regions where they did not exist previously. Some of the newly introduced diseases affected the Western honey bee severely, driving considerable losses in colonies. Among the most serious diseases are those caused by viruses and mite parasites (Staveley et al., 2014). However, no other

pathogen has had a comparable impact in the long history of beekeeping as the mite *Varroa destructor*.

i.1.3. The mite *Varroa destructor*

The ectoparasite *Varroa destructor* (Anderson and Trueman, 2000) is recognised as the biggest pest to honeybees worldwide, being the predominant threat to modern apiculture. This mite is compromising the survival of managed and feral honey bees, the beekeeping industry, and, due to the role of bees in pollination, the future of many agricultural crops. The disease condition in a honey bee colony caused by the infestation of *Varroa* mites and the detrimental effects of their parasitism is called varroosis (Boecking and Genersch, 2008; Shimanuki et al., 1994; Wegener et al., 2016).
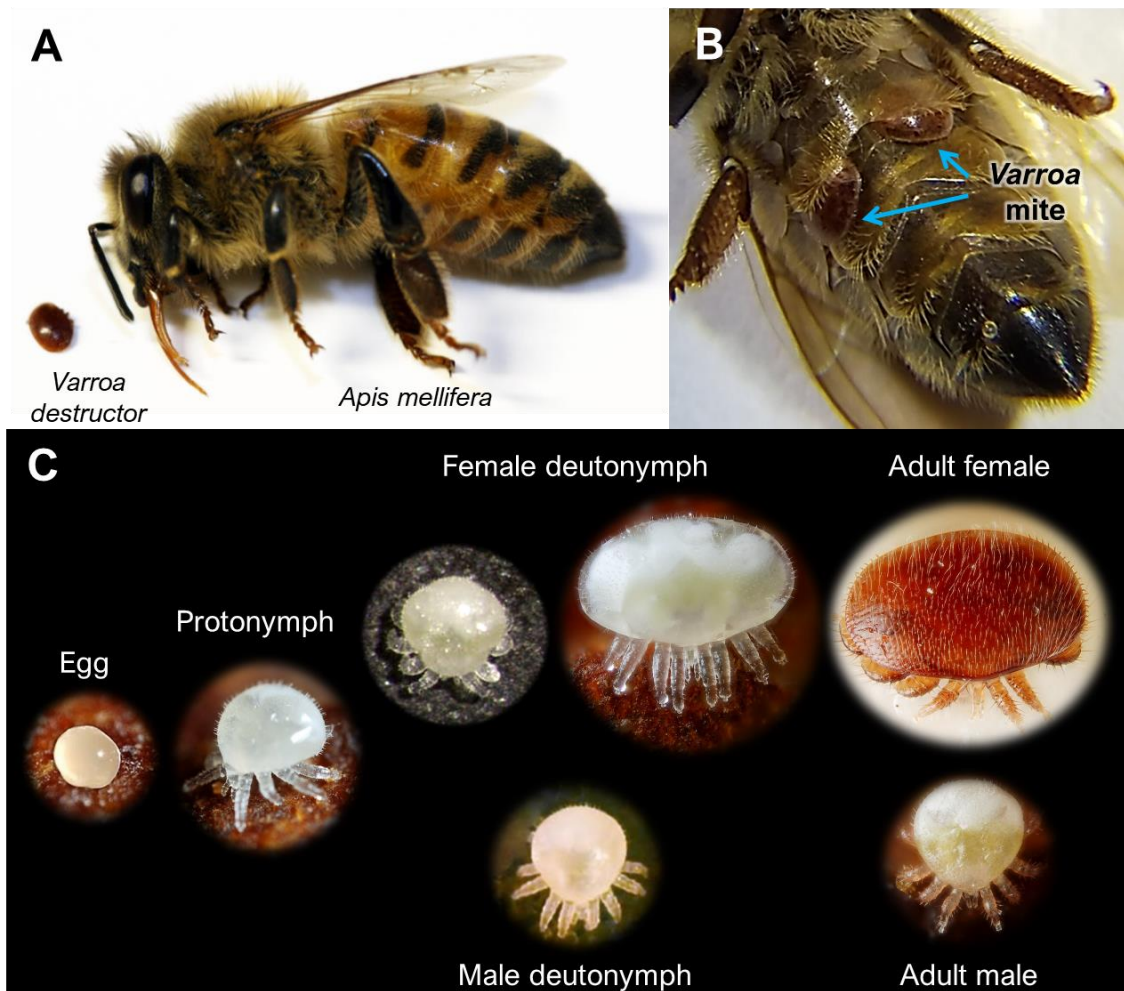
Figure i.2. Adult female *V. destructor* next to *A. mellifera* (A). *Varroa* mites hiding beneath the abdominal sclerites of a bee (B). *Varroa destructor* female and male stages (C). Photos by Andrew Bradley (A), Scott Koppa (B) and Gilles San Mantin (C).

Varroa mites show a distinct sexual dimorphism. Adult females are flat, with an oval-shaped body of approximately 1.1 mm long and 1.7 mm across, making them easily identifiable to the naked eye. The dorsal and ventral shields of mature females are highly sclerotized with a reddish-brown coloration. The male and immature female stages show only weak sclerotization (Fig. i.2C). The female body is dorsoventrally compressed, allowing the mite to fit beneath the bee's abdominal sclerites (Fig. i.2B), thus lessening water loss from transpiration; and hiding there reduces *Varroa's* vulnerability to grooming and to dislodgment during host activity. The male body is pear-shaped and is clearly smaller than females at any developmental stage (Fig. i.2C) (Rosenkranz et al., 2010; Sammataro et al., 2000). The females' chelicerae are structurally modified. The fixed digit is lacking, and the moveable digit is a saw-like blade capable of piercing and tearing the host's integument. Male chelicerae are also modified, but for sperm transmission in the copula (Rosenkranz et al., 2010). This is a brief summary of the distinctive features and sexual dimorphism of *V. destructor*. For a more detailed morphological description of *V. destructor*, see Anderson and Trueman (2000).

i.1.4. Taxonomy and classification of *Varroa* mites.

The family *Varroidae* includes two genera, *Varroa* and *Euvarroa*, both obligate ectoparasites of bees from the *Apis* genus. The genus *Varroa* and the species *Varroa jacobsoni* were named and first described by A. C. Oudemans in 1904, after he had received four adult female mites, found by Mr. Edward Jacobson in a colony of *Apis cerana javana* Fabr. (formerly called *A. indica* Fabr.) from Java, Indonesia (Oudemans, 1904). See annex I.1 for the complete taxonomic classification of *V. destructor*

The *Varroa* genus is currently represented by four species of obligate ectoparasitic mites:
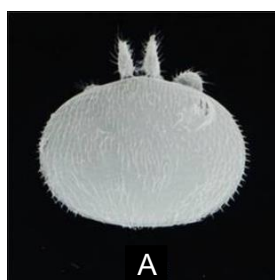
- ***Varroa jacobsoni*** (Oudemans, 1904) (Fig. i.3A). It infests five honey bee species throughout Asia and Indonesia, including *A. cerana, A. mellifera, A. koschevnikov, A. nigrocincta*, and *A. nuluensis*. It was found in the debris of *A. dorsara* in Malaysia (de Guzman and Delfinado-Baker, 1996; Delfinado-Baker et al., 1989; Koeniger et al., 2002; Otis and Kralj, 2001).
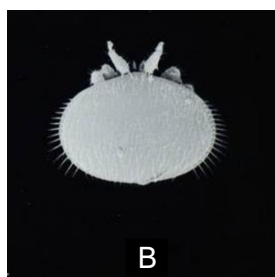
- ***Varroa underwoodi*** (Delfinado-Baker and Aggarwal, 1987) was first described parasitizing *A. cerana* in Nepal (Fig. i.3B).
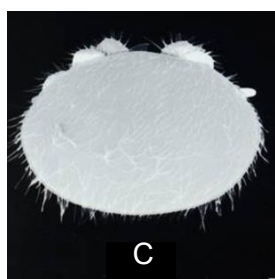
- ***Varroa rindereri*** (de Guzman and Delfinado-Baker, 1996) is only described in Borneo and restricted to *Apis koschevnikovi*, but was also collected from *A. dorsata* debris along with *V. jacobsoni* (Koeniger et al., 2002) (Fig. i.3C).
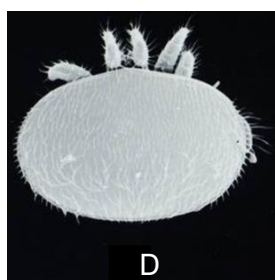
- ***Varroa destructor*** was described in both *A. cerana* (original host) and *A. mellifera* (new host). It was previously misidentified as *V. jacobsoni* until 2000 (Anderson and Trueman, 2000) (Fig. i.3D).

Figure i.3. Adult female appearances of the four species in the *Varroa* genus. Dorsal surfaces of adult females of *V. jacobsoni* (A), *V. underwoodi* (B), *V. rindereri* (C) and *V. destructor* (D). Scale bar approxiomately 500 µm. Figure adapted from Anderson and Trueman (2000).

i.1.5. *Varroa jacobsoni* and *V. destructor*: redefinition of sibling species

Initially, *V. destructor* mites were misclassified as *V. jacobsoni* since there are no clear morphological differences between the two species (Anderson and Trueman, 2000). However, evidence of differences in virulence and reproductive ability in *A. mellifera* (Anderson, 1994; Anderson and Sukarsih, 1996) suggested that *V. jacobsoni* may be more than one specie. Studies on the genotypic, phenotypic, and reproductive variation revealed that the so-called *V. jacobsoni* was, in fact, a species complex of 18 different genetic variants belonging to two reproductively isolated sibling species, the one originally described by Oudemans (1904) as *V. jacobsoni* and the newly named *V. destructor* by Anderson and Trueman (2000).
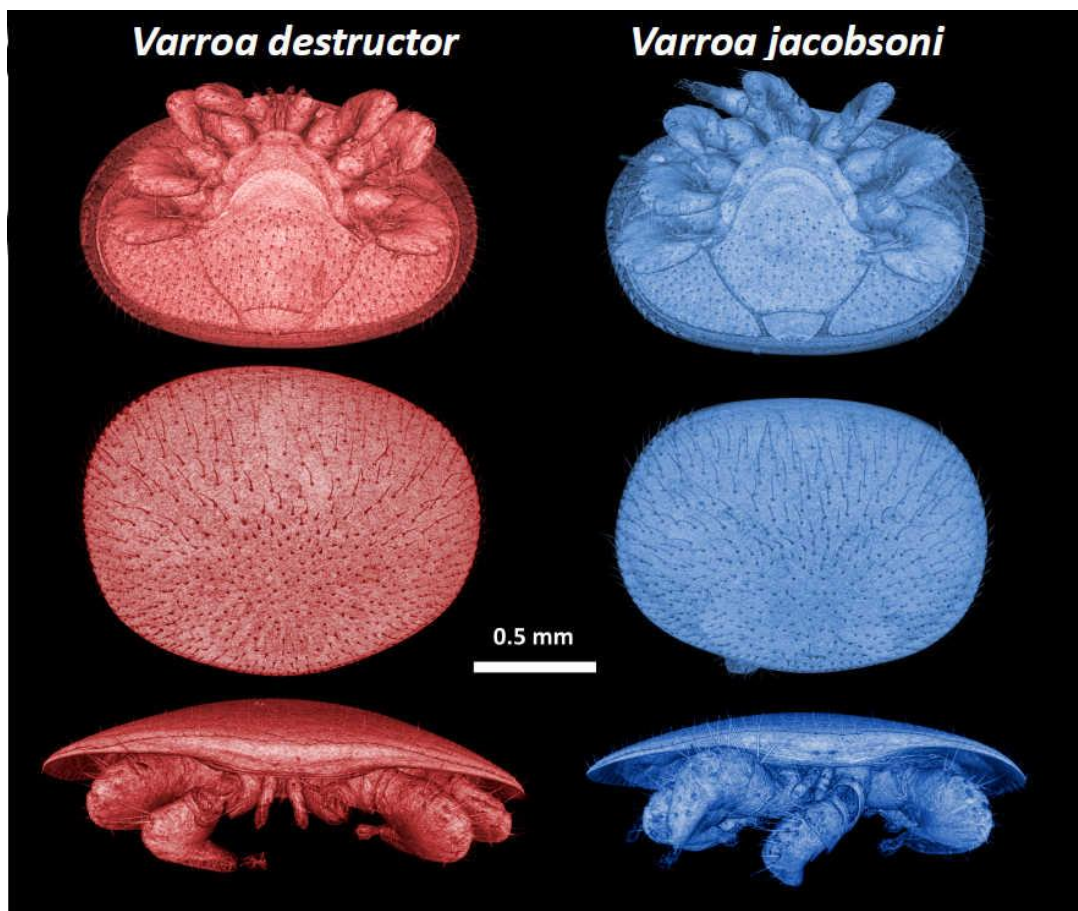
Figure i.4. A comparison of two adult females of the sibling species, *V. destructor* and *V. jacobsoni*. From top to bottom, ventral, dorsal and frontal view, respectively. Figure adapted from Techer et al. (2019).

INTRODUCTION

Body size and mitochondrial cytochrome oxidase I gene (*cox1* gene) sequences (GenBank database; *V. jacobsoni*: AF106902–AF106910; *V. destructor*: AF106897–AF106901) were used to redefine these species (Anderson and Trueman, 2000). The mitochondrial DNA (mtDNA) sequences for the cytochrome oxidase I gene differ by 6.4% between the sibling species, while the genetic distance for haplotypes within the same species is below 2% (Anderson and Trueman, 2000). Phenotypically, the members of both species are very similar, and it is challenging (often difficult) to distinguish them physically, but adult females of *V. destructor* are slightly larger and less spherical in shape than females of *V. jacobsoni* (Fig. i.4). The average body length and width is for *V. jacobsoni* are 1063.0 µm (± 26.4 µm) and 1506.8 µm (± 36.0 µm) respectively, and 1167.3 µm (± 26.8 µm) and 1708.9 µm (± 41.2 µm) for *V. destructor* (Anderson and Trueman, 2000).

The virulence towards *A. mellifera* of *V. jacobsoni* and *V. destructor* is not uniform, as is that of their haplotypes. At least nine haplotypes are described for *V. jacobsoni* and seven for *V. destructor* (Anderson and Trueman, 2000; Navajas et al., 2010), based on a 458 bp fragment of the mitochondrial *cox1* gene. This variation is higher when more sensitive markers are used, consisting of 2700 base pairs of concatenated sequences of the mitochondrial genes *cox1*, *cox3*, *atp6* and *cytb*, finding 18 sub-haplotypes for *V. destructor* only in Asia (Navajas et al., 2010). More recently, two novel haplotypes, the Serbia 1 (S1), and Peshter 1 (P1), were described infecting *A. mellifera* colonies in Serbia; differing from the original K1 haplotype (see below) in single nucleotide polymorphisms (SNPs) within cytochrome c oxidase 1 (*cox1*) and cytochrome b (*cytb*) (Gajic et al., 2013). *Varroa destructor* haplotypes were named after the population where they were first described: China 1 (C1), China 2 (C2), China 3 (C3), Japan-Thailand 1 (J1), Korea 1 (K1), Vietnam 1 (V1), Nepal (N1), Serbia 1 (S1), and Peshter 1 (P1) (GenBank accession numbers: C1: AF106900, C2: AY372063, C3: GQ379068, J1: AF106897, K1: AF106899, V1: AF106901, N1: AF106898, S1: JX970938, and P1: JX970939) (Anderson and Trueman, 2000; Gajic et al., 2013; Navajas et al., 2010).

Only two out of the eight haplotypes described for *V. destructor* can reproduce on *A. mellifera*, the Japan-Thailand (J1) and the Korean (K1) haplotypes. The other six haplotypes are unable to reproduce successfully in *A. mellifera*, and hence they are just temporary inhabitants (vagrant guests) in their colonies (Anderson and Sukarsih, 1996; Anderson and Fuchs, 1998; Roberts et al., 2015). Like those latter, *V. jacobsoni* does not

reproduce in *A. mellifera* (Rosenkranz et al., 2010). Recently, though, a population of *V. jacobsoni* was found breeding on *A. mellifera* in Papua New Guinea (Andino et al., 2016; Roberts et al., 2015). Haplotypes J1 and K1 can reproduced on *A. cerana* and *A. mellifera* worker brood, but K1 shows better fecundity in the new host than in the original host (Li et al., 2019b). Mites of the K1 haplotype are considered more virulent and have globally spread on *A. mellifera*. Besides, mites of the J1 haplotype have a more restricted distribution, having only been reported in Japan, Thailand, and North and South America (Anderson and Trueman, 2000; de Guzman et al., 1999; Garrido et al., 2003); but apparently, they are being displaced in some regions by mites of the K1 haplotype (Garrido et al., 2003; Octaviano-Salvadé et al., 2017). This, together with the lower frequencies found for the J1 haplotype mites, suggests a lower reproductive success for the K1 haplotype (Beaurepaire et al., 2019b). Genetic differentiation within the two haplotypes in worldwide populations is highly difficult, with almost no polymorphism, and considered to have a quasi-clonal population structure (Navajas et al., 2010; Solignac et al., 2005; Solignac et al., 2003). Presumably reflecting the effect of the strong bottlenecks tied to host-shift events and the subsequent rapid expansion around the world, along with its reproductive traits (see below) (Solignac et al., 2005; Techer et al., 2019). In summary, the only mite of economic importance is *V. destructor*, and the studies about *Varroa* in *A. mellifera* from the last century refer to *V. jacobsoni*, although *V. destructor* was the subject (Rosenkranz et al., 2010).

i.1.6. Host-shift and worldwide dispersion

Before the human-mediated movement of honey bees, there was no geographical area of contact between *A. mellifera* and *A. cerana*, the original host of *V. destructor* (see Fig. i.1, p.38). The first observations of *Varroa* mites parasitizing *A. mellifera* were reported a few years after its introduction into Asia for commercial purposes. Despite this, the details of the host shift are unknown, but it most likely occurred during the first half of the twentieth century, when both species become close in contact, possibly through mutual robbing or beekeeping practises (De Jong et al., 1982b).
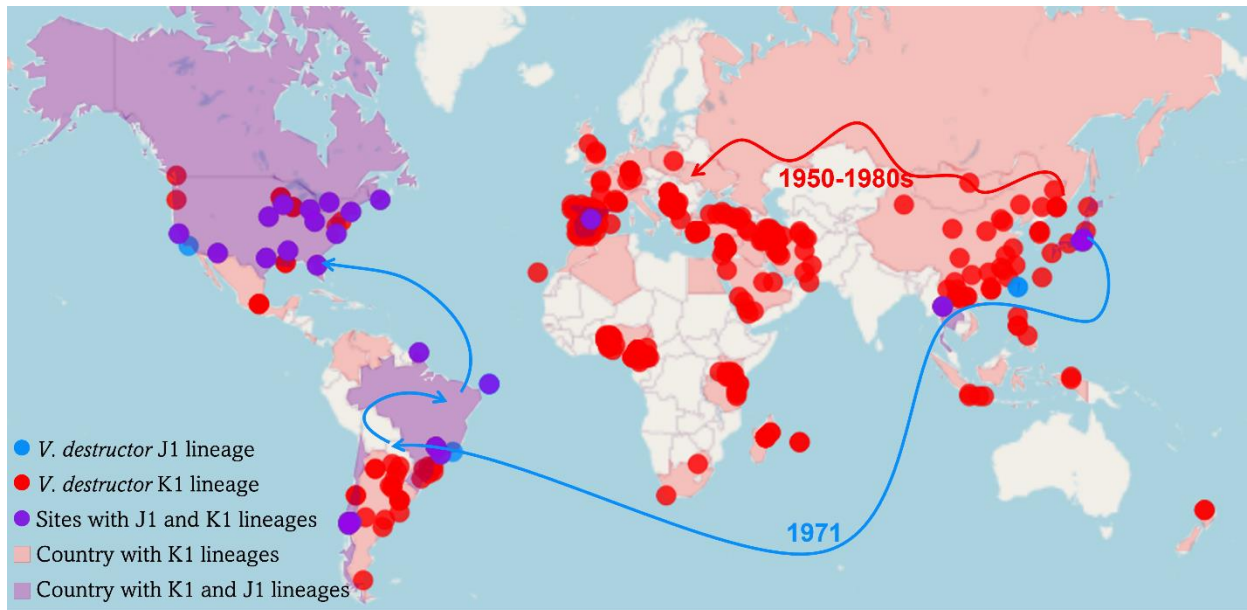
Figure i.5. The global distribution of *V. destructor* Japan-Thailand (J1) and Korean (K1) haplotypes parasitising *A. mellifera*. Colored points indicate the locations reported by literature and the GenBank database for K1 and J1 haplotypes of *V. destructor* on *A. mellifera*. The arrows indicate the directions of dispersal of the K1 and J1 haplotypes from their region of origin after the host change to *A. mellifera*. Figure adapted from Traynor et al. (2020). Interactive map: https://mikheyevlab.github.io/varroa-mtDNA-world-distrib/

It seems likely that the switch of *V. destructor* to the new host occurred with success at least twice, in parallel events, leading to the K1 and J1 haplotypes (Anderson and Trueman, 2000; Navajas et al., 2010). Probably, the J1 first shifted from *A. cerana* to *A. mellifera* in Japan, after the introduction of the latter in 1957 (Sakai and Okada, 1973). It spread on *A. mellifera* into Thailand and Paraguay (1971), and then into Brazil, North America (1987), and other south America countries (Fig. i.5) (Anderson and Trueman, 2000; de Guzman et al., 1999). In the USA, *V. destructor* was first detected in late September 1987 in hives transported from Florida after these experienced sudden declines in colony size. A further national survey revealed the presence of *Varroa* in the states of Maine, New York, Rhode Island, Pennsylvania, Ohio, Michigan, South Dakota, Nebraska, Illinois, Wisconsin, Florida, and Mississippi. By 1995, *V. destructor* was widespread across the USA, assisted by the distribution of queen and package bees, as well as the movement of colonies for pollination services and over-wintering (Wenner and Bushing, 1996).

The K1 haplotype is thought to have shifted from *A. cerana* to *A. mellifera* in the Ussuria region, near Vladivostok (former Soviet Union, north of the Korean peninsula) following the introduction of *A. mellifera* from Ukraine during the late 1950s (Crane, 1978). *Apis mellifera* colonies, or queen packages, were exported from Ussuria to geographically distant places, such as the Caucasus, and from there to Bulgaria, Romania, and Tunisia, with the subsequent spread of *V. destructor* to Pakistan (1955), China (1959), Bulgaria (1967), and from Europe in the 1960s (Germany (1977), Czechoslovakia (1978), France in the 1980s) to around the world, arriving in America and Africa (Fig. i.5) (Crane, 1978; de Guzman et al., 1997; Kamler et al., 2016; Oldroyd, 1999; Ruttner and Ritter, 1980; Sammataro et al., 2000). On the webpage of the Invasive Species Compendium (www.cabi.org) an extensive table of country distribution and the associated reference can be found. An interactive map of *Varroa* haplotype distribution can also be found at http://mikheyevlab.github.io/varroa-mtDNA-world-distrib/ .

It was around the 1950s and 1960s that *Varroa* became an economic concern, causing severe damage to *A. mellifera* colonies in Japan and China, followed by Europe in the late 1960s and 1970s, and Israel and North America in the 1980s (Sammataro et al., 2000). Aided by honey bee commerce and trade, *V. destructor* has spread almost worldwide within a short time period, changing worldwide beekeeping profoundly. Today, only a handful of *A. mellifera* populations in the world are not infested by *V. destructor*, and it may be difficult to find a "*Varroa*-free" honey bee colony anywhere. Most of these are on small islands with small-scale beekeepers. Meanwhile, Australia is the exception to the global *Varroa* crisis. This country has a large commercial-scale beekeeping industry but remains free of *V. destructor* thanks to the exhaustive control of its borders (AQIS, Australian Government: http://www.daff.gov.au/aqis/quarantine/pests-diseases/honeybees).

i.1.7. Life cycle and reproductive characteristics

Members of the genus *Varroa* are obligated parasites, lacking a free-living stage, with a life cycle closely linked to their host. The life cycle of *Varroa* females is divided into two phases: the reproductive phase, inside the sealed brood cell, and the dispersal phase, also called the phoretic phase, on adult honey bees. A female mite can normally complete two to three of these cycles during her lifetime (Fries and Rosenkranz, 1996).

Varroa males and female nymphal stages are short-lived and can only be found in sealed brood cells and never as phoretic mites.

The reproductive phase takes place exclusively inside the capped brood cells of the honey bee host, and therefore is highly dependent on brood availability (Beaurepaire et al., 2017). No brood equals no mite breeding. The gonotrophic cycle of *V. destructor* has been suggested to be influenced by the hormonal milieu of the host (Beetsma and Zonneveld, 1992). Besides, mites show a marked preference for drone brood cells as the drone brood produces a kairomone (a compound, analogous to a hormone, secreted by an individual of one species that modifies the behaviour of individuals of another species) that is more attractive to the mite than that produced by the worker brood. Also, fecundity is higher in drone cells than in workers, maybe due to their larger post-capping period (15 days for drones, vs. 11 days for workers) (Boot et al., 1992). Nonetheless, drone broods are much less available as they are reared only during the swarming season, and their cell numbers are always lower than those of workers. *Varroa* mites do not reproduce in queen cells because of the repellence of royal jelly and the short post-capping stage (7 days) (Calderone et al., 2002).

The reproductive phase starts when adult females of *V. destructor* (a "foundress" mite) slide into a brood cell of advanced larval stages before nurse bees seal the cell with a wax capping (Fig. i.6); around 20 hours before for worker bees and 40 hours before for drone brood (Beetsma et al., 1999; Beetsma and Zonneveld, 1992). Mites find drone honey bee brood significantly more attractive to breed in than worker brood, giving rise to multiple infestations of the same cell. The mite slides past the bee larva to the bottom of the cell and becomes immobile, immersed (sinks itself into) in the larval food, which remains unnoticed, exposing only the peritremes (breathing tubes). Only after the cell has been sealed and the larva has consumed the food, the mite is released (Ifantidis, 1988). Then, the mite moves onto the immature bee. Using the chelicera, it perforates the soft portions of the host's integument, making a single feeding hole through which it will suck feed from the developing bee larvae's fat body (Calderón et al., 2009; de Lillo et al., 2001; Li et al., 2019a; Ramsey et al., 2019). The feeding wound is relatively large (around 100 μm) (Kanbar and Engels, 2004; Ramsey et al., 2019), and remains open via suppression of host healing by anti-coagulant proteins found in the mites' saliva (Becchimanzi et al., 2020; Richards et al., 2011). This single feeding hole would be used repeatedly and communally
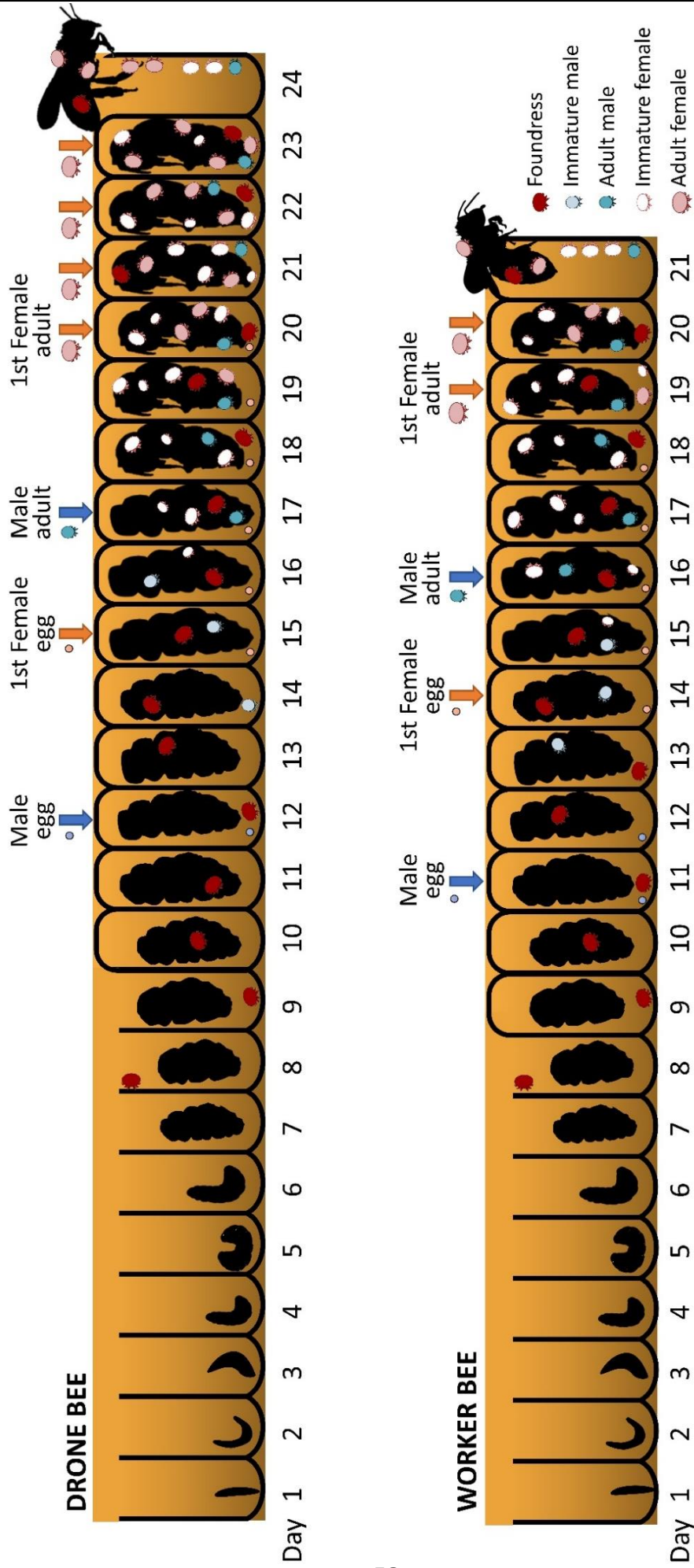
Figure i.6. *Varroa destructor* reproductive cycle in honey bee drones and workers. *Varroa* reproduces in capped cells of developing honey bees.

by the mother mite and her progeny residing in the same capped cells (Calderón et al., 2009; Egekwu et al., 2018; Kanbar and Engels, 2005; Li et al., 2019a). *Varroa* mites do not show particular preference for any body part to create the feeding hole, while the host is on the prepupae stage (Calderón et al., 2009), but on adult bees, mites show a strong preference for the underside of the abdomen metasoma (Egekwu et al., 2018; Ramsey et al., 2019). About 60 hours after the brood cell has been sealed, the mother mite produces the first egg, which is usually haploid (7 chromosomes) and develops into a male. Subsequent eggs laid at 24-30-hour intervals are diploid (14 chromosomes) and develop into females (Ifantidis, 1983). The actual timing may vary due to external factors. In a regular reproductive cycle, up to five and six eggs are laid in the worker brood and drone brood, respectively (Fig. i.6) (Garrido et al., 2003; Martin, 1994; Rosenkranz et al., 2010). The development from larva to adult mite occurs through two nymphal stages. The mite larva (6-legged) develops inside the egg, hatching into a protonymph (8-legged), that moults into a deutonymph and finally to the adult form (Delfinado-Baker, 1984) (see Fig. i.2, p.39). Around 6 days after oviposition, the offspring become mature and begin to mate inside the sealed brood; approximately the tenth day after capping for the son and first daughter (Rehm and Ritter, 1989). Matting is triggered by a female sex pheromone perceived by the male via tarsal sensory pits (Häußermann et al., 2015; Ziegelmann et al., 2013). The male mates with his sisters multiple times. Nevertheless, males prefer freshly moulted females, which emit the sex pheromone more strongly (Häußermann et al., 2020). This way, it is ensured that all mature females have been fertilised before leaving the cell. After the copula, the spermatozoa are stored inside the spermatheca of female mites, where they will undergo a further maturation process before being able to fertilize oocytes, the so-called capacitation, which takes about 5 days (Alberti and Hänel, 1986; Häußermann et al., 2020; Häußermann et al., 2016).

Adult bee workers and drones emerge around 11 and 15 days after cell capping, respectively, and adult female mites leave the cell attached to them (Fig. i.6). On average, besides the mother, one or two adult daughters emerge from a worker brood (1.30–1.45 adult female) cells and up to three or four daughters from a drone brood cells (Martin, 1994; Rehm and Ritter, 1989). Only adult female mites are able to survive outside the brood cell, in contrast to younger and more sensitive immature stages like protonymphs and deutonymphs. Likewise, male mites are unable to feed by themselves since their chelicerae (the structure that permits active feeding on the honey bee host) are modified

for sperm transfer, and die soon after the emergence of the honey bee host (Delfinado-Baker, 1984).

The adult females stay on the young host bee until they enter a brood cell to reproduce, starting a new cycle. Emerged female mites usually remain in the phoretic phase for 1 to 13 days on the same adult bee, or they can move to another worker or drone bee (Beetsma et al., 1999; Martin, 1998; Xie et al., 2016). Generally, mother mites or foundresses have been fertilised when they enter the brood cell. Nonetheless, recent studies have demonstrated that virgin female mites are also capable of occasionally producing haploid males and mating with their sons (oedipal mating). However, the fecundity and offspring resulting from oedipal mating is reduced (Häußermann et al., 2020). Consequently, the sex in *V. destructor* is determined by arrhenotokous parthenogenesis (female mites can produce offspring without a previous mating), even though the parthenogenetic reproduction is not very frequent (Häußermann et al., 2020).

In zoology, the term "phoretic" refers to a non-permanent interaction in which one organism attaches itself to another solely for the purpose of travel, without causing harm (Houck and OConnor, 1991; White et al., 2017). However, in the case of *Varroa* mites, this is not used in the *sensu stricto* since *Varroa* feeds on the adult bee during its phoretic phase (Ramsey et al., 2019). When on adult bees, *Varroa* females usually hide under the sternites of the bee (Beetsma, 1994; Ramsey et al., 2018), to prevent being noticed when transported to a new brood cell for reproduction or to limit the possibility of falling during flight, when moving to new bee colonies (Kuenen and Calderone, 1997) (see Fig. i.2, p.39).

i.1.8. Spread of *Varroa* mites to different honey bee colonies

Varroa mites are wingless and unable to crawl between spaced honey bee colonies. Despite these limitations, they have a great potential for dispersal, first through host honey bees and then through human-mediated movement for trade and pollination (Sammataro et al., 2000). It is clearly evidenced by their worldwide distribution within a few decades and almost ubiquitously infested honey bee colonies. Even managed colonies successfully treated against *V. destructor* are at risk of re-invasion in a short period of time (Frey and Rosenkranz, 2014; Frey et al., 2011; Greatti et al., 1992).

Drones as well as workers are used for the dispersal of *Varroa* mites in their phoretic phase. The mites can be transferred between bee colonies either directly, from bee to bee, or indirectly, when a mite drops from their host to a neutral location, such as a flower, waiting for a new host. Adult mites are quite capable of living for more than five days without the presence of honey bees, but the indirect transmission is unlikely to move a large number of mites between colonies (Peck and Seeley, 2019). *Varroa* mites are very agile and fast in their movement and can move among nearby bees as they pass by. Thus, it is likely that most mite transmission occurs directly when a bee flies between its nest and another colony's nest while carrying a mite (Peck and Seeley, 2019).

❖ **Bee and human behaviours contributing to *Varroa* dispersal to new colonies:**

Foraging   By visiting blossoms to collect nectar and pollen, worker bees can meet other bees. Also, *Varroa* mites can step off and wait for a new host bee to arrive at the flower (Peck et al., 2016).

Robbing   When a bee enters another colony to steal honey and nectar. Weak colonies are targets for robbers, such as bees from another colony, which take advantage of the vulnerability of the colony to loot their honey and nectar, also taking phoretic mites with them.

Drifting   Sometimes worker or drone bees leave their natal nest and travel to another nearby colony, sometimes by disorientation, carrying the mites with them. This is particularly important for drones that are accepted into colonies for queen mating. Premature foraging on parasitised bees, before the full development of their orientation faculties increases the incidence of these bees drifting to nearby apiaries because of disorientation (see section i.1.10, p.53) (Bowen-Walker and Gunn, 2001).

Migration   Bees from collapsing colonies escape from their own hive and find other colonies.

Swarming   A swarm from an infested colony will always carry mites with it. Swarms from feral colonies can spread the mite naturally by 3-5 km per year.

Beekeepers   Manipulative management by the beekeeper can transfer affected bees to other colonies in the apiary or to other apiaries. Migratory beekeeping can cause a rapid spread across large distances.

i.1.9. Low genetic diversity in the *Varroa* population infecting *A. mellifera*

The genetic diversity of *V. destructor* outside Asia, its natural geographical range, is very low. Mitochondrial and microsatellite DNA studies revealed almost no genetic variation within the two main *V. destructor* haplotypes that infest *A. mellifera* colonies worldwide, being those almost clonal populations (Anderson and Trueman, 2000; Solignac et al., 2005). This quasi-clonal population worldwide is attributed to the rapid geographical spread preceding the strong genetic bottlenecks undergone during the host shift, combined with their intense inbreeding behaviour.

Its reproductive characteristics, including male haploidy and full sibling mating in the sealed brood cells, result in extreme inbreeding with no genetic exchange among lineages in the population as long as a single female mite infests a cell. Apart from mutation, the only mechanism for introducing variation in a *Varroa* population is by admixture of different lineages. Population admixture can occur only when two genetically dissimilar mites co-invade a brood cell and the non-sibling offspring of the foundresses may mate (Fuchs and Langenbach, 1989). This phenomenon is more prone to happening latter in the season (summer and fall) as the mite population in the hive increases and the available brood decreases, and foundress mites inevitably have to co-infect cells for reproduction. At the beginning of the brood season, when the number of brood cells available is higher than the number of mites in the colony, the cells will typically be infected by single foundresses (single infestation), and mating will occur between the offspring of this mite. Eventually, as a result of the more frequent incestuous mating, multiple lineages of highly inbred mites would coexist in the colony. However, as the season progresses, the mite population grows and the proportion of mites per brood cell rises. Then, random cell invasion by multiple foundresses ("multiple infestations") becomes more frequent, increasing the probability of progeny mixing up (Beaurepaire et al., 2019a). In addition, the mite population in a hive is not completely closed off, receiving the influx of foreign mites carried by worker drifting and drones, particularly towards the end of the season. The introduction of new mite lineages from different colonies would increase the heterozygosity beyond the plain recombination of the resident mite lineages. At this point, the level of heterozygosity in the colonies would increase (Beaurepaire et al., 2017; Calis et al., 1999). In short, the dynamic genetic structure of the mite population in a hive is characterised by a drastic drop in heterozygosity at the beginning of the brood

season, followed by an increase of recombination toward the end of the season (Beaurepaire et al., 2019a; Beaurepaire et al., 2017).

It is thought that the main factor responsible for the rapid adaptation of the mite to its host is the strong selective forces guided by antagonistic co-evolution (Beaurepaire et al., 2019b; Paterson et al., 2010; Thrall et al., 2012). Genetic diversity is a key component in the antagonistic co-evolution race between host and parasites (Ebert and Fields, 2020; Nee, 1989). Despite the reduced genetic diversity in *V. destructor* populations, the adaptation of the mite in response to its host and the environment is widely proven. Examples such as the ability of the mite to acquire resistance to acaricide treatments show how quickly populations of this parasite can adapt to selection pressures. Gene flow among colonies is an important factor in the population dynamics of *V. destructor*. The drift of mites among colonies ensures the presence of a high number of different lineages in all colonies in the apiary. Selection will act on these different lineages, promoting the best adapted ones, and high inbreeding will facilitate the fixation of selected alleles by increasing the homozygous state in the progeny. In the case of acaricide resistance, the inbreeding will result in more resistant mites in the colony (see below). Therefore, the strong endogamy that could limit the probability of recombination of different linages and the introduction of genetic variability in the population, could also be of high adaptative value, accelerating the fixation of beneficial alleles.

i.1.10. Effect of *V. destructor* parasitism on honey bees

Varroa mites and *A. cerana* co-evolved together, implying a mutual co-adaptation to the selective forces exerted by each other (Rath, 1999). The Asian honey bees cope well with this parasite and the impact of *Varroa*'s parasitism is minimal on the colony (Chantawannakul et al., 2016). Conversely, in evolutive terms, *V. destructor* is a new parasite for *A. mellifera*. Therefore, a balanced host–parasite relationship is lacking (so defensive behaviour is poorly developed), and beekeepers do not have long-term experience in dealing with this pest. The effect of *V. destructor* parasitism on *A. mellifera* colonies is so detrimental that its introduction has eclipsed the impact of other relevant honeybee parasites on bees, such as tracheal mites (Sammataro et al., 2000).

In its original host, *A. cerana*, *V. destructor* breeds exclusively on drones brood (Harris and Harbo, 2000; Roberts et al., 2015). In contrast, *V. destructor* infesting *A. mellifera*

colonies can reproduce successfully on worker as well as on drone brood, being largely invasive into the hives (Rosenkranz et al., 2010). Undoubtably, the ability to reproduce in worker brood emerges as a critical adaption to the new host, increasing significantly the growth potential of the *V. destructor* population, as well as causing much greater damage to the health and production capacity of *A. mellifera* colonies (De Jong, 1988). In addition, *A. cerana* exhibits remarkable behavioural defences against phoretic and reproducing mites that have been proven essential factors in limiting mite populations within the colony to tolerable levels. This is also called "hygienic behaviour" or "*Varroa* sensitive hygiene" and includes: **(a)** grooming, which involves the removal and killing of phoretic mites from adult bees (Büchler et al., 1992; Peng et al., 1987; Pritchard, 2016; Rath, 1999); and **(b)** the detection of parasitized brood followed by the uncapping and removal of the mites (Boecking and Spivak, 1999; Carreck, 2011; Rinderer et al., 2010), or conversely, **(c)** the "entombing" of parasitized brood cells beneath propolis, and consequently the non-emergence of both bee and parasites (Rath, 1999). The hygienic behaviour has also been observed at variable intensity in some subspecies of *A. mellifera*, but is poorly developed (less intense) when compared to *A. cerana* (Boecking and Spivak, 1999; Božič and Valentinčič, 1995; Büchler et al., 2010; Büchler et al., 1992; Guzman-Novoa et al., 2012; Morais et al., 2009; Pritchard, 2016). Rearing *A. mellifera* strains performing *Varroa*-tolerant behaviour is considered the most sustainable and long-term possible solution to the *Varroa* problem (Beetsma, 1994; Dietemann et al., 2012; Hunt et al., 2016). Even so, efforts to breed a productive and *Varroa*-tolerant honey bee stock may take decades to become commercially available (Jack and Ellis, 2021).

In *A. mellifera*, the physical and physiological effects triggered by *V. destructor* parasitism on individual bees and on the colony as a whole have been extensively investigated in an attempt to clarify why this parasite is so devastating. On the one hand, the direct effect of the parasitism is caused by feeding on the fat body of adults and immature bees (Ramsey et al., 2019). Until recently, *Varroa* mites were assumed to be haemolymphagous parasites; therefore, all literature to date refers to *Varroa* feeding on haemolymph. Likewise, the harmful effect of parasitism was thought to be largely based on the infection by secondary pathogens. However, in 2019, Ramsey *et al.* demonstrated that *V. destructor* feeds on fat body tissue, entailing more direct damage to the bee. The diverse array of debilitating pathologies observed in parasitized bees is better explained by the fat body intake rather than that of haemolymph (Table i.1) (Ramsey et al., 2019).

Moreover, it has been demonstrated that there is a direct correlation between the intensity of the detrimental effect on the bee with the number of mites parasitizing it and hence the amount of fat body tissue ingested (Beetsma, 1994; De Jong et al., 1982a; Duay et al., 2003).

Table i.1. The primary function of the fat body in honey bees and the pathologies related to these functions resulting from *Varroa* parasitism. Adapted from Ramsey *et al.* (2019).

FAT BODY FUNCTION	Associated pathology reported in *A. mellifera* parasitized by *V. destructor*
Regulation of growth, development and metamorphosis (Amdam et al., 2003; Arrese and Soulages, 2010; Martins et al., 2008; Stell, 2012)	Stunted growth, malformed organs, precocious foraging (Amdam et al., 2004; Bowen-Walker and Gunn, 2001; Rosenkranz et al., 2010)
Nutrient storage and mobilization (Arrese and Soulages, 2010; Bordier et al., 2017; Martins et al., 2008)	Inability to replace and store amino acids; reduction in amino acid and carbohydrate levels (Bowen-Walker and Gunn, 2001; van Dooremalen et al., 2013)
Protein and lipids synthesis (Arrese and Soulages, 2010; Locke, 1980)	Decrease in lipid and amino acid production (Amdam et al., 2004; Bowen-Walker and Gunn, 2001)
Production of antimicrobial peptides (Arrese and Soulages, 2010)	Diminished immune response (Amdam et al., 2004; Erban et al., 2019; Nazzi et al., 2012)
Regulation of metabolic activity (Arrese and Soulages, 2010; Bordier et al., 2017)	Reduction in oxidative phosphorylation and overall metabolic rate (Bowen-Walker and Gunn, 2001; Erban et al., 2019)
Pesticide detoxification (Chan et al., 2013; Locke, 1980)	Increased susceptibility to pesticides (Blanken et al., 2015; Drescher and Schneider, 1988; van Dooremalen et al., 2018)
Osmoregulation (Arrese and Soulages, 2010; Cohen, 2013)	Increased water loss and associated weight loss (Annoscia et al., 2012; Bowen-Walker and Gunn, 2001)
Thermoregulation (Arrese and Soulages, 2010; Locke, 1980)	Greater overwinter mortality (Amdam et al., 2004; van Dooremalen et al., 2012)
Vitellogenesis (Amdam et al., 2003; Arrese and Soulages, 2010; Nilsen et al., 2011)	Reduction in vitellogenin titers; decreased lifespan; increased overwinter mortality (Amdam et al., 2004)

The fat body is the primary organ for the synthesis and storage of proteins and lipids. It also regulates the metabolism and takes part in thermoregulation (Arrese and Soulages, 2010). Parasitized bees are less able to replace and store amino acids. The synthesis of lipids and proteins is also hampered. They show increased loss of water and

also a higher metabolic rate (Beetsma, 1994; Bowen-Walker and Gunn, 2001; De Jong et al., 1982a; Duay et al., 2003; Ramsey et al., 2019).

In holometabolic insects, the fat body plays a crucial role during the maturation process, as it stores the macromolecules resulting from the disintegration of the larval organs and slowly releases them to form the adult organs during the pupal stage (Stell, 2012). This step is critical in the development of the adult bee, and also coincides with the time when the parasitism of *Varroa* is most acute, strongly impacting the future of the colony. Inside the brood cells, the developing bees are parasitized by one, or sometimes more, foundress mites and their progeny, that feed on their fat body hampering the metamorphosis, resulting in impaired development, malformed organs, reduced weight and health implications, and a consequently shorter lifespan (Beetsma, 1994; Bowen-Walker and Gunn, 2001; De Jong and De Jong, 1983).

The fat body in insects also plays a leading role in pesticide detoxification by absorbing and sequestering harmful xenobiotics. Recent work showed that parasitized honey bees were more vulnerable to the effect of neonicotinoids than non-parasitized bees (Blanken et al., 2015). Besides, the fat body is an essential organ for the immune response, producing and storing antimicrobial peptides and vitellogenin. The latter is responsible for the reduction of oxidative stress, extending considerably the lifespan of the bees during the winter (Amdam et al., 2004; Amdam et al., 2003).

The suppression of immune activity is directly related to the most destructive effect of *Varroa* mites on honey bees, because they are capable of vectoring an extensive set of honey bee viruses (Table i.2), as well as activating dormant viruses (Beaurepaire et al., 2020; Chen and Siede, 2007; Gisder and Genersch, 2017; Grozinger and Flenniken, 2019; McMenamin and Flenniken, 2018). So far, more than 20 viruses have been identified infecting honey bees, predominating the positive sense single-stranded RNA viruses (+ssRNA) from the order Picornavirales. The recent advances and affordability of next-generation sequencing technologies have boosted the discovery of unnoticed bee-associated viruses, revealing that the vast majority are cryptic viruses, and only a small

Table i.2. Viruses infecting *A. mellifera* that have been related to *Varroa*-mediated transmission. Reviewed in Beaurepaire et al. (2020); McMenamin and Genersch (2015); Yañez et al. (2020). +: transmission confirmed; Sugg.: transmission suggested but non-demonstrated; unclear: unclear.

	Apis mellifera virus	Abbr.	Family	*Varroa* vector status	
	Black queen cell virus	BQCV	*Dicistroviridae*	unclear	(Bailey and Woods, 1977; Beaurepaire et al., 2020)
AKI complex	Acute bee paralysis virus	ABPV	*Dicistroviridae*	+	(de Miranda et al., 2010)
	Kashmir bee virus	KBV	*Dicistroviridae*	+	(Shen et al., 2005a)
	Israeli acute paralysis virus	IAPV	*Dicistroviridae*	+	(Di Prisco et al., 2011)
DWV clade	Deformed wing virus	DWV	*Iflaviridae*	+	(Santillán-Galicia et al., 2010; Shen et al., 2005a)
	Varroa destructor virus-1	VDV-1	*Iflaviridae*	+	(Ongus et al., 2004)
	Kakugo virus	KV	*Iflaviridae*	+	(Fujiyuki et al., 2006)
(Serologically related to DWV)	Egypt bee virus	EBV	*Iflaviridae*	Sugg.	(Bailey et al., 1979; Beaurepaire et al., 2020)
	Sacbrood virus	SBV	*Iflaviridae*	Sugg.	(Beaurepaire et al., 2020; White, 1913)
	Slow bee paralysis virus	SBPV	*Iflaviridae*	+	(Santillán-Galicia et al., 2014)
	Apis mellifera filamentous virus	AmFV	*Baculoviridae*	unclear	(Bailey et al., 1981; Gauthier et al., 2015)
	Apis iridiscens virus	AIV	*Iridoviridae*	unclear	(Bailey et al., 1976)
	Bee macula-like virus	BeeMLV	*Tymoviridae*	+	(de Miranda et al., 2015)
	Varroa tymo-like virus	VTLV	*Tymoviridae*	+	(de Miranda et al., 2015)
	Apis/Bee rhabdovirus-1	ARV-1/BRV-1	*Rhabdoviridae*	Sugg.	(Levin et al., 2017)
	Apis/Bee rhabdovirus-2	ARV-2/BRV-2	*Rhabdoviridae*	Sugg.	(Remnant et al., 2017)
	Varroa orthomyxovirus-1	VOV-1	*Orthomyxoviridae*	+	(Levin et al., 2019)
	Tobaco ring spottled virus	TRSV	*Secoviridae*	+	(Li et al., 2014)
	Chronic bee paralysis virus	CBPV	unclassified	Sugg.	(Olivier et al., 2008)
	Cloudy wing virus	CWV	unclassified	Sugg.	(Carreck et al., 2010a; 2010b)

proportion of them cause disease (Deboutte et al., 2020; Grozinger and Flenniken, 2019; McMahon et al., 2015). The longest-known bee-infecting viruses of concern are those that are revealed through symptomatic infections, affecting either the morphology (DWV, CWV, AmFV, AIV), the development (SBV, BQCV) or the behaviour of the host (CBPV, ABPV, SBPV, IAPV) (Geffre et al., 2020). In acute infections, some of these viruses can

dramatically impact both the individual and colony levels (de Miranda and Genersch, 2010). It is worth highlighting the impact of viruses of the Deformed Wing Virus clade and the Acute Bee Paralysis Virus complex (**A**BPV, **K**BV and **I**APV, also called the AKI-complex). The co-pathogenic interaction of these viruses and *V. destructor* is thought to be a key driver of the recent increase in colony losses (de Miranda et al., 2010; de Miranda and Genersch, 2010; McMenamin and Genersch, 2015; Posada-Florez et al., 2019). It is most notably that, in the absence of *V. destructor* parasitism, these viruses co-exist with honey bees as covert infections without triggering any apparent negative impact on host fitness and, therefore, no major issues for apiculture (Grozinger and Flenniken, 2019; McMenamin and Genersch, 2015; Roberts et al., 2017; Shen et al., 2005b; Stanimirović et al., 2019). Immunosuppression induced by the feeding of mites leads to a raise in pre-existing viral titres and disease outbreak (Ball and Allen, 1988; Francis et al., 2013; Nazzi et al., 2012; Yang and Cox-Foster, 2007). Consequently, symptomatic and overt infection outbreaks are generally displayed when *V. destructor* is parasitizing honey bees (de Miranda and Genersch, 2010; Gauthier et al., 2007; Locke et al., 2017; Locke et al., 2021; Roberts et al., 2017; Roberts et al., 2020; Staveley et al., 2014; Sumpter and Martin, 2004; Thaduri et al., 2019). With the introduction and dispersion of *V. destructor*, the prevalence and pathogenicity of these viruses increased significantly, with the mite acting as a viral reservoir and incubator, allowing direct transmission into the bees and bypassing conventional transmission routes (Beaurepaire et al., 2020; Gisder et al., 2009; Sumpter and Martin, 2004; Wilfert et al., 2016). In addition, the global spread of *V. destructor* has led to the co-occurrence of viruses that did not exist in sympatry (Beaurepaire et al., 2020; Wilfert et al., 2016).

At the colony level, *Varroa* parasitism disrupts the homeostatic system of the colony as a superorganism. Honey bees, like many social insects, display a well-established hierarchical pattern of behavioural development that regulates the colony's division of labour (Seeley, 1989). They begin adult life performing in-hive tasks (nurse bees), and delay leaving the nest to forage until later in adult life (Robinson, 1987; Winston, 1991). The transition from nursing to foraging is regulated nutritionally and socially. Therefore, if the colony suffers from a loss of foragers or colony starvation, young bees will accelerate their behavioural development and start foraging precociously (Huang and Robinson, 1996; Leoncini et al., 2004a; Leoncini et al., 2004b; Toth and Robinson, 2005). Similarly, it has been documented that the earlier onset of foraging on bees parasitized on the brood is probably because of the reduction in lipid content, which is also characteristic

of older bees (Bowen-Walker and Gunn, 2001; Ramsey et al., 2019; Toth and Robinson, 2005). Nonetheless, precocious foragers may not have their orientation faculties fully developed, and the incidence of failure because of disorientation is higher (Kralj and Fuchs, 2006; Perry et al., 2015). In this scenario, the foraging crew of the colony became progressively younger and less effective, until they could no longer sustain maintenance tasks and food levels in the colony. This triggers a rapid terminal decline, as food limitation prompts the accelerated recruitment of nurse bees for foraging, exacerbating the cutting down of nurse crews and the neglect of nest maintenance tasks (Annoscia et al., 2015; Perry et al., 2015; Zanni et al., 2018). At this stage, viral and bacterial diseases and other opportunistic parasites can thrive and exacerbate the terminal collapse (Benoit et al., 2004; Budge et al., 2016; Burritt et al., 2016).

Hence, the result of *V. destructor* parasitism is adult bees with deficiencies in metabolic functions and immune response, being less tolerant to pesticides and dehydration, and having shortened longevity (Beetsma, 1994; De Jong et al., 1982a), drastically cutting the chances of the bee to survive the winter, or cope with other stressors. Combined, this impoverishes the structure of the colony and leads to its collapse.

Some other factors that have been linked to colony decline are pesticides, climatic conditions, environmental pollution, nutrition deficit and shortage of high-quality pollen, limited access to water, loss of feral populations and the low genetic variability of managed strains, beekeeping management and migration of the colonies, etc. (Doublet et al., 2015; Neumann and Carreck, 2010; Oldroyd, 2007; Potts et al., 2010; Ratnieks and Carreck, 2010; Rucker et al., 2019; Stanimirović et al., 2019). However, as described above, there is sufficient evidence to consider honey bee pathogens and their interactions as the major threat to bee colonies. Among these pathogens, the combination of *V. destructor*'s direct feeding debilitating effect plus its high vectoring capacity and enhanced viral pathogenicity is considered by many as the major contributor to the very high losses of colonies in Europe and the USA in the last decades (Brodschneider et al., 2018; Guzmán-Novoa et al., 2010; Ramsey et al., 2019; Roberts et al., 2017; Staveley et al., 2014; Steinhauer et al., 2018; vanEngelsdorp et al., 2009).

i.1.11. The impact of varroosis on the beekeeping industry: economic, environmental, and agricultural consequences

As soon as beekeepers started noticing dramatic losses in their colonies, State and federal agricultural agencies, university researchers, and the beekeeping industry began working together to understand the cause and develop Best Management Practices to reduce losses (some examples are honeybeehealthcoalition.org; beeinformed.org; and coloss.org). For example, since 2006, the annual survey in the United States has recorded consistent losses of more than 30% of the colonies (BIP, 2020). These high rates of colony losses require that beekeepers rebuild their colonies at a higher pace with a substantial increase in expenses, placing commercial beekeeping in jeopardy as a viable industry and threatening the crops dependent on honey bee pollination (vanEngelsdorp et al., 2008; vanEngelsdorp et al., 2007). Consequently, the economic impact of *Varroa* parasitism is estimated to be millions of US dollars per year (Cook et al., 2007; Iwasaki et al., 2015). Even so, it is difficult to quantify the actual economic cost of *V. destructor* in beekeeping, partly because most colonies suffer from multiple threats, which may also act synergistically. Some examples of the well-documented implications of *Varroa* parasitism on national apiculture are found in the United States, Canada, New Zealand and Australia (see below).

Prior to the introduction of *Varroa* mites into the **USA**, beekeepers reported 5–10% winter losses. These losses rose to 15–25% after the introduction of *Varroa* and tracheal mites (*Acarapis woodi*), with considerable variation in both, average and total loss by State (vanEngelsdorp et al., 2008). For instance, Pennsylvania suffered an epidemic of colony losses that averaged 53% between 1995 and 1996 (Finley et al., 1996). Beekeepers who treated their colonies against *Varroa* with fluvalinate (Apistan®) or antibiotics (oxytetracycline (Terramycin) and fumagillin (Fumidil B) reported significantly lower colony mortality (Finley et al., 1996). It was around 2006 when higher-than-normal overwintering losses began to be reported across the country (Ellis et al., 2010; vanEngelsdorp et al., 2007), exceeding by far the average of 15% of acceptable losses considered by beekeepers (vanEngelsdorp et al., 2008). These concerns about higher losses promoted the annual national survey, conducted by the Bee Informed Partnership, which has been reporting average loss rates of about 39% annually (BIP, 2020; vanEngelsdorp et al., 2007).

INTRODUCTION

In **Canada**, the incursion of *Varroa* in 1989 also dramatically changed the structure of the beekeeping industry, initially dominated by part-time hobby operations and now by full-time commercial beekeepers. The winter losses doubled from 5-15% in 1992 to around 35% between 2007 and 2009, identifying *Varroa* as the main cause of the increased mortality (Guzmán-Novoa et al., 2010; Hafi et al., 2012).

Following the discovery of *Varroa* in **New Zealand**, the number of registered beekeepers fell by half, mostly because they were unable to make a profit due to the increased hive mortality and additional cost of maintenance. The government estimates that *Varroa* would likely cost the country between $400 and $900 million over the next 35 years (Stevenson et al., 2005).

Similarly to managed bees, the *Varroa* mite has also contributed to the eradication of most feral honey bee colonies, greatly reducing the pollination service they provide, because in the case of feral bees, there is no opportunity for mite control via treatment with miticides (Büchler et al., 2010; Sammataro et al., 2000). The loss of feral colonies in the **USA** was estimated at 95 to 98% after *Varroa* settled in (Cornell University 1997). **New Zealand** is also an excellent example of the consequences of the *Varroa destructor*'s invasion in terms of ecosystem services to agriculture (Iwasaki et al., 2015). The decline of feral colonies has been estimated at about 99% since *Varroa*'s introduction in 2000 (Goodwin et al., 2006), negatively impacting on the pollination services of local farmers and pastoral plants (Iwasaki et al., 2015). The environmental impact of *Varroa* mites in natural habitats is difficult to quantify, but it is obvious that the decline of feral bees will lead to a fast reduction of plant diversity followed by ecosystem instability and reduced potential for restoration (Boecking and Veromann, 2020; Potts et al., 2010). This void of wild bees has been especially noticed by homeowners and growers who had relied on local bees to pollinate their crops, and now require ever more pollination services (Sammataro et al., 2000). The role of *Varroa* parasitism in honey bee colony losses, along with the worldwide decline of natural pollinators, may exacerbate future problems for pollination (De la Rúa et al., 2009). Today, agricultural production depends heavily on managed bees to pollinate many varieties of commercial orchards. This, together with the increased costs incurred by beekeepers for pest control and recouping losses, will have an impact on the price of honey and inhive products, as well as on the fees charged for pollination services. For example, the cost of renting honey bee hives for almond pollination in the **USA** rose from about $50 in 2003 to $150-$175 per hive in 2009 (Li, 2021). And in **New**

Zealand, from an average of $80 per hive in 2001 (one year after the first detection of *V. destructor*), to $150 in 2012 (Goodwin et al., 2006).

Australia currently has a unique scenario to assess the actual impact of *Varroa* on a global scale. The country is considered free of *Varroa* and has not experienced similar losses in honey bee colonies. This advantage has been maintained over time thanks to the country's relative isolation and the substantial investment in quarantine measures and surveillance programmes for protection against incursions of exotic pests and diseases (AQIS, Australian Government: https://www.daff.gov.au/aqis/quarantine/pests-diseases/honeybees). It is believed that Australia's freedom from *Varroa* confers a considerable benefit to its competitive position over other countries in areas such as agricultural production and foreign trade (Reeves and Cutler, 2005). Remarkably, Australia has a large commercial-scale beekeeping industry, exposed to similar agrochemical and pathogenic stressors as North America and Europe, but has not experienced the increase in colony losses that they report. A report conducted by the Australian Bureau of Agricultural and Resource Economics and Sciences (ABARES) estimated the cost associated with the introduction and spread of *Varroa* in the country to range from $0.36 to $1.31 billion over 30 years (Hafi et al., 2012).

i.2.   Pesticide treatments against *V. destructor*

In the years following the large numbers of bee colony deaths in eastern and western European countries, beekeeping research concentrated on pesticide screening against the *Varroa* mite, including herbs, natural compounds, and synthetic chemicals. A good varroacide treatment must meet some requirements. It has to be effective in killing *Varroa*, but also show low toxicity for non-target bees and a low risk of contamination of bee products (Stanimirović et al., 2019). These requirements greatly limit the acaricides that can be used in hives, narrowing them down to the few active ingredients officially permitted for use in bee colonies (Rosenkranz et al., 2010). Soon, these acaricides were widely used by beekeepers and, by giving one treatment per year to all their colonies, they were able to keep mite populations at a low level. Still, today, beekeepers control *V. destructor* infestations in their honey bee colonies using several mechanical and chemical approaches based on the few treatments available, including synthetic (hard) and/or organic (soft) acaricides.

i.2.1. Organic acaricides

Organic treatment regimens include organic acids, such as formic, oxalic, and lactic acids, or essential plant oils (e.g., thymol) (Table i.3) (Calderone and Spivak, 1995; Imdorf et al., 1999; Umpiérrez et al., 2011). The general advantages of natural compounds are the low risk of residue accumulation in bee products and the lower probability of eliciting resistance (Rosenkranz et al., 2010). However, beekeepers reported failures to adequately control colony mite levels by some of these products.

There are multiple ways to treat the colony with these compounds. Usually, they are applied as liquid or gel, either directly to the colony or using different matrices soaked in the product that evaporates afterwards. But, on some occasions, they can be powdered or vaporised over the bees. These formulations require greater handling and training by the beekeeper to ensure adequate efficacy of treatment. This is because insufficient doses are incapable of controlling the mites properly, but also because some natural treatments, such as formic acid and oxalic acid, can show negative effects on bees at high concentrations (Bolli et al., 1993; Damiani et al., 2009; Ebert et al., 2007; Pietropaoli and Formato, 2019).

Table i.3. List of organic acids (OA) and essential oil (EO) treatments shown to have significant efficacy for *Varroa* control.

Primary site of action	Chemical class	Active ingredient	Product trade name
Unknown	organic acid	Oxalic acid	Ecoxal®, Apibioxal®, generic
Unknown	organic acid	Oxalic acid dihydrate	Oxybee®
Unknown	organic acid	Formic acid	MAQS®, generic
Unknown	organic acid	Lactic acid	generic
Unknown	organic acid	Formic acid and oxalic acid dihydrate	Varromed®
Unknown	essential oil	Thymol	Apiguard®, Thymovar®
Unknown	essential oil	Thymol, eucalyptol, menthol, camphor	Api-Life Var®

The main disadvantage of organic acaricides is that their effectiveness is variable as the outcomes are highly dependent on external factors such as climatic and in-hive conditions (environmental temperature and humidity, hive size, presence of brood, mite population size, etc.), and means of application (i. e., chosen evaporator and the area covered by it) (Calderone, 1999; Calderone, 2010; Calis et al., 1998; Eguaras et al., 2003; Eischen, 1998; Rosenkranz et al., 2010; Underwood and Currie, 2003). This makes them not as reliable as synthetic acaricides, but their use is highly recommended as alternatives to other pesticides in Integrated Pest Management (IPM) programs. (Calderone, 1999; Rosenkranz et al., 2010; Stanimirović et al., 2019; Umpiérrez et al., 2011; Underwood and Currie, 2003).

A range of other substances (e.g., mineral/vegetable oil, neem oil, wintergreen oil, icing sugar) show some promise as *Varroa* control treatments (Aliano and Ellis, 2005; Fakhimzadeh et al., 2011). However, there is currently insufficient research data available for these substances to be considered as suitable control treatments.

i.2.2. Synthetic acaricides

Synthetic acaricides are the most effective and widely used method for controlling *Varroa* (Haber et al., 2019). These are based on three active ingredients, with the nervous system as the primary site of action (Table i.4).

Usually, synthetic varroacides are applied as plastic polymer (LDPE or PVC) strips impregnated with the active compound. The strips should be placed in the hive, hung between frames, so that both sides of the strip are in contact with the bees. The bees rub against the strips as they move through the brood chamber, and then pass the chemical on to other bees as they rub up against each other in the hive. This way, the active compound comes into contact with phoretic mites. As mites inside capped brood cells are protected from the treatments, but as the strips with the acaricide are kept in the hive for such a long time (periods of 6-8 weeks), mites in brood cells also become exposed when they emerge from the capped cells.

Table i.4. Synthetic acaricides authorised for use against *V. destructor*.

MoA Group	Chemical class	Active ingredient	Action	Product trade name
Acetylcholinesterase (AChE) inhibitors	1B: Organophosphates	Coumaphos	Inhibit AChE, causing hyperexcitation. AChE is the enzyme that terminates the action of the excitatory neurotransmitter acetylcholine at nerve synapses.	Checkmite® Asuntol® Perizin®
Sodium channel modulators	3A: Pyrethroids	*Tau*-fluvalinate Flumethrin	Keep sodium channels open, causing hyperexcitation and, in some cases, nerve block. Sodium channels are involved in the propagation of action potentials along nerve axons.	Apistan® Klartan® Mavrik® Bayvarol® Polyvar®
Octopamine receptor agonists	19: Amitraz	Amitraz	Activate octopamine receptors, leading to hyperexcitation. Octopamine is the insect equivalent of adrenaline, the fight-or-flight neurohormone.	Apivar® Apitraz® Amicel® Taktic®

Historically, synthetic acaricides have been the preferred choice for beekeepers since they are highly effective, killing an average of 95-99% of susceptible mites; they show low toxicity to honey bees; and they are easy to apply. The lipophilic nature of these compounds limits the residues in honey. Notwithstanding, increasing studies have reported their accumulation in wax and beebread (Bonzini et al., 2011; Calatayud-Vernich et al., 2018; Orantes-Bermejo et al., 2010). The biggest drawback of synthetic acaricides is the evolution of resistance in mite populations. Currently, resistance to all three families of active ingredients has been reported (Bąk et al., 2012; Elzen et al., 1999a; Elzen et al., 1998; González-Cabrera et al., 2018; Gracia-Salinas et al., 2006; Lodesani et al., 1995; Maggi et al., 2009; Maggi et al., 2010; Martin, 2004; Milani, 1995, 1999; Miozes-Koch et al., 2000; Pettis, 2004; Rinkevich, 2020; Rodríguez-Dehaibes et al., 2005; Trouiller, 1998). The present work is focused on the investigation related to the evolution of resistance to synthetic pyrethroids in *V. destructor*.

i.3. Pyrethroids

i.3.1. History and general characteristics

Pyrethroids are a major class of synthetic pesticides used worldwide for controlling indoor and agricultural pests (Gajendiran and Abraham, 2018). They are synthetic analogues of the natural pyrethrins, plant defence active compounds naturally occurring in the flowers of some species of the genus Chrysanthemum (formerly Pyrethrum) (Family *Asteraceae*) (Ross, 2011; Schechter et al., 1949).

The pyrethrum (a term referring to the dried and powdered flower heads of the mentioned plants) extracts show a strong repellent and toxic effect on arthropods and a low toxicity on mammals and avians (Richter and Steuber, 2010). The insecticidal and insect-repellent properties of pyrethrum daisy and pyrethrum extracts have been known for centuries. The use of dried flowers as insect repellent is mentioned in early ancient Chinese history, and it is thought to have passed into Central Asia and Europe along the silk routes (Sun et al., 2020). In the 19th century, the powder obtained from crushing dried flower heads of Dalmatian and Persian chrysanthemum (*Tanacetum cinerariifolium* and *Tanacetum coccineum*, respectively), known as 'Persian dust' or 'Dalmatian dust', was used as a botanical insecticide for controlling ticks, fleas, mosquitoes, and flies (Fig. i.7A) (Davies et al., 2007; Glynne-Jones, 2001). The full-scale production of these flowers for the commercialization of pyrethrum started in the mid-19th century and continues until today, with the increasing demand for natural biopesticides. Nonetheless, these plants require certain conditions for flowering that greatly limit their production (Sun et al., 2020).

Pyrethrum extracts contain six natural active pyrethrins: pyrethrin I and II, jasmolin I and II, and cinerin I and II (Sun et al., 2020). Chemically, they are esters of the cyclopropane carboxylic acid (chrysanthemic acid moiety in pyrethrins type I, and pyrethric acid in pyrethrins type II) that vary in the alcohol moiety (Fig. i.7B) (Glynne-Jones, 2001). Pyrethrins act as neurotoxins, altering nerve function and causing paralysis in a wide range of arthropod species, rapidly knocking down flying insects and eventually resulting in death. However, they are quite unstable in sunlight and outdoors, which is good for the environment but limits their use for agricultural purposes (Ross, 2011). The identification of pyrethrum active elements and the investigations to elucidate the structure of pyrethrins, started by H. Staudinger and L. Ružička in the 1920s, permitted

the development of analytical methods to undertake fundamental studies on pyrethrins and their insecticidal applications (Glynne-Jones, 2001). The complete characterization of the structure and further studies on structural modifications of pyrethrins during the

A)

B)

Pyrethrin I	R1= H	R2= CH=CH$_2$
Pyrethrin II	R1= CO$_2$	R2= CH=CH$_2$
Cinerin I	R1= H	R2= CH$_3$
Cinerin II	R1= CO$_2$	R2= CH$_3$
Jasmolin I	R1= H	R2= CH$_2$CH$_3$
Jasmolin II	R1= CO$_2$	R2= CH$_2$CH$_3$

C)   Allethrin

Acid Moiety   Alcohol Moiety
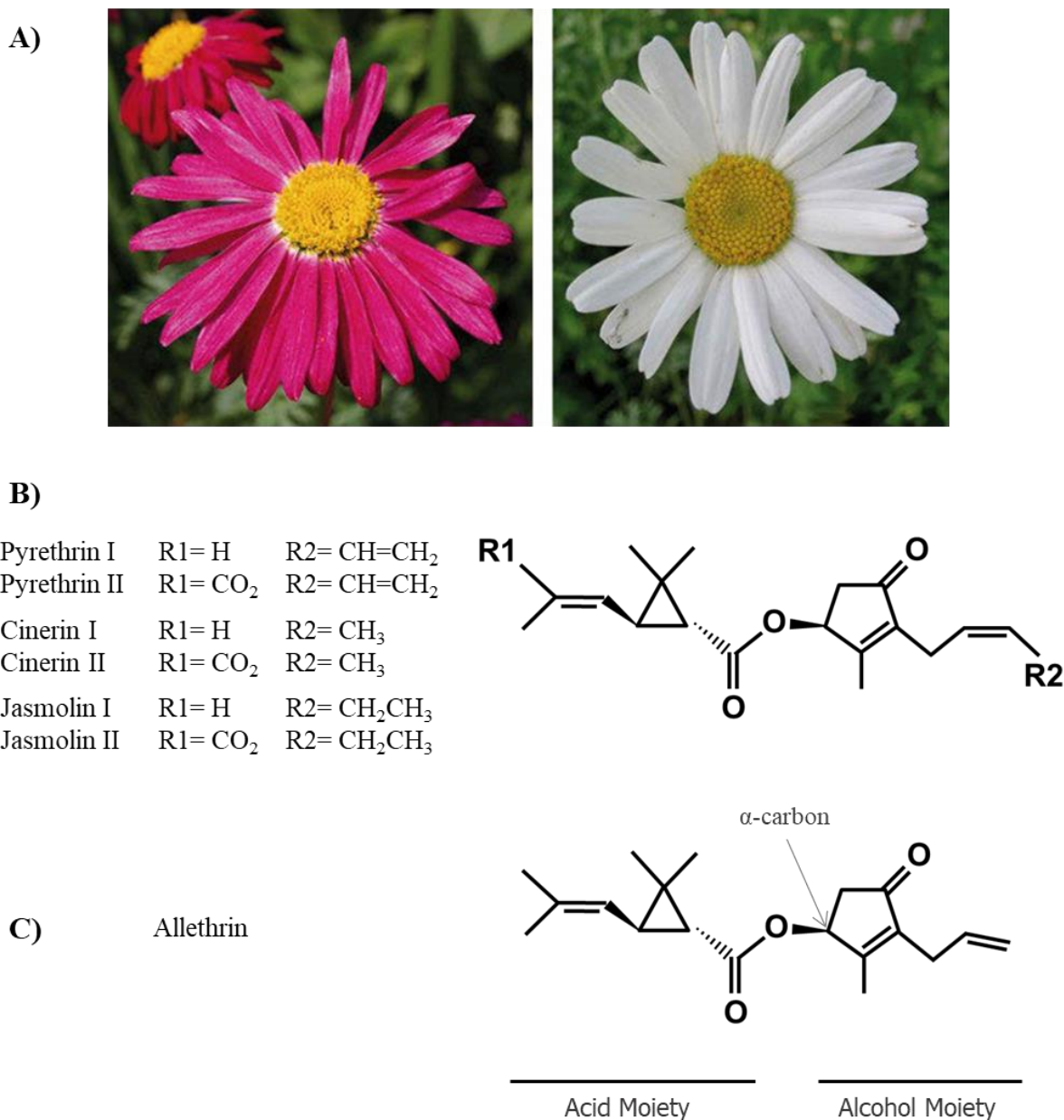
Figure i.7. Pyrethrum flowers of *Tanacetum coccineum* and *Tanacetum cinerariifolium*, respectively (A). The chemical structure of the natural pyrethrins (B) and the first pyrethroid synthesised (allethrin) (C).

period from 1924 to 1974 led to the development of the first generation of synthetic pyrethroids (Davies et al., 2007). Pyrethroids represented a breakthrough in chemistry that reproduced and modified the chemical structures of natural pyrethrins to improve their chemical properties in terms of stability as well as better biological performance (higher selective toxicity) (Aznar-Alemany and Eljarrat, 2020; Elliott, 1976).

In 1949, M. S. Schechter and colleagues announced the development of the first totally synthetic pyrethroid, the allethrin (Sanders and Taff, 1954; Schechter et al., 1949), which closely mimics the structure of cinerin I (Fig. i.7C). The discovery of allethrin coincided in time with the identification of problems associated with DDT, which was the major pesticide used at the time (finally banned in the 1970s) (EPA, 1975). Allethrin was much more effective than DDT, but without the severe environmental or health effects associated with it (Elliott, 1976). This prompted chemists worldwide to investigate structural modifications of the pyrethroid alcohol and acid moieties, and later even the essential ester function (Elliott and Janes, 1978). These efforts resulted in the development of a number of pyrethroids with diverse characteristics. Between 1964 and 1970, pyrethroids such bioallethrin, tetramethrin, resmethrin and bioresmethrin were produced and marketed; they were more potent than natural pyrethrins but still unstable to UV light (Davies et al., 2007; Matsuo, 2019).

Since 1973, subsequent synthetic chemical modifications have helped to obtain more environmentally stable derivatives, giving rise to the second generation of synthetic pyrethroids. Permethrin, cypermethrin and deltamethrin were the first of these pyrethroids, developed by the research group led by M. Elliott at Rothamsted Research Institute, United Kingdom (Rothamsted Experimental Station at the time) (Davies et al., 2007; Elliott, 1977; Elliott et al., 1973a; Elliott et al., 1973b). These are substantially more resistant to degradation by light and air, but more importantly, they are more effective against a wider range of insects, so farmers need to apply fewer insecticide products to their crops. This also means that although they are more persistent and therefore more likely to build up to hazardous levels in the environment. Overall, the development of this new family of high photo-stable pyrethroids with lower acute toxicity than organophosphates and carbamates has dramatically increased their use in agriculture, accounting for approximately 25% of the global insecticide market today (Gajendiran and Abraham, 2018; Ross, 2011).

Subsequent pyrethroids developed were mostly analogues of those developed by Elliott and colleagues. This is the case of **flumethrin**, a modification of cypermethrin, currently used as a varroacide in many countries. In the same period, further key contributions to pyrethroid chemistry came with the development of the first non-cyclopropane pyrethroid, fenvalerate, developed by the Japanese Sumitomo Chemical Company (Nakayama et al., 1979; Ohno et al., 1976). Later, many fenvalerate analogues with different substitutes in the acyl moiety were discovered, including **fluvalinate**. This pyrethroid, like **flumethrin**, exhibits broad-spectrum insecticidal and miticidal activity, but in contrast to other pyrethroids, it is essentially non-toxic to bees. Indeed, given these features, fluvalinate has been used for decades as the most popular acaricide to control *V. destructor* in honey bee colonies (Roth et al., 2020). For a more extensive and comprehensive review of the development of the synthetic pyrethroids and their chemical structures, see Elliott (1989); Katsuda (2012); Khambay and Jewess (2005); Matsuo (2019); Ujihara (2019).

After contact with pyrethrum or pyrethroids, arthropods initially show excitation and hyperlocomotion with coordination disorders, as nerve cells are stimulated to produce repetitive discharges. Then follows a sublethal so-called "*knockdown* effect" that eventually causes paralysis or death. The high lipophilicity of pyrethroids and pyrethrins permits them to pass passively through the insect's cuticula, making them much more effective when absorbed topically, by contact, than when ingested orally (Gunjima and Sato, 1992). Furthermore, higher lipophilicity gives better knockdown rates as the pyrethroid penetrates the channel target more quickly. Based on their chemical structure and the symptoms they produce in response to acute poisoning, synthetic pyrethroids are classified into two classes: type I and type II (Table i.5) (Aznar-Alemany and Eljarrat, 2020; Davies et al., 2007; Gammon et al., 1981; Gunjima and Sato, 1992; Nasuti et al., 2003; Ray and Forshaw, 2000; Richter and Steuber, 2010; Ross, 2011; Verschoyle and Aldridge, 1980).

Table i.5. Characteristics of type I and type II pyrethroids.

| | **Pyrethroids** | |
	type I	type II
General structure	R1—O—R2 with O (Cyclopropane carboxylic ester)	R1—O—R2 with O and CN (Addition of a cyano-group at the α-benzylic position (see Fig. i.7C, p.67))
Action site	Peripheral nervous system	Central nervous system
Duration of modified sodium currents	Tens to hundreds milliseconds	Milliseconds to a few seconds, or longer
Effect in neurons	Induce repetitive firing in axons	Do not induce repetitive firing in the cercal sensory nerves. Irreversible depolarization of the nerve axons and terminals
Consequence *(Characteristics as pesticides)*	Restlessness and hyperactivity followed by exhaustion and paralysis. Good *knockdown* agents	Cause a pronounced convulsive phase that results in better kill
***Acute poisoning symptoms *** *(in mammals)*	T-syndrome: Tremors, hyperexcitation, ataxia and convulsions	CS syndrome: Choreoathetosis (uncontrolled contractions, twitching and writhing), Salivation seizures and hyperexcitability

*Some pyrethroids appear to exhibit characteristics of both syndromes, termed T-CS or mixed syndrome

| ***Examples*** | allethrin, bifenthrin, permethrin, phenothrin, resmethrin, tefluthrin, tetramethrin | cyfluthrin, cyhalothrin, cypermethrin, deltamethrin, fenvalerate, fenpropathrin, flucythrinate, **flumethrin**, **fluvalinate**, tralomethrin. |

i.3.2. Pyrethroid target site and mode of action

Pyrethroids and pyrethrins share the same mode of action. They are grouped together in IRAC's group 3A as modulators of the voltage-gated sodium channel (VGSC) (Sparks and Nauen, 2015). The VGSC is a large transmembrane protein located in the membrane of neurons and other excitable cells that plays an essential role in the initiation and propagation of the action potential in the nerve impulse (Dong et al., 2014; Field et al., 2017; O'Reilly et al., 2006). Thus, they affect both the peripheral and central nervous systems of arthropods.

This protein forms a transmembrane pore of high ionic selectivity, allowing only the passage of sodium ions, and is characterised by its fast kinetics of activation (opening) and inactivation (closing) (Catterall, 2000). The primary structure of Arthropoda's VGSC is similar to that of mammalian sodium channel α-subunits, with four homologous domains (I–IV), each of them arranged in six transmembrane segments (S1–S6) (Dong et al., 2014). In each domain, the transmembrane segments 1 to 4 (S1-S4) constitute the voltage-sensing module (VSM), whereas segments S5, S6 and the membrane-reentrant loop connecting them (called the P-loop) form the pore module (PM) (Fig. i.8) (Bass et al., 2014). Each P-loop is formed by helices P1 and P2 and the extra-cellular link between helices P2 and S6. In the turn region, between helices P1 and P2, are located the residues that form the DEKA motif that plays a key role in the ion selectivity filter of the channel. These are four amino acids (aspartate (D)-glutamate (E)-lysine (K)-alanine (A)), each of which maps into the analogous position of the P-loop in each domain (Fig. i.8) (Soderlund, 2005).

The S4 transmembrane helix from each domain alternates one positively charged residue for every two hydrophobic residues, acting as the voltage sensor of the channel. In response to local membrane depolarization, the S4 segment is proposed to move outward along a spiral path, initiating conformational changes that lead to pore opening and inactivation (Catterall, 2000). The short intracellular linker connecting segments S4 and S5 (L4-5) transfer the movements of the voltage sensing modules to the segments S6 and the pore opens, allowing sodium ions entry into the cell by passive diffusion. The rapid influx of positively charged sodium ions is responsible for the depolarization of the neighbouring membrane potential and the rapid increase in action potentials, which then triggers the activation of nearby VGSCs.
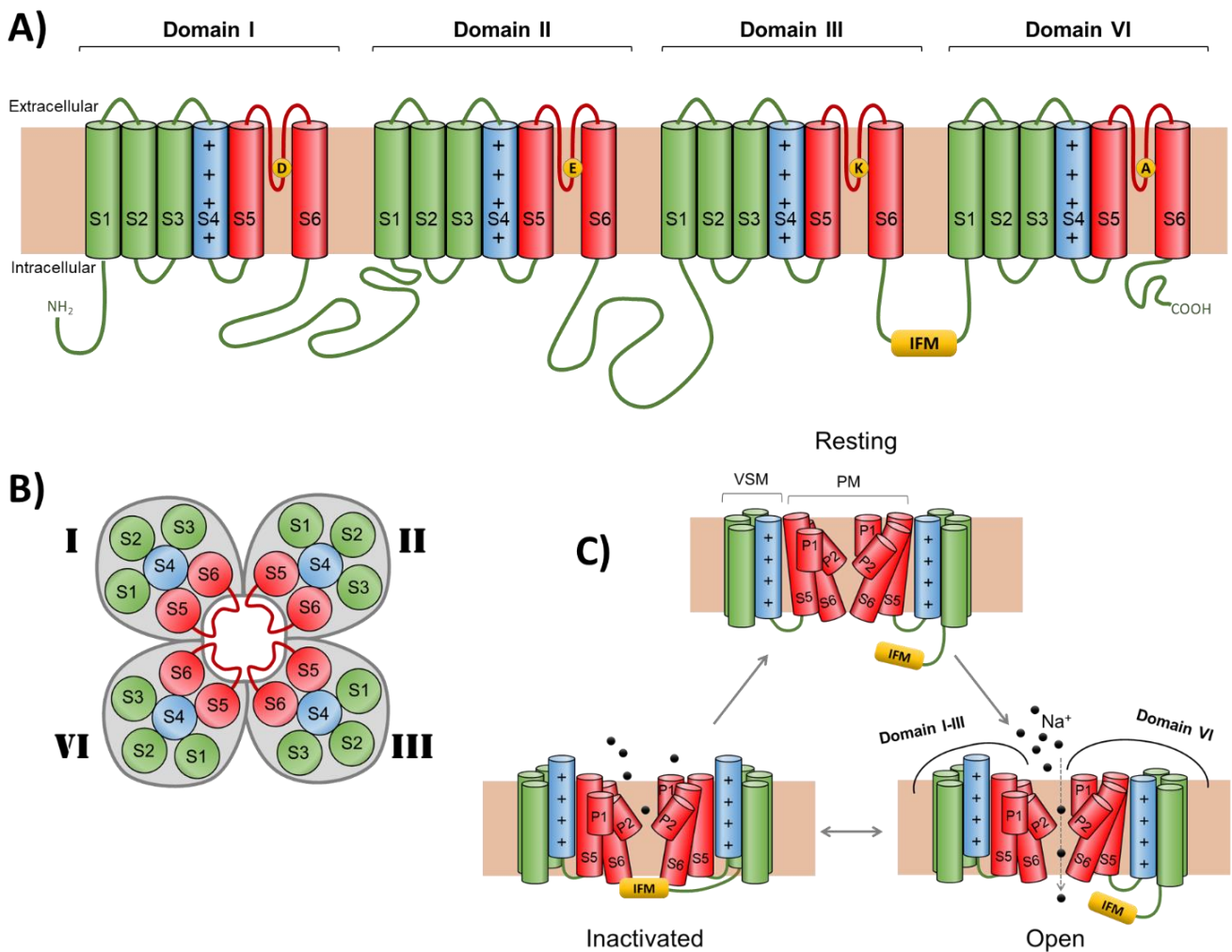
Figure i.8. A graphic representation of the voltage-gated sodium channel structure. **(A)** VGSC topology indicating the sequence features that are critical for channel function. The VGSC protein contains four homologous repeats (Domains I to IV), each having six transmembrane segments (S1-S6). From each domain, the S4 segment (in blue) is enriched in positive-charged residues and acts as a voltage sensor. Together with segments S1 to S3 (in green), they constitute the voltage-sensing module (VSM). The Pore Module (PM) is formed by segments S5, S6 and the connecting S5–S6 linker, called the P-loop (P1 and P2 helices) (in red). In the P-loop are located the residues that form the DEKA motif (indicated as yellow dots) that play a key role in the ion selectivity filter of the channel. **(B)** A schematic representation of the sodium channel's extracellular view, showing the position taken by the segments of each domain to form the channel conformation. **(C)** An overview of the VGSC gating cycle is depicted in a diagram. In the **resting** state, the DI-DIV S4 segments are drawn towards the intracellular side because of the excess of positive charges on the extracellular side polarising the membrane, giving the closed conformation (down state of the S4). Upon membrane depolarisation, the forces that maintain the downstream state are alleviated and the S4 segments of DI-DIII are rapidly pulled extracellularly (upstream state of S4), pushing the S6 segment and opening the channel (**open** state of the channel). The S4 segment of Domain IV moves slowly upwards compared to S4 DI-DIII and leads to intracellular occlusion of the pore by the IFM motif, also known as fast inactivation (**inactivated** state of the channel). After cell repolarization, the channel returns to a closed (resting) state (Dongol et al., 2019).

INTRODUCTION

Inactivation can be divided into two separate subprocesses: fast and slow inactivation. Fast inactivation occurs within a few milliseconds after the opening of the channel pore when this is physically occluded by the inactivation gate, formed by the IFM motif (Isoleucine-Phenylalanine-Methionine) found in the intracellular linker that connects domains III and IV (Catterall, 2000). Fast inactivation is typically observed as a sharp decrease in ion conductance following activation and plays a critical role in the termination of action potentials. It also prevents excessive depolarization of the resting membrane potential. Fast inactivation is highly vulnerable and affected by many toxins such as **pyrethroids** and other sodium channel modulators (sodium channel modulators act contrary to sodium channel blockers, prolonging the opening of sodium channels and causing hyperexcitation). The slow inactivation takes longer (milliseconds to seconds) and comprises the steps of deactivation (closing the pore), recovery from inactivation (removal of the inactivation gate from the inner pore) and return to the resting-excitable state. The sodium-potassium pump acts to repolarize the membrane, so the voltage sensors of the sodium channel can slip inward, returning to their initial position, inducing the conformation changes of the pore to come back to the resting state (deactivation step). The next step is to remove the inactivation gate from the inner pore aperture (recovery from inactivation) and return to the resting, excitable state. Until the entire inactivation process is completed, the channel remains refractory and unable to open again until full recovery. The local positive changes in membrane potential caused by the sodium inflow trigger the opening of the adjacent sodium channels, thus propagating forward the signal along the axon. The lag period (refractory period) from inactivation to deactivation and recovery prevents nearby channels from being activated again in an upstream direction, so the signal transduction always travels in a forward direction to the terminal axon (Catterall, 2000; Dongol et al., 2019; Ulbricht, 2005).

Analysis of the currently sequenced insect genomes suggests that, contrary to mammals, most insects have only one sodium channel gene and achieve the required functional diversity of sodium channels by alternative splicing and RNA editing (Dong et al., 2014). Besides, no orthologs of mammalian β subunits are found in insects. Instead, functionally analogous to β subunits are the TipE and TipE-homologous proteins (TEH1 to 4) in *D. melanogaster* (Feng et al., 1995; Wang et al., 2013; Warmke et al., 1997) and their orthologs in other insects (Bourdin et al., 2015; Bourdin et al., 2013; Derst et al., 2006; Li et al., 2011; Tseng et al., 2007) are considered as auxiliary subunits of insect sodium channels,

playing roles in modulating the expression and gating properties of sodium channels (Wang et al., 2015; Wang et al., 2013). In *Varroa*, non-auxiliar subunits of the sodium channel have been described to date.

Pyrethroid action over the VGSC inhibits the fast inactivation of channels, in such a way that they stay open (activated) for longer. Then, the prolonged inflow of sodium ions results in a continuous depolarization. When the amplitude of the sodium current continues unrelieved, the level of hyperexcitability overwhelms the cell's capacity to maintain the activity of the sodium-potassium pump, triggering hyperexcitation and, in some cases, nerve block. Eventually, cells become exhausted, resulting in incapacitation of the organism and the *knockdown* phenotype. Nevertheless, if interaction ceases, the membrane potential could be shifted, so the nerve cells function in a new, and relatively stable, state of abnormal hyperexcitability.

i.3.3. Acaricidal pyrethroids used in hives

In general, most pyrethroids are highly toxic to insects, and therefore to bees. However, certain pyrethroids show high selectivity for Acari (ticks and mites), offering a great advantage for controlling some pests in the presence of non-target insects (Field et al., 2017). Among them, the pyrethroids *tau*-fluvalinate and flumethrin have been proven to be very successful in the control of *Varroa* in beehives. These selective pyrethroids show an elevated toxicity against mites, while they are tolerated at relatively high concentrations by honey bees. The structure of the acid moiety could be the key to how this specificity can be achieved. In contrast to other pyrethroids highly toxic to insects, *tau*-fluvalinate and flumethrin have an aromatic ring and halogenated groups in the acidic moiety (Fig. i.9).
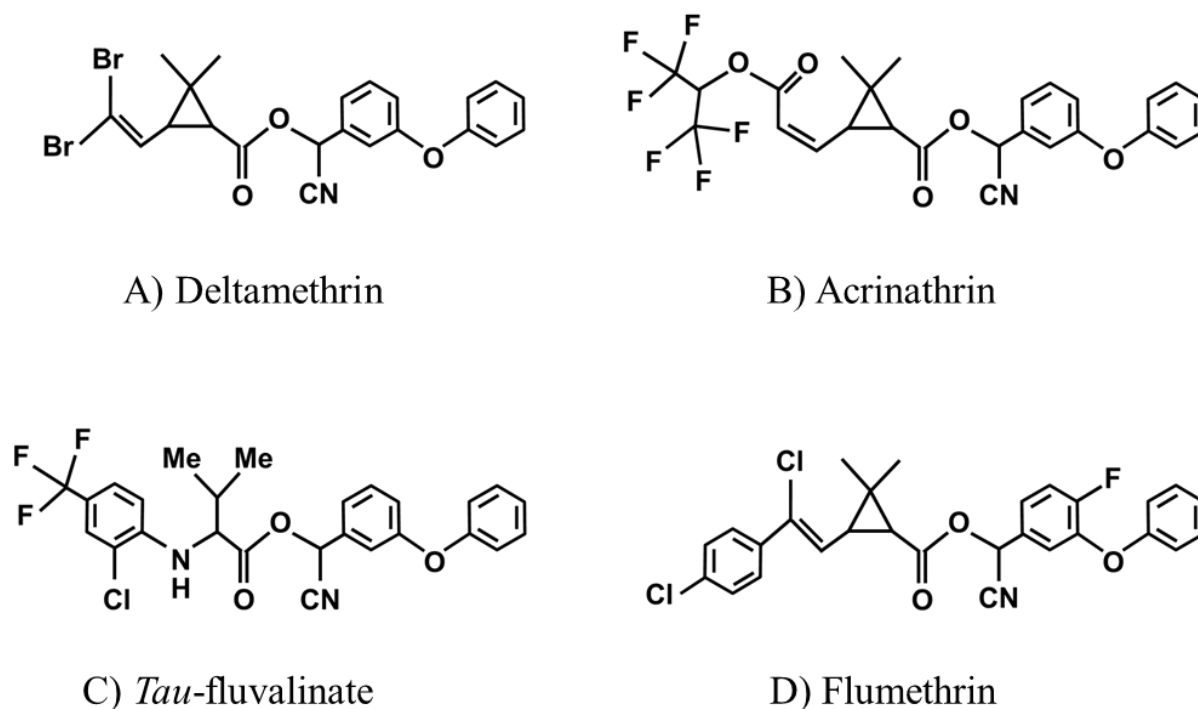
Figure i.9. The chemical structure of a generalist pyrethroid (A) and acari-selective pyrethroids (B, C, and D). Deltamethrin (A) is highly toxic for both insects and acari. Acrinathrin (B), *tau*-fluvalinate (C) and flumethrin (D) are selective for mites, having a larger acid moiety. The *tau*-fluvalinate (C) and flumethrin (D) have an extra aromatic ring in their structure.

Computer modelling studies simulating the interaction of pyrethroids with acarine and insect VGSCs suggest that the amino acid at position 933 may be crucial for the selectivity of these pyrethroids. Position 933 maps to the region suggested to be the point-of-contact for the acidic moiety of pyrethroids within the channel. In the case of pyrethroids displaying acaricidal selectivity, the acidic moiety contains larger halogenated groups. In insects, the residue 933 is always a cysteine (933C), while an alanine, glycine, or valine can be found in acarine species (933A/G/V), which turns out to be smaller compared to cysteine. The bigger side chain of cysteine at 933 would impede the proper accommodation of the acari-specific pyrethroids, making the insect channel less sensitive to them. On the other hand, the smaller amino acids at this position in VGSCs from acarine species allow the pyrethroid to have the necessary room to fit and thus bind more tightly, making it a good acaricide (Lynd et al., 2018; O'Reilly et al., 2014).

In addition, the ability of honey bees to tolerate high concentrations of these pyrethroids is largely dependent on the rapid detoxification rate by cytochrome P450 monooxygenases (P450s) (Johnson et al., 2006), since one of the many reactions catalysed by P450s is the oxidation of aromatic rings (Guengerich, 2020). In *tau*-fluvalinate and flumethrin, the additional aromatic ring in the acid moiety (Fig. i.9) might provide an extra target for the P450 detoxification enzymes and may possibly enhance the detoxification activity contributing to the lower toxicities exhibited by these two pyrethroids in honey bees (Johnson et al., 2006).

Acrinathrin, a pyrethroid derived from hexafluoro-2-propanol, is also an insecticide and an acaricide formerly authorised for use against *Varroa* until the detection of high toxicity to bees. Interestingly, acrinathrin shows selectivity against mites and ticks, most likely due to the halogenated groups in its acidic fraction. However, it does not contain an aromatic ring in the acid moiety, hence it is not rapidly detoxified in the honey bee. Currently, acrinathrin is used as an agricultural pesticide, but it is not an approved product for beehive treatment (Mutinelli, 2016). Despite restrictions, this pyrethroid has been detected in beeswax and pollen, suggesting an irregular use by beekeepers in some apiaries (Calatayud-Vernich et al., 2018; Jiménez et al., 2005; Lodesani et al., 2008; Orantes-Bermejo et al., 2010).

Tau-fluvalinate and flumethrin are registered in several countries worldwide for the control of mites (*Varroa* and tracheal mites) in honey bee colonies. Flumethrin (German patent 2730515, 1979; Bayer AG, Leverkusen) has been registered in EU member states for use on companion and food-producing animals since 1986. Commercial formulations are composed of a mixture of two diastereomers. The pyrethroid *tau*-fluvalinate refers to a subset of isomers of fluvalinate (Katsuda, 1975). Initially, a commercial product, registered under the name fluvalinate, contained all four active diastereoisomers of the fluvalinate. Later, in 1994, chemical advances permitted the use of only two of these diastereoisomers with insecticidal activity in product formulation, and it was renamed *tau*-fluvalinate to reflect this change. In 1987, the pyrethroid *tau*-fluvalinate was among the first synthetic varroacides approved in the USA for use in beehives (Ellis et al., 1988). In Spain, *tau*-fluvalinate was authorised for use in bee hives on 1989 (https://cimavet.aemps.es/cimavet/).

Initially, the treatments were applied using plywood strips soaked in an agricultural formulation and placed into hive matrices (Watkins, 1997). This methodology implies greater risks given the low control over the dose of the applied treatment. Either too high or too low treatment dosage can create problems in the form of bees and/or beekeepers' poisoning, hive product contamination, or by promoting the selection of mites resistant to the product. In 1990, commercial plastic strips impregnated with pyrethroid replaced the homemade plywood strips. This made treatments easier with a more controlled dose of the active ingredient and safer for bees and beekeepers. According to the label, a single strip contains 0.7 g of *tau*-fluvalinate or 0.36 g of flumethrin, of which as much as 10% may diffuse from the plastic strip into hive matrices (Bogdanov et al., 1998). Since *tau*-fluvalinate and flumethrin belong to the group of the more stable α-cyano-pyrethroids, it is possible to maintain a constant treatment for as long as 6 to 8 weeks. Yet, this stability could also have a negative impact due to its persistence in beehive matrices (Calatayud-Vernich et al., 2018).

Tau-fluvalinate and flumethrin have been used with success to control *V. destructor* for decades, being among the most popular acaricides for beekeepers. Unfortunately, the extensive use of these products and the continuous treatments based on a single active ingredient have led to the development of resistance in many locations since the mid-1990s (Alissandrakis et al., 2017; Bąk et al., 2012; Elzen et al., 1998; González-Cabrera et al., 2018; Gracia-Salinas et al., 2006; Kim et al., 2009; Macedo et al., 2002; Martin, 2004; Milani, 1995; Miozes-Koch et al., 2000; Panini et al., 2019; Stara et al., 2019a; Thompson et al., 2002; Wang et al., 2002). In many cases, the resistance was associated with the use of agricultural formulations or the misuse of the varroacide strips (Milani, 1999; Thompson et al., 2002).

i.4. Pyrethroid resistance

i.4.1. Evolution of pyrethroid resistance in *V. destructor*

The first report of pyrethroid resistance in a *V. destructor* population was in 1991 (confirmed in 1992) in the Italian region of Lombardy, in the district of Bergamo. A reduction in the effectiveness of Apistan® (*tau*-fluvalinate) was detected by the weakening and collapse of colonies that remained heavily infested after being treated

(Loglio and Plebani, 1992). By the summer of 1992, more apiaries across Lombardy provinces suffered from a high mortality rate of hives due to failure of the treatment (Lodesani et al., 1995). For the first time, the average efficacy of Apistan® was much lower (20.5%) than the 95% reported until then (Lodesani et al., 1995; Milani, 1993). Although resistant mites were officially detected in the north of Italy, it is possible that these mites came from Sicily, where similar problems may have been occurring. They may have reached the north through migratory beekeeping, via the well-established movement of colonies between these regions (Hillesheim et al., 1996; Martin, 1994; Watkins, 1997). In 1995, mites resistant to pyrethroid treatments were detected in the neighbouring regions of southern Switzerland, the south-east of France and Slovenia (Colin et al., 1997; Hillesheim et al., 1996; Martin, 2004; Trouiller, 1998; Vandame et al., 1995), a situation most probably associated with migratory beekeeping (Trouiller, 1998). From there, it continued spreading throughout Europe, most probably via human-mediated bee movement, being detected in Austria (1996), Poland (1996), Belgium (1997), Hungary (1997), Germany (1997), Finland (1998), Spain (2001), UK (2001) and also in Israel (1997) (Gracia-Salinas et al., 2006; Lipiński et al., 2007; Miozes-Koch et al., 2000; Thompson et al., 2002; Trouiller, 1998).

In America, the first detection of pyrethroid treatment failure was detected in 1997 in the USA, in the State of South Dakota, USA (Baxter et al., 1998). These resistant mites were quickly linked to bees relocated from Florida, where the presence of pyrethroid resistant mites was confirmed (Elzen et al., 1998; Elzen et al., 1999b). Florida is a major commercial beekeeping region for bee breeding and distribution of bee packages to the rest of the country. Besides, it was also the place where *Varroa* mites were initially introduced in the country, in 1987. In just seven years, almost all States had reported problems associated with mites resistant to treatment with *tau*-fluvalinate (Macedo et al., 2002; Martin, 2004). Outside the USA, pyrethroid resistant mites have also been reported in other American countries, like Argentina and Mexico (Maggi et al., 2009; Rodríguez-Dehaibes et al., 2005).

Although it is not known whether the distribution of resistant mites was a result of mite dispersion or whether new outbreaks have arisen independently, the pattern of resistant mites spread throughout mainland Europe, the UK islands and the USA was quite similar to the pattern of spread exhibited originally after the introduction of *V. destructor* in these regions. This is characterised by a slow local spread by flying bees

moving mites between colonies, with irregular long-distance jumps caused by beekeepers moving infested colonies. Supporting this hypothesis is the initial patchy pattern distribution of resistant mites, with a higher proportion of resistant mites noticed in areas with active migratory beekeeping (Martin, 2004; Milani, 1999).

i.4.2. General mechanisms of pesticide resistance

Resistance may be defined as "a heritable change in the sensitivity of a pest population that is reflected in the repeated failure of a product to achieve the expected level of control when used according to the label recommendation for that pest species" (IRAC, irac-online.org). So far, four main mechanisms of resistance have been described. They can act alone or in combination to counteract the effect of the pesticide on the target organism:

- **Metabolic resistance** involves overexpression or the expression of more efficient forms of the enzymes that degrade or remove the toxin from the body of resistant mites faster than in susceptible individuals. It is the most common mechanism in insects, and it often presents the greatest challenge, because some detoxifying enzymes may have a broad activity spectrum against different pesticides.

- **Target-site resistance** implies a genetic modification in the pesticide target protein that prevents the binding or interaction of the toxin, thereby reducing or eliminating the pesticidal effect.

- **Penetration resistance** occurs when the insect's outer cuticle develops barriers, slowing or delaying the absorption of the chemicals into their bodies. This can protect arthropods from a wide range of pesticides that penetrate passively by contact. Usually, it is caused by a thickening of the cuticle, which slows down the absorption of toxins. This mechanism often occurs in conjunction with other forms of resistance, and the reduced penetration intensifies the effects of these other mechanisms.

- **Behavioural resistance** is when the arthropod avoids the toxin by changing its behaviour. The arthropod could somehow detect the threat and evade it, for example, by moving to a non-exposed area or by stopping feeding. This resistance mechanism has

been reported for several classes of pesticides, including organochlorines, organophosphates, carbamates, and pyrethroids.

i.4.3.   Resistance to pyrethroids in insects

In arthropods, resistance to pyrethroids is generally associated with different forms of metabolic and/or target site resistance (Davies et al., 2007; Dong et al., 2014; Kostaropoulos et al., 2001; Oppenoorth, 1985; Riveron et al., 2013; Wang et al., 2020). The latter has been reported to be the most common and is often known by the term "*knockdown* resistance", in reference to the lack of the characteristic *knockdown* effect of pyrethroids, pyrethrins, and DTT in arthropods (Williamson et al., 1993).
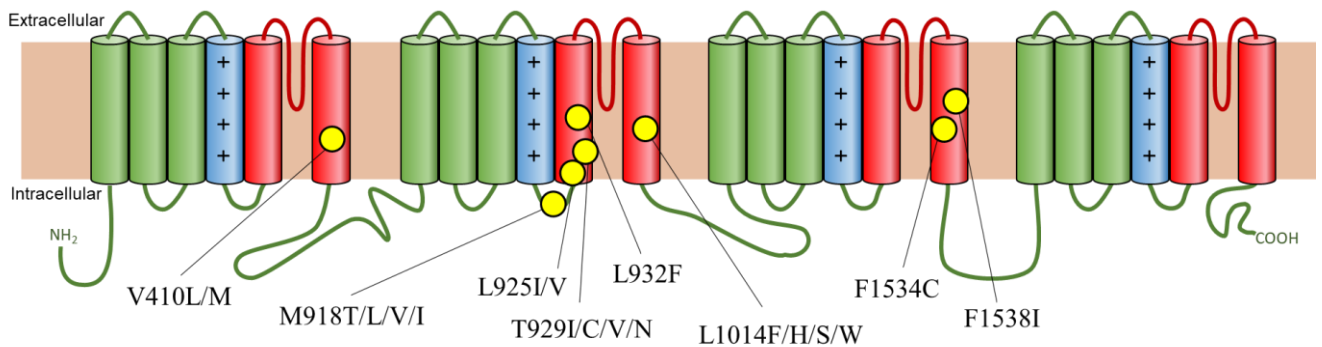
Figure i.10. Position in the voltage-gated sodium channel of the most typical mutations associated with pyrethroid resistance.

Busvine was the first to identify and characterise the resistance to the early *knockdown* effect by DTT and pyrethrins in housefly strains (*Musca domestica*) that was not correlated with metabolic degradation or cuticle penetration (Busvine, 1951, 1953). In the early 1990s, pyrethroid resistance was found to be genetically linked to the VGSC, in particular, associated with point mutations in the gene (Williamson et al., 1993; Williamson et al., 1996). The first mutations described as responsible for pyrethroid resistance were the substitutions of L1014F and/or M918T in the housefly, which were named *knockdown resistance* (*kdr*) (L1014F) or super-*kdr* (M918T), due to the enhanced level of resistance recorded in the flies combining the two mutations (Williamson et al., 1996). Further studies detected these and also other point mutations in the sodium channel related to resistance in other species. These mutations include the substitution of Methionine 918

(M918T/L/V/I), Leucine 925 (L925I/V), Threonine 929 (T929I/C/V/N), Leucine 932 (L932F), Leucine 1014 (L1014F/H/S/W), Phenylalanine 1534 (F1534C) and Phenylalanine 1538 (F1538I) (numbered after the housefly *para*-type sodium channel protein) (Reviewed in Rinkevich *et al.* (2013) and Dong *et al.* (2014)). The functional characterisation of some of these mutations in *Xenopus spp.* oocytes demonstrated their role in pyrethroid resistance (Dong et al., 2014). These point mutations, often referred to as *kdr*-type (*knockdown* resistance-type) mutations, are mostly located in some transmembrane helices of domains II and III (IIS5, IIS6 and III6) and the linker between helices 4 and 5 of domain II (IIS4-S5) (Dong et al., 2014) (Fig. i.10). Computer modelling studies of protein structure predicted that these regions would shape into a hydrophobic pocket wherein pyrethroids would be accommodated (O'Reilly et al., 2006; O'Reilly et al., 2014). Thus, any viable modification of the amino acid mapping in this region may cause resistance.

i.4.4. Resistance mechanisms to pyrethroids in *V. destructor*

The cross-resistance documented in *V. destructor* to fluvalinate, flumethrin, and acrinathrin (Milani, 1995) evidenced a similar resistance mechanism for the three different pyrethroids. As in other arthropods, the mechanism of resistance to pyrethroids in *V. destructor* has been associated with amino acid substitutions in the VGSC. In particular, the mutations found associated with *kdr*-type resistance to pyrethroids are substitutions at position 925 of the VGSC (numbered after the housefly *para*-type sodium channel protein). To date, three different resistant alleles have been described at this position, replacing wild-type Leucine by Valine (L925V), Isoleucine (L925I) or Methionine (L925M) (González-Cabrera et al., 2013; 2016).

The substitution from the wild-type Leucine to Valine at position 925 of the channel protein (L925V) was first found in mites that have survived *tau*-fluvalinate treatment in the United Kingdom and the Czech Republic (González-Cabrera et al., 2013; Hubert et al., 2014). Later, the screening of *Varroa* populations in different European countries confirmed that the mutation L925V was distributed along the continent and also correlated with resistance to pyrethroids (Alissandrakis et al., 2017; González-Cabrera et al., 2018; Panini et al., 2019; Stara et al., 2019a). Further studies conducted with samples collected in the Southeastern USA showed that mites surviving *tau*-fluvalinate treatment

were also mutants at position 925, but the amino acid changes were to Isoleucine (L925I) or Methionine (L925M), rather than the L925V found in European mites (González-Cabrera et al., 2016). These three different resistant alleles are found in different mite populations around the world, showing a clear geographical separation, with the mutation L925V found only in European mite populations, while L925I and L925M were first detected in the USA (González-Cabrera et al., 2018; González-Cabrera et al., 2016; Panini et al., 2019; Stara et al., 2019b), although L925I was recently reported in some resistant mites collected in Greece (Alissandrakis et al., 2017).

As mentioned above, position 925 maps into the transmembrane segment 5 of domain II (IIS5), right into the hydrophobic pocket considered the main binding site of pyrethroids within the channel (O'Reilly et al., 2006; O'Reilly et al., 2014). Besides, the substitution of Leucine 925 has been previously associated with pyrethroid resistance in many arthropod species (Benavent-Albarracín et al., 2020; Capriotti et al., 2014; Kapantaidaki et al., 2018; Katsavou et al., 2020; Morgan et al., 2009; Morin et al., 2002; Yoon et al., 2008). Furthermore, electrophysiological analysis confirmed that the substitution L925I reduces the sensitivity to pyrethroids and DTT in mutated *Drosophila melanogaster* VGSC expressed in *Xenopus laevis* oocytes (Usherwood et al., 2007).

Exceptionally, other mutations and mechanisms of resistance have been described for *V. destructor*. In this instance, Wang (2002) found the mutations L1596P + M1823I in resistant mites from Michigan and Florida, plus two more mutations only in the resistant mites from Florida (F1528L and I1752V). Later, Liu and colleagues (2006) substituted in the cockroach (*Blattella germanica*) VGSC the analogue position L1596 from Phenylalanine (found in insects) to Leucine (found in *Varroa* and *Rhipicephalus microplus*, cattle tick), to make the cockroach channel more "alike" to that of acarine species (*Varroa* and *R. microplus*). The modified channel resulted in a five-fold increase in susceptibility to fluvalinate, suggesting that this residue could be involved in the selectivity of acaricidal pyrethroids. These mutations are located in regions of the channel not usually associated with resistance in other species (L1596P in the IIIS6-IVS1 linker region, M1823I in the IVS6, F1528L in the IIIS6, and I1752V in the IIIS6) (Dong et al., 2014; Rinkevich et al., 2013). Besides, no further publications have reported their association with resistance in mite populations from other locations. In fact, the mutation M1823I was indeed detected in mites from the UK but distributed evenly between susceptible and resistant mites to the pyrethroid treatment (González-Cabrera et al., 2013).

On the other hand, an increase of P450 monooxygenase activity was documented and suggested to take part in the detoxification of pyrethroids in resistant *Varroa* from Israel and Europe (Hillesheim et al., 1996; Miozes-Koch et al., 2000). However, pyrethroid detoxification was not achieved at a significant level to support the hypothesis that metabolic resistance was primarily responsible. Besides, data from the USA indicated that these metabolic pathways were not involved in their mite resistant population (Bell et al., 1999). Currently, no studies have been published on mite-resistant populations capable of reducing or preventing pyrethroid penetration through changes in the physical properties of the cuticle. Not on populations exhibiting behavioural resistance, e.g., by reducing the time spent in the phoretic stage, thus minimising the chance of exposure (Evans and Cook, 2018).

In summary, the point modification of position 925 of the VGSC is currently the only mechanism associated with resistance to a pyrethroid treatment in *V. destructor* populations from apiaries around the world. However, very little was known about the evolution of these mutations, their incidence in apiaries or even their actual implication in the channel sensitivity to pyrethroids, which is the subject of the present research.

OBJECTIVES

- **Impact of the research and scope of the thesis.**

As it has been previously exposed, it is well known that, in the absence of more environmentally friendly alternatives, pyrethroid miticides are one of the safest and most effective ways of removing mites from a hive. Nevertheless, its continuous use has led to the evolution of resistance in many locations, potentially compromising the efficacy and overall usefulness of these miticides in the near future.

The overall aim of the present thesis was to study the pyrethroid resistant-associated mutations at position 925 in *V. destructor* VGSC to achieve a better understanding of the current scenario of the pest and aid in the development of new control mechanisms. The better knowledge of the resistance mechanism will allow us to design methodologies that would guarantee the future use of the current *Varroa* treatments for pest management strategies that would better suit the needs of beekeepers and stakeholders. Physiological and pharmacological characterization of 925 residue mutations in the VGSC of *V. destructor* can help to confirm the genetic linkage with the resistant phenotype, and it can expose whether these mutations entail any impairment of the channel function (**Chapter 1**).

Furthermore, it is of high relevance to study the evolutionary origin of the different mutations in mite populations to know if they originated from single or multiple mutation events. By unravelling the phylogenetic relationship between the resistance alleles, we can identify past mutation events that have resulted in the present distribution of resistance mites. Understanding the evolutionary history of the resistant alleles is a key step to anticipating future events of emerging resistance, and therefore contributes to designing more finely tuned management strategies (**Chapter 2**).

Previous research has shown that the L925V mutation has spread across Europe, but in the United States, mutations reports were limited to few South-eastern apiaries. Knowing the spread and incidence of these mutations throughout the country will let to comprehend the current scenario for USA beekeepers and will allow us to address the situation more effectively (**Chapter 3**).

In a short-term perspective, as mentioned above, detecting these mutations prior to the treatment would allow us to predict its efficacy and provide advice for selecting the most convenient way to deal with the mite. Nowadays, high-throughput genotyping

technologies are available for monitoring resistance in apiaries. However, their cost and accessibility greatly restrict their use as a routine assay for low-resourced laboratories. The availability of cheaper and more accessible methodologies for the detection of resistance would be of great value to beekeepers and stakeholders, so they can make informed decisions regarding the best management strategy to preserve their honey bee colonies. (**Chapter 4**).

Furthermore, it is of utmost importance to develop approaches and implement methodologies that allow better control of the pest in the apiaries with the available treatments. In the **Discussion chapter,** the results of the whole study will be discussed in a broader context, taking into consideration their implications and utility towards an effective Integrated Pest Management.

To that end, the following specific objectives were stablished:

- **Objective 1**: Functional and pharmacological characterization of the *Varroa destructor* VGSC and its alleles associated with pyrethroid resistance (**Chapter 1**).

- **Objective 2**: Phylogenetic analysis of the mutations associated with the pyrethroid resistance in the *Varroa destructor* VGSC (**Chapter 2**).

- **Objective 3**: Determine the prevalence of pyrethroid resistance mutations in the *Varroa destructor* population from the United States (**Chapter 3**).

- **Objective 4**: Development of a new methodology for detecting *Varroa destructor* resistant to synthetic pyrethroids (**Chapter 4**).

CHAPTER 1

Functional and pharmacological characterization of the *Varroa destructor* VGSC and its alleles associated with pyrethroid resistance

1.1. Introduction

The pyrethroid analogues *tau*-fluvalinate and flumethrin has been used with success to control *V. destructor* for many years since they show some selectivity for *Acari* (ticks and mites), which limit their effect on honey bees. However, there is growing evidence of resistance evolution to these toxicants in populations around the world (Alissandrakis et al., 2017; Almecija et al., 2020; Bąk et al., 2012; Elzen et al., 2000; Elzen et al., 1998; Gracia-Salinas et al., 2006; Higes et al., 2020; Kim et al., 2009; Milani, 1995; Mitton et al., 2021; Mozes-Koch et al., 2000; Sammataro et al., 2005; Thompson et al., 2002; Wang et al., 2002). The most common mechanism of resistance to pyrethroids is the modification of certain residues in the voltage gated sodium channel (VGSC), the target of pyrethroids (Davies et al., 2007; Dong et al., 2014). In *V. destructor*, three different mutations have been detected in the VGSC as associated with resistance. These are substitutions of the amino acid residue at position 925, that change the wild-type Leucine for Valine, Methionine, or Isoleucine (Alissandrakis et al., 2017; González-Cabrera et al., 2018; González-Cabrera et al., 2013; González-Cabrera et al., 2016; Hernández-Rodríguez et al., 2021; Hubert et al., 2014; Mitton et al., 2021; Ogihara et al., 2021; Stara et al., 2019a). However, so far there is no actual demonstration of their actual role in reducing the sensitivity to pyrethroids.

Pyrethroid molecules display a high lipophilic nature that favours their membrane embedding, reaching the target more quickly and giving better *knockdown* levels. However, the extremely high levels of nonspecific attachment to cellular membranes makes unfeasible the use of direct binding methodologies (e.g., radiolabelling) to determine the effect of *kdr*-type mutation in the binding of pyrethroids (Dong and Scott, 1994; Lombet et al., 1988; Pauron et al., 1989; Rossignol, 1988; Soderlund et al., 2002; Soderlund et al., 1983). Alternatively, electrophysiological approaches using heterologous expression in *Xenopus* spp. oocytes have been used with success to shed light on the mechanism of action and resistance to pyrethroids and other toxins in several insect sodium channels (Fig. 1.1B) (Feng et al., 1995; Gosselin-Badaroudine et al., 2015; Lee et al., 1999; Smith et al., 1997; Tan et al., 2002; Tatebayashi and Narahashi, 1994; Vais et al., 2000b; Warmke et al., 1997; Wu et al., 2017).

Electrophysiological techniques allow to explore the role of toxins and molecular alterations into the biophysical properties of functional voltage-gated ion channels. The basis for electrophysiology is the measurable potential difference across the lipid
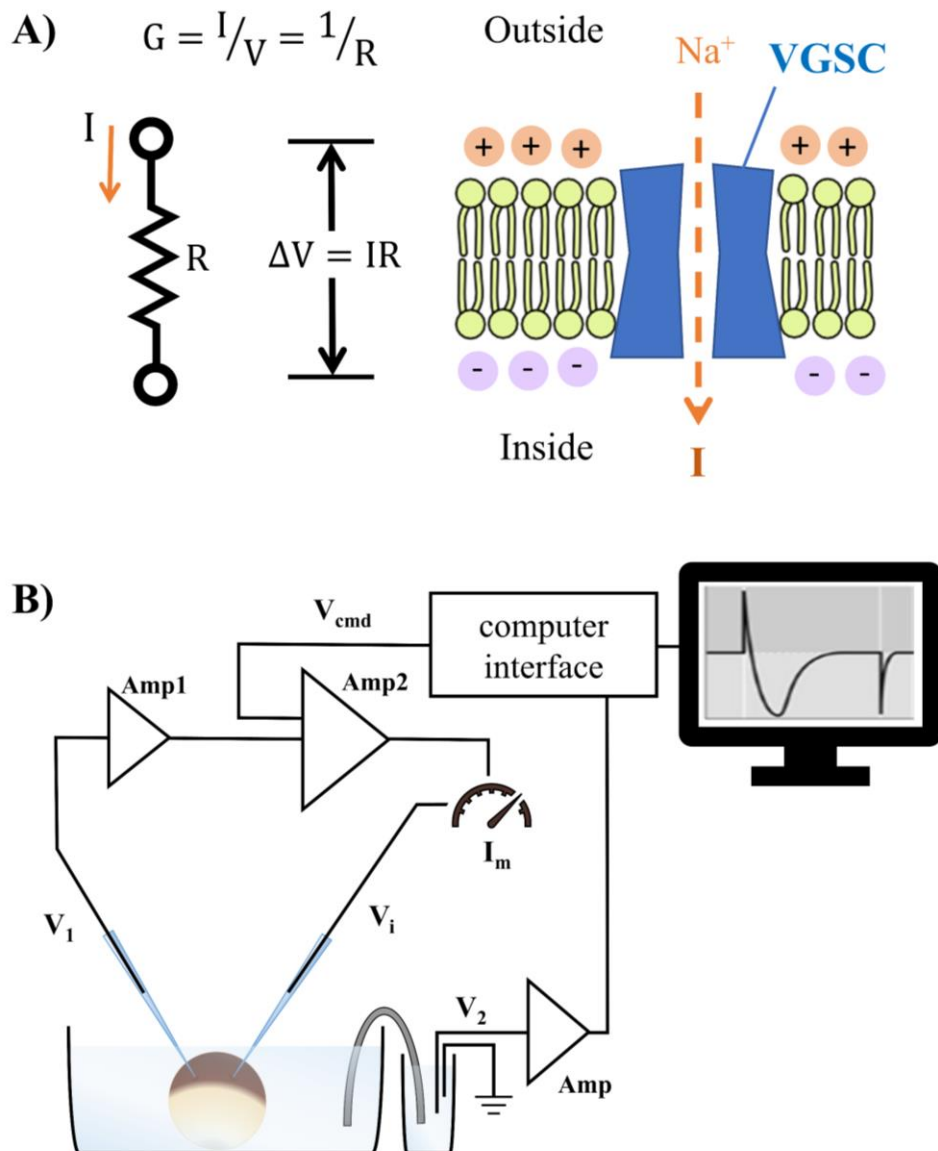
Figure 1.1. TEVC principle. (A) Graphical representation of Ohm's law adapted to the cell membrane. **(B)** Schematic illustration of TEVC circuit. TEVC technique allows to measure ion flow across the cell membrane as an electric current under controlled transmembrane potential. The oocyte is impaled by two microelectrodes, one for voltage sensing (V_1), and one for current injection (V_i), and the transmembrane potential is held under constant experimental control with a feedback amplifier. The transmembrane potential (V_m) is monitored by a unity-gain amplifier (Amp1) connected to the voltage-sensing microelectrode (V_1). This are connected to a high-gain differential amplifier (Amp2) that compares the V_m and the V_{cmd} (Voltage commanded) and rapidly injects current to the cell via the microelectrode V_i to maintain a constant V_m. The magnitude of the injected current needed to keep V_m constant is equal to the membrane current but opposite in sign, thus, it is an accurate measurement of the total membrane current (I_m). The bath electrode or reference electrode (V_2) verifies that the bath is clamped. The amplifiers and computer are connected by a computer interface, which converts analogue signal to digital, and vice versa (Guan et al., 2013).

control the cell's membrane potential, so changes in membrane conductance (G) can be measured by monitoring the current flow of charged ions (I) across the membrane at specific voltages (V). According to Ohms' law (I=V/R), the current between two points (I) is directly proportional to the voltage (V, e.g., the membrane potential) across them, and inversely proportional to the resistance (R). Conductance is opposite to resistance (G = 1/R = I/V) and can be defined as the ease of an electric current to pass between two points, in this specific case from outside to inside the cell (Fig. 1.1.A). Hence, conductance will be conditioned by the activation and inactivation of the heterologous-expressed VGSC, for instance, when the channel opens by the depolarization of the membrane and let in sodium ions. The art of the technique permits the study of voltage-gated ion channels properties and exploration of the role of toxins and molecular variations in the physical behaviour of the ion channel (Guan et al., 2013).

In electrophysiological studies, the *Xenopus laevis* oocyte provide a versatile heterologous expression system particularly suited for the study of (exogenous) ion channels and membrane transporters (Musa-Aziz et al., 2010) . The expression of the heterologous ion channel in *Xenopus* oocytes is achieved by the microinjection of synthetic cRNA (mRNA synthesised using cDNA as template). The first step is therefore to clone the sodium channel coding sequence (CDS) into a suitable vector to create the constructs for microinjection into oocytes.

The challenge of cloning VGSC.

Research with recombinant VGSCs entails special challenges when it involves propagation into bacterial hosts (Feldman and Lossin, 2014). Undoubtedly, the top drawback is the instability of the sodium channel DNA once introduced into a bacterial host. Pitfalls during cloning and bacterial propagation result from re-arrangements of the sodium channel CDS (it comprises four very similar domains, see Fig. i.8, p. 72), fragment deletion and point mutations that lead to a truncated protein. The CDS of the VGSC are long, typically around 6 kb in length, so the final size of the insert-vector plasmid construct is usually in excess of 10 kb. Plasmids carrying sodium channel DNA will almost invariably emerge mutagenized and unusable. Furthermore, the protein seems to be highly toxic for bacteria (not surprisingly, as it is a pore membrane protein), even at basal expression. So, cloning and plasmid multiplication in bacterial host requires the adoption of special conditions.

1.2. Objectives

Mutations at position 925 of the *V. destructor* VGSC (*Vd*VGSC) has been correlated with mites surviving to treatments based on *tau*-fluvalinate and flumethrin. Functional and pharmacological characterization of these mutated channels is essential to elucidate the role of the discovered mutations in pyrethroid resistance (Burton et al., 2011; Usherwood et al., 2007). Comparing the effects of the different pyrethroids upon the wild-type and mutated *Vd*VGSC will let to a better understanding of the basis of *tau*-fluvalinate and flumethrin selectivity for mites.

This chapter aims to further explore the *kdr*-type position L925, and the three mutations found in *V. destructor* (L925V/I/M), providing empirical data for channel kinetics and sensitivity of each pyrethroid molecule. Thus, the major objective of this chapter is the examination of the pharmacologic characteristics that modifications at position 925 confers to the *Vd*VGSC. But in order to achieve this, it is necessary to accomplish several prior objectives to prepare the necessary elements to carry out the electrophysiological study:

- First, is the cloning of the four allelic variants (wild-type and mutants at position 925 of the channel protein to Valine, Isoleucine, and Methionine) of the *Vd*VGSC in a vector specially designed for protein expression in *Xenopus* oocytes.

- Second, to perform a throughout electrophysiological characterization of the wild-type and mutated *Vd*VGSCs by voltage clamp using the *Xenopus* oocyte expression system.

- Subsequently, the pharmacological characterization of wild-type and mutated *Vd*VGSCs and their sensitivities to pyrethroids.

1.3. Materials and methods

1.3.1. Construction of wild-type and mutant *Vd*VGSC constructs

The wild-type (analogously known as *para*-type in insects) VGSC coding sequence (CDS) from *V. destructor* (*Vd*VGSC) was cloned into the pGH19 vector (construct pGH19-*Vd*VGSCwt) by Dr. Joel González-Cabrera during his post-doctoral period at the Rothamsted Research institute, UK. The vector pGH19 is a derivate of the pGEMHE
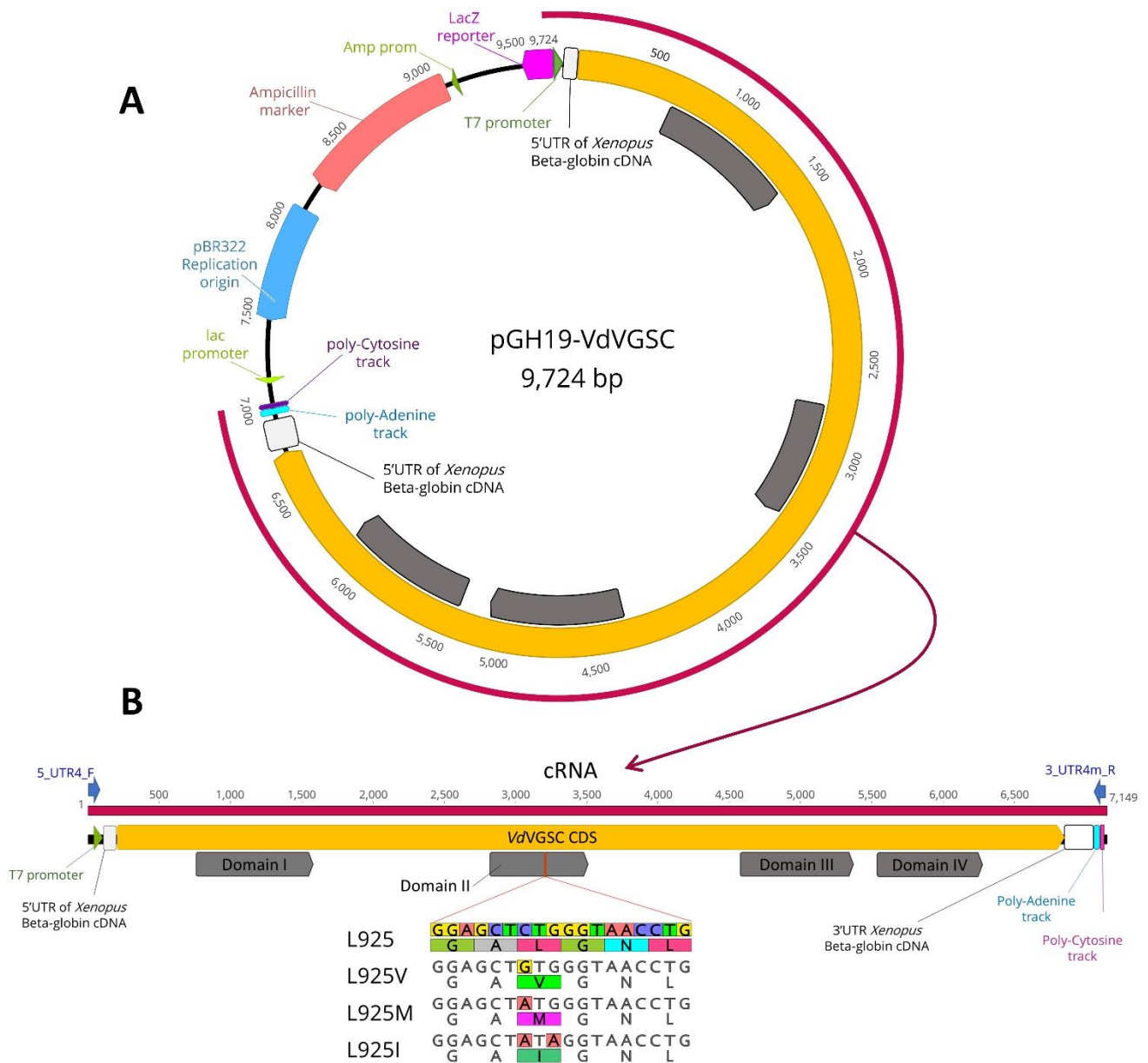
Figure 1.2. Schematic illustration of plasmid constructs (A) and the amplified region for RNA transcription (cRNA) with primers 5_UTR4_F and 3_UTR4m_R (B). Plasmid features and necessary elements for protein expression in *Xenopus* oocytes are indicated. DNA region including the position of 925-residue of the *Vd*VGSC is amplified, showing the nucleotide differences in the mutated constructs.

specially designed for expression in *Xenopus* oocytes (Fig. 1.2). Besides the T7 promoter, needed for *in vitro* transcription of the cRNA, this vector includes both 5'- and 3'-untranslated regions (UTRs) from the *Xenopus* β-globin gene at the corresponding ends of the cloned CDS, followed at 3' by a poly-Adenine track (23 As) and a poly-Cytosine track (31 Cs) (Liman et al., 1992). These modifications stabilize the injected cRNA in the *Xenopus spp.* oocytes, even beyond 48 h, and thereby, boost the protein expression (Shin et al., 1998; Venkatachalan et al., 2007).

Primers for site-directed mutagenesis, amplification and sequencing were designed using primer3 (Untergasser et al., 2012) (Supplementary Table S1.1, p.240). L925V/I/M mutations were introduced into the pGH19-*Vd*VGSCwt construct using the QuikChange Lightning site-directed mutagenesis kit (Agilent technologies Inc., Santa Clara, CA, USA) following the manufacturer's instructions with some modifications. Mutant strand synthesis reactions were performed in a final volume of 50 µL containing 125 ng of each primer from the pair designed to introduce the mutation (Supplementary Table S1.1, p. 240), and 400 ng of template plasmid pGH19-*Vd*VGSCwt. Thermocycling conditions for PCR were carried out as follows: 95°C for 2 min, followed by 15 cycles of denaturation at 95°C for 20 s, annealing at 63°C for 15 s, and elongation at 68°C for 15 min, with a final extension of 5 min at 68°C. Subsequently, reaction products were digested with *Dpn*I at 37°C for 60 min and precipitated by 1-Butanol before bacteria transformation.

The wild type (*para*-type) and mutated VGSC plasmid constructs were used to transform *E. coli* ElectroMAX™ Stbl4™ (11635-018, ThermoFisher Scientific) by electroporation (1.2 kV, 25 µF, 200 Ω) using 0.1 cm gap electroporation cuvette (1652083, Bio-Rad). Plasmid propagation procedure were adapted following the indications from Feldman and Lossin (2014). Sodium channel is apparently toxic for the bacterial host, since proper propagation is hampered in bacteria carrying the whole VGSC CDS cloned in a plasmid. Consequently, mutations throughout the sodium channel CDS are frequent and prevalent, and bacteria carrying the correct VGSC sequence use to grow slowly. Thus, to minimize undesired random mutations in the plasmid, all bacteria cultures were incubated at 30°C or less.

Transformed bacteria were incubated in 1 mL of 2xYT medium (1.6% (w/v) bacto-tryptone, 1% (w/v) yeast extract and 85.6 mM NaCl, pH 7.0-7.5) at 30°C for 2 hours, with a constant shaking of 225 rpm, prior to be plated for bacteria propagation in S.O.B.

medium (2% (w/v) bacto-tryptone, 0.5% (w/v) yeast extract, 8.56mM NaCl and 2.5mM KCl, pH 7.0-7.5) supplemented with 20 mM Glucose and 1.5% agar, containing Ampicillin (50 µg/mL) and Tetracycline (5 µg/mL) for selection. Plates were incubated at 30ºC for 2 to 4 days before selecting colonies. After 48 - 72 hours of incubation, two types of colonies were well-differentiated by their size, large and tiny (Fig. 1.3). Large colonies are bacteria growing at a normal rate for *E. coli*. Usually, these colonies are very likely to carry plasmids that had suffered alterations in the sodium channel DNA sequence, such as rearrangements, deletions, or insertions. Large colonies checked initially in this work contained corrupted plasmids (data not shown), and subsequently were avoided. Slow-growing (tiny) colonies were selected for growing in liquid media (S.O.B medium + 20 mM Glucose + 50 µg/mL Ampicillin + 5 µg/mL Tetracycline) for 36 to 48 hours at 29ºC with a constant shaking of 200 - 250 rpm. Plasmids were isolated following the manufacturer's instructions using the NucleoSpin® Plasmid Kit (740588, Macherey-Nagel). Isolated plasmids were checked by digestion with a set of restriction enzymes (*Bam*HI + *Xba*I, *Eco*RI, *Pvu*I, *Xho*I and/or *Pst*I), before sequencing the complete ORF to verify that the coding sequence was the expected.
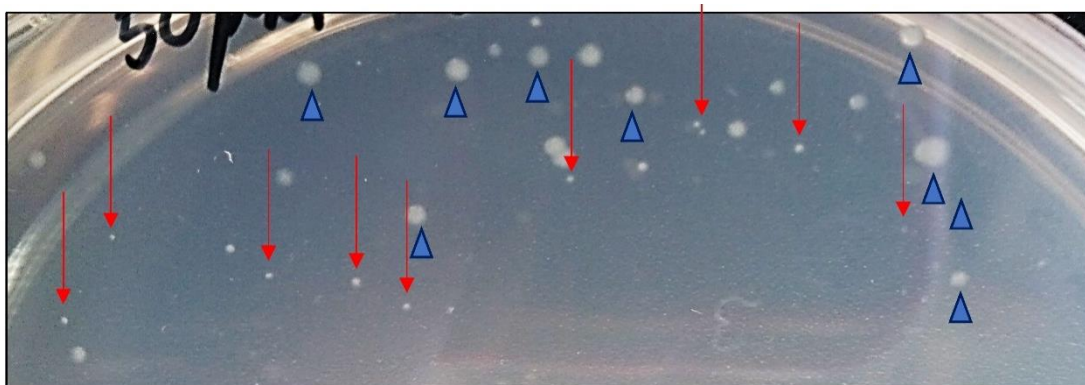
Figure 1.3. Detail on culture plate showing bacterial colonies of transformed *E. coli* with the plasmid pGH19-*Vd*VGSCwt. Red arrows and blue triangles indicate tiny (slow grower) and large colonies (fast growers), respectively.

The complete DNA sequence containing all necessary elements for cRNA transcription and expression in *Xenopus spp.* oocytes (see Fig. 1.2B, p.92) were amplified by PCR using the Q5® High-Fidelity DNA Polymerase (M0491, New England BioLabs) with primers 5_UTR4_F and 3_UTR4m_R (0.5 µM/each) (Supplementary Table S1.1, p. 240), and 0.4 mM of dNTPs in a final volume reaction of 50 µL. Reaction were subjected to the following cycling conditions: Initial denaturation step at 98ºC for 30 s, following 35 cycles of denaturation at 98ºC for 10 s, annealing at 68ºC for 20 s, and elongation at

72º for 7 min; ending with a step of 72ºC for 5 min. RNA transcripts were synthesised using PCR products as templates (Fig. 1.2B, p.92), using the T7 mMESSAGE mMACHINE kit (Ambion Inc., Austin, TX, USA) adding 6 mM of Cap Analog [m^{7}G(5')ppp(5')G] (AM8048, Ambion Inc., Austin, TX, USA), following manufacturer's instructions. cRNA transcripts of either the wild-type or a mutant *Vd*VGSC were diluted for injection to a concentration of 400 ng/µL in RNAase-free water.

1.3.2. Oocyte preparation and microinjection

Xenopus laevis oocytes were supplied as ovarian lobes by the European *Xenopus* Resource Centre (University of Portsmouth, UK). Animal care and treatment were conducted in compliance with national and international laws and policies. *Xenopus laevis* oocytes were isolated and treated before injection according to standard procedures (Burton et al., 2011; Furutani and Kurachi, 2012; Kachel et al., 2016).
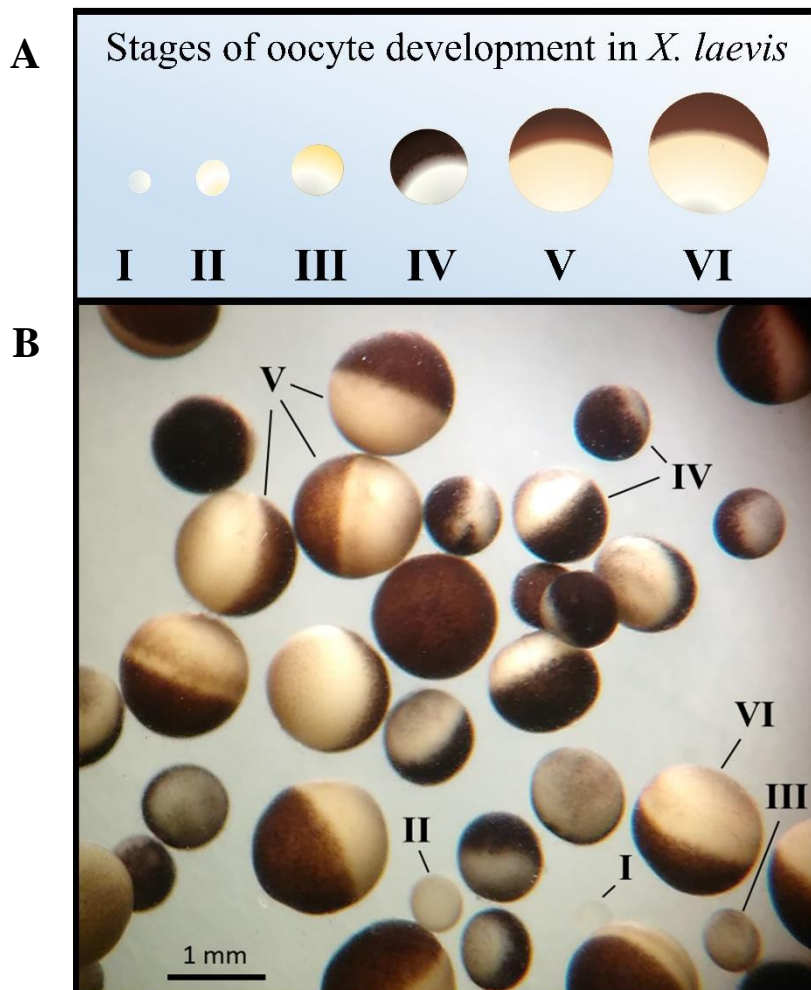
Figure 1.4. *Xenopus laevis* oocytes. Graphical representation (A) and photo (B) showing the different developmental stages of the *X. laevis* oocytes. Scale bar indicates 1 mm.

Oocytes were washed with calcium-free Barth's solution (96 mM NaCl, 2 mM KCl, 5 mM HEPES, 2.5 mM pyruvic acid, 0.5 mM theophylline and 0.05 mg/ml of gentamicin, adjusted to pH=7.5 with NaOH) prior to be treated with 1 mg/ml of type 1A collagenase (C9891, Sigma, Poole, Dorset, UK) for 60 min in calcium-free Barth's solution. Collagenase treatment was followed by three rinses with fresh Barth's solution (96 mM NaCl, 2 mM KCl, 1.8 mM CaCl2, 5 mM HEPES, 2.5 mM pyruvic acid, 0.5 mM theophylline, adjusted to pH7.5 with NaOH), and oocytes of stages V–VI were selected for manual defolliculation using precision tweezers to remove the connective and follicular tissue. Defolliculated oocytes were microinjected with 50 nl of 400 ng/μL cRNA transcript for either the wild-type or mutant sodium channels, using a Nanoliter injector (World precision instruments, Florida, USA), and incubated in Barth's GTP solution (96 mM NaCl, 2 mM KCl, 1.8 mM CaCl2, 5 mM HEPES, 2.5 mM pyruvic acid, 0.5 mM theophylline and 0.05 mg/ml of gentamicin, adjusted to pH7.5 with NaOH) at 18 °C for 3 to 7 days, for protein expression before recording.
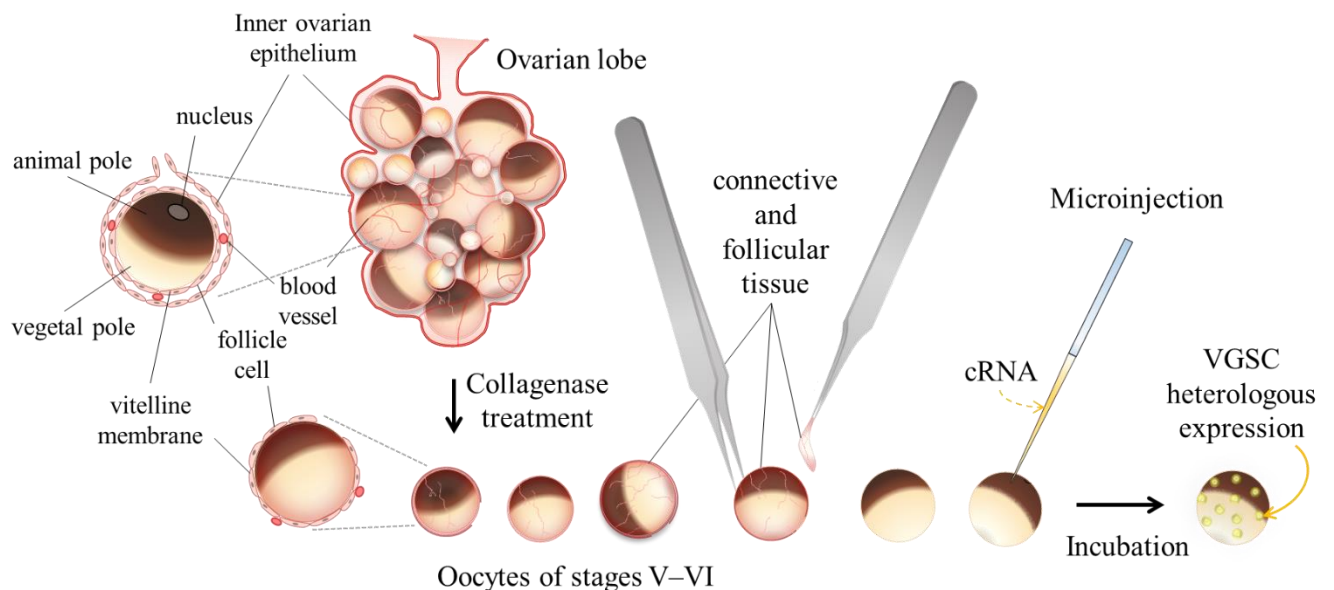
Figure 1.5. Scheme of *Xenopus* oocyte preparation for microinjection in the heterologous expression system.
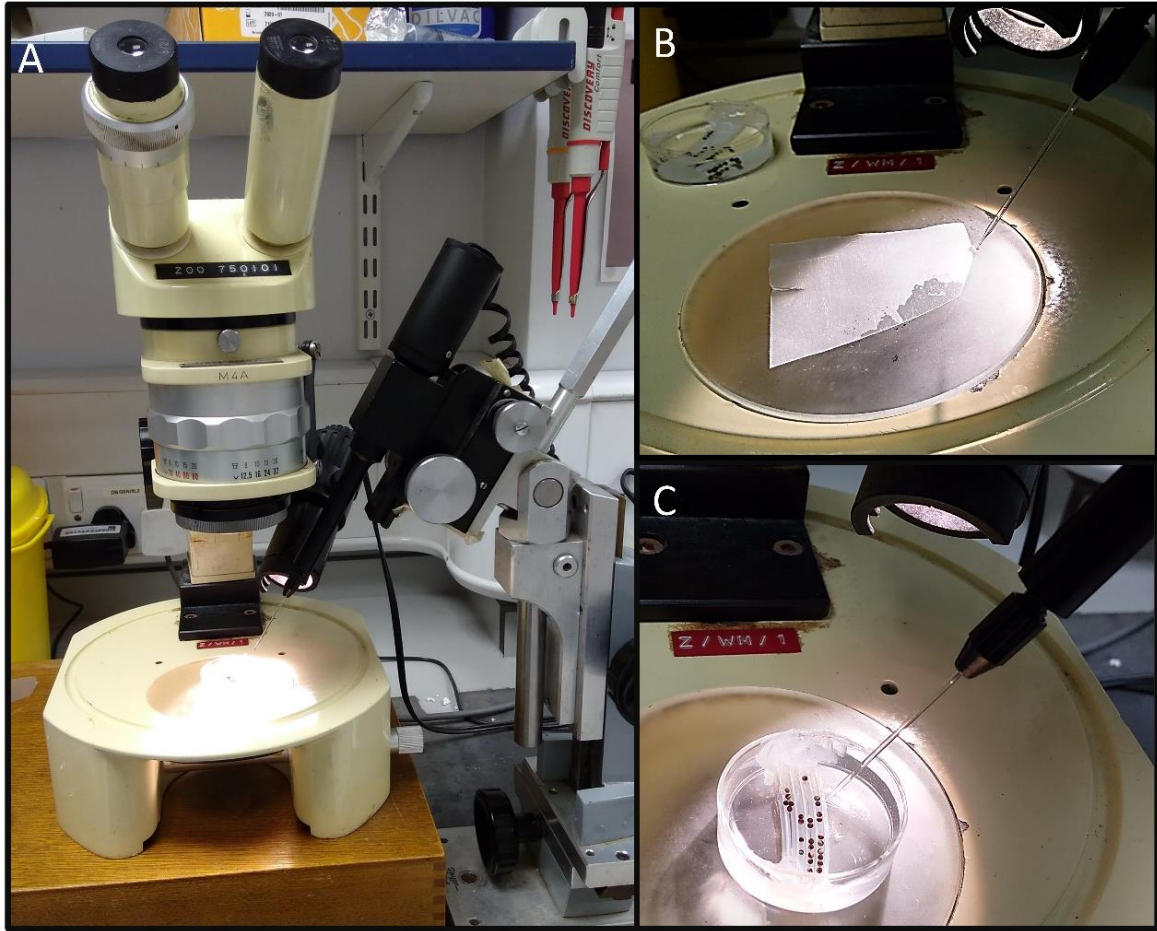
Figure 1.6. Oocyte microinjection. A) Stereomicroscope and Nanoliter 2010 injector. Fine pipettes were pulled from OD 1.14 mm glass capillaries (#504949, world precision instruments, USA) using a Flaming/Brown micropipette puller Model P-97 (Sutter Instrument Co., USA). The tips of the pulled capillaries were broken using sterile tweezers giving a slanted point of approximately 10 μm in diameter. The micropipettes were filled with sterile paraffin oil and clamped on to the needle of the nanoliter injector. B) The cRNA solution was disposed on clean parafilm and sucked into the micropipette avoiding the introduction of air bubbles. C) Selected oocytes were then injected with 50 nL of cRNA solution.

1.3.3. Electrophysiological measurements

The two-electrode voltage-clamp (TEVC) experiments were conducted using a Dagan CA-1B amplifier (Dagan Instr., Minneapolis, MN, USA) with experimental protocols and data acquisition performed using WinWCP V5.4.1 software (Dr John Dempster, University of Strathclyde, UK) (Dempster, 1997).

Oocytes were placed in a disposable 35 mm diameter petri dish, with 2 ml of *Xenopus* ringer solution (95 mM NaCl, 2 mM KCl, 2 mM $CaCl_2$, 1 mM $MgCl_2$, 5 mM
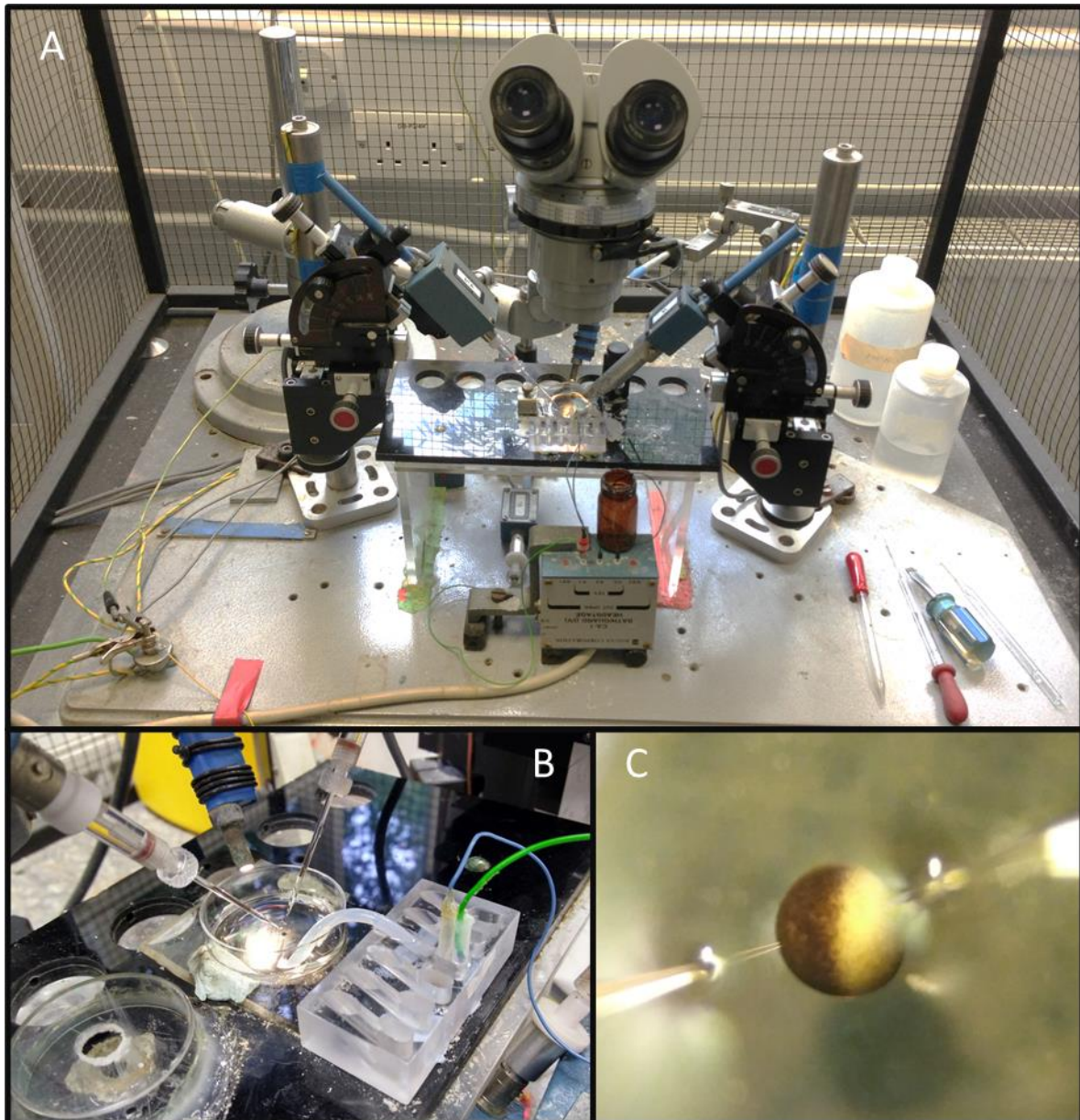
Figure 1.7. Two-electrode voltage clamp (TEVC). (**A**) TEVC workstation. It consists in an anti-vibration table, a Faraday cage, a stereomicroscope, micromanipulators, amplifiers, and data acquisition system. (**B**) Intracellular electrodes for recording and stimulation, and bath electrode (**C**) Clamped oocyte.

HEPES, adjusted to pH7.5 with NaOH) (Fig. 1.6). The oocytes were clamped by intracellular microelectrodes, for recording and stimulation, whilst the bath solution was voltage clamped by a platinum wire in an agar bridge (resistance lower than 7 kOhm) (Fig. 1.7). Intracellular electrodes were pulled from fire polished borosilicate glass capillaries (GC150TF-10, Harvard apparatus, Edenbridge, UK) on a Flaming/Brown micropipette puller (model P-97, Sutter Instrument Company, USA). Current-injecting electrodes were filled with pipette solution of 0.7 M KCl and 1.7 M K-citrate to get a

resistance of 0.5-1.5 MOhm. The adequate quality of the oocytes, required for TEVC analyses, was verified by checking the resting membrane potential before clamping (values from -10 to -40 mV), and the leakage current (less than -150 nA) when the oocyte was clamped to a holding potential of -80 mV. The oocytes were clamped at -80 mV and subjected to depolarizing pulses applied to cause activation of the VGSCs, measurable as an inward sodium current, and challenged with increasing concentrations of the tested pyrethroids diluted in the *Xenopus* Ringer's solution.

1.3.4. Voltage clamp protocols

Various well-established protocols, adapted for mite sodium channels, were applied in order to investigate the voltage dependence of activation, rate of fast inactivation and deactivation (see below for details) (Burton et al., 2011; Usherwood et al., 2007; Vais et al., 2000a). Electrophysiological measurements were made first in the absence of toxicants and then sequentially after exposure to increasing concentrations of pyrethroids. Experiments were replicated using at least 5 oocytes per condition (5 biological replicates). All experiments were carried out at room temperature, approximately 21 to 23 ºC.

> **P.1) Voltage dependence of activation**: This protocol lead us to estimate the voltage at which half maximal activation occurs ($V_{50,act}$) and this provides a measure of the channel's sensitivity to membrane potential (Usherwood et al., 2007). Repeating this in the presence of pyrethroid allows a comparison of $V_{50,act}$s (Fig. 1.8).
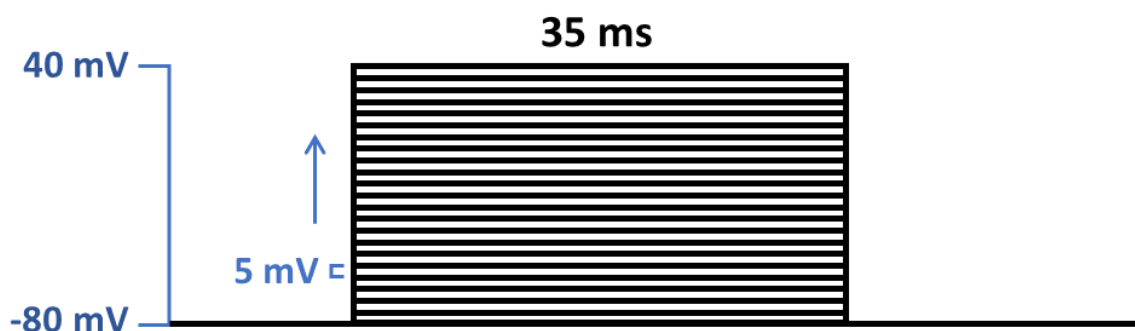
Figure 1.8. Illustrated protocol for Voltage dependence activation.

PROTOCOL: The membrane potential was held at -80 mV, then a series of 25 depolarising voltage test pulses of 35 ms duration were applied at 1 s intervals, starting at -75 mV and then increasing in 5 mV increments until rise up to +45 mV (Fig 1.8).

Resultant sodium currents were measured and normalised for each cell, then mean values plotted against test pulse voltage. Peak current (I_{peak}, peak amplitude of sodium inward current) was plotted against the tested potential (V_T) and fitted with a modified Boltzmann equation (Boltzmann IV) (**Equation 1**) to obtain the reversal potential (V_{rev}), membrane potential when channel response (I_{peak}) reaches 0 again after inactivation). The data was then converted to conductance (G) (**Equation 2**), normalized for each oocyte (**Equation 3**), and plotted against their corresponding V_T. Normalized values were fitted with a Boltzmann sigmoidal equation to permit the estimation of the half-maximal activation voltage ($V_{50,act}$) and the slope factor (k_{act}).

Equation 1
$$I_{peak} = G_{max} \frac{V_{T.act} - V_{rev}}{1 + \exp(\frac{V_{T.act} - V_{50,act}}{k})}$$

Equation 2
$$G = \frac{I_{peak}}{V_{T.act} - V_{rev}}$$

Equation 3
$$G_{norm} = G/G_{max} = \frac{1}{1 + \exp(\frac{V_{T.act} - V_{50,act}}{k})}$$

Where **I_{peak}** is the peak sodium current amplitude; **G** is the sodium (Na^+) conductance values at each V_T; **G_{max}** is the total sodium conductance, or maximal conductance; **G_{norm}** is the Conductance normalized; **$V_{T.act}$** is the Test potential, or membrane potential tested (mV); **V_{rev}** is the Reversal potential (mV); **$V_{50.act}$** is the voltage for half maximal current activation, in other words, the voltage at which 50% of the available channels are activated, or half of maximal current response is elicited; and **k** is the slope factor (mV).

The fast activation and inactivation kinetics of the channel can be obtained from records obtained by the voltage dependence of activation protocol. Inward current plots

were fitted with a single exponential (**Equation 4**) on the onset or decay of the induced current elicited by the step depolarisation (see Fig. 1.9). This allows obtaining the time constant of the exponential, also known as *tau* onset (τ_{onset}) or decay (τ_{decay}) in the respective case. The time constant represents an estimate of the speed of channel for activating or inactivating at a given depolarising membrane voltage.

Equation 4 $\quad\quad\quad\quad I_{(t)} = a_0 + a_1 \exp(-t/\tau1)$

Where $\mathbf{a_0}$ is the initial value for the amplitude of the exponential, $\mathbf{a_1}$ is the height of the exponential (i. e. the span of the onset or decay); $\mathbf{t}$ is time and τ_1 (*tau*) is the time constant of the exponential. The time constant (τ_1) values for each test potential were plotted against the step depolarization values.
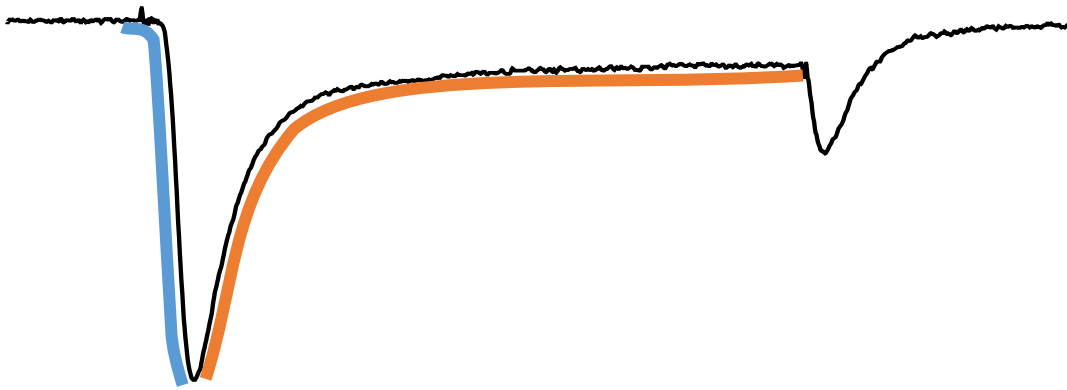
Figure 1.9. Illustrated example of fitting a single exponential function to the onset (blue line) and decay phase (orange line) of the inward sodium current. The *tau* value of the fast activation (τ_{onset}) and inactivation kinetics (τ_{decay}) is the time constant of the exponential fit.

P.2) Steady-state inactivation: this protocol allows the estimation of voltage dependence on fast inactivation (also known as steady-state inactivation). This could be measured when in two consecutive activation pulses, the membrane potential of the first pulse alters the response in the second activation pulse. The level of activation in the second pulse will be influenced by the time required for completing inactivation and deactivation of the channels that have been opened on the first pulse. With this protocol we could estimate the membrane potential voltage for half inactivation

(V$_{50,inact}$), the potential at which approximately half of the available channels are in an inactivated state.
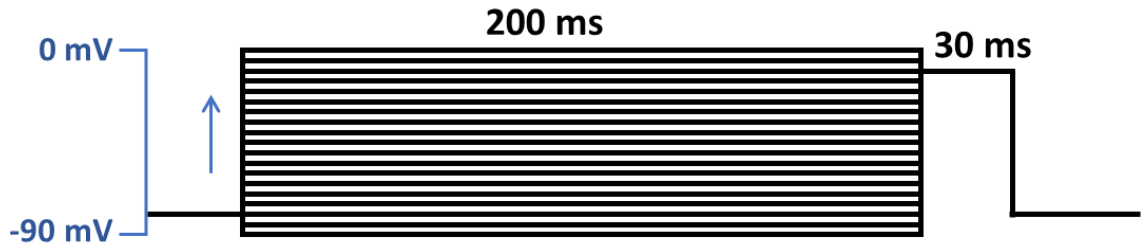
Figure 1.10. Illustrated protocol for Steady state inactivation.

PROTOCOL: from holding current (-80mV), application of a 200 ms inactivation pre-pulse in the range of -90 mV to 0 mV, in 5 mV increments, followed by a 30 ms test pulse to -20 mV (Fig. 1.10).

The test pulse at -20 mV would trigger immediate channel activation, but this would be influenced by the pre-pulse potential. The more positive pre-pulse potential the more channels would be in an inactivated state in the test pulse, and consequently, would not being activated by the second pulse, thus the smaller the second sodium current. The analysis of the peak sodium current produced by the -20 mV test depolarisation, for each pre-pulse value, would enable to establish voltage dependence of steady-state inactivation of the channel (V$_{50,inact}$). Peak current data for test depolarization (I$_{peak}$) were plotted as normalized current (I$_{peak}$/I$_{max}$) against inactivating pre-pulse voltage (V$_{T,inact}$), and fitted with a Boltzmann sigmoidal equation to obtain the voltage for half maximal inactivation (V$_{50,inact}$) (**Equation 5**).

$$\textbf{Equation 5} \qquad I_{peak} = \frac{Bottom + (Top\text{-}Bottom)}{1 + e^{(\frac{V_{T,\,inact} - V_{50,\,inact}}{k})}}$$

Where **I$_{peak}$** is the peak sodium current amplitude elicited for a single inactivating pre-pulse; **V$_{T.inact}$** is the pre-pulse voltage (mV); **V$_{50.inact}$** is the voltage at which it is estimated 50% of the channels are inactivated; k is the slope factor (mV); **Bottom** represents the bottom plateau (I$_{min}$ minimal peak current elicited for a series of test pulses) and **Top**, the top plateau (I$_{max}$, maximal peak current elicited for a series of test pulses).

P.3) Tail currents: To quantify the effects of mutations at position 925 on the affinity of acaricidal pyrethroids, it is necessary to have a measure of the fraction of sodium channels modified by this ligand. This protocol can give a good measure and visualisation of channel sensitivity to pyrethroids. The repeated activation (see above) maximizes the effect of the pyrethroids in the channel, since they are known to bind most effectively to the open (activated) channel. Upon repolarisation, following a test depolarisation, the channel should be closed so any residual current indicates pyrethroid modification of the channel by the pyrethroids.
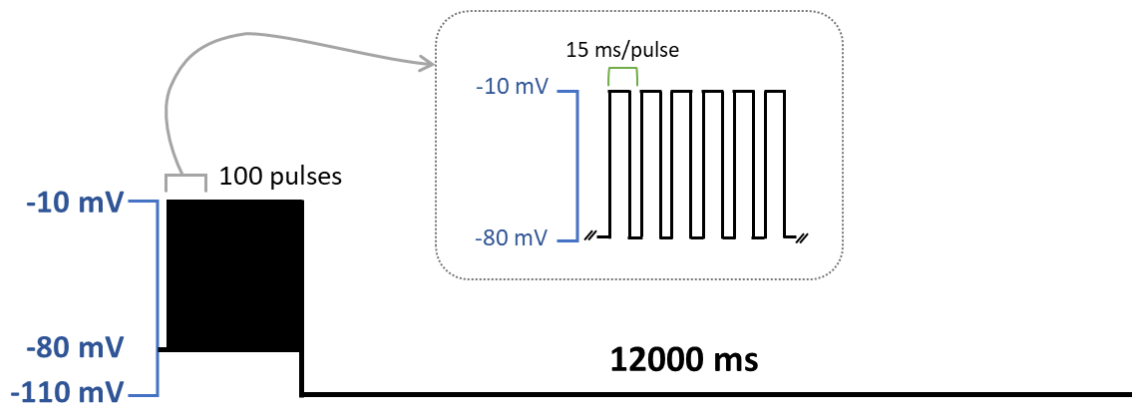
Figure 1.11. Illustrated tail current protocol.

PROTOCOL: 100 depolarisation pulses (5 ms, 66 Hz) from holding potential at -80 mV to -10 mV were applied to repeatedly activate the channels, in 15 ms intervals (sufficient time for recovery from open state inactivation), followed by repolarization of the membrane to -110 mV for 12 s (Fig. 1.11). The tail current is measured during this final repolarizing phase.

Taking into account the elicited amplitude and length of tail currents, we can estimate the percentage of sodium channels modified (M) by the pyrethroid at a given concentration and the potency of the given pyrethroid (M_I) (Vais et al., 2000b).

The conductance of pyrethroid-modified channels ($G_{Na,pm}$) can be calculated by the **equation 6**; where I_{tail} is the amplitude of the peak current, V_{tail} is the voltage of the tail current measurement (-110 mV in our studies) and V_{rev} is the reversal potential (obtained by **equation 1**).

Equation 6 $\qquad G_{Na,pm} = \dfrac{I_{tail}}{V_{tail} - V_{rev}}$

Tail currents were normalized to the maximum sodium conductance for each cell (G_{max}, obtained by **Equation 1**) and expressed as percentages of modified channel (**Equation 7**). In the absence of pyrethroid the tail current is effectively zero.

Equation 7 $\qquad M(\%) = \dfrac{G_{Na,pm}}{G_{Max}} \times 100 = \dfrac{\left(\dfrac{I_{tail}}{V_{tail} - V_{rev}}\right)}{G_{Max}} \times 100$

To estimate the potency of the pyrethroids effect on the channel, we need to consider the duration of the tail current. By introducing the time constant value of exponential fit (*tau* or $I_{tail,integ}$, measured in seconds) we can obtain the integral modification (M_I) (**Equation 8**).

Equation 8 $\qquad M_I(\%) = I_{tail,\ integ} \times M(\%) = I_{tail,\ integ} \times \dfrac{\left(\dfrac{I_{tail}}{V_{tail} - V_{rev}}\right)}{G_{Max}} \times 100$

M_I was plotted against pyrethroid concentration and fitted by a four-parameter logarithmic equation to estimate the maximum integral modification ($M_{I,max}$) and the half maximal effective concentration for the pyrethroid (EC_{50}, is equal to half $M_{I,max}$). The resistant factor (RF), that estimates the resistant level exhibited by the mutations, was calculated by **equation 8**, according to Burton *et al.* (2011).

Equation 9 $\qquad RF = \left(\dfrac{WT\ M_{I,\ max}}{Mut\ M_{I,\ max}}\right) \times \left(\dfrac{Mut\ EC_{50}}{WT\ EC_{50,}}\right)$

Where **$M_{I,max}$** is the maximal modification for each concentration of pyrethroid; ant the **EC_{50}** is the half of $M_{I,max}$.

1.3.5. Data analyses

Sodium currents and *tau* values (time constants or $I_{tail,integ}$) were measured by WinWCP V5.4.1, following the plotting, curve fitting and statistical analysis using Graphpad Prism 7 software (Graphpad Software inc., La Jolla, CA). Values of current amplitudes, conductance and modification percentages are expressed as mean ± standard error of the mean (SEM). The statistical significance was determined by one-way or two-

way ANOVA with Dunnett's post-test, indicated in any case. Differences among the confidence intervals was inferred by Tukey test for the $V_{50,act}$ (Supplementary Fig. S1.1, p. 243), $V_{50,inact}$ (Supplementary Fig. S1.2, p. 244), k_{act} (Supplementary Fig. S1.3, p. 245) and k_{inact} (Supplementary Fig. S1.4, p. 246) at increasing concentrations of pyrethroids. Significance was set at $P<0.05$ or as indicated in the table and figure legends.

1.3.6. Chemicals

Pyrethroid reagents were purchased from Sigma (Poole, Dorset, UK).

- **Deltamethrin** ((S)-a-cyano-3-phenoxybenzyl(1R,3R)-3-(2,2-dibromovinyl)-2,2-dimethylcyclopropane-carboxylate) PESTANAL ® (45423, SIGMA). Delivered as powder, the 10 ml stock solution at 10^{-2} M deltamethrin (molecular weight 505.2) was made up by dissolving 50.52 mg of deltamethrin in 10 ml of dimethyl sulphoxide (DMSO, Sigma, St Louis, MO).

- **_tau_-fluvalinate** (_N_-[2-Chloro-4-(trifluoromethyl)phenyl]-D-valine(_RS_)-cyano(3-phenoxyphenyl) methyl ester) PESTANAL® (46294, SIGMA). Delivered as liquid, dissolved in acetonitrile, with a purity of 96.9%. The 0.1 M stock solution was prepared by adding to the vial containing 100 mg of _tau_-fluvalinate (molecular weight: 502.91) DMSO to a final volume of 1.92 mL.

- **Flumethrin** (Cyano(4-fluoro-3-phenoxyphenyl)methyl 3-[2-chloro-2-(4-chlorophenyl) ethenyl]-2,2-dimethylcyclopropanecarboxylate) PESTANAL (46417, SIGMA). 100 mg of Flumethrin (molecular weight 510.38) at 95.7 % purity were provided dissolved in acetonitrile. For a 0.1 M stock solution, DMSO was added to a final volume of 1.87 mL.

Serial dilution from 10^{-2} to 10^{-6} M of each pyrethroid were made up in DMSO. These were applied directly to the 2 ml bath volume to give the final bath concentration of pyrethroid, ranging between 1 nM – 10 μM. Upon application, the pyrethroids were let to diffuse in the bath for 10 min before the voltage protocols lectures were made.

The maximum concentration of DMSO in the bath solution did not exceed of 1% in any case. Previous studies have proven that concentrations of DMSO up to 1% did not have negative effect on oocyte cell (Burton et al., 2011). However, concentration above

1% can be detrimental to oocyte stability, and when this is above 5%, all oocytes perish (Ian Mellor personal communication) (Burton, 2012).

1.4. Results

1.4.1. Sequence and cloning

The complete CDS of the *Vd*VGSC was cloned in the plasmid pGH19 for the wild-type (*para*) channel and the mutant variations at position 925. Despite the modification in the bacterial propagation procedure, we found plasmids that had random mutations in the *Vd*VGSC DNA with high frequency. These mutations ranged from large-scale rearrangement to point mutations, such as deletions, or insertions. Even bacterial colonies that had been verified by sequencing to carry the plasmid correctly suffered subsequent mutations when further cultures were performed (data not shown).

Cloned wild-type and sodium channels mutated at position 925 were fully sequenced to discard the presence of any unwanted mutations that would disrupt the proper translation of the channel. The predicted amino acid sequences were compared with the corresponding sequences from the previous *Vd*VGSC functional expression studies published to date (Du et al., 2009; Gosselin-Badaroudine and Chahine, 2017). The wild-type *Vd*VGSC cloned and expressed in this work featured several variations with respect to the amino acid sequence of the previous *Vd*VGSC functionally characterized by electrophysiological methods (Fig. 1.12, Table 1.1).

Our sequences contained the optional exon B-like sequence (VSIYYFST) documented in the Nav1 channel (VGSC) of *Blattella germanica*, which corresponds to aa 818-825 in *V. destructor* (Du et al., 2009; Song et al., 2004). Our constructs also contained the optional exon 2 (position 1147-1152) (Figure 1.11, Table 1.1) named by Gosselin-Badaroudine and Chahine (2017) and absent in their *Vd*VGSC construct. The additional sequence differences were single amino acid changes resulted from single-nucleotide mutations, that can be attributed to the genomic variation (Fig. 1.12). These variations were inspected using Phyre2 protein simulator with the SuSPect package (Kelley et al., 2015; Yates et al., 2014). None of them entail any position reported to alter pyrethroid susceptibility, nor does it seem to have any effect on protein functionality (Fig. 1.12; Supplementary Fig. S1.5, p. 247).
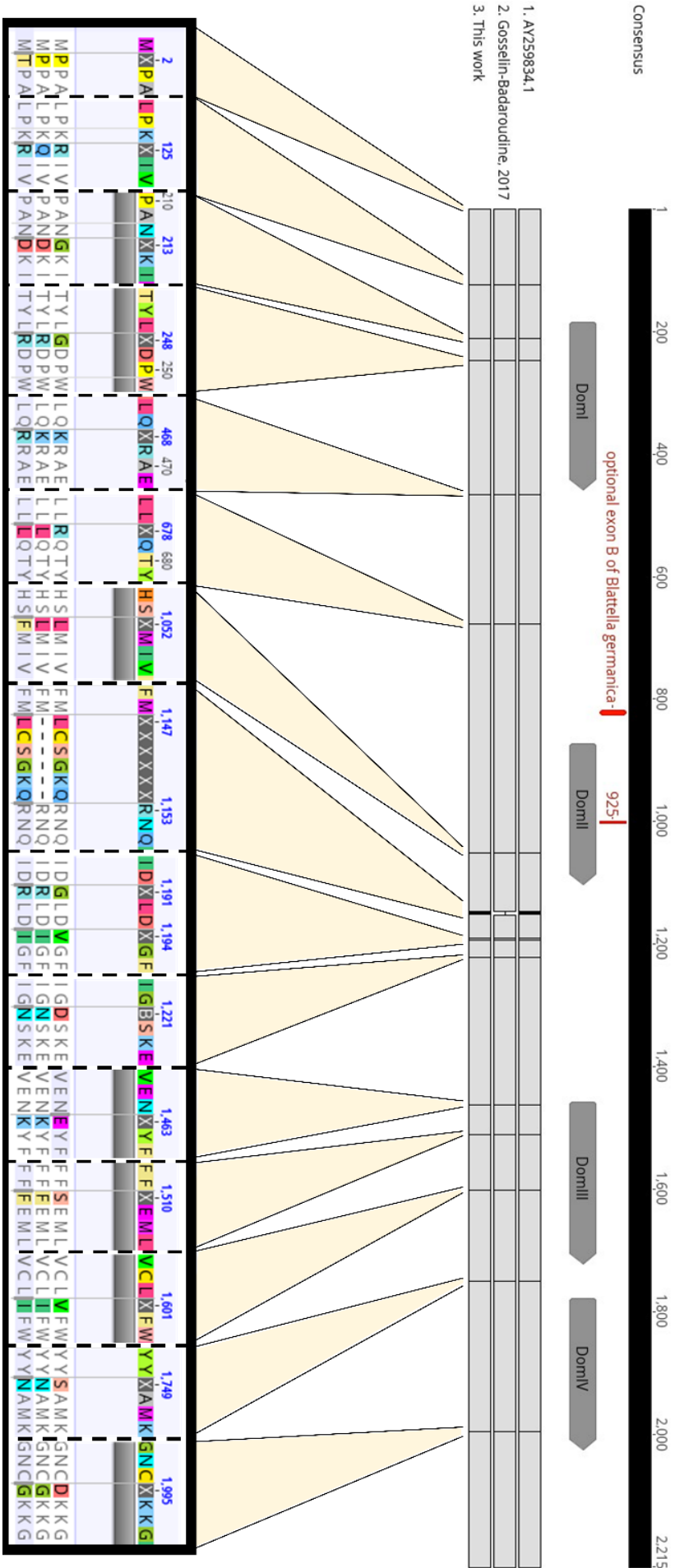
Figure 1.12. Amino acid sequence comparison of the wild-type VGSC construct of this work with the constructs of previous TEVC works published to date: AY259834.1 (Du et al., 2009) and Gosselin-Badaroudine and Chahine (2017). The analogue optional exon B of *B. germanica* and the residue L925 location are indicated.

Table 1.1. Amino acid differences with respect to the *V. destructor* sodium channels in TEVC studies to date (Du et al., 2009; Gosselin-Badaroudine and Chahine, 2017).

Residue position	AY259834 (Du et al., 2009)	Gosselin-Badaroudine and Chahine (2017)	This work	Location
2	Phe	Phe	Thr	N-terminal tail
125	Arg	Gln	Arg	N-terminal tail
213	Gly	Asp	Asp	IS1-IS2 linker
248	Gly	Arg	Arg	IS2-IS3 linker
468	Lys	Lys	Arg	I-II linker
678	Arg	Leu	Leu	I-II linker
1052	Leu	Leu	Phe	II-P1
1147 - 1153	LCSGKQ	Deletion	LCSGKQ	II-III linker
1191	Gly	Arg	Arg	II-III linker
1194	Val	Ile	Ile	II-III linker
1221	Asp	Asn	Asn	II-III linker
1463	Glu	Lys	Lys	II-III linker
1510	Ser	Phe	Phe	IIIS2
1601	Val	Ile	Ile	IIIS3
1749	Ser	Asn	Asn	III-IV linker
1995	Asp	Gly	Gly	IVS5-IVS6 linker
Amino acid properties:	**Non-polar**	**Polar**	**Acidic** (Positive charged)	**Basic** (Negative charged)

Table lists the 16 differences between the three constructs (wild-type channels, L925), indicating the residue position that is different (numbered after the *Vd*VGSC amino acid sequence, AY259834.1) and its location in the VGSC protein structure. Cell colours denote the side chain properties of the amino acid, being green for non-polar, pink for polar, orange for acidic, and green for basic.

The CDS of the channel for the mutation L925V and L925I only differs on this specific amino acid from the wild-type (*para*) channel. An additional modification at position 1400 (K1400E) was found in the L925M construct, located in the linker connecting domains II and III (Figure 1.13). This variation does not imply any reported position altering pyrethroid susceptibility, nor does it seem to have any effect on protein function, as predicted by Phyre2 protein simulator with the SuSPect package (Figure 1.12) (Kelley et al., 2015; Yates et al., 2014).
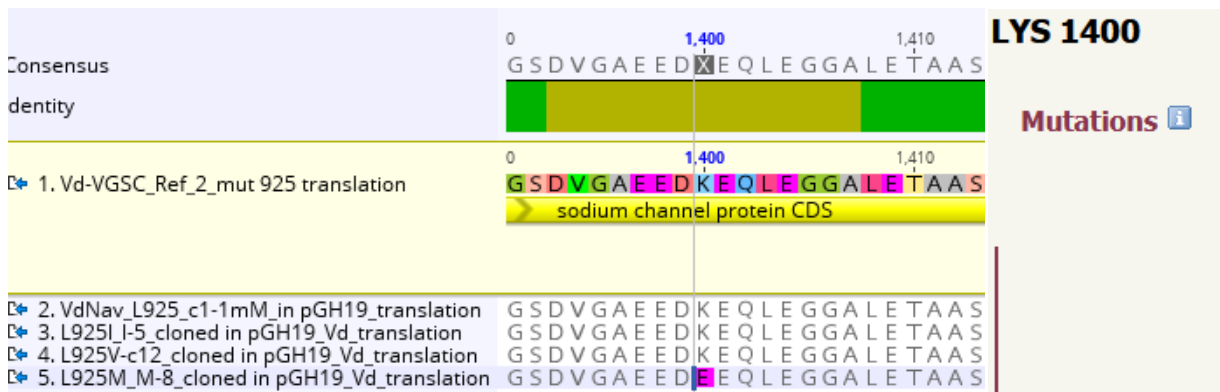
Figure 1.13. Prediction of the mutation effect on protein function are made using the SuSPect method (Yates et al., 2014). The mutational analysis graph represents the predicted effect of mutations at a particular position in the sequence. The coloured bars indicate the probability that a mutation to the corresponding residue will have some effect on function of the protein or on the phenotype of the organism. The warmer colour (max. red, min. dark blue) and tallest the bar, the highest likelihood that mutation affects the protein function.

1.4.2. Electrophysiological characterization of the wild-type and mutated channels at position 925.

All three modified channels examined as well as the wild-type channel were found to be functionally expressed in *Xenopus* oocytes. For all channels tested, sodium currents were detected five to ten days after cRNA injection. Even though the amplitude of the peak obtained were variable depending on the oocyte, the detected sodium currents were robust and sufficient for functional characterization (> 1uA) (Fig. 1.14). All expressed *Vd*VGSC exhibited the typical kinetics of a voltage-gated sodium channel (Fig. 1.14 and 1.15), featuring step voltage dependence of activation and fast inactivation (Fig. 1.16). As expected, the activation and inactivation response were function of the magnitude of the voltage steps (membrane depolarization). Table 1.2 shows the voltages for half-maximal activation ($V_{50,act}$) and inactivation ($V_{50,inact}$), and the associated slope factor (k) for each channel construct analysed.
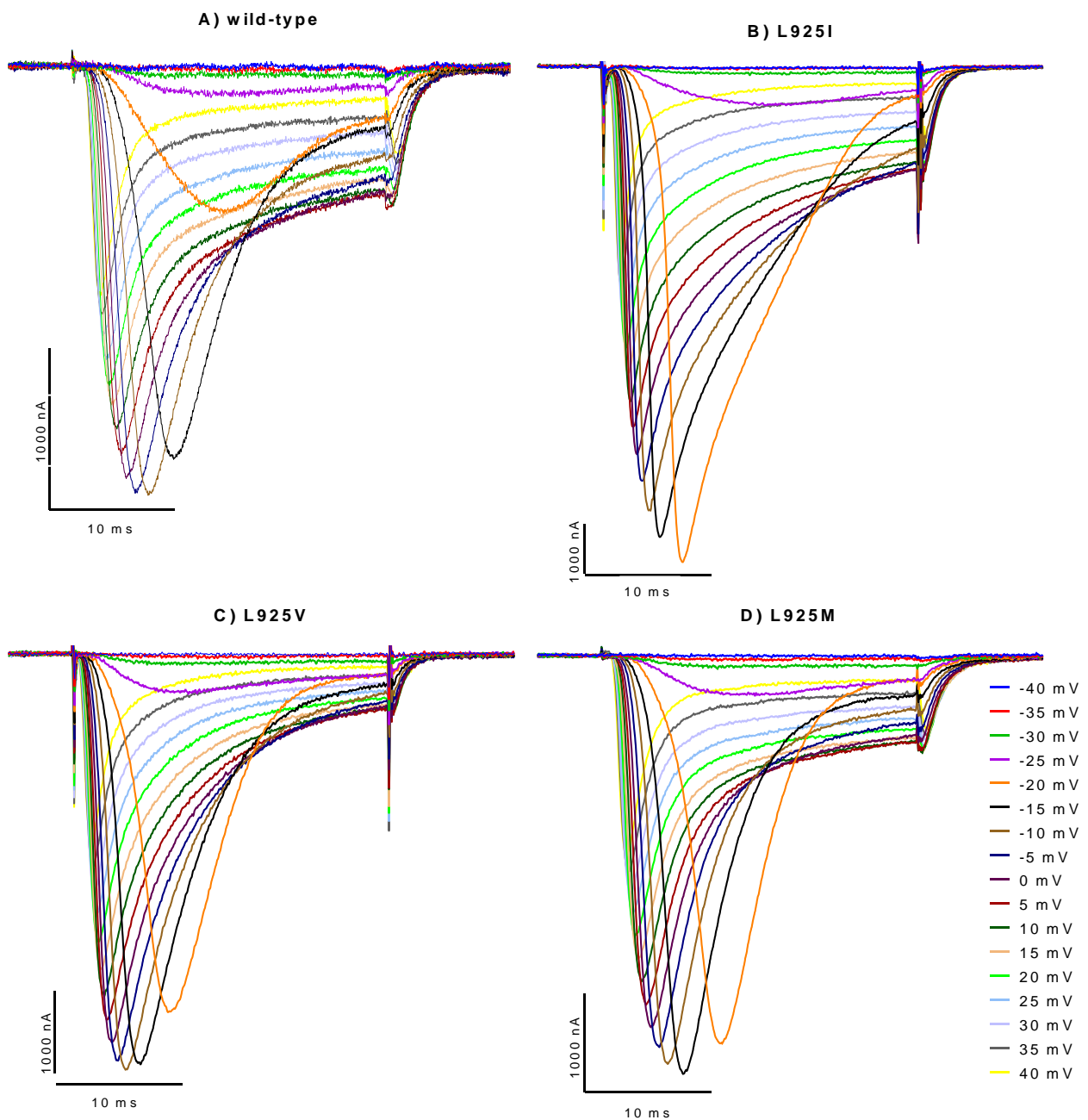
Figure 1.14. Sodium current traces recorded in response to increasing depolarization steps (see voltage dependence of activation protocol (protocol P.1), p. 99) for the wild-type channel of *V. destructor* (A) and the three mutants L925I (B), L925V (C) and L925M (D). Figures show inward currents elicited for membrane potentials (V_T) in the range of -45 to +40 mV in 5 mV increments. Legend indicates the V_T in mV. Data recordings corresponds to a single oocyte. Peak inward currents (I_{peak}) at each step were recorded and analysed. Traces recorded using WinWCP V5.4.1 software (University of Strathclyde, UK).

Activation

V_T (mV)
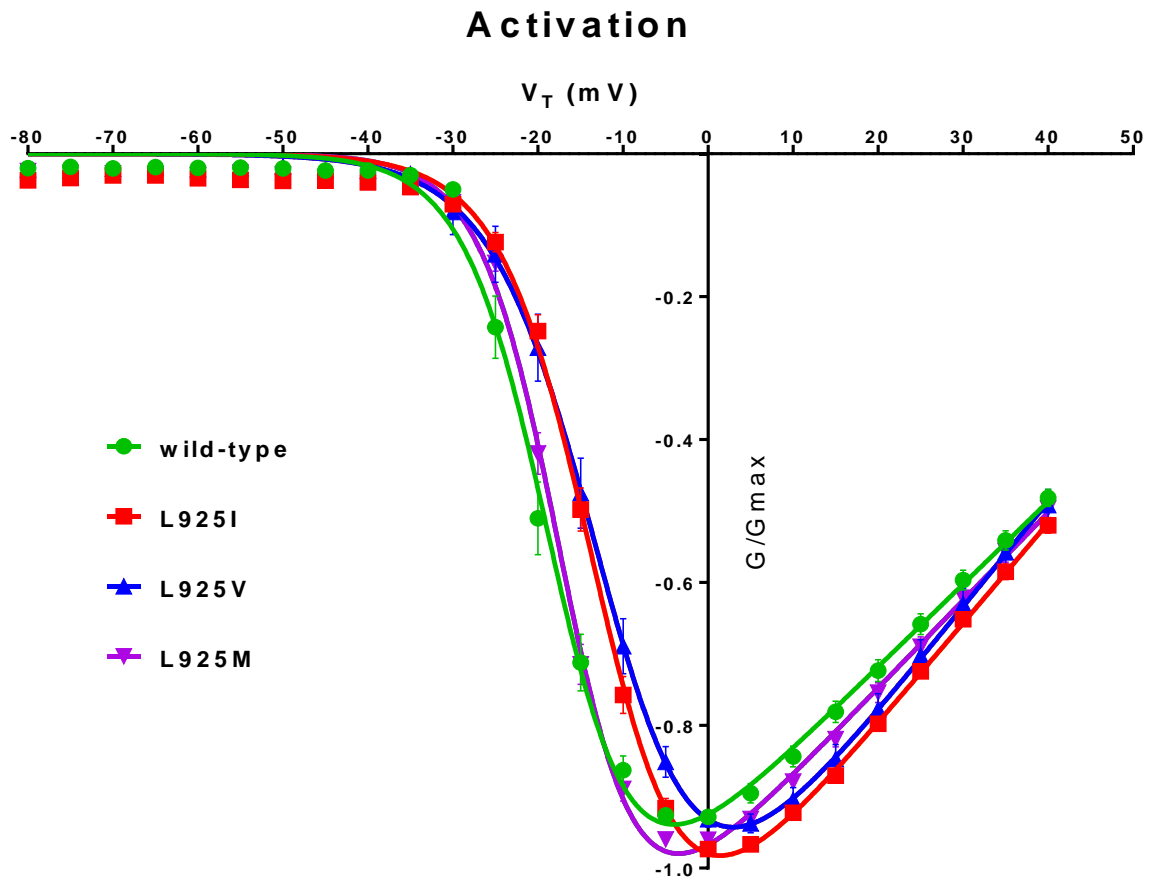
Figure 1.15. Relation between membrane voltage and normalised current for the wild-type and L925 mutant *Vd*VGSC constructs. Values are given as mean ± SEM. Legend: Green dots for the wild-type channel, red square for L925I, blue triangle for L925V; and pink inversed triangle for L925M.

In absence of pyrethroids, all three 925 mutant channels have their $V_{50,act}$ significatively shifted towards the depolarizing direction. However, this shift was more acute for mutants L925I and L925V, shifting more than 5 mV in the positive direction. The shift was 'only' 2 mV for L925M. On the other hand, only the $V_{50,inact}$ for L925M showed a significant shift to more negative voltage when compared to the wild-type channel (Fig. 1.16, Table 1.2). All channels showed a rapid activation and inactivation (Fig. 1.16), exhibiting a 5-10% post-inactivation residual current (also known as late sodium or non-inactivation current), that was slightly lower in the three mutant channels (Fig. 1.16B and C).

Table 1.2. Gating properties for activation and steady-state inactivation for the wild-type and mutant VGSC of *V. destructor* expressed in *Xenopus* oocytes.

		Activation	**Inactivation**
wild-type	V_{50}	**-18.39** $\pm$ 0.2507	**-31.04** $\pm$ 0.1265
	k	5.05 $\pm$ 0.2181	4.873 $\pm$ 0.1102
	n	26	28
L925I	V_{50}	**-12.96** $\pm$ 0.1871 ****	**-31.4** $\pm$ 0.2294
	k	5.399 $\pm$ 0.1629	5.189 $\pm$ 0.2002
	n	25	25
L925V	V_{50}	**-12.94** $\pm$ 0.3492 ****	**-31.73** $\pm$ 0.1567 *
	k	5.993 $\pm$ 0.3047 **	4.909 $\pm$ 0.1366
	n	19	19
L925M	V_{50}	**-16.45** $\pm$ 0.1619 ****	**-33.91** $\pm$ 0.1302 ****
	k	4.767 $\pm$ 0.1408	4.771 $\pm$ 0.1136
	n	32	29

Values are expressed as mean $\pm$ SEM (mV). V_{50} is the voltage for half-maximal activation or inactivation ($V_{50, act}$ and $V_{50, inact}$, respectively), k is the slope factor (k_{act} for activation and k_{inact} for inactivation), and n is the number of oocytes tested. Statistical comparisons were drawn for all values of mutant channels compared to the wild-type channel. One- way ANOVA with Dunett's post-test, *$P<0.05$, **$P<0.01$, ***$P<0.001$, ****$P>0.0001$.

All channels displayed a substantial overlap in the voltage dependence of activation and inactivation curves, creating a potential window current at which channels can open but not inactivate completely (Fig. 1.16C). At the crossing point of the activation and inactivation curves, at voltages of -26 to -20 mV, there are about 25% of the wild-type and 18% of the mutant channels that do not inactivate. Therefore, these channels have the potential to open and produce inward currents.
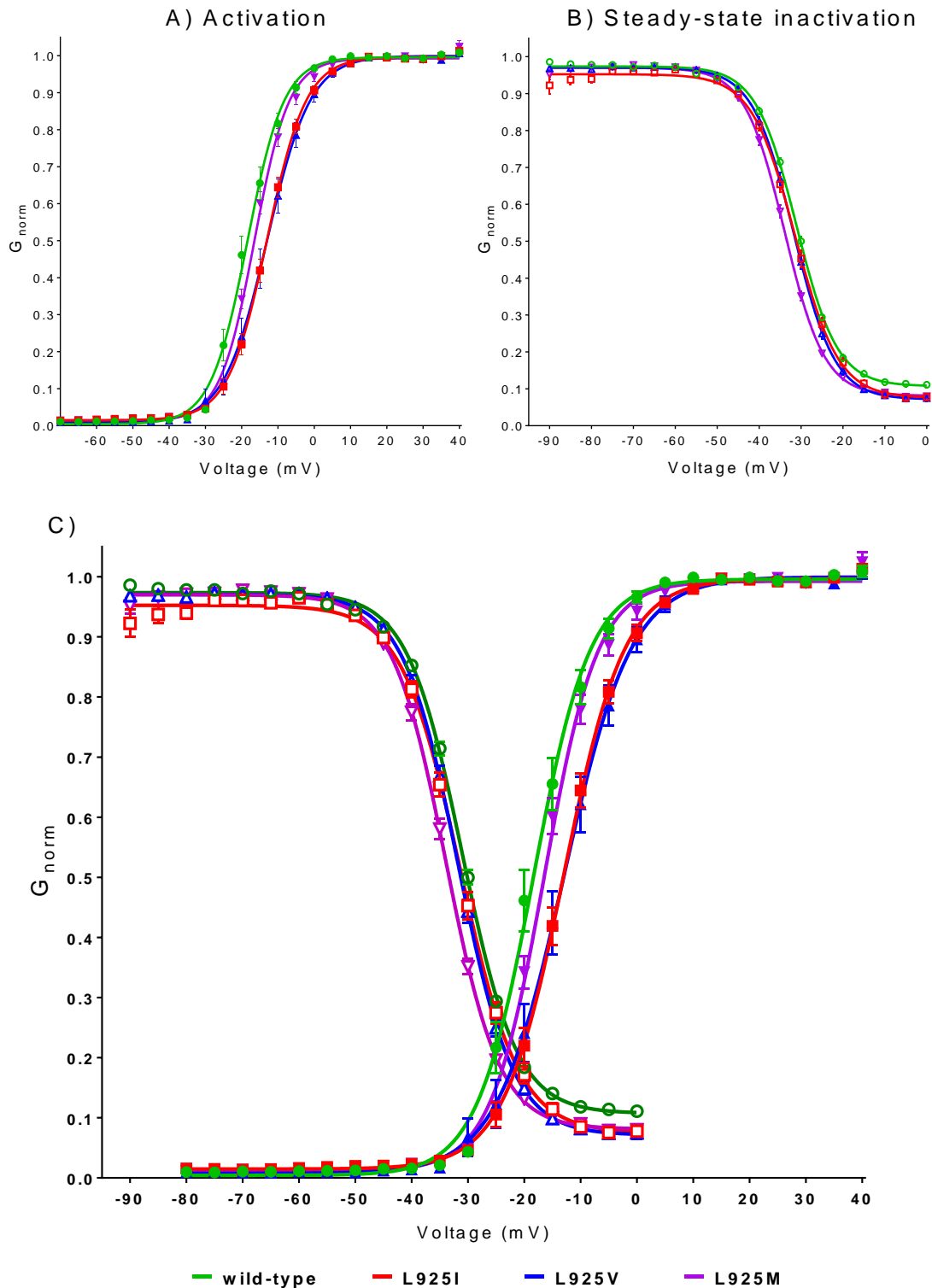
Figure 1.16. Functional characteristics of wild-type and L925 modified *Vd*VGSCs expressed in *Xenopus* oocytes. Voltage dependence of activation (**A**) and inactivation (**B**) is shown as mean normalized conductance (± SEM) fitted with a Boltzmann equation and plotted against Voltage (mV) (see protocols for activation (P.1) and steady-state inactivation (P.2), p. 99-101). Data values of V_{50} and the curve slope for activation and inactivation are given in Table 1.2. (**C**) Merged curves of activation (filled symbols) and inactivation (empty symbols) conductance dependent of voltage. Legend colour: wild-type in green, L925I in red, L925V in blue, and L925M in pink.

Fast activation and inactivation

Inward currents records were also analysed to determine the onset and decay time constants (τ_{onset} and τ_{decay}, respectively). The time constant at onset and decay are measures that indicate the rate of rapid activation and recovery from activation (fast inactivation) for a sodium channel at a certain membrane voltage. By comparing the *tau* onset and *tau* decay values of the wild-type *Vd*VGSC with the 925-mutant *Vd*VGSCs, it is possible to determine whether these amino acid substitutions influence the rapid activation or inactivation of the channels at different depolarisation voltages. Thus, the fast activation (τ_{onset}) and inactivation kinetics (τ_{decay}) of each L925-mutant channel were examined and compared to the wild-type channel.

Fast activation

The *tau* onset was obtained by fitting a single exponential function spanning from the point of the membrane depolarising stimuli to the peak of the inward current (see Fig. 1.9, p. 101). The *tau* onset value exemplifies the fast of channel for activating, measured in milliseconds (ms). All channels showed decreasing values of the time constants of activation as membrane depolarisation steps increased (Table 1.3, Fig. 1.17), indicating that the activation is sharper at highest depolarizing potentials. The wild-type channel has a significantly slower activation than the mutated L925V and L925M channels at membrane voltages of -20 mV. No significant differences were found between the wild-type and the 925-mutated channels for depolarizing voltages above -20 mV.

Table 1.3. Onset time constant (τ_{onset}) of *Vd*VGSC activation for wild-type and 925-mutant VGSC of *V. destructor* between -25 and +40 mV test depolarizations.

	τ_{onset} (ms)			
V_T	wild-type	L925I	L925V	L925M
-25	3.56 ± 0.64 (11)	3.63 ± 0.49 (6)	3.25 ± 0.90 (6)	2,77 ± 0.27 (11) **
-20	2.42 ± 0.12 (23)	2.84 ± 0.29 (15)	2.91 ± 0.29 (10) *	3.47 ± 0.23 (19) ****
-15	2.51 ± 0.14 (32)	2.52 ± 0.21 (15)	2.41 ± 0.21 (16)	2.44 ± 0.18 (19)
-10	2.12 ± 0.15 (33)	2.08 ± 0.19 (17)	2.16 ± 0.18 (17)	1.92 ± 0.13 (19)
-5	1.73 ± 0.11 (33)	1.72 ± 0.15 (17)	1.90 ± 0.17 (17)	1.52 ± 0.09 (19)
0	1.39 ± 0.07 (33)	1.39 ± 0.11 (17)	1.53 ± 0.12 (17)	1.27 ± 0.07 (19)
5	1.23 ± 0.07 (33)	1.20 ± 0.09 (17)	1.23 ± 0.08 (17)	1.09 ± 0.06 (19)
10	1.10 ± 0.06 (33)	1.03 ± 0.07 (17)	1.12 ± 0.08 (17)	0.97 ± 0.05 (19)
15	0.97 ± 0.05 (33)	0.93 ± 0.06 (17)	0.97 ± 0.07 (17)	0.87 ± 0.04 (19)
20	0.90 ± 0.05 (33)	0.85 ± 0.06 (17)	0.88 ± 0.05 (17)	0.80 ± 0.04 (19)
25	0.83 ± 0.04 (33)	0.79 ± 0.05 (17)	0.82 ± 0.05 (17)	0.74 ± 0.04 (19)
30	0.77 ± 0.04 (33)	0.72 ± 0.05 (17)	0.78 ± 0.05 (17)	0.69 ± 0.03 (19)
35	0.72 ± 0.04 (33)	0.74 ± 0.05 (16)	0.74 ± 0.04 (17)	0.65 ± 0.03 (19)
40	0.71 ± 0.03 (29)	0.71 ± 0.05 (15)	0.69 ± 0.05 (16)	0.65 ± 0.04 (19)

Values are shown as mean ± SEM (ms). Number of oocytes tested are between brackets. Statistical comparisons were made between the mutant channels and the wild-type. One-way ANOVA with Dunnett's post-test, *$P < 0.05$; **$P < 0.01$; ****$P < 0.0001$.
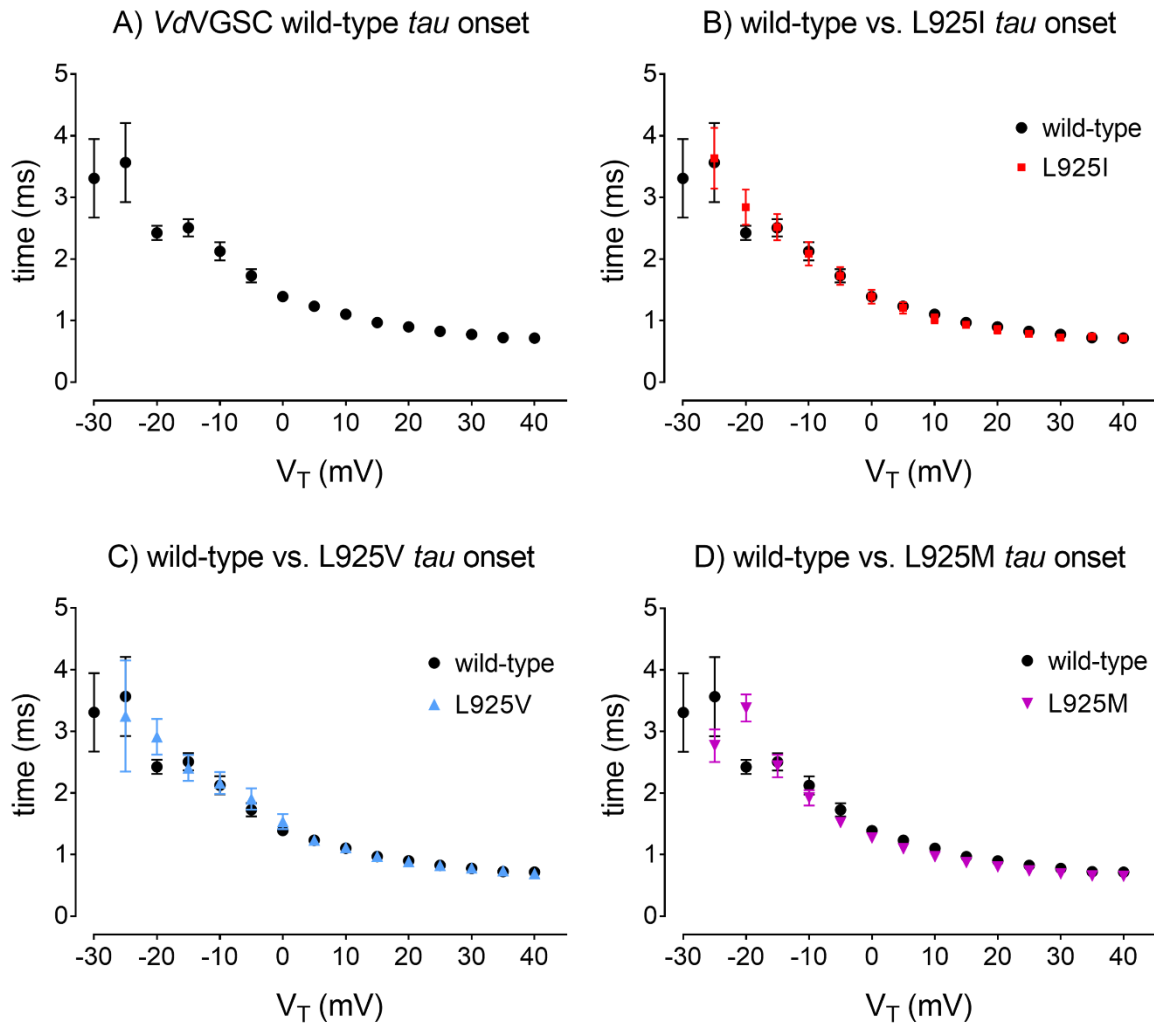
Figure 1.17. Wild-type and 925-mutant *Vd*VGSC fast-activation kinetics. The rate of sodium current onset for each channel construct shown as onset time constants (τ_{onset} (ms)) was plotted against the corresponding test depolarization (V_T (mV)). The wild-type τ_{onset} values (**A**) were compared with the values obtained for the mutant channels L925I (**B**), L925V (**C**) and L925M (**D**). Data is shown as mean ± SEM. Black symbols indicate the values for the wild-type channel, and coloured symbols are for the mutant channels (red square for L925I, blue triangle for L925V; and pink inversed triangle for L925M).

Fast inactivation

The current decay after inward peak current was also fitted with a single exponential function to obtain the time constant on decay. This value reflects the time (in ms) needed for the channel to recover after being activated by a depolarizing pulse. In other words,

the fast inactivation of the channel. So, smaller time decay constant indicates a faster inactivating channel.

The *tau* decay values were obtained by fitting a single exponential to the decay current in the recordings from the Voltage dependence of activation protocol (P.1) (see Fig. 1.9, p. 101). The obtained values for *tau* decay were plotted as a function of the voltage applied (Fig. 1.18). Similarly to the activation, the time constant on decay for all the channels were dropping with the increasing steps of depolarization, suggesting a lower time required for the fast inactivation in relation to higher depolarization voltages.

Table 1.4. Time constant on decay (τ_{decay}) of fast-inactivation rate for wild-type and 925-mutant VGSC of *V. destructor* for currents evoked between -10 and +40 mV test depolarisations.

	τ_{decay} (ms)			
V_T	wild-type	L925I	L925V	L925M
-15	8.10 ± 0.62 (24)	8.31 ± 0.90 (17)	8.23 ± 0.93 (11)	5.62 ± 0.84 (14) ****
-10	6.78 ± 0.82 (28)	6.20 ± 0.56 (17)	7.52 ± 0.82 (15)	5.01 ± 0.31 (19) **
-5	5.54 ± 0.33 (30)	5.07 ± 0.33 (17)	6.27 ± 0.56 (17)	4.44 ± 0.22 (19) *
0	5.09 ± 0.27 (30)	4.56 ± 0.32 (17)	5.26 ± 0.34 (17)	4.07 ± 0.19 (19)
5	4.48 ± 0.20 (30)	4.08 ± 0.27 (17)	4.62 ± 0.30 (17)	3.80 ± 0.18 (19)
10	4.13 ± 0.19 (30)	3.63 ± 0.22 (17)	4.24 ± 0.26 (17)	3.47 ± 0.17 (19)
15	3.67 ± 0.18 (30)	3.40 ± 0.20 (17)	3.94 ± 0.29 (17)	3.28 ± 0.19 (19)
20	3.37 ± 0.19 (30)	2.97 ± 0.15 (17)	3.61 ± 0.28 (17)	3.05 ± 0.19 (19)
25	2.96 ± 0.19 (30)	2.68 ± 0.16 (17)	3.06 ± 0.24 (17)	2.76 ± 0.19 (19)
30	2.52 ± 0.18 (30)	2.34 ± 0.14 (17)	2.74 ± 0.22 (17)	2.50 ± 0.19 (19)
35	2.10 ± 0.14 (30)	2.06 ± 0.14 (17)	2.30 ± 0.17 (17)	2.22 ± 0.20 (19)
40	1.75 ± 0.13 (30)	1.73 ± 0.11 (17)	1.95 ± 0.16 (17)	1.91 ± 0.18 (19)

Values are shown as mean ± SEM (ms). Number of oocytes tested are between brackets. Statistical comparisons were made between the mutant channels and the wild-type. One-way ANOVA with Dunnett's post-test, *$P < 0.05$; **$P < 0.01$; ****$P < 0.0001$.

Recovery from inactivation is faster for L925M mutant sodium channels than for the wild-type at membrane voltage steps from -15 to -5 mV (2-way ANOVA; -15 mV, *P* value= 0.0001; -10 mV, *P* value= 0.0005; -5 mV, *P* value= 0.042). In the depolarizing steps from 0 mV to 10 mV it can be appreciated in the *tau* decay values (Table 1.4, Fig.

1.18D) also a slightly faster inactivation for the L925M than for the wild-type channels, however, these values were not big enough to be statistically significant (2-way ANOVA: 0 mV, *P* value= 0.067). No significant differences in the recovery from inactivation was observed between the L925I and L925V mutant channel compared to the wild-type (Table 1.4, Fig. 1.18).

Comparison of the *tau* decay values with the wild-type channel at a depolarizing voltage of -10 mV revealed that only the L925M mutant channel showed a significant faster recovery from activation. However, no differences were observed between the L925I or L925V compared with the wild-type (Table 1.4, Fig. 1.18).
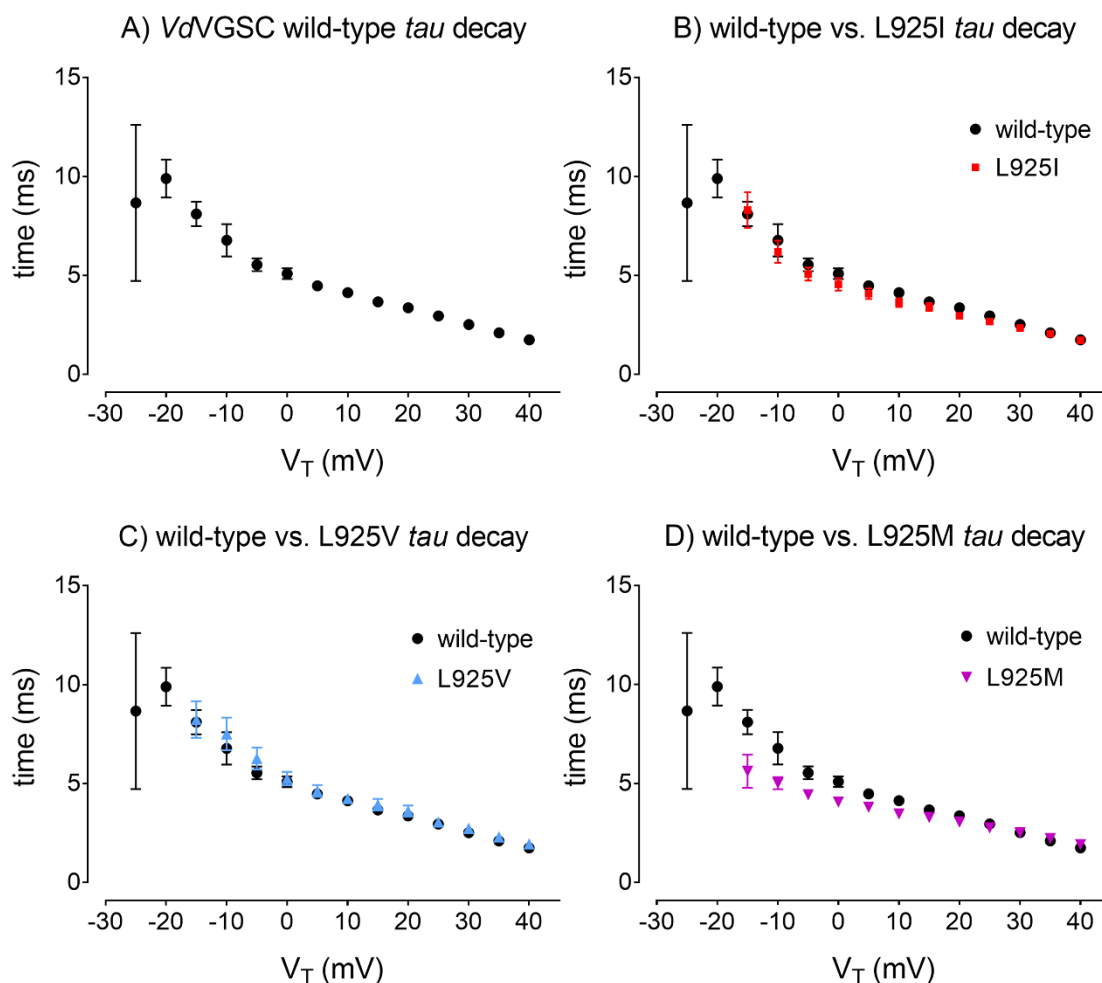
Figure 1.18. Wild-type and mutant *Vd*VGSC fast-inactivation kinetics. The rate of sodium current decay for each channel construct shown as onset time constants (τ_{decay} (ms)) was plotted against the corresponding test depolarization (V_T (mV)). The wild-type τ_{onset} values (A) were compared with the values obtained for the mutant channels L925I (B), L925V (C) and L925M (D). Data is shown as mean ± SEM.

1.4.3. Effect of deltamethrin, flumethrin and *tau*-fluvalinate on wild-type and 925 mutated *Vd*VGSCs

The effect of pyrethroids upon VGSC can be detected by the modification of the gating kinetics in the opening and fast inactivation processes, usually by hampering their rapid action. The inhibitory effect of pyrethroids on these processes can give rise to characteristic features known as tail currents, manifested as a residual sodium current after inactivation (Burton et al., 2011; Thompson et al., 2020; Vais et al., 2000b). Modification on the gating kinetics have been tested for all four variants in the presence of increasing concentration of mite selective (*tau*-fluvalinate and flumethrin) and non-selective (deltamethrin) pyrethroids.

The extremely hydrophobic nature of pyrethroids and their limited solubility in aqueous solution pose difficulties in analysing accurately the exposure to higher concentrations. Thus, concentration response curves for the tail current do not reach the upper plateau, and resistance factors could not be reliably calculated. In addition, the high lipophilicity of pyrethroids may affect the integrity of the oocyte membrane, which may become excessively leaky (permeable) and unsuitable for recording. Therefore, only oocytes of sufficient quality were used for subsequent pyrethroid testing.

1.4.3.a. Effect of deltamethrin upon *Vd*VGSCs

Increasing concentrations of deltamethrin affect the wild-type and L925M channels by shifting the $V_{50,act}$ to more positive membrane potentials. This effect can be observed at concentrations as low as 10 nM. On the contrary, the $V_{50,act}$ of the L925I and L925V channels seems not being influenced by deltamethrin until concentrations higher than 1 µM (Fig. 1.19 and 1.20, Table 1.5). In contrast, the $V_{50,inact}$ of the wild-type channel was not significantly altered until reaching much higher concentrations. It was only after exposure to 1 µM deltamethrin that the $V_{50,inact}$ of the wild-type channel shifted significantly towards more positive voltages. In comparison, $V_{50,inact}$ was not significantly affected in the mutant channels under the experimental conditions (Fig 1.21, Table 1.5). Nevertheless, in all channels tested, the exposure to deltamethrin appears to increase the post-inactivation residual current (late sodium current). The proportion of channels that are not completely inactivated rises in relation to the concentration of toxicant, generating

this late sodium current. This effect is illustrated in the bottom plateau of the inactivation curve (Fig. 1.21).

Activation
Deltamethrin
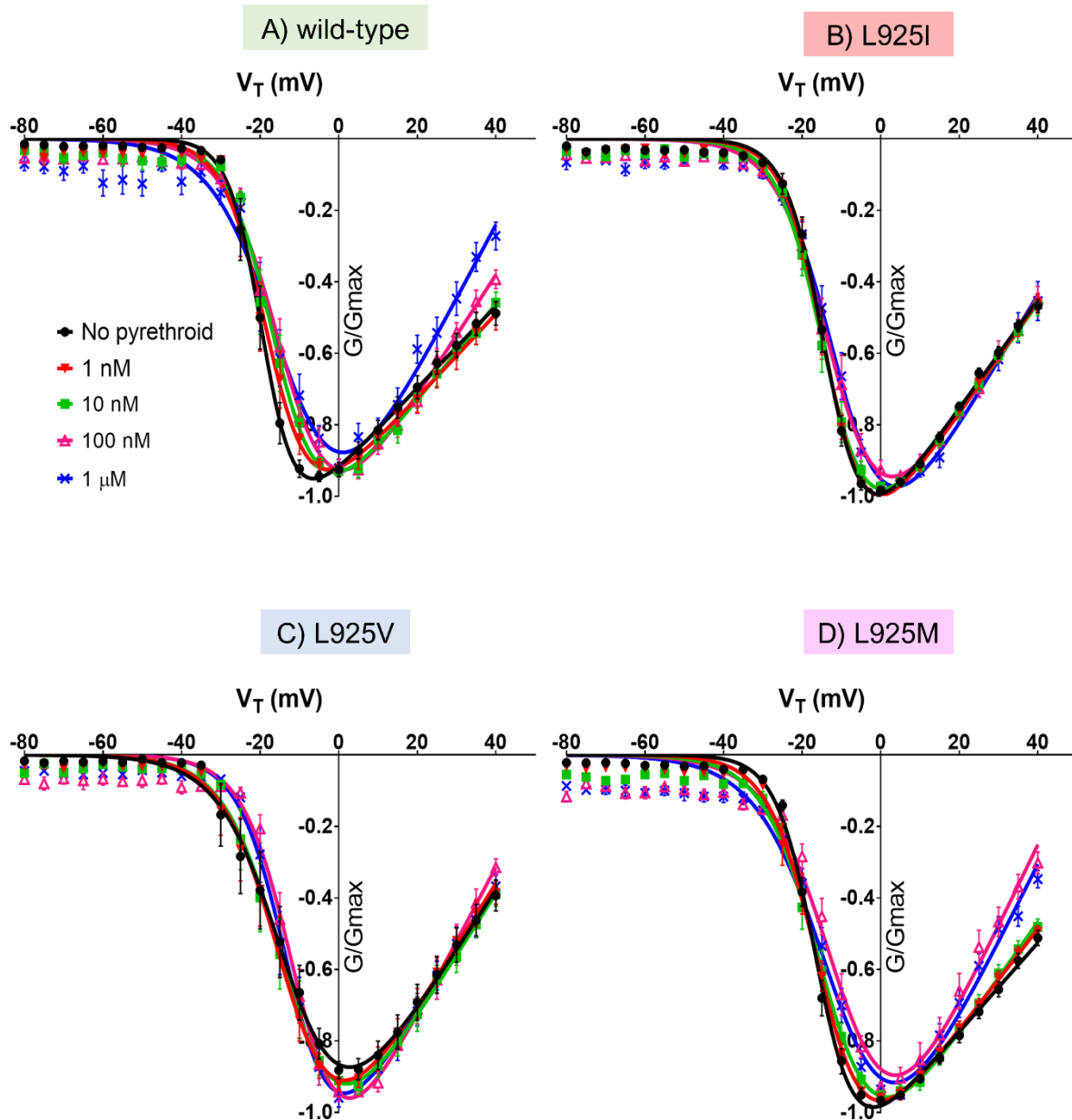
Figure 1.19. Current-voltage relationship for the wild-type (A), L925I (B), L925V (C) and L925M (D) mutant VGSC in presence of increasing concentrations of deltamethrin. Injected oocytes were subjected to a step depolarization protocol (see protocol P.1, p. 99) from -80 mV to +40 mV in 5 ms increments in presence of increasing concentrations of deltamethrin. The normalized peak inward current was plotted against the tested membrane voltage. Legend colour: Black for No-pyrethroid, red for 1 nM, green for 10 nM, purple for 100 nM and blue for 1 µM of deltamethrin.

Activation
Deltamethrin
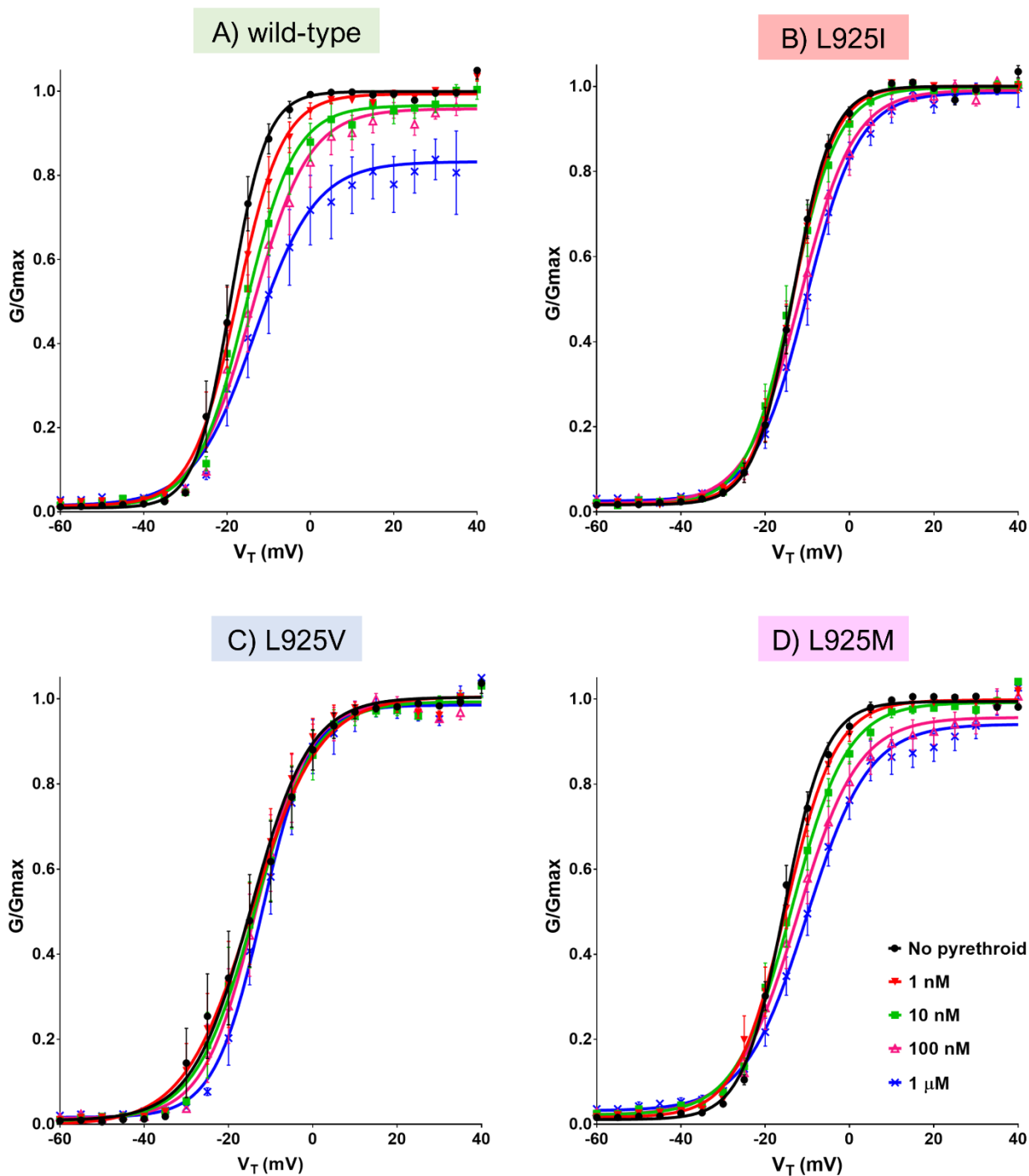
Figure 1.20. Voltage dependence of Activation for *Vd*VGSC wild -type (A) and L925 mutant channels (L925I (B), L925V (C) and L925 (M)) in the presence of increasing deltamethrin concentrations. Conductance normalized, shown as mean ± SEM (mV), was fitted with a Boltzmann equation and plotted against Voltage (mV) (see protocol P.1, p. 99). Data values of $V_{50,act}$ and the curve slope are given in Table 1.5. Legend colour: Black for No-pyrethroid, red for 1 nM, green for 10 nM, purple for 100 nM and blue for 1 µM of deltamethrin

Steady-state inactivation
Deltamethrin

Figure 1. 21. Voltage dependence of steady-state inactivation for *Vd*VGSC wild -type (A) and L925 mutant channels (L925I (B), L925V (C) and L925 (M)) in the presence of increasing deltamethrin concentrations. Conductance normalized, shown as mean ± SEM (mV), was fitted with a Boltzmann equation and plotted against Voltage (mV) (see protocol P.2, p. 101). Data values of $V_{50,inact}$ and the curve slope are given in Table 1.5. Legend colour: Black for No-pyrethroid, red for 1 nM, green for 10 nM, purple for 100 nM and blue for 1 µM of deltamethrin.

Table 1.5. The effects of increasing concentrations of deltamethrin on the gating kinetics of wild-type and L925 modified sodium channels of *V. destructor*.

		DELTAMETHRIN			
		wild-type	**L925I**	**L925V**	**L925M**
No pyrethroid	$V_{50,act}$	-19.12 ± 0.37 (7)	-13.44 ± 0.25 (6)††††	-14.56 ± 0.95 (7)††††	-15.58 ± 0.23 (10)††††
	k_{act}	4.23 ± 0.32	4.65 ± 0.22	7.99 ± 0.84 ††††	4.92 ± 0.20
	$V_{50,inac}$	-31.11 ± 0.21 (7)	-30.39 ± 0.62 (6)	-30.65 ± 0.25 (7)	-34.49 ± 0.22 (10)††
	k_{inact}	4.65 ± 0.19	4.37 ± 0.54	4.56 ± 0.22	4.88 ± 0.19
1nM	$V_{50,act}$	-17.56 ± 0.49 (7)	-13.34 ± 0.27 (6)	-14.71 ± 0.75 (7)	-15.1 ± 0.34 (10)
	k_{act}	5.44 ± 0.43	4.91 ± 0.23	6.99 ± 0.66	5.92 ± 0.30
	$V_{50,inact}$	-30.52 ± 0.28 (7)	-30.3 ± 0.52 (6)	-31.07 ± 0.32 (7)	-33.61 ± 0.36 (10)
	k_{inact}	4.83 ± 0.24	3.95 ± 0.45	4.89 ± 0.27	5.2 ± 0.31
10nM	$V_{50,act}$	-15.54 ± 0.60 (7)***	-13.55 ± 0.36 (6)	-13.86 ± 0.75 (6)	-13.74 ± 0.39 (10)*
	k_{act}	5.92 ± 0.53	5.46 ± 0.31	7.02 ± 0.66	6.6 ± 0.34 *
	$V_{50,inact}$	-29.91 ± 0.45 (7)	-30.29 ± 0.62 (6)	-30.75 ± 0.45 (6)	-33.3 ± 0.63 (10)
	k_{inact}	4.54 ± 0.39	4.97 ± 0.54	5.14 ± 0.40	5.38 ± 0.55
100nM	$V_{50,act}$	-13.96 ± 0.73 (7)****	-11.71 ± 0.55 (5)	-13.5 ± 0.67 (5)	-12.37 ± 0.59 (10)****
	k_{act}	6.78 ± 0.64 **	6.36 ± 0.48	6.23 ± 0.59	7.20 ± 0.52 **
	$V_{50,inact}$	-28.2 ± 0.71 (7)	-28.6 ± 1.05 (5)	-30.69 ± 0.54 (5)	-32.56 ± 0.88 (10)
	k_{inact}	5.45 ± 0.61	4.61 ± 0.91	5.48 ± 0.47	5.99 ± 0.78
1 µM	$V_{50,act}$	-13.34 ± 1.24 (6)****	-10.19 ± 0.44 (5)**	-12.01 ± 0.58 (5)*	-10.24 ± 0.59 (10)****
	k_{act}	7.32 ± 1.09 ***	6.21 ± 0.38	5.7 ± 0.51 *	7.39 ± 0.52 ***
	$V_{50,inact}$	-25.59 ± 2.43 (6)****	-27.32 ± 1.27 (5)	-30.63 ± 0.61 (5)	-32.67 ± 1.28 (10)
	k_{inact}	8.77 ± 1.94 ***	4.6 ± 1.10	4.33 ± 0.53	7.08 ± 1.14 *

The data included in the table for No pyrethroid treatment are those obtained from oocytes that were subsequently subjected to deltamethrin treatment. Data are expressed as means ± SEM (mV). Table shows the values of the voltages for half-maximal activation ($V_{50,act}$) and inactivation ($V_{50,inact}$), and the slope factor for activation (k_{act}) and inactivation (k_{inact}). Numbers in parentheses are the number of oocytes tested. Statistical comparisons were plotted for all V_{50}s and slope factors assessing differences without pyrethroids for mutant channels and the wild-type (†), and within individual channels in the absence of and at specific deltamethrin concentrations (*). Two-way ANOVA with Dunnett's post-test: *,†: $P < 0.05$; **,††: $P < 0.01$; ***,†††: $P < 0.001$; and ****, ††††: $P < 0.0001$.

The most evident detrimental effect of pyrethroids on VGSC channels can be visualized in the induced tail currents. Increasing concentrations of deltamethrin lead to a considerable tail current enhancement for the wild-type and L925M mutant VdVGSC. While, in comparison, the elicited tail current is almost non-detectable in the L925I and L925V mutant VdVGSC. The effect of deltamethrin upon the elicited tail current in the wild-type VGSC revealed that the upper value of modified channels was not reached at concentrations of 3 µM. Consequently, the top plateau of the curve was not achieved, and the %IM and EC_{50} values were estimated through the curve tendency, giving an EC_{50} of 5.5 µM and a maximum integral modification of the channels of around 391%.
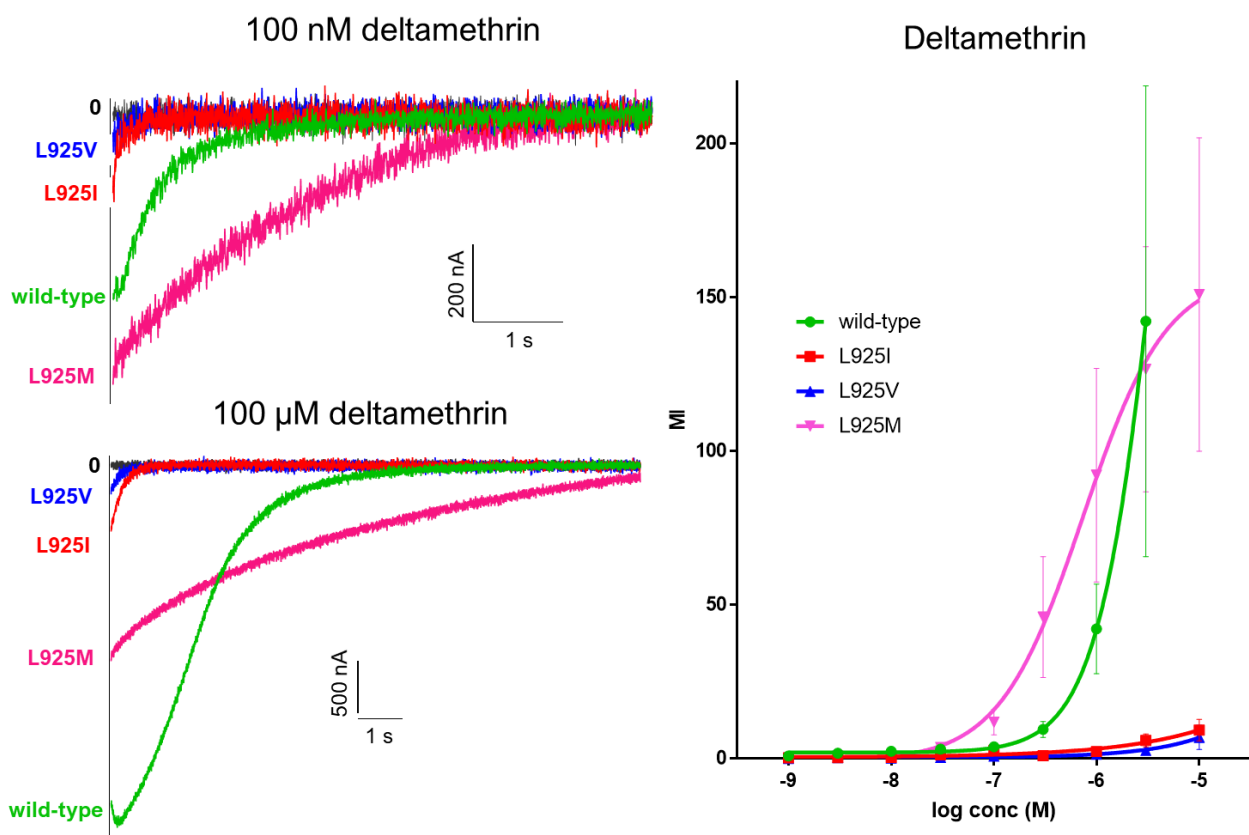
Figure 1.22. Analysis of the tail current elicited by deltamethrin treatment**.** Illustration of a typical tail current recorded from single *Xenopus* oocytes injected with *Vd*VGSC constructs of the wild-type (green), L925I (red), L925V (blue) and L925M mutations (pink) in the presence of 100 nM (A) and 1 µM (B) of deltamethrin. The 0 (black line) indicates the absence of deltamethrin. C) Integral modification (%) of the channels were plotted against the deltamethrin concentration and fitted with a four-parameter logistic equation. EC50, M_{max} and $M_{I,max}$ values are given in Table 1.6 (see tail current protocol P.3, p. 103).

Table 1.6. Resistance to deltamethrin analysed through the elicited tail currents for L925I, L925V an L925M *Vd*VGSC.

Deltamethrin	wild-type	L925I	L925V	L925M
EC_{50} (uM)	4.5	~ 3552	~ 2439	0.7387
$M_{(I),max}$ (%)	391.1	~ 197.3	~ 468.9	158.3
RF_I	1	~86.85	~86.74	2.47
n	6	6	6	9

$EC_{50,I}$, $M_{I,max}$ and RF_I values were determined from plots of MI (based on tail current amplitude and decay time constant) vs. concentration of deltamethrin. Values for the L925I and L925V are estimated by the tendency of the curve since they did not reach the EC_{50}.

We can observe that lower concentrations of deltamethrin have a bigger effect on L925M channels than to the wild-type, but the potential percentage of channels that can be modified by the toxicant is lower for the L925M than for the wild-type (Table 1.6). On the contrary, deltamethrin induced a much lower tail current effect in channels with L925I and L925V mutations. For this mutant construct, the highest % of integral modified channels obtained did not reach the 10% applying 10 µM of deltamethrin. The wide error bar displayed by wild-type and L925M mutated channels indicates the variability found between the oocytes analysed, most probably consequence of the reduced solubility of pyrethroids in the buffer solution at high concentrations.

1.4.3.b. Effect of *tau*-fluvalinate upon *Vd*VGSCs

Tau-fluvalinate shows a similar effect as deltamethrin on the activation kinetics of the *V. destructor* wild-type channel, by shifting the $V_{50,act}$ toward more positive values of voltage (the depolarizing direction). However, this displacement seems enhanced under the influence of *tau*-fluvalinate at the same toxicant concentration. A comparable effect on the $V_{50,act}$ for the modified L925M and L925V channels can be observed, showing also pronounced shifts toward depolarizing voltages in response to increasing exposure to *tau*-fluvalinate. Otherwise, L925I mutant channels revealed no significant variation in $V_{50,act}$ until concentrations of 1 µM (Table 1.7, Fig. 1.23 and 1.24; Supplementary Fig. S1.1, p. 243)

As observed with deltamethrin, the $V_{50,inact}$ values for the wild-type channel were not significantly altered until exposition to 1 µM of *tau*-fluvalinate. The L925M channels shifted to a more positive value from 100 nM of *tau*-fluvalinate. For mutations L925V and L925I, there was no significant change in $V_{50,inact}$ (Table 1.7, Fig. 1.25; Supplementary Fig. S1.2, p. 244). Still, *tau*-fluvalinate displayed an effect upon inactivation as well by boosting the late sodium current (Fig. 1.25). The effect was specially denoted for the wild-type channel, reaching 40% at 1 µM. L925M and L925V channels displayed a similar increase on the post-inactivation residual current, but not as pronounced as the wild-type. This effect was much lower for L925I mutation, that went from 6% without toxicant to 16% at the highest concentration of *tau*-fluvalinate (1 µM).

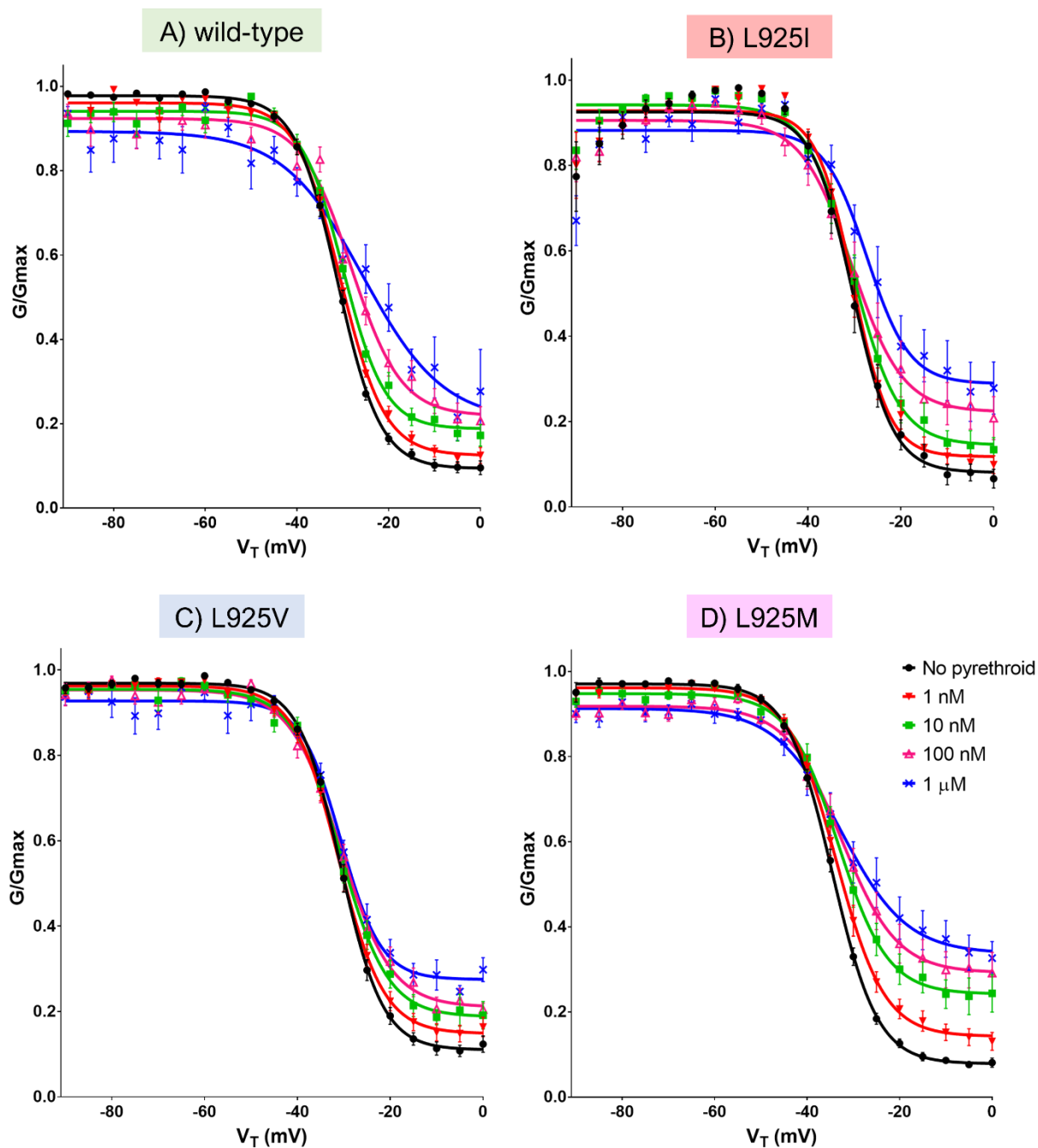# Activation
tau-fluvalinate
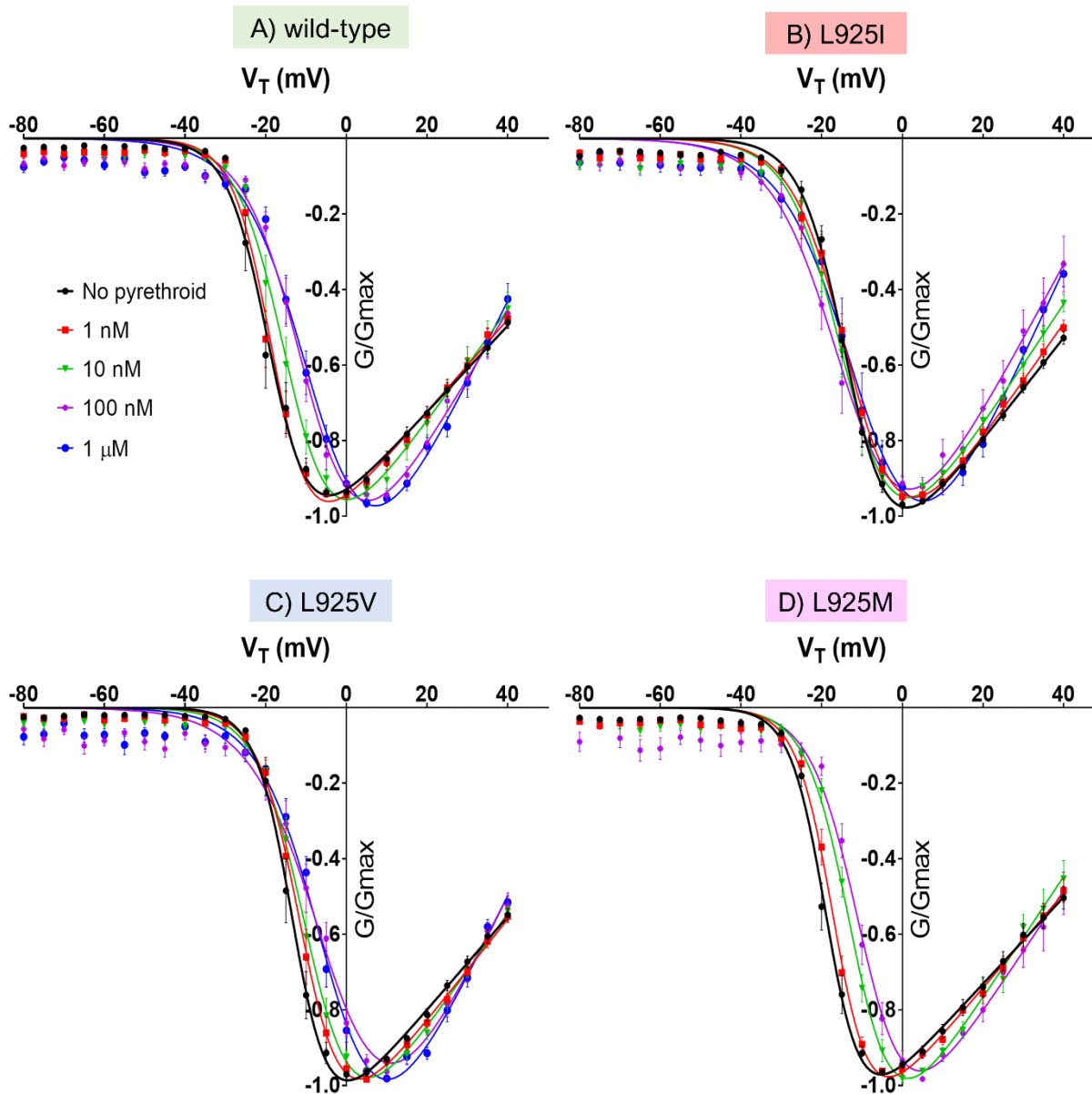
Figure 1.23. Current-voltage relationship for the wild-type (A), L925I (B), L925V (C) and L925M (D) mutants VGSC in the presence of increasing concentrations of *tau*-fluvalinate. Injected oocytes were subjected to a step depolarization protocol (see protocol P.1, p. 99) from -80 mV to +40 mV in 5 ms increments in the presence of increasing concentrations of *tau*-fluvalinate. The normalized peak inward current was plotted against the tested membrane voltage. Legend colour: Black for No-pyrethroid, red for 1 nM, green for 10 nM, purple for 100 nM and blue for 1 µM of *tau*-fluvalinate.

Activation
tau-fluvalinate
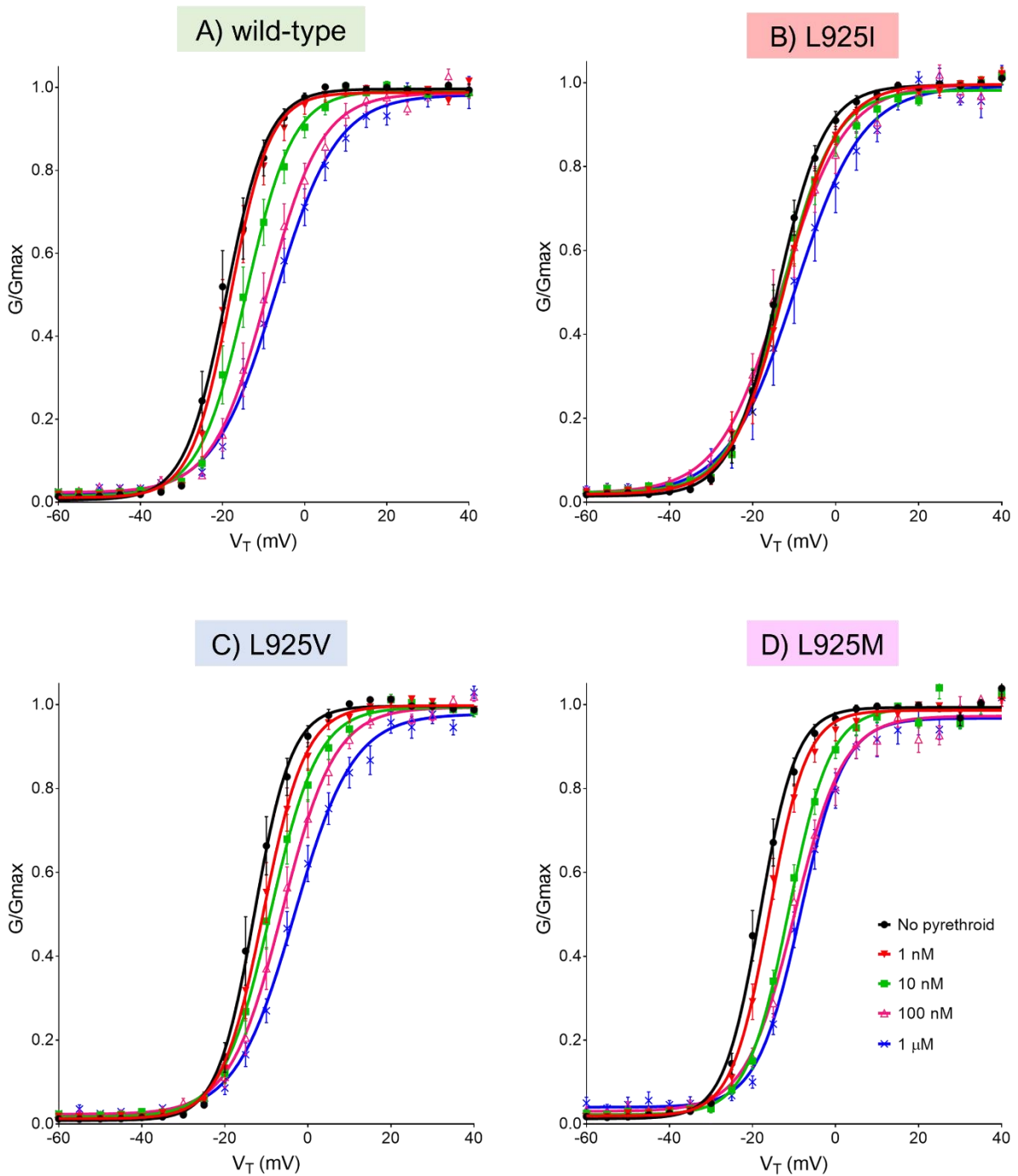
Figure 1.24. Voltage dependence of Activation for *Vd*VGSC wild -type (A) and L925 mutant channels (L925I (B), L925V (C) and L925 (M)) in the presence of increasing *tau*-fluvalinate concentrations. Conductance normalized, shown as mean ± SEM (mV), was fitted with a Boltzmann equation and plotted against Voltage (mV) (see protocol P.1, p. 99). Data values of $V_{50,act}$ and the curve slope are given in Table 1.7. Legend colour: Black for No-pyrethroid, red for 1 nM, green for 10 nM, purple for 100 nM and blue for 1 µM of *tau*-fluvalinate.

Steady-state inactivation
tau-fluvalinate
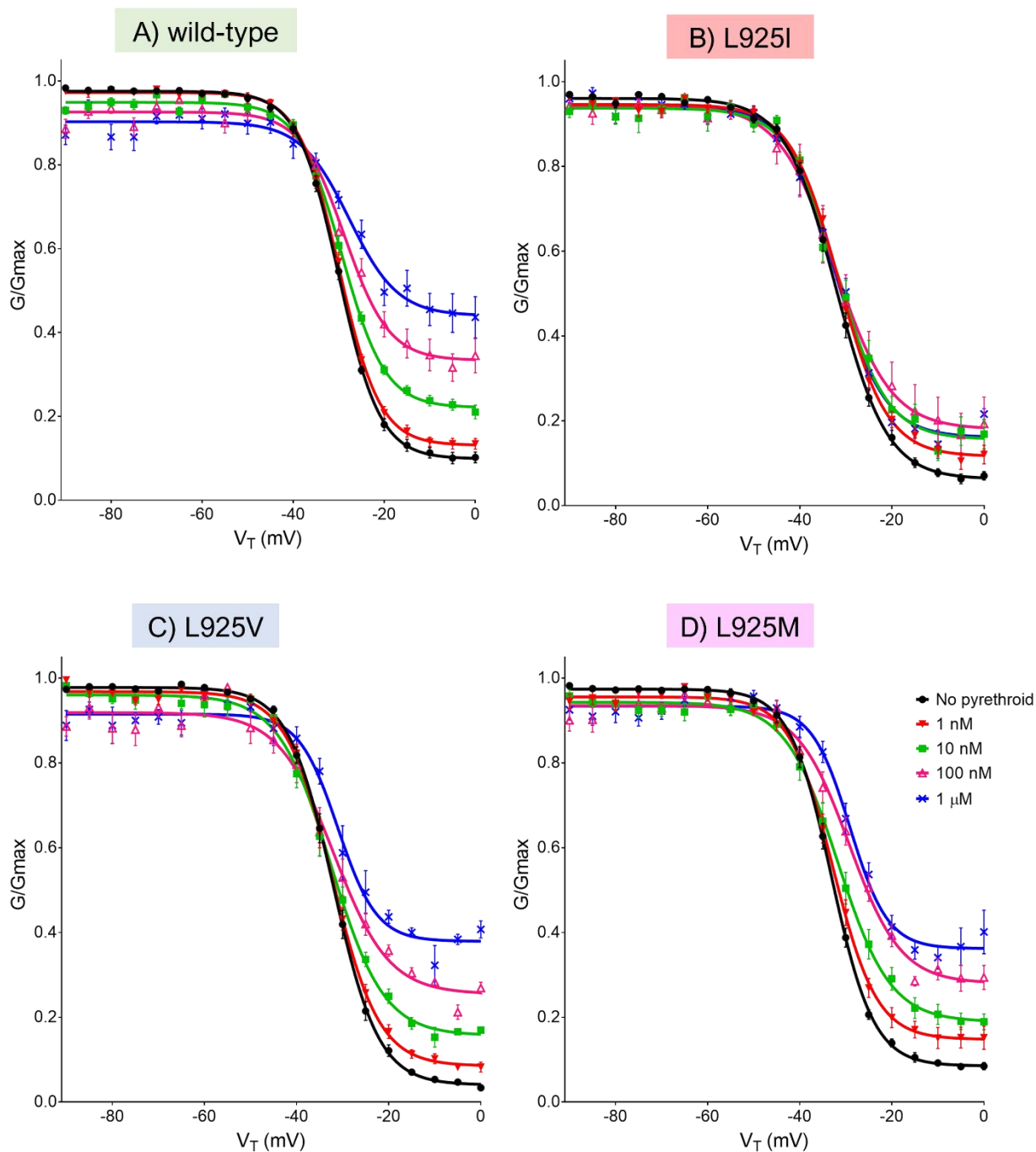
Figure 1.25. Voltage dependence of steady-state inactivation for *Vd*VGSC wild -type (A) and L925 mutant channels (L925I (B), L925V (C) and L925 (M)) in the presence of increasing *tau*-fluvalinate concentrations. Conductance normalized, shown as mean ± SEM (mV), was fitted with a Boltzmann equation and plotted against Voltage (mV) (see protocol P.2, p. 101). Data values of $V_{50,inact}$ and the curve slope are given in Table 1.7. Legend colour: Black for No-pyrethroid, red for 1 nM, green for 10 nM, purple for 100 nM and blue for 1 µM of *tau*-fluvalinate.

Table 1.7. Effects of increasing concentrations of *tau*-fluvalinate on the gating kinetics of wild-type and L925 modified sodium channels of *V. destructor*.

		tau-FLUVALINATE			
		wild-type	**L925I**	**L925V**	**L925M**
No pyrethroid	$V_{50,act}$	-19.06 ± 0.41 (10)	-12.93 ± 0.24 (12)††††	-14.01 ± 0.30 (5)††††	-18.71 ± 0.26 (9)
	k_{act}	5.04 ± 0.36	5.27 ± 0.21	4.02 ± 0.26 ††††	4.08 ± 0.23 ††††
	$V_{50,inact}$	-30.01 ± 0.18 (10)	-32.1 ± 0.26 (12) ††	-32.02 ± 0.22 (5)†	-33.05 ± 0.21 (9) ††††
	k_{inact}	4.53 ± 0.15	5.54 ± 0.23	4.92 ± 0.20	4.56 ± 0.18
1nM	$V_{50,act}$	-18.06 ± 0.37 (10)	-12.41 ± 0.37 (12)	-11.86 ± 0.33 (5)**	-15.96 ± 0.25 (9)****
	k_{act}	4.78 ± 0.32	6.39 ± 0.32 *	4.73 ± 0.29	4.49 ± 0.21
	$V_{50,inact}$	-29.88 ± 0.21 (9)	-31.55 ± 0.32 (12)	-32.21 ± 0.28 (5)	-32.74 ± 0.36 (9)
	k_{inact}	4.47 ± 0.18	5.26 ± 0.28	5.081 ± 0.24	4.76 ± 0.31
10nM	$V_{50,act}$	-14.24 ± 0.4 (8)****	-12.96 ± 0.47 (7)	-10.23 ± 0.35 (5)****	-11.30 ± 0.23 (7)****
	k_{act}	5.7 ± 0.35	6.29 ± 0.47	5.23 ± 0.30	5.03 ± 0.20
	$V_{50,inact}$	-29.29 ± 0.26 (7)	-31.89 ± 0.57 (8)	-32.53 ± 0.43 (5)	-31.74 ± 0.53 (7)
	k_{inact}	4.76 ± 0.23	5.39 ± 0.50	5.74 ± 0.38	5.72 ± 0.47
100nM	$V_{50,act}$	-9.13 ± 0.48 (7)****	-12.99 ± 0.61 (6)	-7.41 ± 0.33 (5)****	-9.85 ± 0.38 (6)****
	k_{act}	6.61 ± 0.42 **	7.59 ± 0.54 ****	5.89 ± 0.28 **	5.89 ± 0.34 **
	$V_{50,inact}$	-28.7 ± 0.66 (6)	-32.34 ± 1.0 (6)	-31.95 ± 0.81 (5)	-29.24 ± 0.65 (6)****
	k_{inact}	4.87 ± 0.57	6.05 ± 0.88	6.0 ± 0.71	5.63 ± 0.57
1 µM	$V_{50,act}$	-7.17 ± 0.54 (7)****	-9.82 ± 0.84 (4)****	-4.57 ± 0.34 (5)****	-8.43 ± 0.39 (5)****
	k_{act}	7.48 ± 0.48 ****	8.04 ± 0.75 ***	6.48 ± 0.29 ***	5.25 ± 0.34
	$V_{50,inact}$	-27.7 ± 1.1 (7)**	-32.38 ± 0.48 (4)	-31.06 ± 0.79 (5)	-29.1 ± 0.61 (5)****
	k_{inact}	5.34 ± 0.96	5.38 ± 0.42	4.23 ± 0.69	4.12 ± 0.53

The data included in the table for No pyrethroid condition are those obtained from oocytes that were subsequently subjected to *tau*-fluvalinate treatment. Data are expressed as means ± SEM. Table shows the values of the voltages for half-maximal activation ($V_{50,act}$) and inactivation ($V_{50,inact}$), and the slope factor for activation (k_{act}) and inactivation (k_{inact}). Numbers in parentheses are the number of oocytes tested. Statistical comparisons were plotted for all V_{50}s and slope factors comparing mutant channels with the wild type without pyrethroids (†), and within individual channels in the absence of and at specific *tau*-fluvalinate concentrations (*). Two-way ANOVA with Dunnett's post-test: *,†: $P <0.05$; **,††: $P <0.01$; ***,†††: $P <0.001$; and ****, ††††: $P <0.0001$.

Tau-fluvalinate only elicited tail currents over wild-type channels (Fig. 1.26). Although, the effect of tau-fluvalinate upon the tail current was not as potent as that induced by deltamethrin. Instead, only 20% of integrally modified channels were induced to produce tail currents at a higher concentration of 100 µM. Notably, only few oocytes expressing the wild-type VdVGSC could resist higher concentrations of tau-fluvalinate, as the majority became too leaky to continue the recordings after being exposed to the pyrethroid for a period of time. The three mutant channels did not display tail currents induced by tau-fluvalinate. The EC_{50} values for tau-fluvalinate could not be calculated because the tested concentrations just reached the initiation of the MI (%) curve, so the M_{max} values could not be accurately estimated.
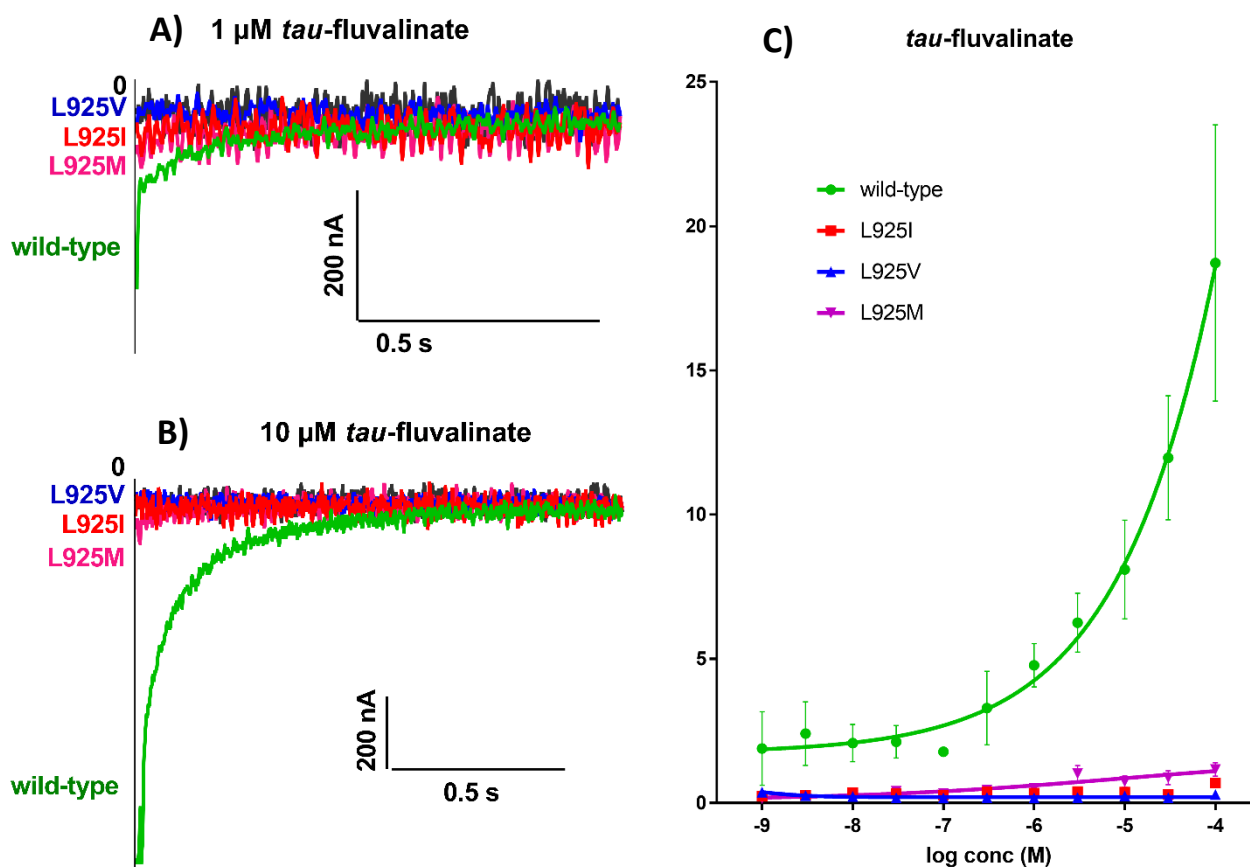
Figure 1.26. Analysis of the tail current elicited by tau-fluvalinate treatment. Illustration of a typical tail current recorded from single Xenopus oocytes injected with VdVGSC constructs of the wild-type (green), L925I (red), L925V (blue) and L925M mutations (pink) in the presence of 1 µM (A) and 10 µM (B) of tau-fluvalinate. The 0 (black line) indicates the absence of tau-fluvalinate. C) Integral modification (%) of the channels were plotted against the tau-fluvalinate concentration and fitted with a four-parameter logistic equation (see tail current protocol P.3, p. 103).

138

1.4.3.c. Effect of flumethrin upon *Vd*VGSCs

The influence of flumethrin upon the activation kinetics can be detected at nanomolar concentrations for all *Vd*VGSC tested. The $V_{50,act}$ of the wild-type, as well as for the L925I and L925V mutant channels, were altered by shifting to more positive membrane voltages even at the lowest concentration of 1 nM. Low concentrations of flumethrin triggers a stronger shift in the wild-type channel than *tau*-fluvalinate and deltamethrin, as evidenced by the 4 mV deviation at 1 nM flumethrin. Similar shifts were produced in the 925-mutant *Vd*VGSC but at higher concentrations (Table 1.8, Fig. 1.27 and 1.28; Supplementary S1.1, p. 243).

Conversely, flumethrin did not modify the $V_{50,inact}$ value in the wild-type channel, even at the highest concentration of 1 µM as it occurred with deltamethrin and *tau*-fluvalinate. By contrast, $V_{50,inact}$ was shifted to more positive values for the L925M and L925I mutant channels after 10 nM treatment, and after 1 µM for the L925V (Table 1.8, Fig. 1.29; Supplementary Fig. S1.2, p. 244).

As with deltamethrin and *tau*-fluvalinate, increasing concentrations of flumethrin also produced an augment of the late sodium current during the inactivation process (Fig. 1.29). Even though the late sodium current (post-inactivation current) is enhanced in all the channels related to the pyrethroid concentration, the effect upon the wild-type and the L925M channels were significantly bigger at lower concentrations. The application of 1 nM of flumethrin increased the late sodium current to 21% and 18% for the wild-type and L925M channels, respectively. The L925I and L925V mutated channels required bigger amounts of flumethrin to achieve those values of late sodium current. As with the *tau*-fluvalinate assays, the EC_{50} values for flumethrin could not be calculated due to the low tail current response of the constructions for the tested conditions. The tested concentrations illustrate the initiation of the MI (%) curve, so the M_{max} and EC_{50} values could not be estimated precisely (Fig. 1.30).

Activation
Flumethrin
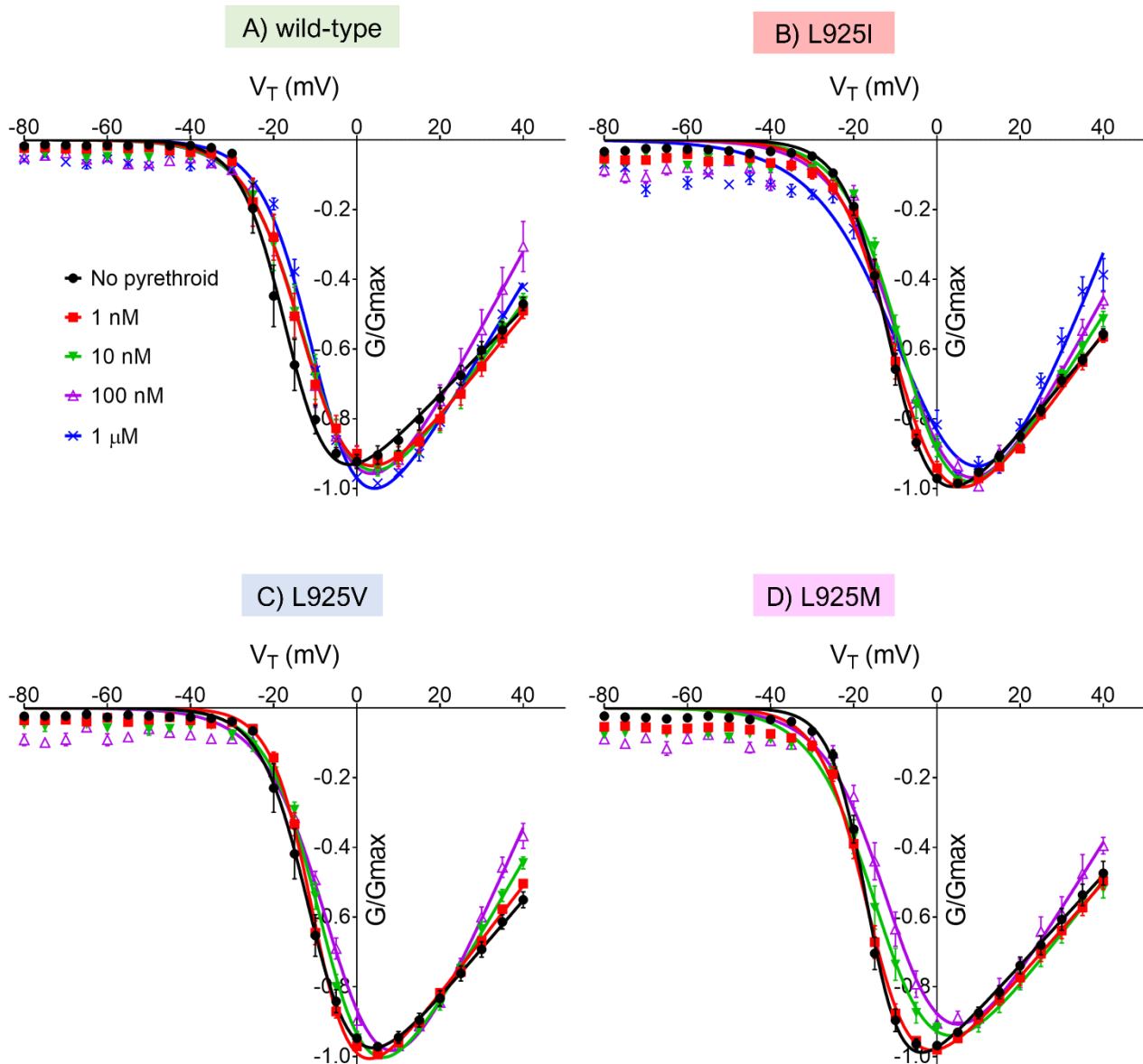
Figure 1.27. Current-voltage relationship for the wild-type (A), L925I (B), L925V (C) and L925M (D) mutants VGSC in the presence of increasing concentrations of flumethrin. Injected oocytes were subjected to a step depolarization protocol (see protocol P.1, p. 99) from -80 mV to +40 mV in 5 ms increments in the presence of increasing concentrations of flumethrin. The normalized peak inward current was plotted against the tested membrane voltage. Legend colour: Black for No-pyrethroid, red for 1 nM, green for 10 nM, purple for 100 nM and blue for 1 µM of flumethrin.

Activation
Flumethrin
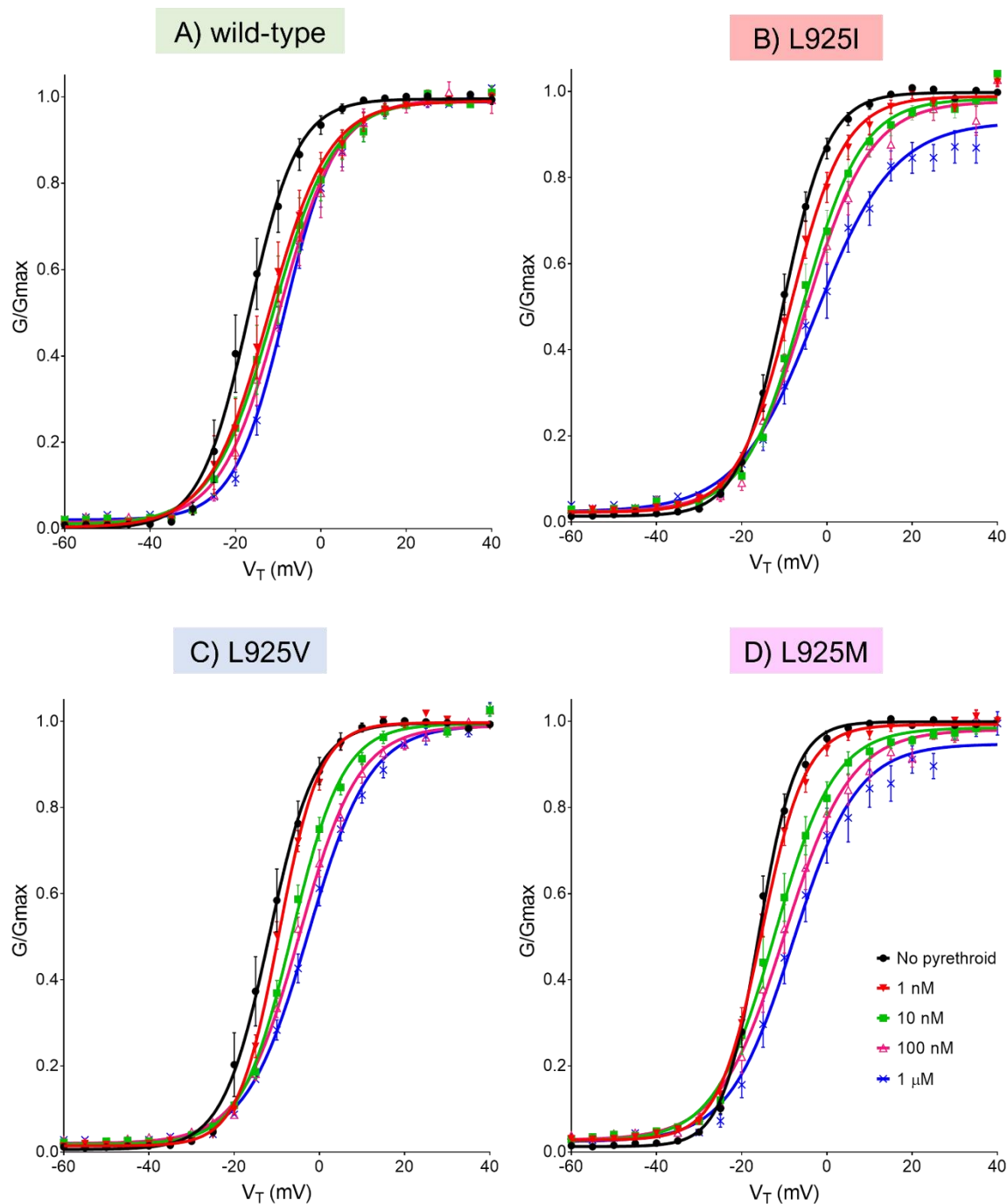
Figure 1.28. Voltage dependence of Activation for *Vd*VGSC wild -type (A) and L925 mutant channels (L925I (B), L925V (C) and L925 (M)) in the presence of increasing flumethrin concentrations. Conductance normalized, shown as mean ± SEM (mV), was fitted with a Boltzmann equation and plotted against Voltage (mV) (see protocol P.1, p. 99). Data values of $V_{50,act}$ and the curve slope are given in Table 1.8. Legend colour: Black for No-pyrethroid, red for 1 nM, green for 10 nM, purple for 100 nM and blue for 1 µM of flumethrin.

Steady-state inactivation
Flumethrin

A) wild-type

B) L925I
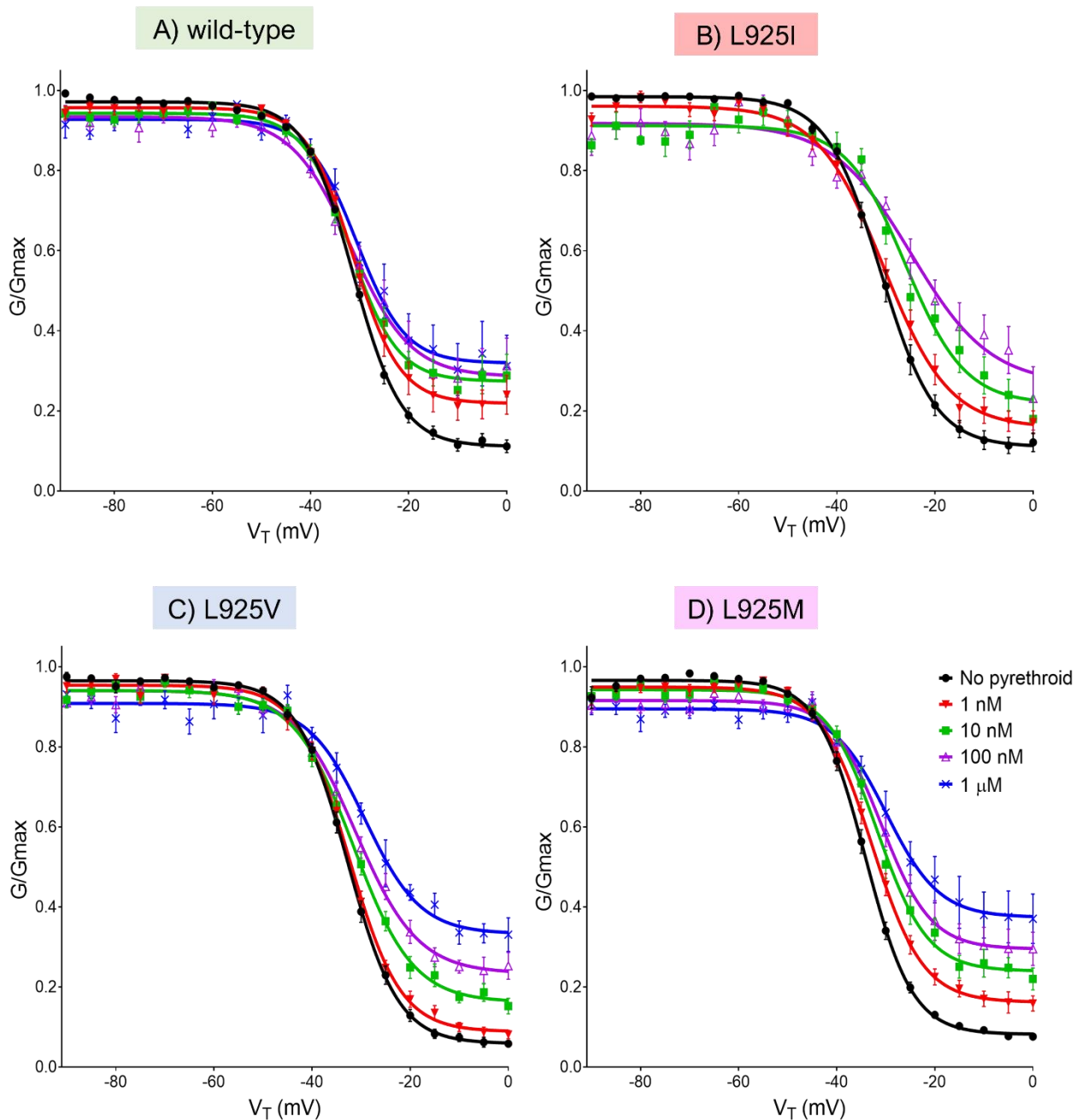
C) L925V

D) L925M

Figure 1.29. Voltage dependence of steady-state inactivation for *Vd*VGSC wild -type (A) and L925 mutant channels (L925I (B), L925V (C) and L925 (M)) in the presence of increasing flumethrin concentrations. Conductance normalized, shown as mean ± SEM (mV), was fitted with a Boltzmann equation and plotted against Voltage (mV) (see protocol P.2, p.101). Data values of $V_{50,inact}$ and the curve slope are given in Table 1.8. Legend colour: Black for No-pyrethroid, red for 1 nM, green for 10 nM, purple for 100 nM and blue for 1 μM of flumethrin.

Table 1.8. Effects of increasing concentrations of flumethrin on the gating kinetics of wild-type and L925 modified sodium channels of *V. destructor*.

		FLUMETHRIN			
		wild-type	**L925I**	**L925V**	**L925M**
No pyrethroid	$V_{50,act}$	-16.87 ± 0.49 (9)	-10.27 ± 0.24 (6)††††	-11.79 ± 0.43 (6) ††††	-15.97 ± 0.24 (10)
	k_{act}	5.68 ± 0.43	5.28 ± 0.21	5.46 ± 0.38	4.32 ± 0.21 †
	$V_{50,inact}$	-31.28 ± 0.21 (9)	-31.06 ± 0.38 (6)	-32.74 ± 0.24 (6)	-34.14 ± 0.23 (10)††
	k_{inact}	4.95 ± 0.18	5.54 ± 0.33	5.15 ± 0.21	4.80 ± 0.20
1nM	$V_{50,act}$	-12.22 ± 0.59 (9)****	-8.487 ± 0.32 (6)*	-9.52 ± 0.16 (6)**	-15.31 ± 0.24 (10)
	k_{act}	7.017 ± 0.52 *	6.284 ± 0.28	4.79 ± 0.14	5.14 ± 0.21
	$V_{50,inact}$	-31.34 ± 0.53 (9)	-30.47 ± 0.62 (5)	-32.42 ± 0.31 (6)	-32.84 ± 0.36 (10)
	k_{inact}	4.78 ± 0.46	6.69 ± 0.55	5.23 ± 0.27	5.23 ± 0.32
10nM	$V_{50,act}$	-11.18 ± 0.60 (7)****	-5.65 ± 0.43 (5)****	-6.45 ± 0.22 (6)****	-12.25 ± 0.45 (9)****
	k_{act}	7.09 ± 0.53 *	6.91 ± 0.37 *	6.03 ± 0.19	7.02 ± 0.40 ****
	$V_{50,inact}$	-31.96 ± 0.60 (7)	-26.00 ± 1.02 (4)***	-31.55 ± 0.48 (6)	-31.76 ± 0.53 (9)*
	k_{inact}	4.85 ± 0.52	6.07 ± 0.87	6.09 ± 0.42	5.14 ± 0.46
100nM	$V_{50,act}$	-9.75 ± 0.54 (6)****	-4.74 ± 0.44 (5)****	-4.68 ± 0.26 (5)****	-9.97 ± 0.52 (9)****
	k_{act}	6.86 ± 0.47	7.50 ± 0.39 **	6.94 ± 0.23	7.716 ± 0.46 ****
	$V_{50,inact}$	-31.74 ± 1.03 (5)	-24.85 ± 1.95 (4)****	-31.11 ± 0.59 (5)	-30.88 ± 0.75 (9)***
	k_{inact}	6.07 ± 0.91	8.07 ± 1.52	6.351 ± 0.52	5.052 ± 0.65
1 μM	$V_{50,act}$	-8.423 ± 0.34 (4)****	-2.82 ± 0.81 (5)****	-2.68 ± 0.31 (5)****	-8.05 ± 0.68 (8)****
	k_{act}	5.986 ± 0.30	9.18 ± 0.71 ****	7.27 ± 0.27 *	7.53 ± 0.60 ****
	$V_{50,inact}$	-30.64 ± 1.11 (4)	-24.02 ± 1.73 (4)****	-29.27 ± 0.95 (4)*	-29.91 ± 1.26 (8)****
	k_{inact}	4.962 ± 0.96	4.101 ± 1.49	5.681 ± 0.83	5.4 ± 1.10

The data included in the table for No pyrethroid condition are those obtained from oocytes that were subsequently subjected to flumethrin treatment. Data are expressed as means ± SEM. Table shows the values of the voltages for half-maximal activation ($V_{50,act}$) and inactivation ($V_{50,inact}$), and the slope factor for activation (k_{act}) and inactivation (k_{inact}). Numbers in parentheses are the number of oocytes tested. Statistical comparisons were plotted for all V_{50}s and slope factors comparing mutant channels with the wild type without pyrethroids (†), and within individual channels in the absence of and at specific flumethrin concentrations (*). Two-way ANOVA with Dunnett's post-test: *,†: P <0.05; **,††: P <0.01; ***,†††: P <0.001; and ****, ††††: P <0.0001.

The tail current produced by flumethrin was the least potent of the three pyrethroid tested. Flumethrin induced relatively minor tail current in wild-type and L925M channels, with a small portion of modified channels found even at higher concentrations. As with the other pyrethroids, L925I and L925V channels showed no tail current response as a result of flumethrin exposure (Fig. 1.30).
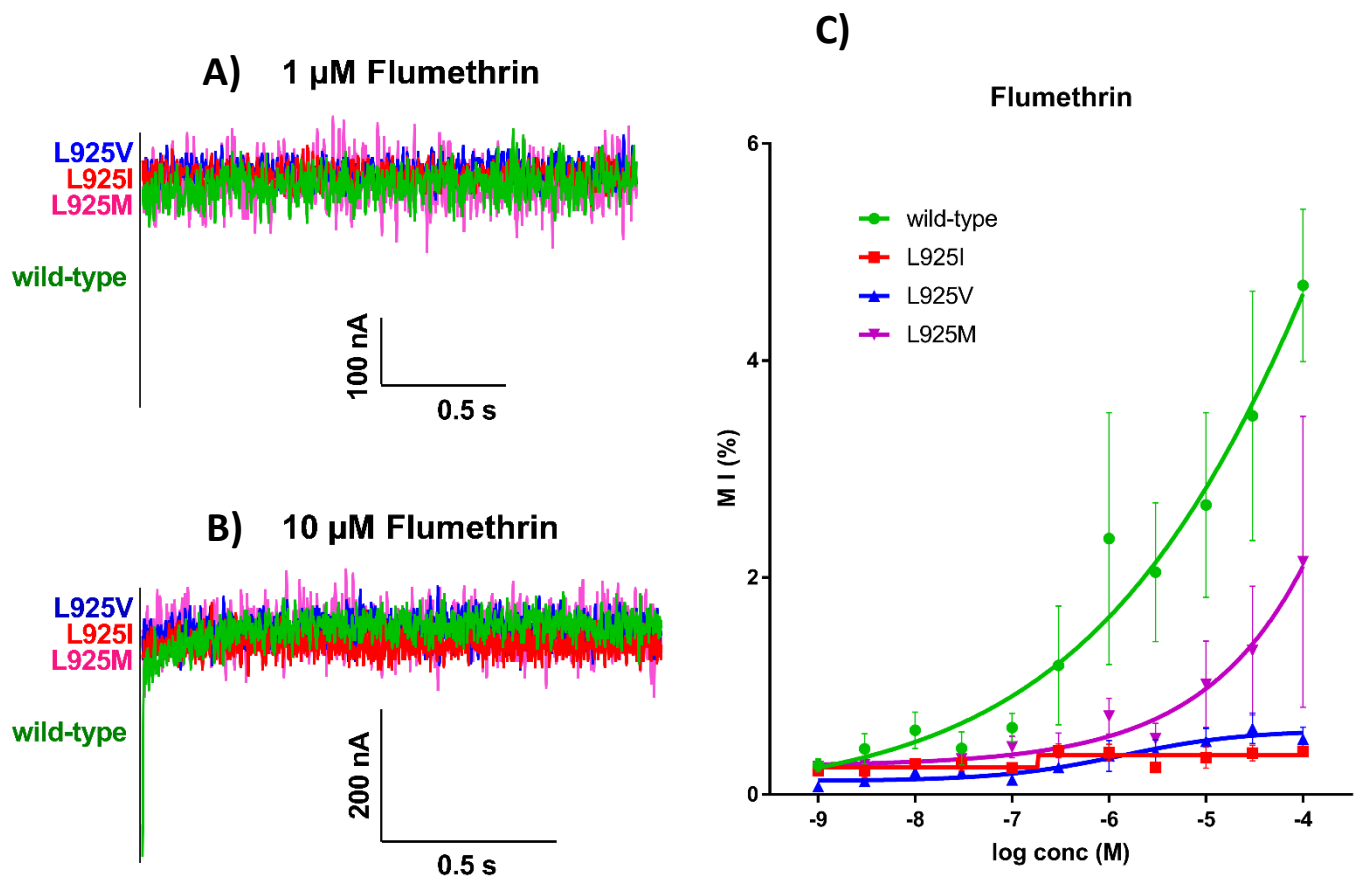
Figure 1.30. Analysis of the tail current elicited by flumethrin treatment. Illustration of a typical tail current recorded from single *Xenopus* oocytes injected with *Vd*VGSC constructs of the wild-type (green), L925I (red), L925V (blue) and L925M mutations (pink) in the presence of 1 µM (A) and 10 µM (B) of flumethrin. The 0 (black line) indicates the absence of *tau*-fluvalinate. C) Integral modification (%) of the channels were plotted against the flumethrin concentration and fitted with a four-parameter logistic equation (see tail current protocol P.3, p. 103).

1.5. Discussion

Varroa destructor mites surviving to *tau*-fluvalinate and flumethrin treatments have been correlated to mutations at position 925 of the VGSC (González-Cabrera et al., 2018; González-Cabrera et al., 2013; González-Cabrera et al., 2016; Hubert et al., 2014; Stara et al., 2019a). Here, the implications of these mutations on the resistance mechanism have been studied in detail functionally and pharmacologically by heterologous expression in *Xenopus* oocytes of the wild-type and mutated channels.

Varroa destructor VGSC constructs and functional expression in *Xenopus* oocytes

In insects, the sodium channel auxiliary proteins, known as TipE or TipE-like subunits, help in modulating the expression and gating properties of sodium channels. When expressing insect VGSC in *Xenopus* oocytes, the co-injection with cRNA of these subunits contributes to enhanced functional channel expression (Feng et al., 1995; Gosselin-Badaroudine et al., 2015; Wang et al., 2013). But, to date, no homologous auxiliar subunits have been identified in *V. destructor*, and the co-expression of *Vd*VGSC with the TipE subunit from *D. melanogaster* resulted in a significant decrease of the detected currents when compared to VGSC expressed alone (Du et al., 2009). Therefore, we did not attempt to co-inject the *Vd*VGSC constructs with the cRNA of auxiliar subunits from insects, such as *D. melanogaster* TipE. Besides, previous research demonstrated adequate expression of *Vd*VGSC in oocytes without co-expression with any accessory protein. In the present study, despite diversity among individual oocytes, all *Vd*VGSC constructs generated 'good' sodium currents in RNA-injected oocytes.

The *Vd*VGSC constructs in this work included the regions of exon B-like and exon 2 described in previous studies (Du et al., 2009; Gosselin-Badaroudine and Chahine, 2017; Song et al., 2004). These exons are located in the intracellular linker for domains I-II and II-III, respectively (see Fig. 1.12, p. 107), and feature phosphorylation sites suggesting a role in the modulation of current expression or activity. This hypothesis is supported by the previous studies that described those optional exons in the *Vd*VGSC. For instance, the deletion of exon B in *B. germanica* and its homologous sequence in *V. destructor* increases considerably the amplitude of peak current (Du et al., 2009; Song et al., 2004). Additionally, Gosselin-Badaroudine and Chahine (2017) reported robust current expression with their *Vd*VGSC construct laking the optional exon 2. Most arthropods,

including *V. destructor*, possess a single sodium channel gene and accomplish the required functional variety of sodium channels by alternative splicing and RNA editing (Dong et al., 2014; ffrench-Constant et al., 2016; Wang et al., 2003). Nonetheless, it is not known whether exon B-like and exon 2 are alternative spliceable exons *in vivo* for *V. destructor*, neither the tissue-specific pattern of transcript isoforms in *Varroa*. Hence, we decided to include these regions in the constructs, as we found them in the mRNA sequenced in our previous work (Accession KF771990) (González-Cabrera et al., 2013).

The biophysical properties of our wild-type *Vd*VGSC construct were found to be very consistent with those obtained by Du *et al.* (2009) for their *Vd*VGSC constructs (named as VdNav1 and VdNav1a in their work, according to the presence or absence of exon B-like respectively) (Supplementary Table S1.2, p. 242). These results differ from those reported by Gosselin-Badaroudine and Chahine (2017) for their *Vd*VGSC construct omitting the optional exon 2 (Supplementary Table S1.2, p. 242). Taken together, these findings show that alternative splicing can produce variant *Vd*VGSC that can be used to meet specific demands in mite tissues.

Characterization of the wild-type and L925 mutated *Vd*VGSCs

In our analyses, the wild-type and the three 925-mutants constructs featured the properties required for functional VGSC. This was to be expected, given that these mutations do not affect any amino acid residue critical for sodium channel function and have been widely reported in field mites (Alissandrakis et al., 2017; González-Cabrera et al., 2018; González-Cabrera et al., 2016; Panini et al., 2014; Wang et al., 2003).

Nonetheless, the characterization of the channels in the absence of pyrethroids revealed variations in gating dynamics between the wild-type and mutant channels. The three mutations at position 925 of the *Vd*VGSC altered the usual gating kinetics of the channel, shifting the activation voltage dependence ($V_{50,act}$) in the depolarising direction as compared to the wild-type (Table 1.2, Fig. 1.15 and 1.16, p. 111-113). When the wild-type Leucine is replaced by a Methionine, our analyses reveal a slight shift towards more positive voltages. However, when the change is to Valine or Isoleucine, this shift is more pronounced and significant, revealing that these channels require stronger membrane depolarization to get activated. On the other hand, Isoleucine and Valine changes did not

alter the voltage dependence of inactivation ($V_{50,inact}$) with respect to the wild-type, while Methionine shifted the $V_{50,inact}$ to more negative voltages.

In brief, as compared to wild-type VdVGSC, L925V and L925I mutant VdVGSCs exhibit a narrower range of membrane voltages at which they get activated, whereas L925M mutant VdVGSC have the activation and steady-state inactivation voltage dependence shifted by about 2 mV, on the positive and negative directions, respectively (Table 1.2, Fig. 1.16, p. 112-113). Besides, the L925M mutant channel displayed a significantly faster recovery from activation than the wild-type (a decrease in the *tau* decay values at a depolarizing voltage of -10 mV) (Table 1.4, Fig. 1.18, p.117-118). This implies that the channel will inactivate faster after it has been activated. Accordingly, the outcome for all three mutations would be VdVGSC having a reduced open-state probability, with this effect being more pronounced in the case of Valine and Isoleucine substitutions.

Given the evidence that pyrethroids have higher affinity for and preferentially target the VGSC in its open state (Vais et al., 2003; Vais et al., 2000b), this variation in the activation and inactivation parameters of the mutated channels may be indirectly counteracting pyrethroid action, hence contributing to the insensitivity to these toxicants. Our results show that 925-mutated VdVGSC require a stronger depolarization of the membrane to switch to open state, making these channels less likely to open and expose the pyrethroid binding site. Furthermore, the L925M channels have a faster recovery from activation rate, which would accelerate the channel shutting process, leaving them out of reach of pyrethroid action. In addition, after an activation step, the wild-type channels exhibited a slightly late sodium current (post-inactivation residual current) higher than the mutant channels, according to our findings (Fig. 1.16, p. 113). This means that following activation, a small fraction of the channels will not be immediately inactivated and will remain open, allowing the docking of pyrethroids, but this fraction is smaller in mutant channels.

In insects, similar changes in gating parameters have been observed in VGSC with *kdr* and *kdr*-like mutations, such as a shift towards the positive direction and faster inactivation (Burton et al., 2011; Lee et al., 1999; Oliveira et al., 2013; Smith et al., 1997; Vais et al., 2001). The positive change in the voltage dependence of activation and/or the increased speed of inactivation *per se* are not thought to be the primary reasons of

pyrethroid resistance; nonetheless, the fact that type II pyrethroids have less access to the binding pocket in the VGSC may be contributing to it. By lowering the proportion of VGSCs that open in response to membrane depolarisation, the channel's high affinity state for pyrethroids is lessened, and thus the chance of pyrethroid docking is reduced. As a result, in addition to pyrethroids' lower affinity for the 925-mutant *Vd*VGSC (see below), these mutations provide additional layers of resistance by reducing the availability of the ideal target state for pyrethroids.

Effect of pyrethroids upon *Varroa destructor* 925-mutant VGSC

In general, pyrethroids alters the kinetics of VGSC by inhibiting of open and closed states inactivation and slowing the deactivation (Burton et al., 2011; Vais et al., 2000b). Inhibition of these processes by pyrethroid interaction can lead to distinctive features known as tail currents, post-inactivation residual currents, and the slowing down of inactivation processes (Vais et al., 2000b).

The effect of pyrethroids on insect VGSC have been well documented by several studies (Burton et al., 2011; Field et al., 2017; Gosselin-Badaroudine et al., 2015; Tan et al., 2002; Tatebayashi and Narahashi, 1994; Vais et al., 2001; Vais et al., 2000b; Wu et al., 2017). On insect VGSC, pyrethroids interaction usually enhance the activation state by shifting the $V_{50,act}$ to more hyperpolarizing potentials (the negative direction) or hampering the fast inactivation; resulting in prolonged opened channels pushing the insect to a state of abnormal hyperexcitability. Surprisingly, in *Vd*VGSC, pyrethroids appear to have the opposite impact on the activation gating voltage as they do in insect VGSC. Our data show that the interaction of deltamethrin, *tau*-fluvalinate and flumethrin with *Vd*VGSC alters the channel kinetics by shifting the $V_{50,act}$ to more positive voltages (Fig. 1.31; see also Fig. 1.20, 1.24, and 1.28; p. 121, 128 and 134, respectively). This variation in the activation properties may indirectly antagonise pyrethroid action, which probably would explain why mite sodium channels are less sensitive to pyrethroids than insect sodium channels (Burton et al., 2011; Gosselin-Badaroudine and Chahine, 2017; Thompson et al., 2020; Vais et al., 2000b; Wu et al., 2017).

The wild-type VdVGSC was sensitive to all three pyrethroids tested at nanomolar concentrations, according to our results. Pyrethroids' action altered the activation potential, shifting the $V_{50,act}$ towards more positive voltages from a concentration of 1 nM of flumethrin and 10 nM of deltamethrin or tau-fluvalinate. The magnitude of the positive shift in the $V_{50,act}$ was significantly bigger for flumethrin, followed by tau-fluvalinate and deltamethrin (Tables 1.5, 1.7 and 1.8; p. 123, 130 and 136, respectively). Besides, the addition of pyrethroids had no significant effect on the steady-state inactivation kinetics parameters in VdVGSC. So, in the presence of pyrethroids, shifting the $V_{50,act}$ to positive voltages while maintaining the same $V_{50,inact}$ and the k_{inact} results in a reduction of the VGSC's open window. The open channel, as previously stated, is the favourable conformation for pyrethroid docking. Therefore, this response does not actually boost pyrethroid action. Nonetheless, the late sodium current (post-inactivation residual current or non-inactivation current) in the steady-state inactivation appears to rise proportionately to the pyrethroid concentration applied (Fig. 1.31.B) This phenomenon corresponds to VGSC that have not been inactivated after they have been opened and continue to produce inward currents. This open channel fraction might be target of further pyrethroid docking.
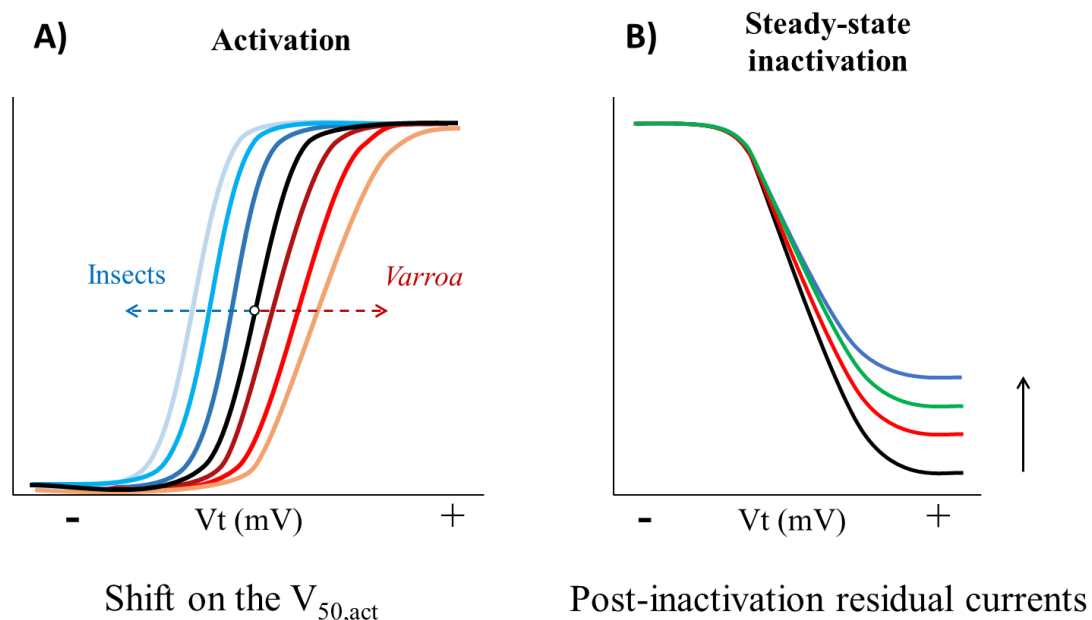
Figure 1.31. Schematic representation of the effect on the opening gating kinetics (A) and fast inactivation (B) in pyrethroid-treated VGSC.

Deltamethrin is a powerful and widely used pyrethroid, but not approved for use in apiaries because it is toxic to bees. In our experiments, both wild-type and L925M channels were highly susceptible to deltamethrin action. Deltamethrin affected the wild-type and L925M channels' activation kinetics by shifting the $V_{50,act}$ to more positive voltages and increasing the k_{act} (Table 1.5, p. 123). In both channels, deltamethrin induced considerable strong tail currents (Fig 1.22, p. 124). On the contrary, the L925I and L925V showed a higher tolerance to deltamethrin. Their channel kinetics remained practically unaltered by deltamethrin, eliciting a smaller tail current that recovered quickly. The L925I mutation is a known resistance-associated mutation in several insects, and their influence on deltamethrin potency upon the channels has been studied in *D. melanogaster* VGSC (Usherwood et al., 2007).

Tau-fluvalinate and flumethrin are mite-selective pyrethroids approved as varroacidal treatments. In the wild-type *Vd*VGSC, both mite-selective pyrethroids generated lower tail currents than deltamethrin. This is a rather common occurrence that has been seen in insect channels as well (Wu et al., 2017). *Tau*-fluvalinate presence induced a moderate tail current in the wild-type channel, whereas none of the mutants displayed a tail current response (Fig. 1.26, p. 131). The activation kinetics of the L925M, L925V, and wild-type channels were also modified at low concentrations of *tau*-fluvalinate, while the kinetics of the L925I channel were almost unaltered until the concentration increased (Table 1.7, p. 130). On the other hand, flumethrin, was the pyrethroid that generated the smallest tail current for the wild-type. L925M channels displayed a tail current lower than that of the wild-type, with none detected for L925I and L925V (Fig. 1.30, p. 137). Although, the influence of flumethrin upon the activation and steady-state inactivation in all channels can be appreciated at nanomolar concentrations for all the VGSC constructions. For L925M and L925I channels, the steady-state inactivation was also altered since 100 nM concentrations, shifting the $V_{50,inact}$ to more positive values (Table 1.8, p. 136). The positive shift of $V_{50,inact}$ for L925M and L925I channels may enhance the rate of inactivation, contributing to channels closed-state, and so reducing pyrethroid toxicity (Vais et al., 2001).

Clearly, pyrethroids interact with the mutant channels, as they modify physiological kinetics properties. However, 925-mutant *Vd*VGSC are less susceptible to their influence, perhaps due to an impaired docking or by speeding the rate of dissociation from the channel (Vais et al., 2000b). The 925-mutations found in *V. destructor*, specially L925V

and L925I, in addition to have a lower affinity to pyrethroids, have also a reduced open state probability, counteracting ligand-induced opening (Vais et al., 2000b). This is also suggesting that mutations at position 925 of *Vd*VGSC are involved in resistance to pyrethroid.

Further, our results for the wild-type *Vd*VGSC exposed to *tau*-fluvalinate are in agreement with those of Gosselin-Badaroudine and Chahine (2017). Our experiments were conducted prior to the publication of Gosselin-Badaroudine and Chahine (2017) work, hence we could not replicate their conditions. In particular, to record the pyrethroid-elicited tail current, we followed a well-established protocol that has been previously used to evaluate the effect of pyrethroids on insect channels (Burton et al., 2011; Gosselin-Badaroudine et al., 2015; Vais et al., 2000b). Instead of the 1000 conditioning pulses required for *Vd*VGSC to reach the maximum fraction of modified channels described in their study, we applied a total of 100 pulses (see Protocol P.3), which are sufficient to activate all insect VGSC. However, Gosselin-Badaroudine and Chahine (2017) have shown that *Vd*VGSC requires more conditioning pulses to reach the maximum amplitude of the tail current. This might explain why the number of total modified channels registered in our experiments was lower than in theirs.

According to our findings, the change of the wild-type Leucine at position 925 of the *Vd*VGSC makes them less sensitive to pyrethroids. We also revealed that the L925M-mutated *Vd*VGSC was more susceptible to pyrethroids than the L925I and L925V, but still less so than the wild-type. Consequently, the L925M/V and I mutation are implicated in resistance to pyrethroids in *V.destructor*.

The mutations at position 925 of the VGSC in *V. destructor* seems to cope with the toxic effect of pyrethroids by an additive combination of effects. First, since mutated *Vd*VGSC have a lower excitability, they open less frequently, reducing the availability of the high affinity binding state for pyrethroids. Second, the weaker interaction between mutant *Vd*VGSC and pyrethroids leads to a faster dissociation, allowing for quicker recovery and no escalation of the pyrethroids effect. In addition, the L925M *Vd*VGSC showed a quicker inactivation kinetics (recovery from activation), which would aid in removing the bonded pyrethroid, besides leaving the docking site out of reach. These channels showed greater sensitivity to pyrethroids than the L925I and L925V *Vd*VGSC, and also have a soften shift of the activation voltage. Thus, the faster inactivation rate

151

might account for its pyrethroid resistance. Overall, our results demonstrated the implication of the mutations L925I/V and M in the resistance mechanism to pyrethroids in *V. destructor*. However, we cannot rule out that other factors or mechanisms, yet unknown, may be contributing to the resistance phenotype.

Additionally, our results showed that *Vd*VGSC (wild-type) are less sensitive to pyrethroids than insect channels (Burton et al., 2011; Gosselin-Badaroudine et al., 2015; Vais et al., 2000b; Wu et al., 2017). Nonetheless, only a low fraction of the VGSCs modified by pyrethroids can drive a noxious reaction on the cell. When sodium influx is not rapidly interrupted, it can trigger an enhanced effect by keeping the depolarization of the membrane and stimulating the opening of more channels. Pyrethroids amplifies this positive feedback because the altered channels remain open after repolarization, further stimulating the depolarization of the membrane potential and thus further VGSC opening. As a result, the membrane could not completely repolarize after an action potential, that can be lethal for the cell. The VGSC are located in the axon of neurones where they play an essential role in transduction of nerve impulses (Davies et al., 2007; Dong et al., 2014), so even little variations in their response could be critical to the fitness of individuals.

Mutations L925I/V could imply a higher fitness cost in the absence of pyrethroids

For *Varroa* mites in a hive, the mutation at position 925 of the VGSC would confer a better adaptation by reducing their sensitivity to pyrethroid treatments than the wild-type mites. However, in the absence of pyrethroids, the $V_{50,act}$ shift towards more positive voltages in the 925-mutant *Vd*VGSC (especially for L925I/V) may be associated with a reduced fitness cost when compared to the wild-type mites. Since these mutant channels require a higher membrane depolarisation to get activated, they are essentially less excitable channels. Consequently, individuals carrying less excitable neurons might be at a disadvantage in analogy to those mites that require a lower excitatory potential (Burton et al., 2011; Chen et al., 2010).

In relation to this, several studies have described a substantial drop in mite resistant population in hive (L925V) after ceasing the use of pyrethroid-based treatments (González-Cabrera et al., 2018; Milani and Della Vedova, 2002). Although more research is needed, our results may be supporting this decline in the frequency of L925V mites in absence of the selective pressure exerted by pyrethroids. In turn, if our hypothesis is right,

a similar reduction in the fitness would be expected for mites carrying the L925I mutation given their similarities at electrophysiological level.

CHAPTER 2

Phylogenetic analysis of the mutations associated with the pyrethroid resistance of the *Varroa destructor* VGSC

2.2. Introduction

The original distribution of *V. destructor* was limited to East Asia where the Asian honey bee, *Apis cerana* Fabricius (Hymenoptera: *Apidae*) is its natural host. Less than a century ago, the mite jumped host onto *A. mellifera* being managed in East Asia, and has quickly spread reaching near global distribution today (Rosenkranz et al., 2010). Western honey bees are less able to tolerate the mites than *A. cerana* (Lin et al., 2018; Page et al., 2016; Peng et al., 1987; Rath, 1999), and as a result, the mite is now a leading cause of the elevated colony losses reported around the world (Roberts et al., 2015; Solignac et al., 2005; Steinhauer et al., 2018).

Beekeepers worldwide control *V. destructor* infestation in their honey bee colonies with several mechanical and chemical approaches. Historically, the pyrethroid *tau*-fluvalinate was the most popular acaricide used to control *Varroa*. Unfortunately, as has happened with many other pesticides, its intensive use has led to the evolution of resistance in many *V. destructor* populations around the globe (Alissandrakis et al., 2017; Bąk et al., 2012; Elzen et al., 1999b; González-Cabrera et al., 2018; Miozes-Koch et al., 2000; Panini et al., 2019; Stara et al., 2019a; Thompson et al., 2002).

In *V. destructor*, as in other arthropods, the substitution of certain amino acids in the VGSC is a common mechanism involved in loss of pyrethroid sensitivity (Alissandrakis et al., 2017; Dong et al., 2014; González-Cabrera et al., 2018; González-Cabrera et al., 2016; Panini et al., 2019; Stara et al., 2019a). These mutations causing resistance to pyrethroids are found either alone or in combination with other mutations depending on the arthropod species or even the specific population (Alon et al., 2006; Benavent-Albarracín et al., 2020; Karatolos et al., 2012; Williamson et al., 1996). The single change of the amino acid at position 925 of the VGSC has been related with *V. destructor* resistant to pyrethroids in several locations. Three different resistant alleles for this position have been found in different mite populations around the world. The mutation L925V is found mainly in European mite populations (González-Cabrera et al., 2018; González-Cabrera et al., 2013; Hernández-Rodríguez et al., 2021; Hubert et al., 2014; Panini et al., 2019; Stara et al., 2019a) while, L925I and L925M were first reported in USA mite populations (González-Cabrera et al., 2016), but recently have been detected in other locations outside America (Alissandrakis et al., 2017; Koç et al., 2021; Ogihara et al., 2021).

In insect pests such as *Myzus persicae* (Anstead et al., 2005), *Anopheles gambiae* (Pinto et al., 2007), *Leptinotarsa decemlineata* (Rinkevich et al., 2012b) and *Musca domestica* (Rinkevich et al., 2012a), evolutionary studies revealed a multiple origin for *kdr*-type mutations in different populations of the same species. This is presumably the result of a strong selective pressure exerted over field populations since the 1940s after the introduction of DTT which, like pyrethroids, also targets the VGSC (Burton et al., 2011). In *V. destructor*, it is possible to describe a similar scenario since Apistan® (active ingredient: *tau*-fluvalinate) treatment started in the 1980's as a simple and effective management approach that proved very popular among beekeepers around the world.

Understanding the evolutionary history of the resistant alleles is a key step to anticipate future events of emerging resistance, and therefore contribute to design more finely tuned management strategies. In this study, we have analysed mites collected from a diverse number of locations where *V. destructor* resistant to Apistan® have been reported. In these *V. destructor* populations we documented mutations at position 925 of the *Vd*VGSC gene in order to determine if resistant populations originated from a single mutation event or that their distribution is the result of multiple independent events.

2.3. Objectives

In order to assess the evolution of resistant mutations in *V. destructor*, we genotyped a region of the VGSC containing the complete exon codifying for *kdr*-type mutations and partial fragments of the upstream and downstream flanking introns from *V. destructor* samples collected worldwide.

We aim to unravel the phylogenetic relationship between the resistance alleles at position 925 of the *Vd*VGSC. Thereby, we could identify the past mutational events that have led to the current distribution of resistant *V. destructor* mites. Furthermore, it is of great relevance to know the evolutionary origin of the different mutations in the *V. destructor* populations have originated from single or multiple mutation events, and thus understand the selection pressure these *kdr*-type residues are under.

2.4. Materials and methods

2.4.1. *Varroa destructor* samples

Adult female mites were collected from colonies located in different countries around the world (Fig. 2.2, p. 153). The mites were collected from the inspection boards, directly from the brood cells using soft tweezers and a fine paintbrush or from worker honey bees from the inner frames of the hives (phoretic *V. destructor*). They were placed in collection vials and stored at -20 °C in 96% or absolute ethanol until use. All apiaries were sampled once within the framework of different research projects. Therefore, the objectives of this study were adapted accordingly.

2.4.2. DNA isolation and amplification

DNA was extracted from single adult mites using a modified version of the Chelex extraction method (Evans et al., 2013; Walsh et al., 1991). Briefly, single mites were homogenized with a plastic pestle in a microcentrifuge tube containing 50 μL of 5% Chelex solution (Bio-Rad, cat. 1421253), supplemented with 0.5 mg/mL of proteinase K (AppliChem, cat. A3830). The homogenate was then subjected to a five-step incubation cycle as follows: 60 min at 56 °C, followed by 15 min at 99 °C, 15 min at 37 °C, 15 min at 99 °C and then cooling at 4 ºC for at least 15 min. After the incubation cycle, the tubes were centrifuged at $13000 \times g$ for 5 min. The supernatant, containing the genomic DNA, was transferred to a new tube and used for PCR amplification.

PCR was used to amplify a 1526 bp genomic region that contains a complete exon 13 (176 bp, encoding for amino acids 899 to 956 of the *V. destructor* VGSC, along with fragments of the flanking up- and downstream introns of 706 bp and 644 bp, respectively (amino acids were numbered according to the *M. domestica para*-type sodium channel protein sequence, Accession EMBL X96668 (Williamson et al., 1996)) (Fig. 2.1).
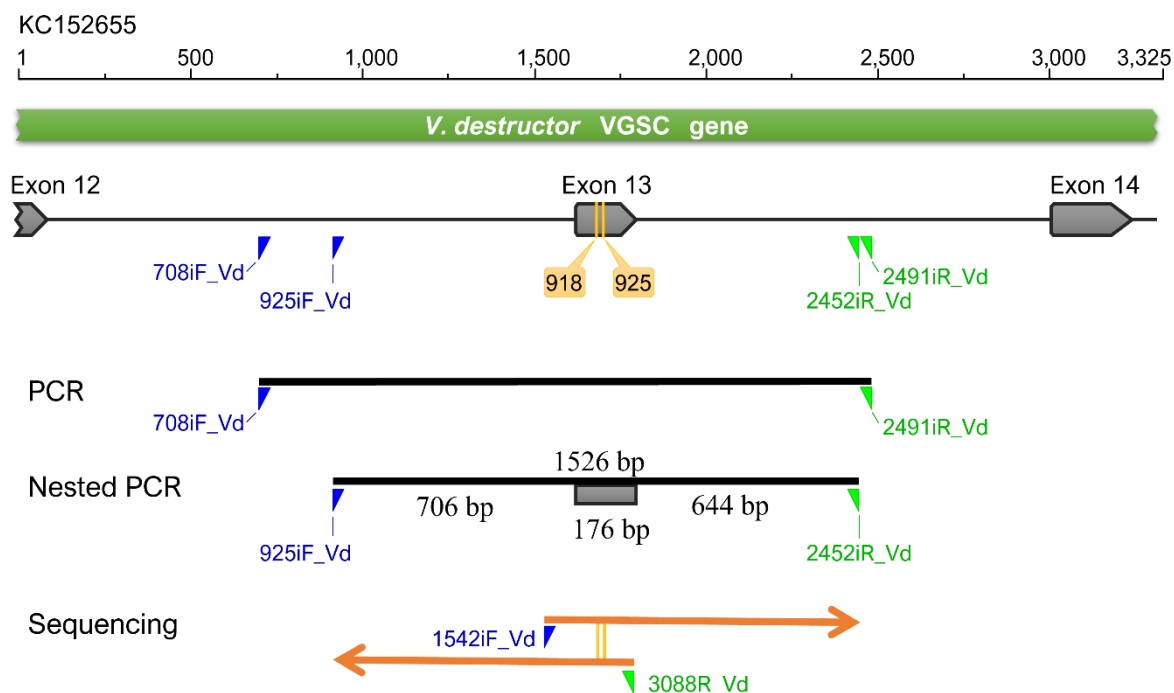
Figure 2.1. Schematic representation of the *V. destructor* VGSC gene region amplified for this study. Positions codifying for residues 918 and 925 of the VGSC are indicated in the exon 13. Blue and green triangles shown position for forward and reverse primers, respectively. GenBank Accession KC152655.2 sequence as reference. Primers info in Supplementary Table S1.1, p. 240).

PCR was performed as follows: 1 µL genomic DNA was added to PCR reaction mixtures containing 0.3 µM of each oligonucleotide primer (Forward primer, 708iF_Vd: 5'-CTGCCAGTGCGTCAACTAGTTGTCT-3', Reverse primer, 2491iR_Vd: 5'-GCGATGGTGGCTTTCTCCCTCTATC-3') and 12.5 µL of DreamTaq Green PCR Master Mix (2x) (Thermo Fisher Scientific) in a total volume of 25 µL. Cycling conditions were: 2 min at 95 ℃, followed by 35 cycles of 30 s at 95 ℃, 30 s at 62 ℃ and 2 min at 72 ℃, with a final elongation step of 5 min at 72 ℃. PCR products were visualised by electrophoresis in 1% agarose gel.

When low or no amplification was detected, a nested PCR was carried out: 1 µL of PCR product was used as template and mixed with 0.3 µM of the nested oligonucleotide primers (Forward, 925iF_Vd: 5'- GCTTCTACCGTATTTTGCTGTCT-3', Reverse, 2452iR_Vd: 5'- TTATTCGGACGGTGTCGGTG-3') and 12.5 µL of DreamTaq Green PCR Master Mix (2x) (Thermo Fisher Scientific) in a total volume of 25 µL. Cycling conditions were: 2 min at 95 ℃, followed by 35 cycles of 30 s at 95 ℃, 30 s at 54 ℃ and 2 min at 72 ℃, with a final elongation step of 5 min at 72 ℃. PCR products were ethanol

precipitated and direct sequenced (Stabvida, Portugal) using the primers 1542iF_Vd (5'-TTCTCTCTGACACATTGCCGC-3') and 3088R_Vd (5'-CGAGATAGTTCTTGCCGAAAAG-3'). Sequences were assembled and analysed in Geneiuos software v.10.2.6 (Kearse et al., 2012). A single representative mite of each genotype was included in further analysis (Supplementary Table S2.1, p. 249). The analysis of DNA sequences polymorphism and haplotypes was carried out with the DnaSP v6 software (Rozas et al., 2017).

2.4.3. Phylogenetic analyses

Sequences were trimmed at 5' and 3' ends to remove bad quality regions leaving a final fragment size of 1413 bp. Heterozygous sequences for 925 codon allele were not included in the analyses to avoid inconsistencies. All sequences were aligned using the multiple alignment functionality of the MAFFT software (Standley and Katoh, 2013). Bayesian phylogenetic inference were conducted in BEAST2 v. 2.5.1 (Bouckaert et al., 2019) with data partitioned for each intron region and codon position to explore the best site model by bModelTest version 1.2.1 (Bouckaert and Drummond, 2017), under a strict clock model, a Coalescence Constant population tree prior and a random tree as starting tree. Six independent runs were conducted, with a chain length of 300 million states each and sampled every 5000 steps. Subsequently, the convergence of the stationary levels were compared and checked with Tracer v1.7.1 (Rambaut et al., 2018), and combined with LogCombiner v.2.5.1 after removing 20% of initial samples. The final effective sample sizes of all inferred parameters were above 700. Tree information was annotated in a consensus tree with TreeAnnotator v.2.5.1 and visualised with FigTree v.1.4.3. The tree was not rooted because when using an outlier sequence from a closer species (*Metaseiulus occidentalis*) to root, all the branches collapsed due to the high identity among the *Varroa* sequences analysed here. This region of the VGSC in *V. jacobsoni* was 100% identical to that in *V. destructor* and was, therefore, not suitable as outlier reference sequence. Finally, the resulting consensus tree was uploaded and customised for publication in the iTOL 4.2 web-platform (Letunic and Bork, 2019).

2.5. Results

A total of 593 *V. destructor* female mites were sequenced in the present study (Table 2.1). These samples were collected from 2008 to 2019, from managed honey bee colonies from 60 locations in 12 different countries, in order to document *kdr*-type haplotype distribution in a wide area across the world (Fig. 2.2).

Table 2.1. Summary of the genotypes found for position 925 of the VGSC of the *V. destructor* samples sequenced for this study, for samples collected from the United States of America (USA) and European countries (EU).

	925L/L	925V/V	925L/V	925M/M	925L/M	925I/I	925L/I	925M/I
EU	224	163	31	3	1	7	None	None
	52.2%	38%	7.2%	0.7%	0.2%	1.6%	0%	0%
USA	91	None	None	18	11	34	5	5
	55.5%	0%	0%	11%	6.7%	20.7%	3%	3%

Sequence analysis revealed a highly conserved sequence of exon 13, corresponding to a region of domain IIS4-S6 of the *Vd*VGSC, and the flanking introns across all different *V. destructor* populations analysed (Fig. 2.1). The lowest sequence identity estimated was 98.4% (Supplementary Table S2.3, p. 255). Given the high sequence similarity among related samples, identical sequences were considered only once, resulting in a dataset of 68 mite genotypes (Supplementary Table S2.1, p.249).

The wild-type allele (L925) was present in all sampled locations. The differences in the exon sequence were reduced to the three already known adaptative substitutions at position 925 (L925V/M/I), a new mutation detected in this study for the first time, a substitution of the Methionine at position 918 by Leucine (M918L) (see below) and a silent mutation at Lysine 903 (AAA to AAG) that was found in a single mite (sequence ESCV7b5_L, haplotype Hap6, Supplementary Table S2.1 and S2.2, p. 249-253). In the non-coding region, corresponding to introns located up- and downstream exon 13, very few changes were found, and these seemed to be random and independent.
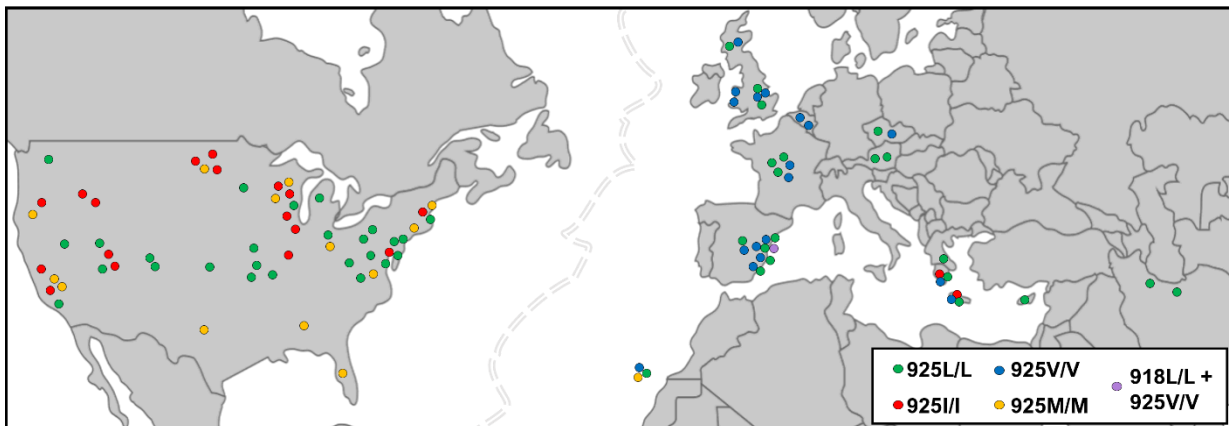
Figure 2.2. Geographic distribution of sampled *V. destructor* populations included in the phylogenetic analyses. Dot colour indicates the genotype for position 925 of the voltage-gated sodium channel (VGSC), being green for L/L, blue for V/V, yellow for M/M, red for I/I and purple for 918L/L + 925 V/V (see Supplementary Table S2.1 for more info, p. 249).

Except for the polymorphisms resulting in changes at positions 918 and 925 (M918L and L925V/M/I) associated with pyrethroid resistance, sequences alignment revealed the presence of 41 additional polymorphic sites (one in the exon and 40 in the intronic regions) and 19 indels in the intronic regions, resulting in 79 haplotypes. (Accession nos. MT859428 to MT859506, Supplementary Table S2.2). These mutations do not appear to be linked to any specific population and therefore lack a biogeographical signal (Supplementary Table S2.1, p. 249).

2.5.1. First detection of mutation L925M outside America.

Concerning to position 925, we did not detect any substitution not previously described in *V. destructor* (L925/V/M/I). As expected, in mites collected in the United States, the substitutions found were only L925M and L925I. On the other hand, more variability was found in mites collected in Europe. In these samples, the most frequent mutation was L925V. However, as we included mites sampled from Greek populations previously reported as carriers of L925I (Alissandrakis et al., 2017), we also detected this amino acid substitution in our sequences (samples GRC3_11_I, GRC3_20_I, GRC5_2_I, GRC5_4_I, GRC5_7_I, GRC8_14_I and GRC8_5_I). More surprising was the detection of L925M in mites collected from El Hierro, one of the seven islands comprising the Canary Islands archipelago (Spain) (Fig. 2.3). Four out of the ten mites sequenced from

El Hierro Island had the L925M substitution. Three of these mites were homozygous 925 M/M (samples ESCN-Fr02_M, ESCN-Fr05_M and ESCN-H82_M), while the other was heterozygous 925 L/M. These samples were collected in 2008 and 2011 and, although they are very few, it might be noteworthy to mention that from the five mites collected in 2008, four were homozygous resistant 925 V/V and only one was 925 M/M. However, in the five mites collected in 2011, the resistant *V. destructor* have the L925M mutation (three out of five). *Varroa* mites collected from other islands in the Canary archipelago showed either the wild-type allele or the L925V mutation (Fig. 2.3).
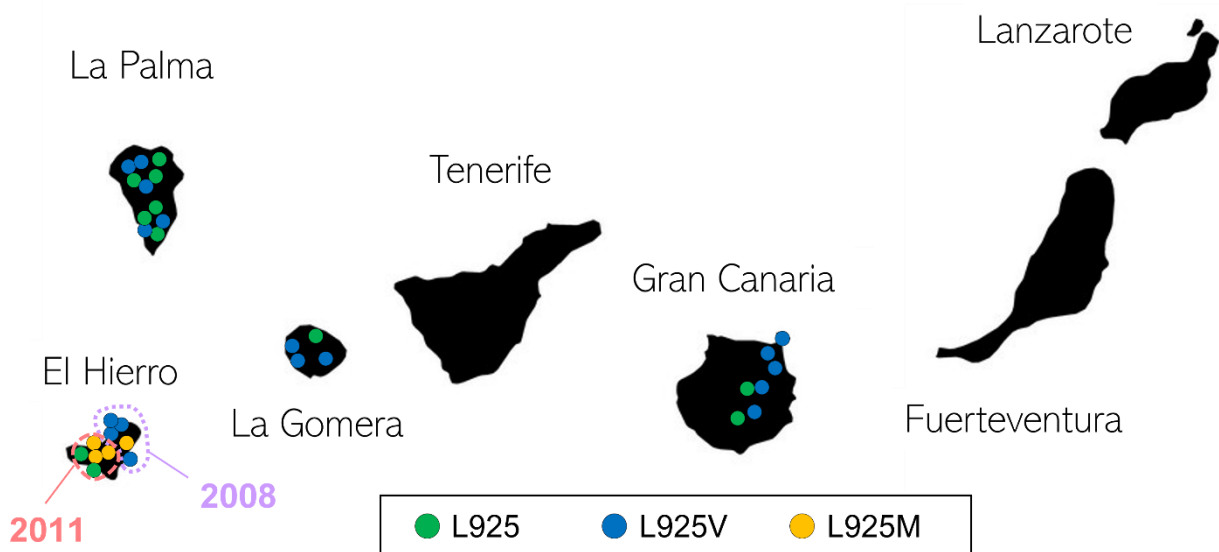
Figure 2.3. Geographical distribution of 925 alleles found in *V. destructor* collected in the Canary Island (Spain). Dot colour indicates the alleles for position 925 of the *Vd*VGSC, being green for L925, blue for V925 and yellow for M925. The year of collection for samples collected on El Hierro island are indicated.

2.5.2. First detection of M918L mutation in *V. destructor*.

In addition to amino acid 925, exon 13 includes other positions known as hot spots for pyrethroid resistance in arthropods (Rinkevich et al., 2013). Among these, substitutions of Methionine 918 have been associated with pyrethroid resistance in *Aphis gossypii* (Carletto et al., 2010), *Dermanyssus gallinae* (Katsavou et al., 2020), *Hyalella azteca* (Weston et al., 2013), *M. persicae* (Fontaine et al., 2011), *Phytoseiulus persimilis* (Benavent-Albarracín et al., 2020), *Thrips tabaci* (Jouraku et al., 2019), *Trialeurodes vaporariorum*

(Karatolos et al., 2012) and *Rhopalosiphum padi* (Zuo et al., 2016), but they have never been detected in *V. destructor* before. In our samples, a single nucleotide polymorphism was detected at the first position of the 918-residue codon (nucleotide position 2983 of the CDS; GenBank Accession AY259834.1), the transversion of Adenine to Thymine, that leads to the substitution of the Methionine at this position for Leucine (<u>A</u>TG (Met) → <u>T</u>TG (Leu)). This mutation was only detected in *V. destructor* samples from the Valencian Community (East Spain) and noticeably, the mutation M918L was always found in combination with L925V (Table 2.2).

Table 2.2. *V. destructor* samples from the Valencian region. Summary of the *V. destructor* samples sequenced in this study collected in the Valencian region (East Spain) during the years 2018 and 2019 in accordance with the alleles detected for positions 925 and 918 of the voltage-gated sodium channel.

	2018			2019		
	925L/L (wild-type)	**925L/V**	**925V/V**	**925L/L** (wild-type)	**925L/V**	**925V/V**
918M/M (wild-type)	15	6	26	24	7	15
	23.8%	9.5%	41.3%	39.3%	11.5%	24.6%
918M/L	None	None	3	None	5	None
	0%	0%	4.8%	0%	8.2%	0%
918L/L	None	None	13	None	None	10
	0%	0%	20.6%	0%	0%	16.4%

The mutation M918L was detected in 10 out of the 26 apiaries sampled from Eastern Spain in 2018 (38.5%), and 17 out of the 34 sampled in 2019 (50%). These apiaries were distributed across the Valencian Community (Fig. 2.4). Thirty-one out of the 124 mites sequenced from this region carried the M918L mutation (8 heterozygotes and 23 homozygotes) (Table 2.2).
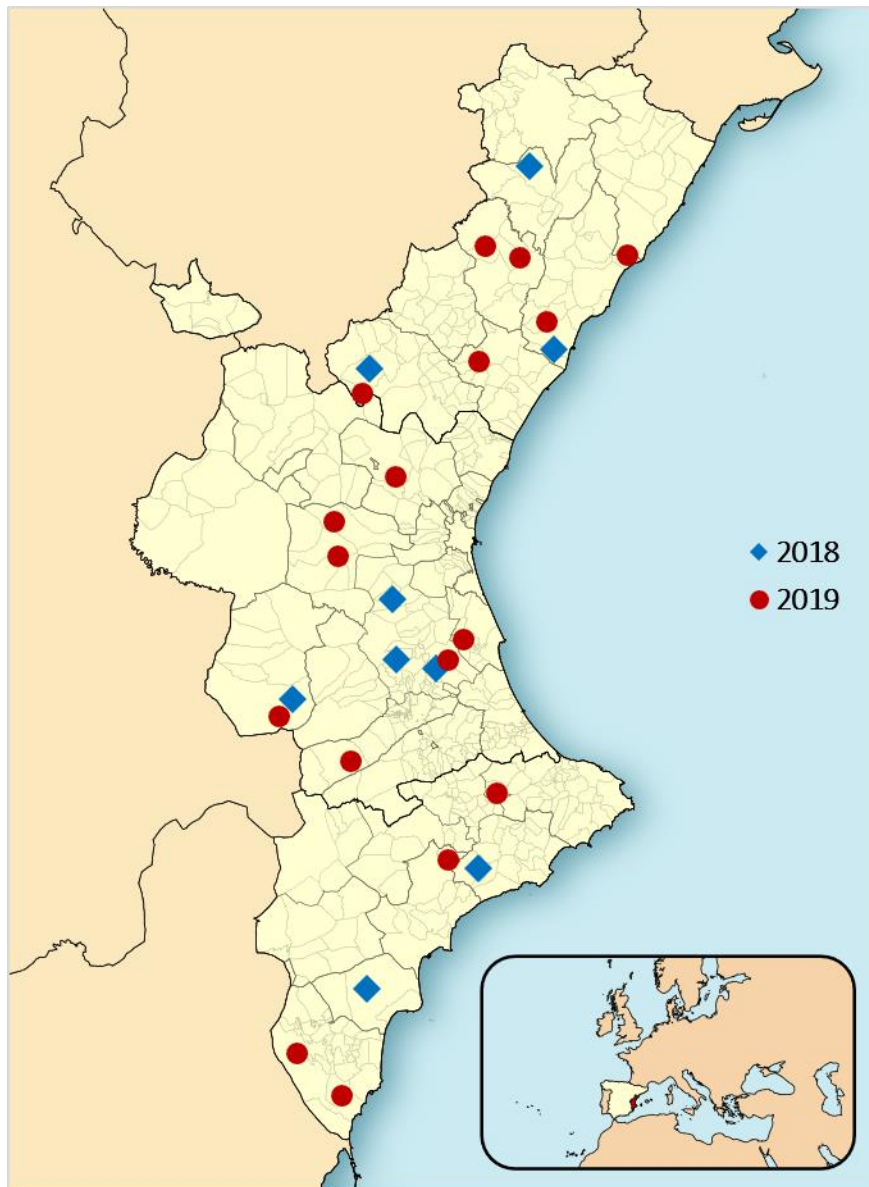
Figure 2.4. Location of *V. destructor* samples bearing M918L mutation in Eastern Spain in 2018 (blue squares) and 2019 (red dots) (see Table 2.2 for more info).

2.5.3. Phylogeny analysis

To explore the phylogenetic relationship among mutations at position 925 of the *V. destructor* VGSC, the 1413 bp sequences were aligned and submitted to a Bayesian MCMC analysis using BEAST2 software. The resulting consensus tree obtained after combination of six independent runs, showed a clear clustering among samples carrying the same substitution at position 925 (Fig. 2.5). Mites carrying the 925V allele clustered together in the same branch while mites with either 925M or 925I grouped in a different branch. Specific features of each of the branches are described below.

Kdr-type alleles
- L925
- L925V
- M918L + L925V
- L925M
- L925I

Tree scale: 0.001
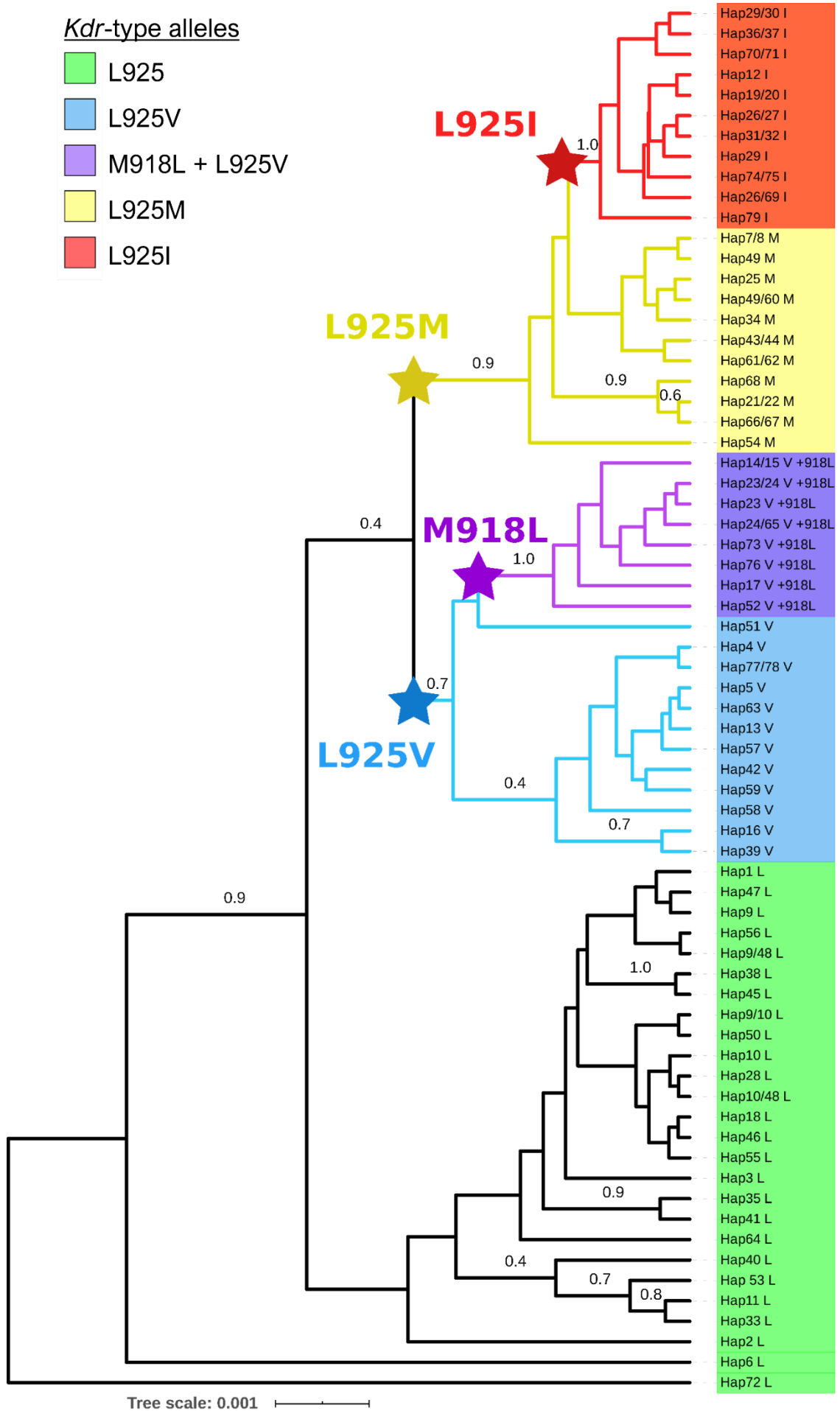
Figure 2.5 (on previous page). Phylogenetic relationship of *kdr*-type mutations for the position 925 of the *Vd*VGSC. Inferred Bayesian phylogenetic tree based on the VGSC genotype sequences comprising exon 13 and the flanking up- and downstream introns. Numbers at branches represent posterior probabilities. For clarity, values of < 0.4 were omitted from the tree. Scale bar indicates distance measured as the average number of substitutions per position. The length of each branch is proportional to the number of nucleotides substitutions per site that have occurred. Tree is unrooted and displayed with a mid-point root for visualisation purposes. Labels are coloured based on the *kdr*-type alleles: green for L925, blue for V925, purple for L918 + V925, yellow for M925 and red for I925. Coloured stars indicate the putative mutation event for L925V, L925M, L925I and M918L in *Vd*VGSC.

The sequence alignment revealed that the amount of phylogenetic signal presented in the sequenced region was small, resulting in many short internal branches difficult to resolve (Fig. 2.5). Pairwise comparison of sequences revealed an identity level ranging from 98.4 to 100% (Supplementary Table S2.3, p. 255). The high level of nucleotide conservation found in the sequences from all the samples made it challenging to resolve the branches nearby the leaves with a confident support. Nevertheless, branches that separate the different resistant alleles from each other showed an adequate support (posterior probability > 0.6) to conclude that each of the substitutions described for position 925 of the *Vd*VGSC share a common and unique origin. The phylogenetic tree exposed that each mutation branching together constituted monophyletic groups, suggesting that the origin of each different substitution was the result of single different mutation events, that subsequently spread to other locations (Fig. 2.5). We did not find any evidence for geographical structuring along the tree for wild-type alleles. Notably, some samples collected from distant geographical locations share a nearly identical sequence at the region studied (Supplementary Table S2.1, p. 249).

The phylogenetic structure of the tree shows a clear relationship between mutations L925M and L925I (Fig. 2.3). They are grouped in the same branch with a clear indication that they are part of a sequential process in which the mutation of Leucine to Methionine (L925M) arose first (CTG → ATG) and that the same codon underwent a second mutation event from Methionine to Isoleucine to generate L925I (ATG → ATA) (Fig. 2.6).

In the case of mites bearing the combination of M918L and L925V, the tree shows that this was also the result of sequential mutation events, but in different codons (Fig. 2.5). The mutation L925V arose first and the mites carrying it forms a monophyletic

group on a branch separated from those containing the other mutations or the wild-type. Then, a second mutation arose within this group causing the substitution of Methionine at 918 for Leucine. Hence, mites bearing M918L and L925V emerge as a monophyletic group from mites carrying L925V (Fig. 2.6).

2.6. Discussion

We used a phylogenetic approach to infer the evolutionary history of target site resistance to pyrethroids in *V. destructor*. The tree topology obtained suggests two different parallel origins for the mutations, one driving the resistance of mites in Europe and another driving resistance in the USA. Overall, our results are consistent with a unique mutation event for each substitution at position 925 (Valine, Methionine and Isoleucine), as well as for the mutation of Methionine to Leucine in the nearby position 918. This suggests that *kdr*-type alleles had evolved in separate events in America and Europe and that their wide distribution throughout each continent is the result of the posterior distribution of mites bearing these mutations. Indeed, given these results, it is possible to hypothesise that the rapid expansion of resistant *V. destructor* bearing these mutations could have been mediated in part by human and bee-mediated transport and by intensive treatments schemes based only on pyrethroid-based acaricides for many years in a row (Rosenkranz et al., 2010).
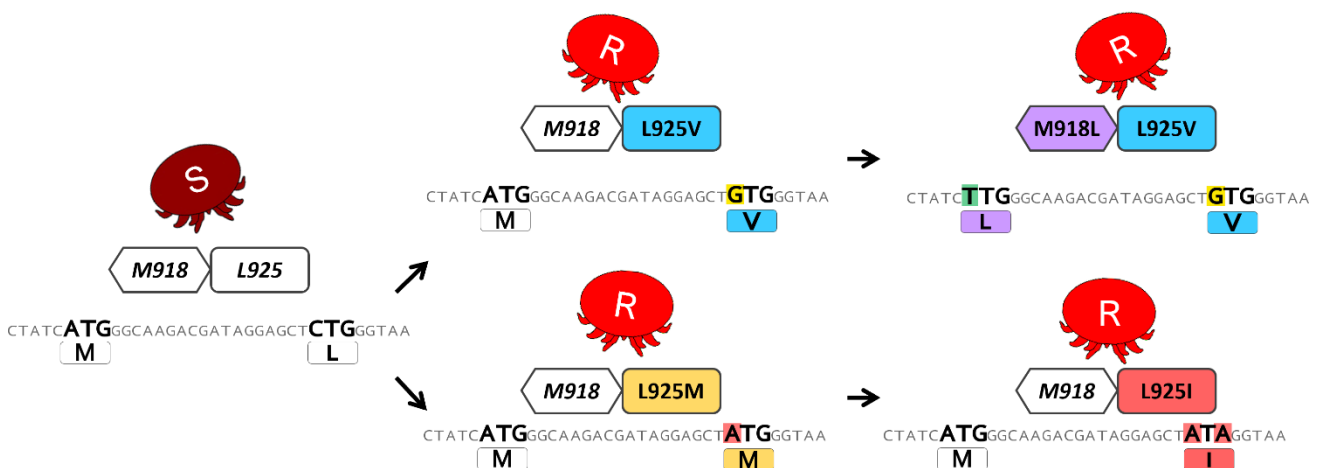
Figure 2.6. Putative sequential evolution of pyrethroid resistance mutations in the *Vd*VGSC. Resistance alleles are indicated by different colours and box shapes. S: Susceptible and R: Resistant to pyrethroids.

The geographical distribution of the resistant alleles correlates well with the results obtained by phylogenetic reconstruction, and therefore also supports the proposal of a single mutation event for each resistance-related amino acid substitution. The mutation L925V is distributed in Europe and L925M and L925I were found mostly across the USA, but also in the Canary Islands and Greece, respectively. However, the L925I and L925M alleles found in Europe appear to be phylogenetically related to the L925I and L925M alleles found in USA mites suggesting that all M925 and I925 alleles share a common origin. Hence, the presence of these mutations in colonies outside America is more likely to be consequence of human facilitated movement rather than to an independent mutation event. In this sense, numerous events have been reported on the introduction of queens and honey bees with different origins on the Canary Islands (De la Rúa et al., 2001; Muñoz et al., 2013), despite the law established in 2001 in La Palma (BOC, 2001) and in 2014 in Gran Canaria (BOC, 2014) which explicitly prohibits the development of beekeeping activities with honey bees other than the local black Canarian ecotype (De la Rúa et al., 1998).

Our results are certainly consistent with the pattern of spread of resistant mites reported at their origins in continental Europe, the UK islands and the USA. Wherein, the initial resistant populations were detected in a specific region and subsequently in nearby or commercially related areas (Martin, 2004; Milani, 1999; Thompson et al., 2002; Trouiller, 1998) (see section 1.1.6 in the introduction chapter).

Given the genetic homogeneity of *V. destructor* populations (Solignac et al., 2005), it is interesting that L925M and L925I mutations were found sharing the same geographical region. The phylogenetic reconstruction suggests that this was likely the result of a sequential process, being the L925M an ancestor of the L925I, that would have arisen in a second parallel mutation event (Leu → Met → Ile). At nucleotide level this hypothesis is the most-parsimonious as well, requiring a single nucleotide change in each step (CTG (Leu) → ATG (Met) → ATA (Ile)) (Fig. 2.6).

An amino acid substitution at position 918 of the VGSC has not been reported before in *V. destructor*, but we have detected mites with a substitution of Methionine for Leucine (M918L) at this position in populations collected in 2018 and 2019 in Valencia (East of Spain). The current restricted distribution of this mutation leads us to hypothesise that it could have emerged recently at some point of the Valencia's area, and that it is

currently spreading, being already found throughout the region (Fig. 2.4, p. 156). The fact that M918L were found linked to L925V and clustering as a monophyletic group inside the L925V group (Fig. 2.5, p. 157), indicates that the origin of the mites bearing the M918L mutation is common and arose in a mite carrying the L925V resistant allele, possibly driven by the high selective pressure of persistent pyrethroids treatments or the accumulation of these acaricides in beeswax. *Tau*-fluvalinate is still one of the most important residues detected in beeswax, but other pyrethroids like flumethrin or acrinathrin are also found in large quantities in samples collected in the Valencian region (Calatayud-Vernich et al., 2017; Calatayud-Vernich et al., 2018). This clearly indicates that there is not only one pyrethroid in use against *Varroa* in the area and that this "enhanced" selective pressure might be contributing to the selection of other mutations, like M918L, not detected before. The M918L is a variant of the well-studied *super-kdr* mutation (M918T) detected for the first time in *M. domestica* with an enhanced *knockdown* resistance phenotype (Williamson et al., 1996). This particular substitution has also been associated with pyrethroid resistance in other pest species, such as *T. urticae* (Wu et al., 2018), *M. persicae* (Fontaine et al., 2011; Panini et al., 2014), *A. gossypii* (Carletto et al., 2010; Chen et al., 2017), *Thrips tabaci* (Jouraku et al., 2019), *T. vaporariourum* (Karatolos et al., 2012) but also in beneficials and non-target arthropods like *P. persimilis* (Benavent-Albarracín et al., 2020) and *H. azteca* (Weston et al., 2013), respectively.

The study of *kdr*-type mutations in arthropod pests, such as *A. gambiae, M. domestica, L. decemlineata* and *M. persicae*, revealed that these mutations arose after independent mutation events occurred in different populations of the same species, likely induced by the strong pressure exerted by pyrethroid pesticides (Alon et al., 2006; Pinto et al., 2007; Rinkevich et al., 2012a; Rinkevich et al., 2012b). Other studies also evidenced that in some insects the *kdr* mutation event was the driving force allowing the spread of the species to new areas to replace more susceptible populations (Haddi et al., 2012). For instance, in *T. absoluta*, the high genetic homogeneity found in populations worldwide and the fact that the *kdr* mutation, L1014F, is almost "fixed", suggested that resistance mutations were key for the spread of this pest (Cifuentes et al., 2011; Haddi et al., 2012).

Varroa destructor populations are not very diverse (Cornman et al., 2010; Farjamfar et al., 2018; Kelomey et al., 2017; Koç et al., 2021; Muñoz et al., 2008; Navajas et al., 2010; Solignac et al., 2005). In fact, the species is considered to have a quasi-clonal structure (Cornman et al., 2010; Solignac et al., 2005; Solignac et al., 2003), although some mite

populations have been described as showing certain level of genetic diversity and population structure as a result of adaptation to the tolerance of their host (Beaurepaire et al., 2019b). This, considering our data, suggests that each mutation (L925V/M/I) would have emerged in a unique event that was subsequently spread through the population on account of pyrethroid pressure. The particular reproductive traits of the mite (adelphogamy - mating between full siblings) (Rosenkranz et al., 2010) and some aspects of honey bee behaviour like drone drifting, foraging, robing and swarming would have led to exponential multiplication of the resistant alleles within the colonies and their successive dispersion to other populations. There are also human related factors like migratory beekeeping, colony displacement for pollination and honey bee trading, contributing to the swift spreading of the mites and resistance alleles across vast areas (Simone-Finstrom et al., 2016). The study of *kdr* mutations in *Bemisia tabaci* MED, or of *ace* (acetylcholinesterase gene) mutations in *Tetranychus urticae* showed that in species with high genetic structure even a low gene flow between geographical populations, probably mediated by human activities, was sufficient to allow resistant alleles of single evolutionary origin to spread across a wide geographic range (Gauthier et al., 2014; Ilias et al., 2014).

Our phylogenetic analysis supports the hypothesis of independent origin for resistant alleles in Europe and the USA, and a close relation between L925M and L925I alleles. Our data also suggest that uncontrolled trading of parasitized honey bees might be an important route for spreading resistant alleles overseas. The substitution M918L, associated with pyrethroid resistance in other species, is reported here for the first time in *V. destructor*, in conjunction with L925V in mites from Spain. The implications of these evolutionary and dispersal processes for *Varroa* mite management are thoroughly discussed in the general discussion section.

CHAPTER 3

Determine the prevalence of pyrethroid resistance mutations in the *Varroa destructor* population from the United States

3.1. Introduction

Beekeepers in the United States (USA) have noted higher than acceptable annual colony losses in the past 14 years (BIP, 2020; Kulhanek et al., 2017). Prior to 2006, colony losses in the USA were estimated to average 5–10% each year (vanEngelsdorp et al., 2008), but they significantly increased to average around 39% annually in the last 10 years (BIP, 2020). These losses can be recovered by replacing the colonies, and therefore have not been accompanied by such a large reduction in the number of colonies in the country, but it has an economic toll and extra management efforts that are estimated to be millions of US dollars per year (Haber et al., 2019; Rucker et al., 2019; vanEngelsdorp et al., 2008; vanEngelsdorp and Meixner, 2010). These high levels of losses are a concern for USA beekeepers, the farmers that relies on beekeepers to provide bees for pollination, and the consumers who benefit from the diversity of food products that honey bee pollination facilitates (Calderone, 2012; Rucker et al., 2012, 2019; Steinhauer et al., 2021).
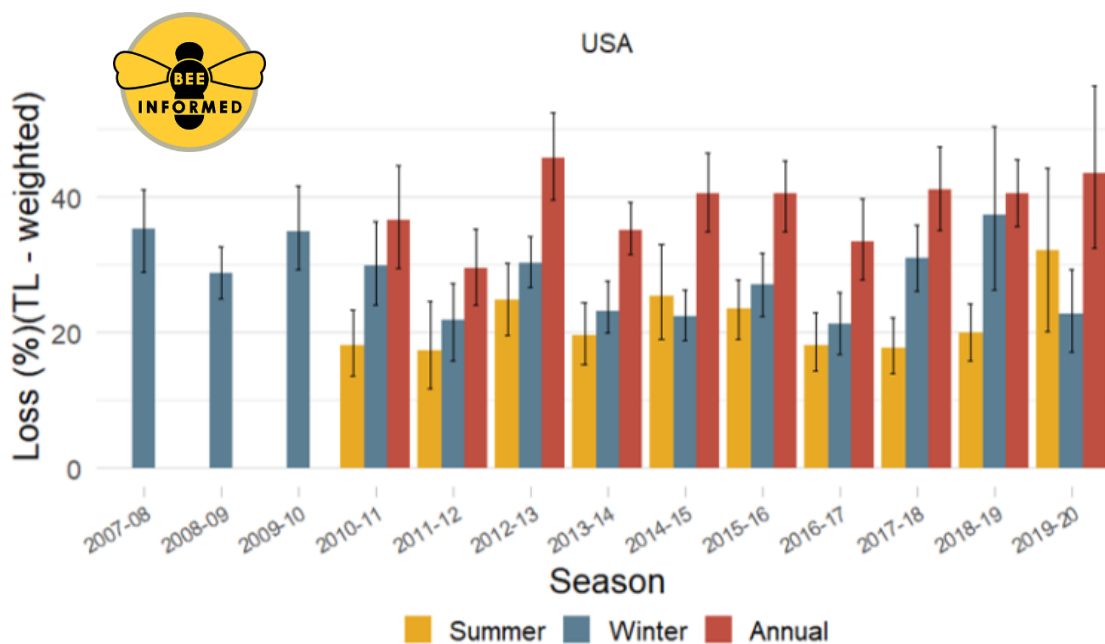
Figure 3.1. Honey bee colony loss rates (in %) in the USA across the years. Result data from the Bee Informed Partnership's national honey bee colony loss survey. Bars represent the total rate of colony loss for summer (yellow bars; 1 April – 1 October), winter (blue bars; 1 October – 1 April), and annual (red bars; 1 October – 1 October). (Source: https://beeinformed.org/citizen-science/loss-and-management-survey/).

Beekeepers and researchers seem to agree that there are different factors, some of them interacting synergistically, that affect bee health (Di Prisco et al., 2016; Genersch, 2010; Goulson et al., 2015; Stanimirović et al., 2019). There is mounting evidence that, of these factors, the largest single driver of colony losses is the parasite *V. destructor* and the viruses this mite vectors (Amdam et al., 2004; Boecking and Genersch, 2008; Di Prisco et al., 2016; Ellis et al., 2010; Francis et al., 2013; Guzmán-Novoa et al., 2010; Martin et al., 2012; Neumann and Carreck, 2010; Ramsey et al., 2019; Roberts et al., 2017; Stanimirović et al., 2019; Sun et al., 2016; Traynor et al., 2020). Currently, *V. destructor* parasitism causes more economic damage than any other bee diseases (Genersch, 2010; Rucker et al., 2012).

Since untreated colonies experience a rapid reduction in health, regular treatment against *V. destructor* have become an essential part of bee management for USA beekeepers. The use of synthetic varroacides, such as the formamidine amitraz, the organophosphate coumaphos, and the pyrethroids flumethrin and *tau*-fluvalinate, have long been in beekeepers "toolbox" (Rosenkranz et al., 2010; Steinhauer et al., 2021). Although there are other non-synthetic acaricides and management techniques available, synthetic miticides are often the preferred choice because of the advantages they offer (Delaplane and Hood, 1997; Haber et al., 2019; Rosenkranz et al., 2010; Roth et al., 2020). Synthetic varroacides are not, however, always effective in reducing colony loss rates. Some mite populations have become resistant to specific compounds. As with other arthropod pests, intensive treatment schemes that rely exclusively on a single compound over consecutive seasons has resulted in the evolution of resistance in mite populations (Bell et al., 1999; Elzen et al., 1998; Elzen et al., 1999b; Macedo et al., 2002; Martin, 2004). Currently, resistance to the three classes of synthetic compounds used for *Varroa* control has been reported in USA (Elzen et al., 1999a; Martin, 2004; Pettis, 2004; Rinkevich, 2020).

In 1987, the pyrethroid *tau*-fluvalinate was approved for use in USA beehives in response to the recent introduction of *V. destructor* (Ellis et al., 1988). This product was a mainstay of mite management until the late 1990s, when mite resistance was widely observed (Bell et al., 1999; Elzen et al., 1998; Elzen et al., 1999b; Macedo et al., 2002; Martin, 2004). The mechanisms of resistance to pyrethroids in *Varroa* has been correlated with the substitution of residue 925 of the VGSC protein (numbered after the housefly *para*-type sodium channel protein). In resistant *Varroa* mites from Europe, the mutation found associated with *kdr*-type resistance to pyrethroids is the substitution from the wild-type Leucine to Valine at position 925 of the *Vd*VGSC (L925V) (Alissandrakis et al., 2017;

González-Cabrera et al., 2013; Hernández-Rodríguez et al., 2021; Hubert et al., 2014; Panini et al., 2019; Stara et al., 2019a). But in the USA, *kdr*-type mutations in *V. destructtor* are associated with an Isoleucine (L925I) or Methionine (L925M) substitutions of the wild-type Leucine at the same position (González-Cabrera et al., 2016).

Previous studies have evidenced the spread of the L925V mutation across Europe, but for USA, their detection was limited to few Southeastern apiaries. Knowing the spread and incidence of these mutations throughout the country's apiaries will let to comprehend the actual scenario for USA beekeepers, and will allow to address the situation more effectively.

3.2. Objectives

A previous study revealed the presence of the L925I and L925M *kdr*-type mutations in *V. destructor* from USA, however this study was limited to few apiaries in the Southeast, namely in the states of Florida and Georgia. Knowing the extent and incidence of these mutations throughout the country's apiaries will facilitate to comprehend the actual scenario/situation for USA beekeepers, and will allow to address the issue of resistance to pyrethroid-based treatments more effectively. The objective of this chapter is to study the incidence of mutations that cause pyrethroid resistance in *V. destructor* populations in USA apiaries.

For detecting the *kdr*-type mutations in *V. destructor*, our group have previously designed and tested a high throughput allelic discrimination assay based on TaqMan®. This method has been demonstrated to be robust, reliable, and fast for genotyping large number of mites individually, hence able to determine the incidence of pyrethroid resistant and susceptible mites in a given apiary (2018; González-Cabrera et al., 2013; 2016). Using this diagnostic tool on mites sampled in 2016 and 2017, we generated a distribution map of pyrethroid resistance mutations across the USA.

3.3. Materials and methods

3.3.1. *Varroa destructor* samples

As part of the US National Honey Bee Disease Survey (NHBDS), female adult *V. destructor* mites were collected from samples at apiary level aggregate across the USA in 2016 and 2017 (Traynor et al., 2016). In brief, samples were collected by apiary inspectors or professional beekeepers in all participating states, included ¼ cup of bees scooped from each of 8 colonies in the same apiary. When possible, collected bees were scooped from a brood nest frame containing open and closed brood cells. The mites were dislodged from the bees using a soapy water shaker (adapted from Rinderer *et al.* (2004)). Collected and counted mites were placed into a 1.5 mL microcentrifuge tube containing 70% ethanol and shipped to the University of Valencia, Spain, for allele frequency determination.

3.3.2. TaqMan® diagnostic assays

A high throughput allelic discrimination assay based on TaqMan® was used to genotype individual mites from 118 and 110 different apiaries sampled across the USA in 2016 and 2017, respectively. The assay accurately discriminates among wild-type mites and those carrying the mutations L925I and L925M in the VGSC (González-Cabrera et al., 2016).

Genomic DNA was extracted from 16 individual adult female mites per apiary (for few apiaries only 15 mites were available) using a modified alkaline hydrolysis method described previously by González-Cabrera *et al.* (2013). Briefly, the mites were placed individually in each well of 96-well flat-bottom microtiter plates containing 20 µL of 0.25 M of NaOH. The mites were then ground using a multiple homogenizer (BA/MH96, Burkard Scientific Ltd., Uxbridge, UK) (ffrench-Constant and Devonshire, 1987). Subsequently, 20 µL of Neutralization buffer (125 mM HCl, 0.5% Triton X-100 and 125 mM Tris/HCl pH 8.0) was added to each well, and the plate was spun at $1000 \times g$ for 5 min. The supernatant containing the DNA was transferred to a new 96-well PCR microplate and stored at -20 ℃ until used.

Primers and probes for the TaqMan® assay were designed using Primer Express™ Software v.2.0 (Life Technologies) against the *V. destructor* genomic sequence (Accession KC152655), as described in González-Cabrera et al. (2016). Primers (Supplementary Table S1.1, p. 249) were designed to amplify a single 97 bp fragment flanking the position 925 of the VGSC (Forward primer, Vd_TM_L925V_F: 5'-CCAAGTCATGGCCAACGTT-3', Reverse primer, Vd_TM_L925V_R: AAGATGATAATTCCCAACACAAAGG-3') (González-Cabrera et al., 2013) (Fig. 3.2).
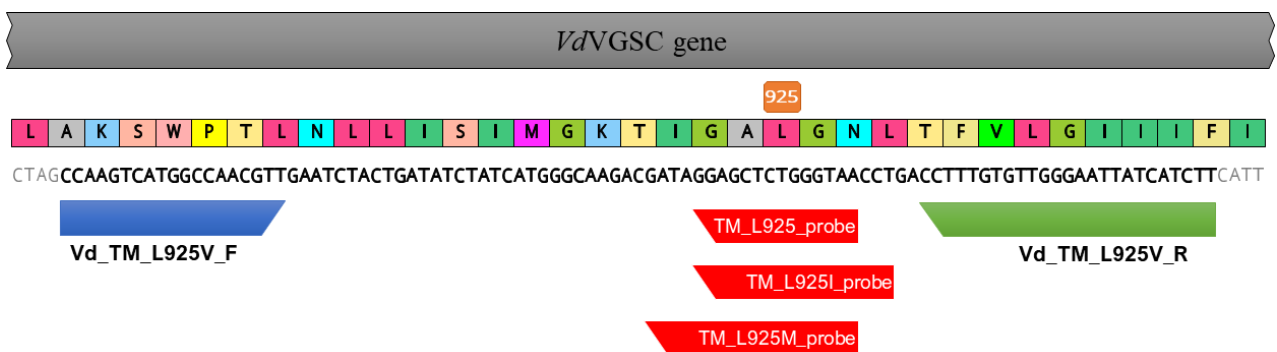
Figure 3.2. Schematic representation of *Vd*VGSC gene section target in the TaqMan® assay described. Forward and reverse primers (showed as blue and green arrowed boxes, respectively) amplify the region spanning 97 nt within exon 13 of the *Nav* gene that encodes the codon for residue 925 of the protein (highlighted in orange). The probes (in red) bind to the specific allelic variants at position 925 (shown in orange) within the region amplified by the primers.

Regular or singleplex TaqMan® assays allow the detection of only two different alleles at a time by using two probes per reaction. Sometimes, this is limited by the detection characteristics or channels of the thermocycler instrument. In our attempt to screen for the three allelic variants of interest (L925, L925M and L925I) in a single reaction, we adapted a multiplex TaqMan® assay, equipping the TaqMan® probes with different fluorogenic dyes and adjusting the instrument settings. Upon adaptation and optimisation of the multiplex TaqMan® assay, it was capable of distinguish between the six possible genotypes that could generate the combination of the three allelic variants (González-Cabrera et al., 2016). Furthermore, multiplex TaqMan assays are more time and cost-effective than performing two singleplex Taq-Man® assays (preparation of two reactions and two qPCR runs instead of one), reducing considerably in experimental time and also cutting down reagent and material consumption, and thus reducing waste.

In order to achieve this, three custom probes labelled with a different fluorophore at the 5'-end were used for the detection of the different alleles at position 925 of the *Vd*VGSC. Thus, the probe specific for the wild-type allele (5'-TTACC<u>CAG</u>AGCTCC-3') was labelled with VIC®, the probe specific for the L925I mutation (5'-AGGTTACC<u>TAT</u>AGCTCC-3') was labelled with 6-FAM™, and the probe specific for the L925M (5'-TTACC<u>CAT</u>AGCTCCTATC-3') mutation was labelled with NED® (codon 925 is underlined). All probes have a non-fluorescent quencher (NFQ) and a minor groove binder (MGB) attached to the 3'-end. The MGB increases the melting temperature of the probe (T_m) by stabilisation of van der Waals forces, thus improving the allele discrimination accuracy (Afonina et al., 1997).

TaqMan® probes are hydrolysis probes in which the fluorescence signal of the fluorophore, covalently attached to the 5'-end, is inhibited by the quencher attached to the 3'-end, as long as they are in close proximity. These probes anneal with high specificity to their complementary DNA sequence, in this instance the region corresponding to residue 925 of the *Vd*VGSC gene. During the elongation step, the 5' to 3' exonuclease activity of *Taq* polymerase degrades the probe that is specifically attached among the template DNA being amplified, releasing the fluorophore and relieving it from the quencher effect. The fluorescence emitted is therefore directly proportional to the fluorophore released and the amount of template DNA present in the PCR.

TaqMan® assay mixture contained 1.5 µL of genomic DNA, 7.5 µL of 2x TaqMan® Fast Advanced Master Mix (Applied Biosystems), 0.9 µM of each primer and 0.2 µM of each probe, in a total volume of 15 µL. Reactions were carried out on a StepOnePlus™ Real-Time PCR system (Applied Biosystems), with the following cycling conditions: 2 min at 50 ℃, 10 min at 95 ℃, followed by 40 cycles of 15 s at 95 ℃ and 1 min at 63 ℃, ending with a post-PCR read of 2 min at 50 ℃.

Since the detection system at our disposal does not allow the detection of three fluorophores at a time, we had to adjust the lectures as follows: Firstly, a pre-PCR readout step for NED® (546 nm excitation and 575 emission) was performed to establish baseline values; subsequently, increasing fluorescence in VIC® (538 nm excitation and 554 nm emission) and 6-FAM™ (494 nm excitation and 518 emission) was monitored in a real-time PCR run.; and finally, a post-PCR readout was performed to detect the fluorescence

increment in NED®. The results obtained were analysed using StepOne Software v2.3 (Applied Biosystems) and combined.
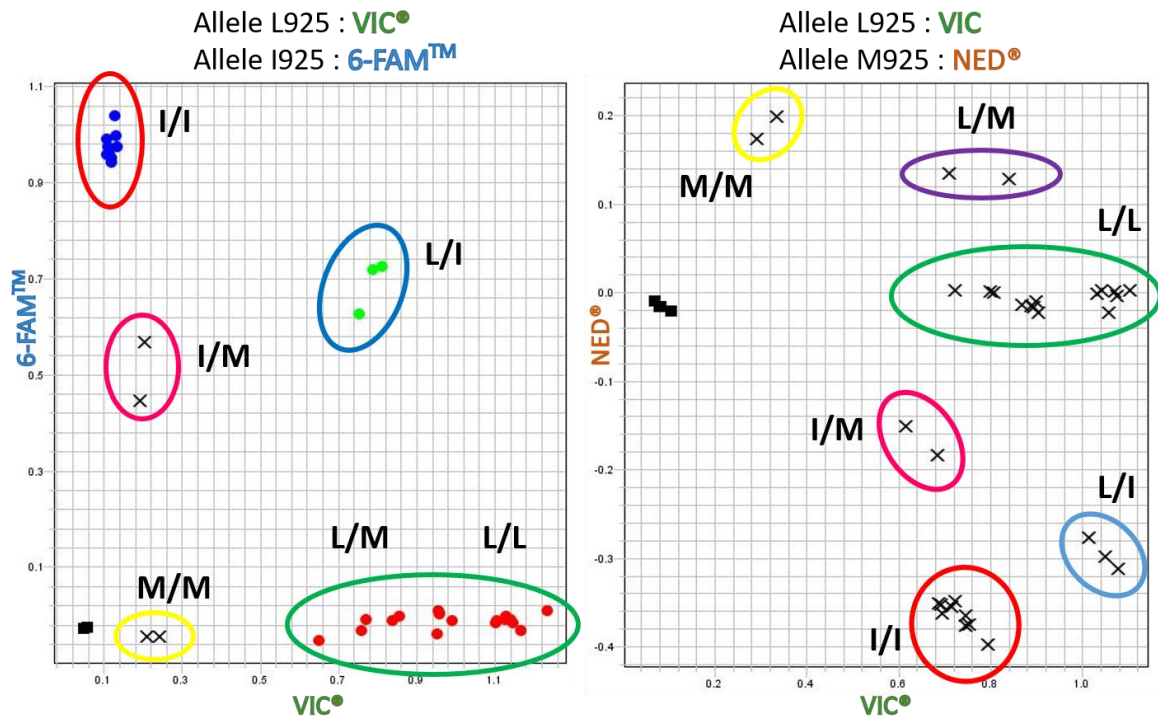
Figure 3.3. Result of an allelic discrimination multiplexed TaqMan® assay for the detection of mutation L925I and L925M in *Vd*VGSC gene. Scatter plot of the fluorescence increment showing the distribution of the six possible genotypes given the three alleles present. Left panel shows the readout 6-FAM™ (allele I925) vs VIC® (allele L925), and the left panel that of NED® (allele M925) vs VIC® (allele L925). Values of X and Y axes are final corrected fluorescence data. Each point represents an individual mite (negative controls represented as squares). L/L: Homozygous for Leucine, M/M: Homozygous for Methionine, I/I: Homozygous for Isoleucine, L/M: Heterozygous for Leucine and Methionine, L/I: Heterozygous for Leucine and Isoleucine and M/I: Heterozygous for Methionine and Isoleucine.

This method discriminates individual mite genotypes by comparing the intensity of fluorescence signals during each cycle of the PCR amplification process. Increment of fluorescence for only one dye indicates that the mite is homozygous for that allele, and intermediate increases in the fluorescence of two dyes indicates that the mite is heterozygous (González-Cabrera et al., 2016). Samples in which no fluorescence increase

was detected or with questionable results were Sanger sequenced to rule out the presence of an allele different from those analysed. In this study, only L925 mutations previously found in the USA were identified (L925I and L925M), so neither the L925V mutation nor any other mutation at position 925 were detected.

3.3.3. Statistical analysis

Statistical analyses were performed using the SPSS v25.0 (IBM SPSS Statistics, Armonk, NY: IBM Corp.) and GraphPad Prism 7 (GraphPad software, Inc, San Diego, CA). The unpaired and nonparametric Mann-Whitney U test was used to compare the differences observed between the year 2016 and 2017 for each genotype, as well as for the expected phenotype, the total sum for each allele and the proportion of homozygotes and heterozygotes. For the comparison of data from the same apiary between the two years, statistical significance was calculated by Fisher's exact test. The differences observed were considered significant if P values were lower than 0.05.

3.4. Results

In this study, a total of 3,576 mites collected from 228 apiaries across the USA territory were genotyped for mutations at position 925 of the VdVGSC, the region associated with pyrethroid resistance in *V. destructor* (2018; González-Cabrera et al., 2013; 2016). We have quantified the allele variation for position 925 of this gene using a multiplex TaqMan® assay and specific probes to detect the wild-type and resistant mutations reported in the USA (L925I and L925M). For each sampled year, obtained data were normalized as percentages of mites with different genotypes and phenotypes, per apiary (Supplementary Table S3.1, p. 256), State (Supplementary Table S3.2, p. 257), and nationally (Supplementary Table S3.3, p. 259).

Nationally, the wild-type Leucine allele at position 925 of the VdVGSC predominated and was found at the same frequency in the mites sampled in both years (54.7% for both years, Mann-Whitney U, $P>0.05$). For the two detected mutant alleles, the frequency of Isoleucine was 25.1% in 2016 and 28.7% in 2017, with no statistically significant differences between the two years (Mann-Whitney U, $p>0.05$). However, a

significant reduction for the Methionine allele was found in 2017 (16.6%) compared to 2016 (20.2%) (Mann-Whitney U, *P*= 0.033).
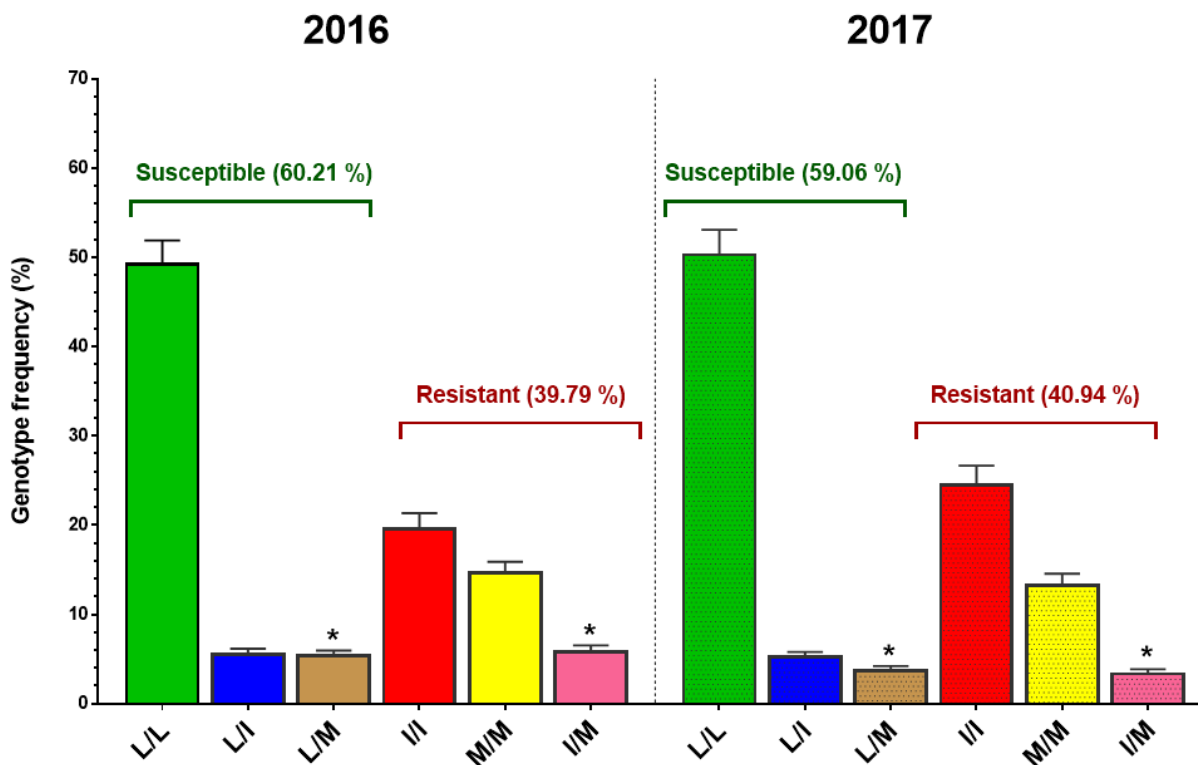
Figure 3.4. Genotype frequency of mutations at position 925 of the VGSC obtained from *V. destructor* collected across the USA in 2016 and 2017, and predicted phenotype for pyrethroid resistance. L: wild-type L925, I: mutant L925I and M: mutant L925M. Values are normalized and shown as percentages for each year. Bars indicate standard error values (SE). Significant differences between the two years for the same genotype are labeled with an asterisk (*) (Mann-Whitney U, *P<0.05).

As it is possible to find the three alleles in the same colony (wild-type allele and the two resistant alleles), six different genotypes can be generated from their combination in female *Varroa* (L/L: Homozygous for the wild-type allele L925, L/I: Heterozygous for L925/I925, L/M: Heterozygous for L925/M925, I/I: Homozygous for the resistant allele I925, M/M: Homozygous for the resistant allele M925, I/M: Heterozygous for I925/M925). The frequency of homozygous mites increased between 2016 and 2017 (83.4 to 87.9%, Mann-Whitney U, *P*=0.016). When considering all data, the susceptible homozygote (L/L) was the most prevalent genotype (49.2 and 50.3% of total mites tested in 2016 and 2017, respectively), followed by the resistant homozygotes I/I (19.5 and

24.4% of total mites tested) and M/M (14.6 and 13.2%). The remaining three heterozygotes had frequencies below 5.8% (Fig. 3.4). A significant reduction in the overall proportion of mites with alleles L/M and I/M was observed between 2016 and 2017 (Mann-Whitney test, P=0.020 in both); the frequency of no other genotypes changed significatively between years.

Kdr-type resistance is inherited as a recessive trait (Brito et al., 2018; Davies et al., 2007; Sun et al., 2016), then only mites with genotypes I/I, M/M and I/M will show the resistant phenotype. On the other hand, mites carrying at least one copy of the wild-type allele would be susceptible to pyrethroid treatment (genotypes L/L, L/I and L/M), as indicated by González-Cabrera et al. (2016). The data reporting the genotypes and predicted phenotypes (Susceptible or Resistant to pyrethroids) for each sampled apiary are shown in the Supplementary Table S3.1 (p. 256). In summary, susceptible mites were more common than resistant mites (Supplementary Table S3.1, p. 256), and the overall frequencies of susceptible and resistance phenotypes remained constant between the two years (Fig. 3.4).

Figure 3.5 (on next page). Distribution map of sampled *V. destructor*. Genotypes for the 925 position in the VGSC of *V. destructor* are shown in A and B for 2016 and 2017, respectively. The predicted susceptibility or resistance to pyrethroid phenotypes are shown in C and D for the 2016 and 2017, respectively. Color legend is shown above each map (genotype's maps (A and B): green for L/L, blue for L/I, light brown for L/M, red for I/I, yellow for M/M, and pink for I/M; and phenotype's maps (C and D): green for susceptible and red for resistant).
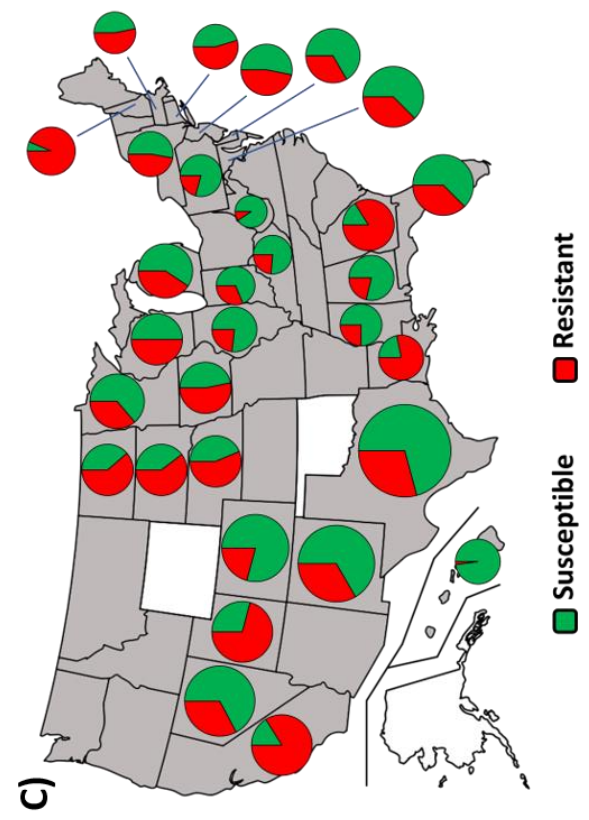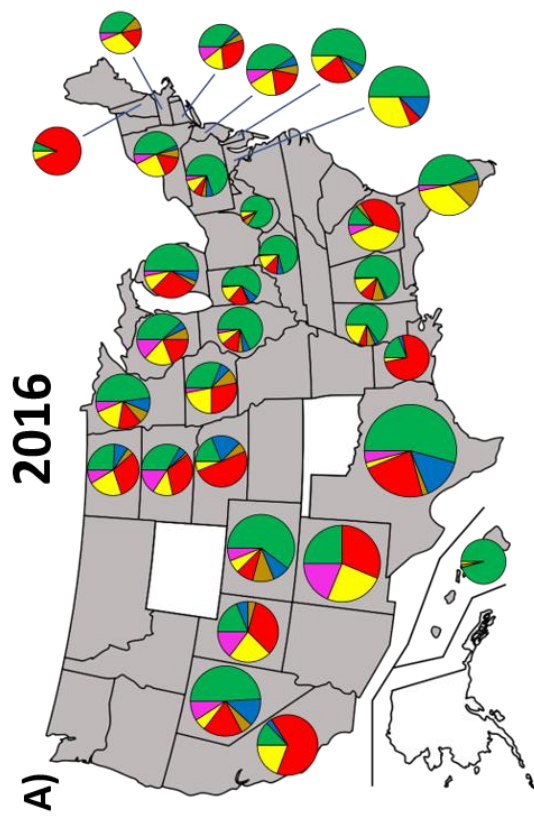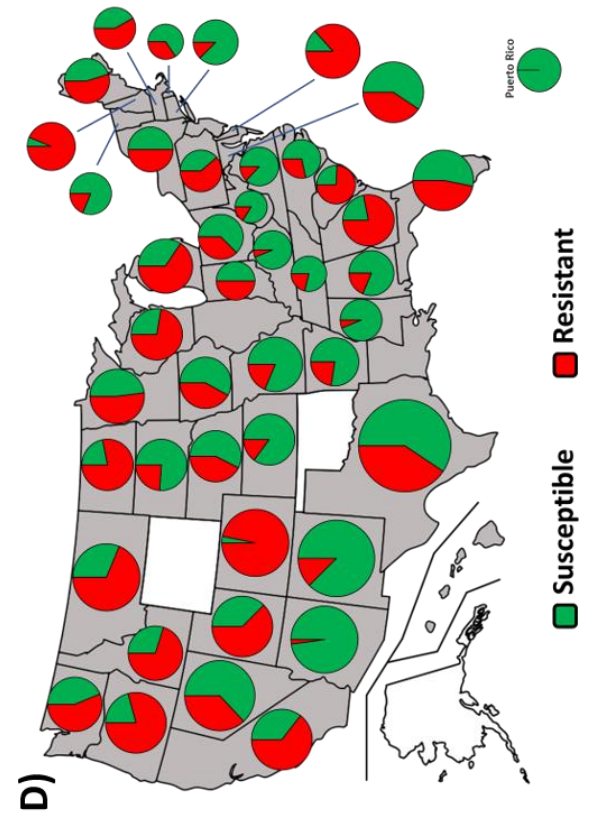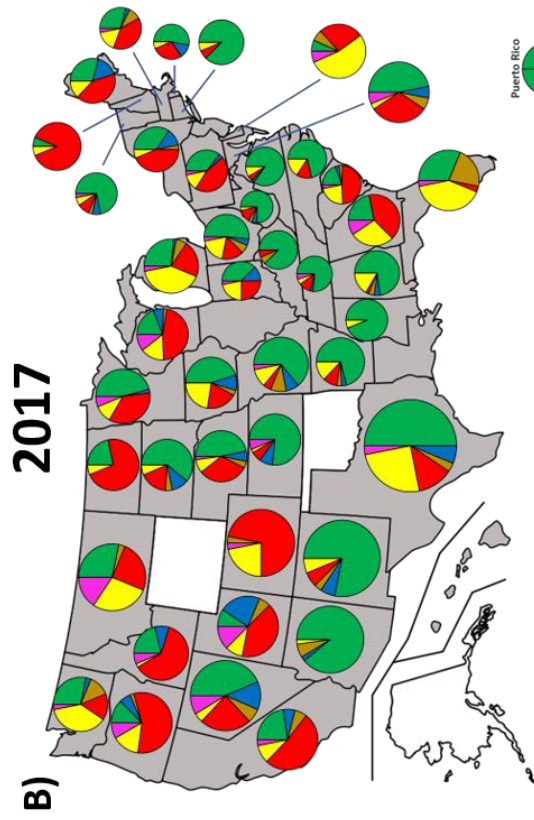
The percentage of apiaries sampled in both years containing fully susceptible mites (i.e. genotypes L/L, L/I or L/M) was low and almost the same in both years, (mean ~9.5%). Worryingly, the proportion of apiaries completely 'free' of mites with resistant mutations was very low (mean 2.2%). Of the 12 apiaries with mites with L/L alleles exclusively, two were from an island in Hawaii and three from the territory of Puerto Rico, places where mites (and presumably mite treatments) occurred relatively recently.

To convey a sense of the distribution of different genotypes and phenotypes across the country, genotype frequencies were grouped by State for each year (Fig. 3.5, Supplementary Table S3.2, p. 257). Our results showed that both mutant alleles are widespread throughout most apiaries in the country. The frequencies of genotypes and phenotypes among States and time, however, showed considerable variability. Notably, of the 25 states that were sampled in both years (Fig. 3.5) shifts in the percentage of mites that were susceptible or resistance changed dramatically, but not in a consistent way across states (Fig. 3.6).
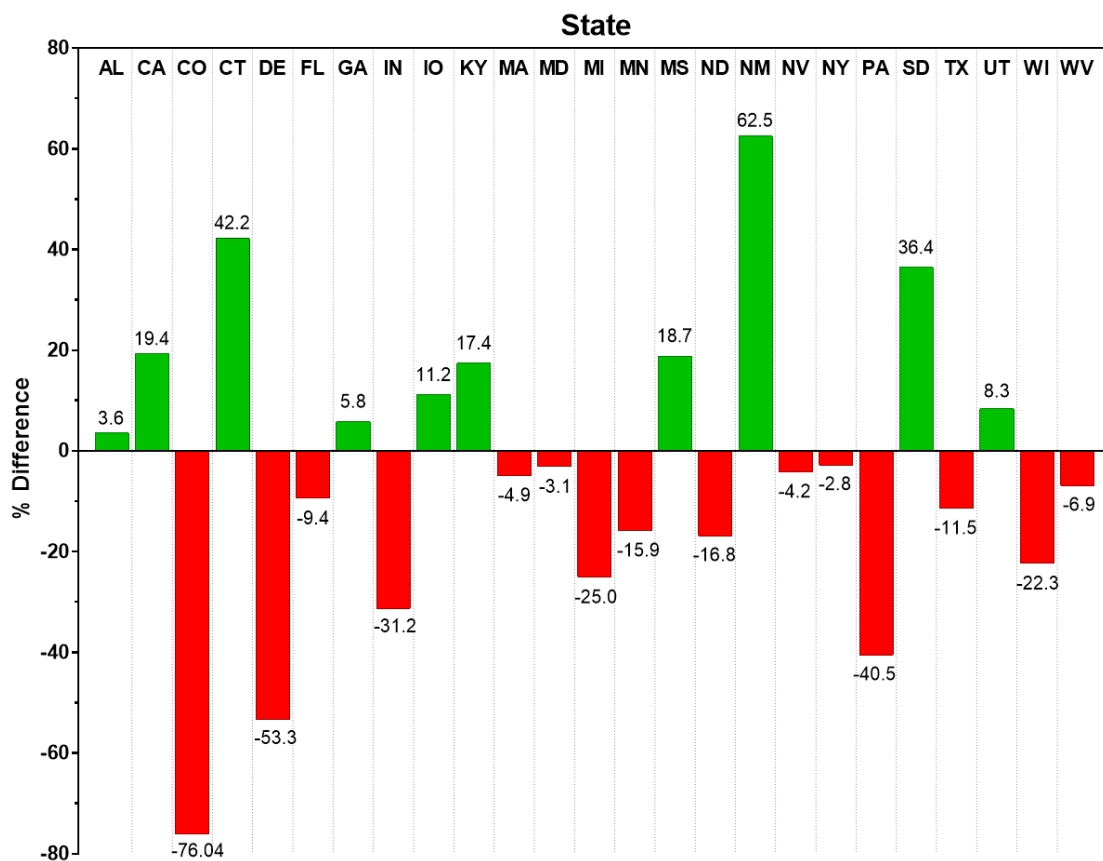
Figure 3.6. Variation between years 2016 and 2017 in the proportion of *V. destructor* susceptible to pyrethroid treatment by State.

Of the 110 samples collected in 2017, eleven had also had samples collected in 2016. The results of these apiaries in both years were compared side by side and are shown in Fig. 3.7 and Supplementary Table S3.3 (p. 259). In seven of these apiaries the frequency of resistant mites differed between years (Fisher's exact test, *P*<0.05), with six out of seven showing an increase in the proportion of resistant mites.
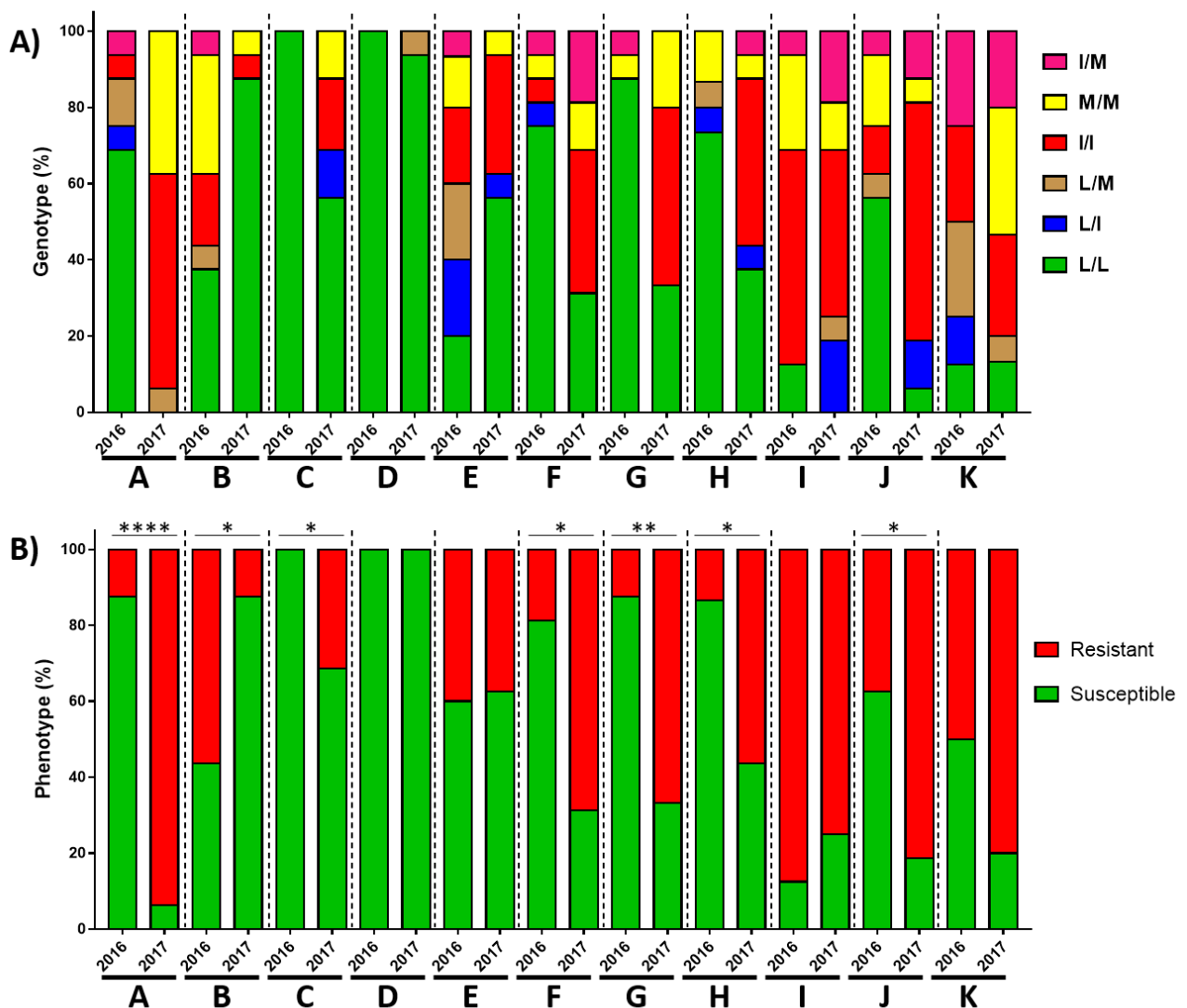
Figure 3.7. Genotype for position 925 of the *Vd*VGSC (A) and the associated pyrethroid susceptibility or resistance predicted phenotype (B) in colonies from the same apiary sampled in 2016 and 2017. A to K code letters refers to the different apiaries. Significant differences between years are labelled as follows: Fisher's exact test, *P* < 0.05, ** *P* < 0.01, **** *P* < 0.0001. Color legend are shown for each graph (genotype (A): green for L/L, blue for L/I, light brown for L/M, red for I/I, yellow for M/M, and pink for I/M; and phenotype (B): green for susceptible and red for resistant). See Supplementary Table S3.3 for more info (p.259).

3.5. Discussion

In this study, we describe, for the first time, the frequency of pyrethroid resistant alleles in *V. destructor* from apiaries across the USA. The results over the two years surveyed suggest that the mutations responsible for pyrethroid resistance are widespread in the mite population of USA apiaries (Fig. 3.5).

The European resistant allele L925V was not detected in the USA, neither other new substitution. However, our results showed that the former reported *kdr*-type mutations, L925I and L925M, are widespread and at high incidence in some States (Fig. 3.5). This confirms a long held understanding that *tau*-fluvalinate or other pyrethroid based products, have limited value for many USA beekeeping operations (Haber et al., 2019). So, the 'general' use of *tau*-fluvalinate or other pyrethroid based products is certainly threatened in a near future if no action is taken to address the situation.

The data presented here is a picture of the situation in 2016 and 2017, but the level of resistance in an apiary's population may fluctuate over a short period of time depending on the treatment regime or the exposure of mites to acaricide residues from previous treatments (González-Cabrera et al., 2018; Lodesani et al., 2008; Martins and Valle, 2012; Orantes-Bermejo et al., 2010). While nationally the overall proportion of genotypes and phenotypes was relatively stable across years (Fig. 3.4), considerable changes were noted at state and apiary level within and between years (Fig. 3.5, 3.6 and 3.7, Supplementary Table S3.1, S3.2 and S3.3, p. 256-259). This high variability suggests that allele frequencies are strongly influenced by external factors, such are recent varroacide applications (González-Cabrera et al., 2018). Such treatment influence have been described for the European L925V substitution (González-Cabrera et al., 2018). Unfortunately, very little treatment data was available for sampled operations as this information is not required as part of the national survey. Samples taken for this study were obtained from a voluntary national survey meant to describe disease incidence in honey bee colonies across the nation (Traynor et al., 2016). The survey was not designed to identify factors that may explain incidence rates *per se*. Ideally, a good understanding of the treatments used by the operations sampled would help us elucidate whether the changes in the frequencies of resistant alleles were influenced by the treatment regime. However, requiring this information would discourage the voluntary participation of beekeepers in the programme.

Nevertheless, a survey of beekeeping practices in USA beekeeping operations from April 2013 to March 2017 reported very low rate of *tau*-fluvalinate use among USA beekeepers (Haber et al., 2019), suggesting that there might be other sources of selection pressure keeping resistant alleles at high frequencies in the USA *V. destructor* population. One possible source is the accumulation of acaricide products in colony matrices like beebread and comb wax. *Tau*-fluvalinate is among the most prevalent and ubiquitous residue detected within colonies, largely because it is a lipophilic product and is sequestered in comb bee's wax (Bernal et al., 2010; Calatayud-Vernich et al., 2018; Johnson et al., 2010). A recent survey of bee wax collected from USA colonies reported that 70.8% of them had detectable levels of *tau*-fluvalinate (USDA-APHIS, 2020). The exposure to accumulated lipophilic acaricides could be exerting a continuous source of selection for resistant genes. Alternatively, selection pressure may be exerted through the contamination of bee forager collected food (nectar or pollen that was exposed to farmer applied products); 37% of bee pollen samples collected in the USA contained fluvalinate, and 46% of the samples contained residues of fluvalinate and other acaricides (Traynor et al., 2021).

Varroa's reproductive biology also plays a role in allele fluctuations. *Varroa destructor* populations are highly inbred, due to full sibling mating inside the brood cell (adelphogamy) along with haplo-diploid sex determination (Rosenkranz et al., 2010). This biology fosters the formation of homozygotes in the offspring making heterozygotes highly scarce. Our data supports this with homozygotes predominating mites, suggesting that resistant alleles might be easily fixed in the population in case of continuous treatments (Beaurepaire et al., 2017). This supposition is also supported by our data which shows worryingly low rate of apiaries with no resistant alleles detected at all. Indeed, the prevalence of resistant genes in mites collected across the country were wide spread, which was facilitated, in all likelihood, by the selection pressure from intensive use of the same treatment for many years (Rosenkranz et al., 2010).

Interestingly, our results here show an overall lower incidence of the 925M allele than the 925I allele. Moreover, a significant decrease for the 925M allele was observed between the two years studied. This observation is in contrast with the postulation in chapter 2 of this thesis about the sequential origin of these mutations, if an equal aptitude is assumed for both alleles. These aspects will be further addressed in the discussion

section. Nevertheless, our monitoring outcome revealed that, although having a variable incidence, both resistant alleles are widespread throughout the USA.

USA beekeepers, specifically, have been suffering of high rate losses over the last 10 years. A national survey of honey bee diseases pointed the *V.destructor* parasitism as the number one stressor for USA operations and suggest that no less than 40% of USA colonies had mite levels well above threshold, particularly in the fall when mite parasitism is most damaging (USDA-NASS, 2020). Nonetheless, approximately 7% of USA beekeepers report not treating their hives for mites in any way (Haber et al., 2019), which makes the incidence of mites and the risk of infection of nearby colonies high. However, even for beekeepers using mite control methods, these are not always effective in reducing colony loss rates, partly because resistance to certain mite control products have evolved in the populations. While resistant alleles are ubiquitous, but not generally fixed in the USA mite populations, it might be possible to implement with success resistance management strategies.

A coordinated Integrated Pest Management strategy that monitors the frequency of resistant mites and promote the appropriate *Varroa* management approaches would be of great benefit to drive resistance frequency to the minimum and prolonging the usefulness of *tau*-fluvalinate, as well as other acaricides, on USA beekeeping operations for the long as possible. Indeed, USA commercial beekeepers who take a diverse approach to mite treatment lose fewer colonies (presumably because of increased mite treatment efficacy) than their less creative colleagues (Haber et al., 2019). Predicting product efficacy through use of genotyping approaches would allow beekeepers to make informed treatment decisions. This point will be further developed in the general discussion.

CHAPTER 4

Development of a new detection methodology for
Varroa destructor resistance to synthetic pyrethroids
based on PCR-RFLP diagnosis

4.1. Introduction

Currently, the distribution of *V. destructor* has become so widespread that in some countries is estimated to be present in every honey bee colony (Dahle, 2010). The biological characteristics and dispersal potential of *V. destructor* make it virtually impossible to prevent parasitism in hives, and mite-free colonies are at high risk of infection (Frey and Rosenkranz, 2014; Frey et al., 2011; Greatti et al., 1992). As it is almost impossible to prevent parasitism with current methodologies, controlling the mite population in hives is often the only thing beekeepers can do to prevent a rapid deterioration in the health of their apiaries. Among the few approaches available to remove mites from hives, synthetic miticides have been proven to be very effective and reliable as long as there is no resistance in the mite colony population. However, the efficacy of the treatment decreases when resistant mites are present in a considerable proportion in the colony.

At present, resistance to the three classes of synthetic compounds used for *Varroa* control has been reported (Elzen et al., 1999a; Martin, 2004; Pettis, 2004; Rinkevich, 2020). The mechanisms of resistance to amitraz and coumaphos in *V. destructor* remain unclear, but resistance to pyrethroids has been largely associated with the *kdr*-type mutations at position L925 of the *Vd*VGSC protein (*Musca domestica* numbering) (Alissandrakis et al., 2017; González-Cabrera et al., 2018; González-Cabrera et al., 2013; González-Cabrera et al., 2016; Hubert et al., 2014; Stara et al., 2019a). The three mutations found to be associated with pyrethroid resistance are the result of non-synonymous nucleotide substitutions in the first (C/GTG in L925V, C/ATG in L925M) or first and third positions (C/ATG/A of the codon triplet for residue L925 in the *Vd*VGSC gene (Fig. 4.1). The early detection of these mutations associated with resistance could be a useful tool for beekeepers wanting to prevent treatment failures. Surveys to monitor mutations associated with resistance have resulted in increased management success of pest species like mosquitoes, aphids, beetles, and ticks (Højland et al., 2015; Lucas et al., 2019; Lynd et al., 2018; MacKenzie et al., 2018; Rosario-Cruz et al., 2009; Willis et al., 2020). These efforts take advantage of the several methodologies currently available for detecting resistant alleles in arthropod pests (Bass et al., 2007; Lynd et al., 2018; Panini et al., 2014; Stara et al., 2019a). In *V. destructor*, our research group have previously designed and tested allelic discrimination assays to detect L925 mutation in the *Vd*VGSC gene based on TaqMan® that proved to be very

robust, fast and reliable (see Chapter 3) (González-Cabrera et al., 2013; González-Cabrera et al., 2016). However, TaqMan® assays require at least two florescence labelled DNA probes, oligonucleotides, an enzymatic preparation and, as they are based on quantitative PCR, the reactions run in sophisticated thermocyclers specially designed for detecting real-time changes in florescence. These requirements limit the possible deploy of these assays to low-resourced laboratories. The availability of cheaper and more accessible methodologies for the detection of resistance would be of great value for worldwide beekeepers and stakeholders, so they can take informed decisions regarding the best management strategy to preserve their honey bee colonies.

4.2. Objectives

To develop a new diagnostic test based on Polymerase Chain Reaction-Restriction Fragment Length Polymorphism (PCR-RFLP) for the detection of mutations at position 925 of the *Vd*VGSC associated with the resistance to synthetic pyrethroids. The PCR-RFLP assay is fast, simple, and affordable to virtually any laboratory.

The aim of this chapter is to provide a simple methodology that can be accessible and adapted as a routine assay in any laboratory. This chapter therefore presents different DNA extraction methods and alternative PCR amplification options; however, the protocol can be adapted to the particular requirements of each laboratory.

4.3. Materials and methods

4.3.1. *Varroa destructor* samples

The three L925 mutated alleles associated with reduced susceptibility to pyrethroids show a marked geographical distribution. The L925V allele has been detected essentially in European mite populations (González-Cabrera et al., 2018; González-Cabrera et al., 2013; Hernández-Rodríguez et al., 2021; Hubert et al., 2014; Panini et al., 2019; Stara et al., 2019a) while the L925I and L925M have been primarily reported in USA hives (González-Cabrera et al., 2016; Millán-Leiva et al., 2021a), although the latter two have been recently reported outside the American continent (Alissandrakis et al., 2017; Koç et al., 2021; Millán-Leiva et al., 2021b; Ogihara et al., 2021).

Adult female mites from apiaries located in the Valencian region (Eastern Spain) were collected in July 2017 from inspection boards separating the mites from colony debris using a fine paintbrush. These mites were collected alive and were immediately frozen in liquid N_2 then stored at -80 ºC until used. *Varroa* samples from USA apiaries were collected in the framework of the US National Honey Bee Disease Survey (NHBDS) and shipped to the University of Valencia in 70% ethanol, as part of a parallel project (see Chapter 3). Previously to this work, all mites were genotyped using a TaqMan®-based allelic discrimination assay as described before (González-Cabrera et al., 2013).

4.3.2. DNA extraction

Genomic DNA was extracted from individual adult mites by two different methodologies, the alkaline hydrolysis and the Chelex® method, used as described in Chapter 3 and Chapter 2, respectively. Both extraction methods are fast, simple to perform and do not require expensive or hazardous reagents.

Alkaline hydrolysis DNA extraction method was performed as described in González-Cabrera *et al.* (2013). This protocol is described here for the processing of up to 96 samples at the same time using a multiple homogenizer, however, it can be carried out by homogenization of single mites with plastic pestles in microcentrifuge tubes. Briefly, the mites were placed individually in each well of 96-well flat-bottom microtiter plates containing 20 µL of 0.25 M NaOH. Then, were ground using a multiple homogenizer (BA/MH96, Burkard Scientific Ltd., Uxbridge, U.K.) (ffrench-Constant and Devonshire, 1987). Subsequently, 20 µL of Neutralization buffer (125 mM HCl, 0.5% Triton X-100 and 125 mM Tris/HCl pH 8.0) was added to each well. The plate was spun at $1000 \times g$ for 5 min for mite debris and fragments to fall to the bottom of the well. The supernatant containing the DNA was transferred to a new 96-well PCR microplate and stored at -20 ºC until used.

Chelex® DNA extraction method protocol was modified from Evans *et al.* (2013). In short, single mites were placed in a microcentrifuge tube containing 50 µL of 5% Chelex® solution (Bio-Rad, cat. 1421253), supplemented with 0.5 mg/mL of proteinase K (AppliChem, cat. A3830) and homogenized with a plastic pestle. Then, the reaction was subjected to a five-step incubation cycle as follows: 60 min at 56 °C, followed by 15 min at 99 °C, 15 min at 37 °C, 15 min at 99 °C and then cooling at 4 ºC for at least 15

min. After the incubation cycle, the tubes were centrifuged at 13000 ×*g* for 5 min. The supernatant, containing the genomic DNA, was transferred to a new tube, taking care of not disturbing the Chelex® resin pellet, and stored at -20ºC until used for PCR amplification.

4.3.3. PCR-RFLP assay

For the sake of simplicity, in this work we used as template a single partial sequence of the *V. destructor* VGSC gene available in Genbank (Accession KC152655.2). All numbering of DNA sequences will be referring to that in this accession (Fig. 4.1).

Different primer pairs (primer pair A, and TM; Table 4.1) were used to amplify the flanking/spanning region containing the position for codon 925 of the channel protein (Fig. 4.1, Table 4.1). Two oligonucleotides were specifically designed for this method (1,273iF and 1,973), which are referred to as primer pair A, giving a PCR product of 701 bp. These primers bind into the intronic region surrounding/neighbouring exon 13 of the *Nav* gene in *V. destructor*, which includes the codon at residue L925. These primers are suitable for genomic DNA as template, such as with the DNA extraction techniques mentioned above. However, they are not appropriate when using as template the coding sequence of the VGSC protein (e.g. cDNA or cloned CDS).

Table 4.1. Primer set used in the protocol described. The table shows for each primer pair the PCR annealing temperature, the length of the DNA product and the length resulting from the *Sac*I digestion.

Pair	Direction	Name	Sequence (5' to 3')	Annealing Temp. (ºC)	PCR product	*Sac*I digestion Susceptible allele	Resistant allele
TM	Forward	Vd_TM_L925V_F	CCAAGTCATGGCCAACGTT	56ºC	97 pb	59 + 38 pb	97 pb
	Reverse	Vd_TM_L925V_R	AAGATGATAATTCCCAACACAAAGG				
A	Forward	1273-iF_Vd	AAGCCGCCATTGTTACCAGA	60ºC	701 pb	264 + 437 pb	701 pb
	Reverse	1973-iR_Vd	GCTGTTGTTACCGTGGAGCA				
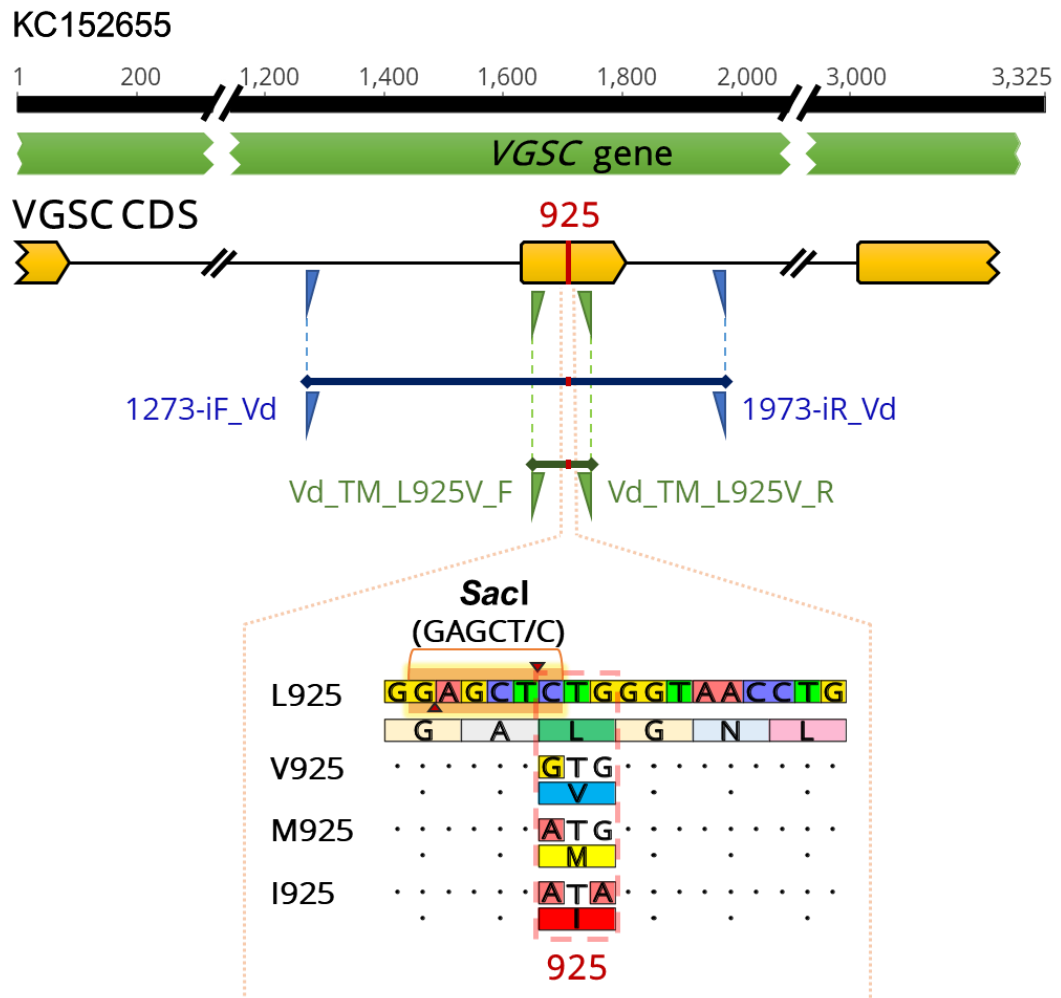
Figure 4.1. Schematic representation of the PCR amplified region of the *Vd*VGSC Domain II. Numbering matches that in Accession KC152655.2. The yellow arrow-shaped boxes indicate the coding sequence (exons) and the black lines connecting them are the non-coding sequence (introns) of the VGSC gene. The insight shows the nucleotide and amino acid sequences flanking the position 925 of the channel protein. Annealing positions for primers pair and amplified DNA fragment are indicated (blue for pair-A, and green for pair-TM). The amino acid at position 925 and the *Sac*I restriction site (5′-GAGCT/C-3′) are highlighted in red and orange, respectively. The red and black triangles indicate the enzyme-cutting site.

The primer pair named TM (Vd_TM_L925V_F and Vd_TM_L925V_R) are the oligonucleotides designed for the genotyping TaqMan assay by González-Cabrera Ket al. (2013) and used in the Chapter 3 of this thesis (Table 4.1). The DNA fragment product of this primer pair is just under 100 bp, consequently, some modifications have been made to allow the detection of small DNA fragments using standard equipment affordable to

any laboratory (see below). These primers bind within the exon 13 (Fig. 4.1) and are suitable for both, genomic DNA and intron-processed DNA as template, giving the same results.

The PCR reaction mixtures contained 1 µL genomic DNA 12.5 µL of DreamTaq Green PCR Master Mix (2x) (Thermofisher Scientific) and 0.5 µM of each primer in a total reaction volume of 25 µL. Thermocycling conditions differ slightly in the annealing temperature and the number of cycles for each primer pair. Thermocycler conditions for primer pair-A were the following: Initial denaturation step at 95 ℃ for 2 min followed by 35 cycles of denaturation at 95 ℃ for 30 s, 20 s of annealing at 56 ℃, and 1 min of extension at 72 ℃, ending with a final extension step at 72 ℃ for 5 min. For the primer pair-TM, the cycling conditions were as follow: 2 min at 95 ℃ followed by 45 cycles of 95 ℃ for 30 s, 56 ℃ for 20 s, 1 min of extension at 72 ℃, and a final extension step at 72 ℃ for 5 min (Table 4.2).

Table 4.2. PCR cycling conditions for amplifying the *V. destructor* VGSC fragment using the primers pair A and TM. Differences in thermocycling condition are shadowed in yellow.

Steps	primer pair-A				primer pair-TM		
	Temp. (°C)	Time	Cycles		Temp. (°C)	Time	Cycles
Initial denaturation	95	2 min	1		95	2 min	1
Denaturation	95	30 s			95	30 s	
Annealing	60	20 s	35		56	20 s	45
Extension	72	1 min			72	30 s	
Final Extension	72	5 min	1		72	1 min	1
Electrophoresis	2% agarose gel				4.5% agarose gel		

Then the PCR product was subjected to an enzymatic digestion by *Sac*I. For the PCR product obtained with the primers pair-A, 5 µL of reaction was mixed with 2.5 U of *Sac*I (Thermofisher Scientific) and 2 µL of 10× buffer L in a final volume of 20 µL. The digestion reaction was incubated at 37 ℃ for 1 hour and then loaded onto a 2% in TBE (89 mM Tris-borate and 2 mM EDTA, pH 8.3) agarose gel and run at 100 V for 30 min.

When using the TM primer pair, the restriction reaction and electrophoresis separation were adapted for the detection of small DNA bands on agarose gels. Thus, 15 to 20 μL of the PCR product was digested by 2.5 U of *Sac*I, in a final volume of 30 μL with 3 μL of 10× L buffer. 20 μL restriction reaction was loaded onto a 4.5% agarose gel in TBE, at 100 V for 45 min.

4.4. Results

The mutations reported at residue L925 of the *V. destructor* VGSC protein are caused by non-synonymous substitutions at nucleotide position 1710 (G/C, Leucine (CTG) for Valine (GTG) or A/C, Leucine (CTG) for Methionine (ATG)), or at positions 1710 and 1712 (A/C and G/A, Leucine (CTG) for Isoleucine (ATA)). The analysis of the sequence revealed a cutting site for the restriction enzyme *Sac*I between positions 1709 and 1710 (Fig. 4.1). Hence, if a DNA fragment containing a region flanking position 925 of the *Vd*VGSC is digested with *Sac*I it will be possible to differentiate each of the three possible phenotypes (SS: Homozygous for the susceptible allele L925; SR: Heterozygous that carries a susceptible allele L925 and a resistant allele (V925, M925 or I925); and RR: mite carrying two resistant alleles (V925, M925 or I925), either in homozygosis or heterozygosis) (Fig. 4.2).

A 701 bp fragment, spanning the relevant Domain II intron-exon-intron region of *V. destructor* VGSC (Fig. 4.1), was PCR amplified using the specific primers pair-A. Digestion with *Sac*I enzyme of PCR fragments amplified from previously genotyped DNA samples resulted in the expected pattern, after gel electrophoresis, given the presence/absence of the restriction site. Thus, samples from mites homozygous for the susceptible allele (S: L925) shows a double band pattern (437 bp and 264 bp, lane S/S), the homozygous or heterozygous for the resistant allele (R: V925, I925 or M925) shows a single 701 bp band (lane R/R) and the heterozygous composed of one susceptible and one resistant copy shows a triple band pattern (701 bp, 437 bp and 264 bp, lane S/R) (Fig. 4.2). In the example in Fig. 4.3A, where mites collected in Spain were tested, the heterozygotes and resistant homozygote correspond to L/V and V/V, respectively. These mites were analysed using the Chelex® DNA isolation method and the primer pair-A.
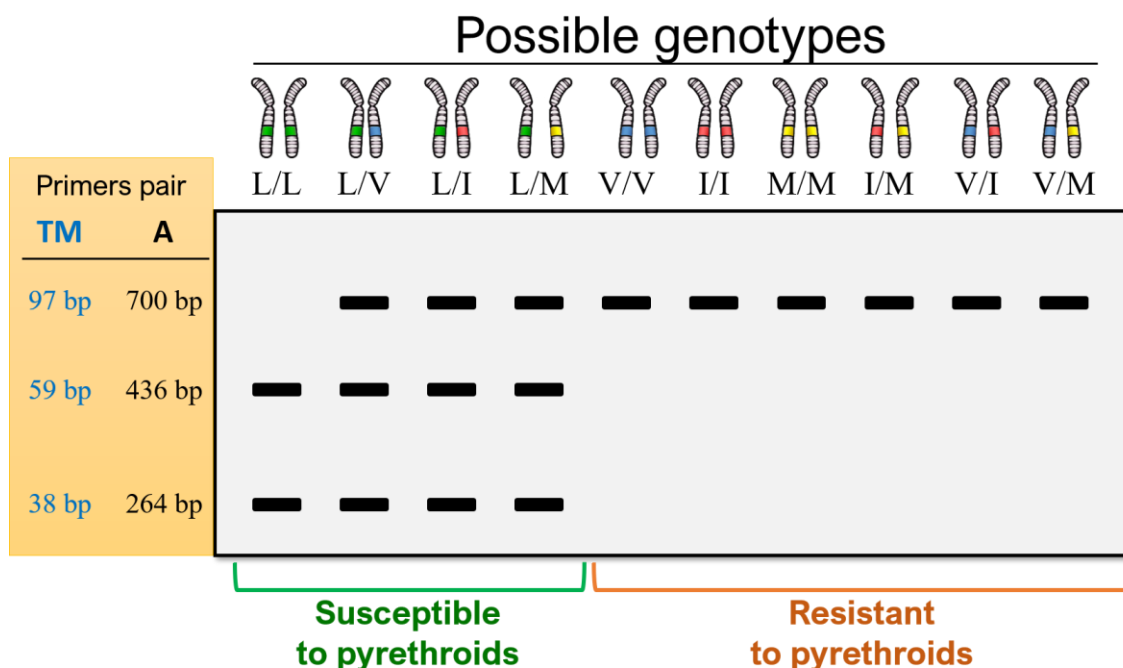
Figure 4.2. Graphical representation of the expected electrophoretic banding pattern for each possible genotype by the of *Sac*I-digested PCR product. The length of the DNA bands obtained depending on whether primer pair A or TM are used is indicated.

Comparable results are obtained when TM primers are used in the PCR. If the *Sac*I restriction site is present (in the L925 allele), the 97 bp amplified fragment of DNA is cut into two smaller fragments of 59 and 38 bp. Therefore, the band pattern associated with the possible mite genotypes is as follows: mites homozygous for the susceptible allele (S: L925) show a double band pattern of 59 and 38 bp (S/S); homozygotes and heterozygotes for any of the three resistant alleles (R: V925, I925 or M925) show a single band of 97 bp (R/R); and lastly, heterozygotes with one susceptible allele and the other resistant exhibit the three-banding pattern of 97, 59 and 38 bp (S/R) (Fig. 4.2). In Fig. 4.3B is shown the PCR-RFLP assay result tested on mites from USA. These mites were stored at -20ºC in 70% EtOH until the DNA extraction by the NaOH method and the amplification with TM-pair primers. The *Sac*I digestion product was run on 4.5% agarose gel for band separation.
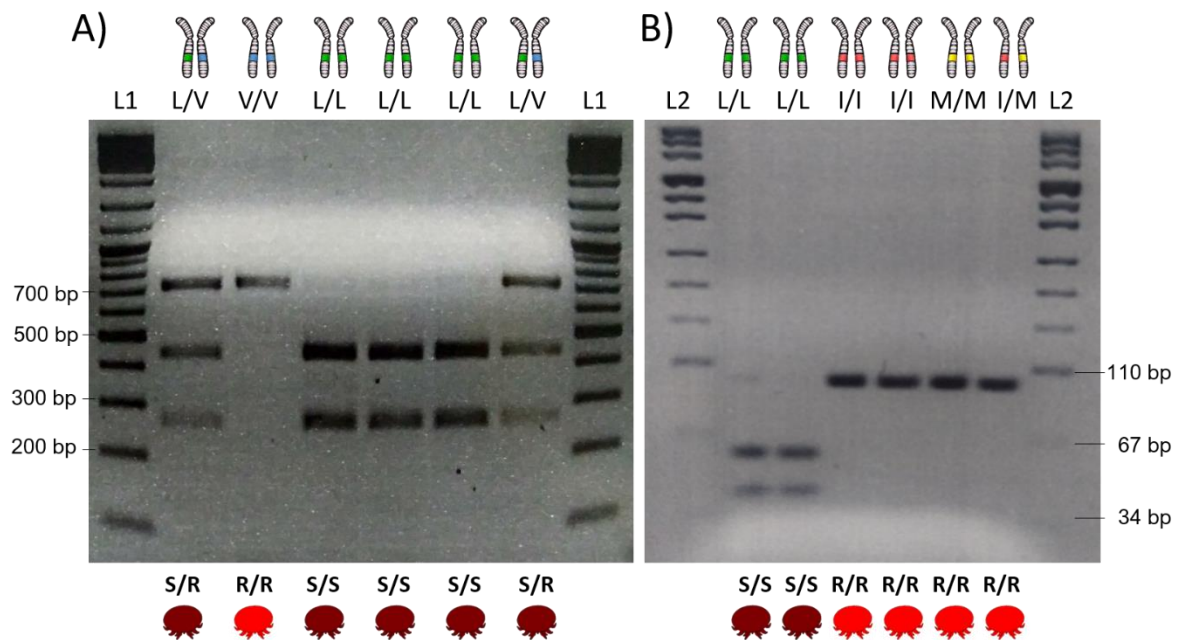
Figure 4.3. Detection of mutations at position 925 of the *Vd*VGSC using a PCR–RFLP assay. **A)** PCR bands migration in a 2% TBE agarose gel amplified with primer pair-A after being digested with *Sac*I (GAGCT/C). **B)** DNA band migration in 4.5% TBE agarose gel amplified with the TM-pair of primers and digested by *Sac*I. The genotype of the mite tested obtained by TaqMan® assay is indicated above each gel lane. **L/L**: homozygote for the susceptible allele L925; **V/V**: homozygote for the resistant allele V925; **L/V**: heterozygote with the susceptible allele L925 and the resistant allele V925; **I/I**: homozygote for the resistant allele I925; **M/M**: homozygote for the resistant allele M925; **I/M**: heterozygote carrying the resistant alleles I925 and M925. **L1**: Molecular weight marker (GeneRuler DNA Ladder Mix, Thermo Scientific), **L2:** Molecular weight marker (Ladder pUC Mix Marker 8, Fermentas, #SM0303). Below each lane is shown the mite genotype assigned to the DNA banding pattern (S: Susceptible allele, and R: Resistant allele). With this outcome, the susceptible or resistant to pyrethroid treatment phenotype can be predicted, represented in the figure as brown or red mite, respectively.

Because *kdr* and super-*kdr* resistant traits are recessively inherited (Davies et al., 2007), only those mites carrying two resistant alleles (R: V925, I925 and M925) will be resistant to a pyrethroid treatment (González-Cabrera et al., 2018; González-Cabrera et al., 2013; Hubert et al., 2014; Stara et al., 2019a) . Those mites will display a single band of 700 bp or 97 bp, depending on the primer pair used, due to that same band pattern is obtained independently of the resistant allele. On the other hand, mites carrying at least one

susceptible allele (L925), such are homozygotes L/L or heterozygotes L/V, L/I and L/M, will be susceptible to pyrethroids.

4.5. Discussion

A target for *Sac*I restriction enzyme was detected in the region of the *V. destructor* VGSC that includes the residue mapping at position 925 of the protein (Fig. 4.1). Based on this finding, a PCR-RFLP methodology was designed to discriminate among mites carrying different residues at position 925 since there are three mutations (L925V, I and M) already described as significantly correlated with resistance to synthetic pyrethroids in *V. destructor* populations (Alissandrakis et al., 2017; González-Cabrera et al., 2013; González-Cabrera et al., 2016; Hubert et al., 2014).

The PCR-RFLP developed here has several advantages over the other high throughput TaqMan®-based screening methodologies used before to estimate the frequency of resistant mites in the populations (González-Cabrera et al., 2013; González-Cabrera et al., 2016). It is significantly cheaper; there is no need for custom made fluorescent-labelled DNA probes, or for expensive enzymatic preparations designed for quantitative PCR. The reactions run in simple thermocyclers now ubiquitous in every laboratory working in molecular biology and there is no need for a dedicated software to assess the results and assign a susceptible or resistant phenotype to a given sample. On the other hand, as there are currently four alleles identified in the populations it is technically very difficult to multiplex a TaqMan® assay to detect the 10 possible genotypic combinations in a single test. It would be necessary to run several tests with the same samples to assign a genotype and subsequently a phenotype regarding resistance. The PCR-RFLP methodology is not as accurate as direct sequencing or TaqMan® assays to assign a genotype to a given sample but it is far more straightforward discriminating whether a sample is coming from a resistant mite or not. As described above, all samples producing a single band (of 700 or 97 bp) after gel electrophoresis of digested PCR fragments come from resistant mites despite the combination of alleles present.

Furthermore, the method explained here is quite versatile and adaptable to the resources of the laboratory running the protocol. For example, it is possible to vary the DNA extraction method or use a different primer set to amplify the DNA fragment as

long as it includes the position coding for residue 925 of the *Vd*VGSC. In fact, this assay has already been successfully applied in several research studies (Ogihara et al., 2021; Stara et al., 2019a; Stara et al., 2019b), besides our own research group.

In a short-term perspective, as mentioned above, detecting these mutations prior to the treatment would allow to predict its efficacy and to provide advice for selecting the most convenient way to deal with the mite. In the current situation, with very few effective treatments to control *V. destructor* parasitism and many reports of resistance to most of them, we believe that coordinated efforts can be made to develop an integrated management strategy that allow the use of an acaricide in a given apiary based on previous knowledge of its expected efficacy. For this to be possible, it is necessary to assess the frequency of resistant mites in the colony before proceeding with the treatment. The new diagnostics methodology presented here would contribute effectively to this scenario since it is able to predict with accuracy the frequency of resistant mites in a given colony but at a fraction of the cost of other technologies. Although this is only applicable to pyrethroids at the moment, we believe that it will be very attractive for beekeepers. They are aware that pyrethroids like tau-fluvalinate or flumethrin are very effective removing mites from the colonies when there is no resistance (Baxter et al., 2000). Thus, previous knowledge of pyrethroid resistance status in their apiaries will help in deciding whether they will be the right choice or not. Further rotation with other available acaricides and management approaches are needed to keep resistance alleles at the lowest possible frequency, contributing to a successful long-term control of the parasite. Accurate pre-treatment detection of resistant mites opens a window for a resistance management strategy aimed at reaching a sufficient control of the mite while protecting the efficacy of pyrethroids for the longer-term possible.

GENERAL DISCUSSION

One of the largest challenges facing beekeepers today is controlling *V. destructor*, a problem exacerbated by the limited number of control products available and the evolution of resistance in mite populations (Davies et al., 2007; Dekeyser and Downer, 1994; Rosenkranz et al., 2010; Steinhauer et al., 2021). Although alternative non-synthetic based treatments are available, their efficacy is variable as outcomes are dependent on external factors such as climatic, in-hive conditions and product application (Rosenkranz et al., 2010; Stanimirović et al., 2019; Umpiérrez et al., 2011; Underwood and Currie, 2003). The development of synthetic miticides based on new active ingredients is becoming harder and more costly (Dekeyser and Downer, 1994; Rosenkranz et al., 2010), so it seems unlikely that new effective varroacides will be available on the market in the near future. Therefore, the focus now must be on keeping current acaricides effective for the longest time possible, but this is threatened by the evolution of resistance.

To develop effective resistance management measures, it is essential to understand the molecular mechanism(s) underlying resistance in *V. destructor* as well as the dynamic factors influencing the incidence of the resistance alleles in the populations. In the present work, we have focused on *kdr*-type mutations at position 925 of the *Vd*VGSC, which have been associated with mites from many locations surviving treatments based on *tau*-fluvalinate and flumethrin (Alissandrakis et al., 2017; González-Cabrera et al., 2018; González-Cabrera et al., 2013; González-Cabrera et al., 2016; Hubert et al., 2014; Panini et al., 2019; Stara et al., 2019a). The intention of this research study was to shed light on the implications of these mutations on pyrethroid resistance, their evolutive relationship, and present status, with the eventual purpose of establishing some basic keystones to develop an effective Integrated Pest Management (IPM) approach. This work is framed within a larger project aimed at elucidating the molecular basis underlying the resistant evolution to the acaricides used for *Varroa* control.

In this thesis, we have evidenced the actual implication of these mutations in the mechanism of resistance using an electrophysiological approach (Chapter 1). Our monitoring results have revealed that, although with varying incidence, both L925I and L925M resistant alleles are widespread throughout the USA, being the most plausible cause of pyrethroid treatment failure in the country (Chapter 3). Moreover, we were the first detecting the substitution M918L associated with resistance in *Varroa* populations (Chapter 2). Our phylogenetic analysis supports the single origin for each *kdr*-type mutation on the *Vd*VGSC and a close relationship between the L925M and L925I alleles

(Chapter 2). We also developed a simple and affordable detection method of 925-mutant alleles based on Polymerase Chain Reaction-Restriction Fragment Length Polymorphism (PCR-RFLP) that can be adapted as a routine assay in any laboratory (Chapter 4).

Varroa destructor's 925-mutated VGSC shows reduced susceptibility to pyrethroid

Mutations at position 925 of the *Vd*VGSC have been correlated with mites surviving treatments based on *tau*-fluvalinate and flumethrin (González-Cabrera et al., 2018; González-Cabrera et al., 2013; González-Cabrera et al., 2016; Hubert et al., 2014; Stara et al., 2019a). In this thesis, the implications of these mutations in the mechanism of resistance have been verified by electrophysiological and pharmacological assays (Chapter 1).

Compared to the wild-type VGSC, the sensitivity to pyrethroids was found to be significantly reduced when mutated sodium channels were expressed in *Xenopus laevis* oocytes. In contrast to the wild-type channel, L925I and L925V mutated sodium channels did not elicit any tail current response when exposed to all tested pyrethroids (deltamethrin, flumethrin, and *tau*-fluvalinate). On the other hand, the mutation L925M seems to be at an intermediate level. It confers more susceptibility to pyrethroids than the L925I/V but displayed a reduced response when compared the wild-type channel.

Clearly, our results are in agreement with previous studies reporting the influence of substitutions at position 925 of the VGSC on the interaction of type II pyrethroids with the channel (O'Reilly et al., 2006). In mutated channels, pyrethroid interaction is most probably hindered by the alternative side chain of the modified residue at position 925, preventing the proper docking of the pyrethroid to its binding pocket (Field et al., 2017; O'Reilly et al., 2014; Yan et al., 2020). Likewise, in the absence of pyrethroids, the three mutations described here modify the physiological kinetics properties of the mite sodium channel, also observed in insect *kdr*-mutated channels (Burton et al., 2011; Usherwood et al., 2007). All three mutated channels exhibit a shift of activation towards a more positive voltage, but the difference is higher in those with substitutions L925I and L925V. Moreover, the L925M channel also inactivates more rapidly than the wild type. In short, the mutated L925V and L925I channels are less likely to open than the wild type, while L925M will switch faster to the closed state.

Pyrethroids have higher affinity and preferentially target the channel in their open state (Vais et al., 2003; Vais et al., 2000b). The formation of bonding contacts between the pyrethroid and the different residues across the predicted binding pocket could stabilise the channel in the open state, prolonging sodium tail currents. Upon return to the closed state, repositioning of the domain II S4-S5 linker would lead to release of pyrethroids due to disturbance of the pyrethroid-binding contacts (O'Reilly et al., 2006; O'Reilly et al., 2014). According to this model, the reduced availability mutated channels in the open state or the faster transition towards the closed state may be counteracting the action of pyrethroids, thus contributing to resistance.

Particularly remarkable is the opposite effect that pyrethroids induce on the activation kinetics of VdVGSC in comparison with that reported in insect VGSCs. In the insect VGSCs, interaction with pyrethroids often enhances the activation state by shifting $V_{50,act}$ to more negative values (Burton et al., 2011; Field et al., 2017; Gosselin-Badaroudine et al., 2015; Tan et al., 2002; Tatebayashi and Narahashi, 1994; Vais et al., 2001; Vais et al., 2000b; Wu et al., 2017). This way the channels become more easily excitable, leading to a hastened and prolonged open state, increasing the exposure of the pyrethroid binding site. However, our results evidenced the opposite effect of pyrethroid interaction upon the activation kinetics of VdVGSC. The interaction of deltamethrin, *tau*-fluvalinate, and flumethrin alters the channel kinetics of VdVGSC by shifting the $V_{50,act}$ to more positive voltages, which could reduce the potential binding of pyrethroids. This difference may be one of the factors underlying the lower sensitivity to pyrethroids of VdVGSC when compared with insect VGSCs (Burton et al., 2011; Gosselin-Badaroudine and Chahine, 2017; Thompson et al., 2020; Vais et al., 2000b; Wu et al., 2017). Further studies are needed to assess if this feature is shared by other acari VGSCs in order to fully characterise the differences between VGSCs from insects and acari since the identification determinants for selectivity and target specificity is essential to further developing highly specific compounds capable of discriminating between target and non-target organisms (e.g., mites and bees).

First detection of the M918L *kdr*-type substitution in *V. destructor*

In the present work, the mutation M918L of the VGSC was detected for the first time in *V. destructor*. Residues M918 and L925 are located in the IIS4-S5 linker and the IIS5 of the channel, respectively. It is predicted that these regions, together with IIIS6, fold into a hydrophobic pocket proposed to be the interaction site of pyrethroids with the channel (O'Reilly et al., 2014). According to this model, any substitution in the amino acids lining the hydrophobic pocket would interfere with the accommodation of the pyrethroid, making the channel less sensitive to these chemicals. In fact, the M918L substitution has been associated with pyrethroid resistance in other arthropod species (Benavent-Albarracín et al., 2020; Carletto et al., 2010; Chen et al., 2017; Fontaine et al., 2011; Jouraku et al., 2019; Karatolos et al., 2012; Panini et al., 2014; Weston et al., 2013; Wu et al., 2018). The effect of the M918L mutation on the *Vd*VGSC channel was not characterised by electrophysiology in this work, as its detection was posterior to the pharmacological characterisation of the mutated channels. Notwithstanding, substitutions of the residue at position M918 have been fully characterised in the past showing that they significantly reduce the susceptibility of the channel to pyrethroids (Lee et al., 2003; Usherwood et al., 2007; Vais et al., 2000a).

Most concerning is the co-occurrence of mutations M918L and L925V in mites collected in the field. In some arthropods, the co-occurrence of more than one *kdr*-type mutation often leads to a resistance level greater than that conferred by a single mutation (Dong et al., 2014). Accordingly, we can hypothesise that the combination of M918L and L925V would trigger a higher destabilisation of the channel than that produced by L925V or M918L alone. In particular, for the M918L substitution, this effect has been described in some species, where the M918L mutation alone confers moderate levels of resistance (Panini et al., 2014), but when combined with other mutations, particularly at position L925, leads to greater resistance (Benavent-Albarracín et al., 2020; Karatolos et al., 2012; Katsavou et al., 2020; Major et al., 2018). Furthermore, there is the possibility that these mutations compensate for potential fitness disadvantages of individual mutations (Dong et al., 2014). To our knowledge, no population of *V. destructor* has been reported with the M918L mutation alone, and in the present study it was always found in combination with L925V. Therefore, at this stage, it is not possible to know how this mutation alone would influence pyrethroid sensitivity in *V. destructor*. Further electrophysiology assays could

unravel the effect of the M918L mutation, alone or in combination with L925V, on the *Vd*VGSC regarding pyrethroid sensitivity.

Phylogenetic relationship of *kdr*-type alleles in *V. destructor*

Understanding the evolutionary history of the resistant alleles is a key step for anticipating future events of emerging resistance and therefore contributes to designing more finely tuned management strategies. Phylogenetic analyses of the gene region linked to position 925 of the *Vd*VGSC revealed a single origin for each *kdr*-type mutation. Furthermore, there is a clear phylogenetic relationship between mutations L925M and L925I, on one hand, and L925V and M918L, on the other. In other words, it suggests two different parallel origins for the mutations: one driving the resistance of mites in Europe, and another driving resistance in the USA. The geographical distribution of the resistant alleles correlates well with the results obtained by phylogenetic reconstruction and therefore also supports the proposal of a single mutation event for each resistance-related amino acid substitution. The mutation L925V is distributed largely in Europe and L925M and L925I is found mostly across the USA. Recently, however, there have been mounting reports of these mutations outside these regions, such as Greece (L925I), Turkey (L925I and L925V), Argentina (L925V), Uruguay (L925V), Japan (L925M), and the Canary Islands (Spain) (L925M, in this work) (Alissandrakis et al., 2017; Koç et al., 2021; Mitton et al., 2021; Ogihara et al., 2021).

Our analyses showed the close relationship between the L925I and L925M alleles found in Greece and the Canary Islands (Spain), respectively, with those found in the USA, suggesting that they share a common origin. Hence, the presence of these mutations in colonies outside America is more likely to be a consequence of human-facilitated movement than that of an independent mutation event. Since they were detected after the publication of our work, we certainly cannot state that the alleles detected in Japan, Turkey, Argentina, and Uruguay also share a common origin with the alleles from the USA and Europe. But given the above evidence, along with the context of global trade in bee queens and colonies, it would not come as a surprise that they share a common origin with those alleles from the USA or Europe.

The phylogenetic reconstruction suggests that L925M and L925I are the results of a sequential process, the L925M mutation being an ancestor of the L925I mutation, that

would have arisen in a second parallel mutation event (Leu → Met → Ile). The wide distribution of these two alleles across the USA territory (Chapter 3) is therefore the outcome of the subsequent distribution of mites carrying these alleles after the mutation events. Our results also prove that the persistent reports of *tau*-fluvalinate treatment failure across the USA can be attributed to these mutations. A similar scenario can be extrapolated to the L925V allele in Europe.

Multiple origin of resistant alleles reflect genetic heterogeneity within a specie. In many other arthropods, the intensive use of pyrethroid pesticides has led to the multiple selection of identical *kdr*-type mutations around the globe (Anstead et al., 2005; Pinto et al., 2007; Rinkevich et al., 2012a; Rinkevich et al., 2012b). Although, in *V. destructor*, recent findings have described certain level of genetic diversity and population structure in Asian mite populations (Beaurepaire et al., 2019b; Dietemann et al., 2019; Dynes et al., 2017), the global genetic variability of mites parasitizing *A. mellifera* is extremely low, with populations considered to be almost clonal (Anderson and Trueman, 2000; Beaurepaire et al., 2015; Cornman et al., 2010; Dynes et al., 2017; Solignac et al., 2005). This is attributed to multiple bottleneck events, together with rapid spread around the world, haplodiploidy, and predominantly sibling mating (Roberts et al., 2015).

Our findings have significant implications for *Varroa* control, revealing that the movement of honey bees has a stronger influence on the current distribution of *kdr*-type alleles than new mutation events. Indeed, given these results, it is possible to hypothesise that the rapid expansion of resistant mites bearing these mutations could have been in part facilitated by human and honey bee-mediated transport, coupled with the intensive treatment schemes based only on pyrethroid acaricides for many years in a row (Rosenkranz et al., 2010). Particularly in the USA, migratory beekeeping has become a crucial element for USA agriculture that can no longer rely solely on local pollinators (Aizen and Harder, 2009; Kremen et al., 2002; National Research Council, 2007). In migratory management, the bee colonies are moved from site to site throughout the year, providing pollination services along well-stablished routes in consolidated migratory itineraries that may cross the entire country (Bond et al., 2014; Burgett et al., 2010; Rucker et al., 2012); but also contributing to the expansion of these mutations (as it helped with the initial dispersion of *V. destructor* around the country). In this regard, the most prominent case is the demand for pollination services by Californian almond orchards. It is estimated that between February and March, 60-75% of all commercial hives in the USA visit almond

orchards, with nearly all migratory routes stopping in California (Bond et al., 2014). This extensive movement and intermingling of honey bees in the USA may certainly account for the higher rates of colony losses from *Varroa* infection in recent years than in countries with less intense migratory habits (BIP, 2020; Brodschneider et al., 2018).

Obviously, it is a challenge to prevent the movement of mites within countries when mites are virtually established in all honey bee populations and can move over long distances stowed away in colonies transported to meet pollination demand or in queen bees' packages. However, several international laws limit the movement of honey bees between nations in order to prevent the spread of diseases (Wilfert et al., 2016). Based on the evidence presented in this work, these regulations are not being sufficiently enforced to prevent the movement of honey bees and their parasites overseas or within Europe, as seen on the Canary Islands, where the spread of the microsporidium *Nosema ceranae* has been related to the introduction of queens from different origins (Muñoz et al., 2014). Our work also suggests that an international law, which recognises diseases and parasites as regulatory reasons to restrict trade, should recognise disease or parasitic strains (e.g., antibiotic resistant bacteria or pyrethroid resistant mites) as sufficient grounds to block trade. The inferred movement of honey bees, and mites with L925M and L925I resistant mutations from the USA to the Canary Islands and Greece, respectively, illustrates the risk associated with inaction, although concern about this event in relation to colony losses and conservation of honey bees has already been highlighted (De la Rúa et al., 2009). In the case of the newly described M918L, it seems critical to avoid its distribution to new locations by restricting the movement of colonies with resistant mite populations, much like restrictions are put in place for other honey bee diseases (Schäfer et al., 2019). For this to occur, however, broader definitions of "disease" for purposes of regulation are needed.

Possible fitness cost associated with *kdr*-type mutations in *V. destructor* in the absence of pyrethroids

Resistance evolution is a costly biological process, involving adaptation to selective pressure that may lead to the spread of resistant alleles in populations that are better adapted to it. Generally, adaptive stresses acting on resistant alleles are more intense for mutations affecting key sites in a protein. Rarely, these alleles are favoured when

selection pressure is absent (Kliot and Ghanim, 2012). Indeed, in some arthropod pests, it is common to observe a certain degree of fitness disadvantage associated with resistant individuals when selective pressure is lacking, which may compromise the prevalence of resistant alleles in the populations (Denholm and Rowland, 1992; Kliot and Ghanim, 2012). The mutations detected in mites at position 925 of the *Vd*VGSC (Valine, Methionine, and Isoleucine) do not compromise the functionality of the sodium channel but entail an alteration of the gating kinetics of the VGSC if compared with the wild-type channel. Hence, considering the key role in the transmission of the nerve impulse played by the VGSC, it is likely that these three substitutions pose certain impact on mites' fitness. In the characterization of the L925 mutants, our results showed a shift towards a more positive voltages in the channel activation potential ($V_{50,act}$) for all of them. Compared to the wild-type, this kinetic modification can be advantageous by counteracting the pyrethroid interaction (see above). However, in the absence of pyrethroids, it could imply higher fitness costs. The positive shift in the activation voltage means that these channels require stronger membrane depolarization to activate than the wild-type channel. Thus, these mutant *Vd*VGSC are essentially less excitable than the wild-type. Accordingly, in the absence of the strong selective pressure exerted by pyrethroids, individual mites with less excitable neurons would be at a disadvantage compared to mites that require a lower excitatory potential (Burton et al., 2011; Chen et al., 2010).

In relation to the associated fitness cost of the mutations, several studies on European *Varroa* populations described a substantial drop of resistant mites in the population after the cessation of pyrethroid-based treatments. Trouiller (2001) documented a reduction of around 50% of resistance after one year following the withdrawal of the active ingredient (Thompson et al., 2002). Further, Milani and Della Vedova (2002) reported a ten-fold decline in resistant mites after three years without fluvalinate treatment. Recently, González-Cabrera *et al.* (2018) related the decline of resistant mites in a hive population to the reduction in the frequency of 925V/V homozygous mites. In line with the previous observations, they reported a reduction in 925V/V mites by almost half after only one year of pyrethroid deprivation. Further genetic studies showed that resistant alleles were few or absent in apiaries not treated with pyrethroids for some years (Alissandrakis et al., 2017; González-Cabrera et al., 2013; González-Cabrera et al., 2016; Hubert et al., 2014). The observations made by these researchers strongly suggest that the L925V mutation has a significant fitness penalty

when the selective action exerted by pyrethroid treatment is discontinued. Our results here provide a plausible explanation for the decline of L925V mites in the absence of pyrethroids, based on the biophysical characteristics of the mutated and wild-type channels (Chapter 1). In turn, if our hypothesis is correct, given the biophysical characteristics of the mutated channels, a comparable fitness cost would be expected for mites carrying the L925I mutation.

The lack of treatment regime information in our study on the incidence of resistance in USA apiaries prevented us from correlating treatment influence with the proportion of resistant alleles to speculate whether there is a similar fitness penalty in mites with mutations L925I or L925M. However, a closer look at the results for resistant alleles monitored in USA shows an overall lower incidence of the 925M allele when compared to the 925I allele across the country, with a significant decrease of 925M between the two years sampled (Chapter 3). However, the phylogeny of these alleles has shown that 925I evolved from the previously originated 925M in the USA (Chapter 2). These results would not be an expected outcome if both substitutions had an equivalent fitness cost and the L925M mutation had arisen before or at the same time as the L925I. If these two alleles had comparable fitness, as would be expected to have about similar frequencies, or even higher for the previously arisen L925M allele. It is possible to hypothesise that 925M is posing a higher fitness cost to the mites when compared to 925I. Our pharmacological analyses revealed that the L925M mutated channel was more sensible to the tested pyrethroids (deltamethrin, flumethrin and *tau*-fluvalinate) than the L925I and L925V mutations (Chapter 1). Furthermore, of the three amino acid substitutions, Methionine is the biggest and heaviest, containing a sulphur atom. It has also been described in bacteria as the most "metabolically expensive" amino acid of all twenty in terms of moles of ATP consumed per molecule produced (Kaleta et al., 2013). Therefore, it is presumably associated with a higher biological cost, making this variant less efficient than the cohabiting Isoleucine. Altogether, these results may suggest that Isoleucine is more stable at position 925 than Methionine. In this scenario, we propose that L925M, even conferring resistance, would be an intermediate through the more stable resistant allele L925I. Nevertheless, further studies on the prevalence and fitness cost associated with these mutations are needed to validate or reject this hypothesis. Reinforcing our theory is the fact that L925I is widely reported to be associated with high resistance levels to pyrethroids in many arthropod species, including *Bemisia tabaci, Cimex lectularius,*

Trialeurodes vaporariorum, Rhipicephalus microplus, and *Hyalella azteca* (Karatolos et al., 2012; Morgan et al., 2009; Morin et al., 2002; Weston et al., 2013; Yoon et al., 2008). On the other hand, L925M has been described only in the mite *V. destructor* (González-Cabrera et al., 2016) and the poultry red mite *Dermanyssus gallinae* (Katsavou et al., 2020). In the latter two cases, the nucleotide triplet coding for the residue 925 needs the change of two nucleotides to switch from Leucine to Isoleucine (CTG to <u>AT</u>A), while only one for changing to Methionine (CTG to <u>A</u>TG) and Valine (CTG to <u>G</u>TG). However, in the species mentioned above, bearing L925I but with no L925M reported so far, only one nucleotide substitution is required to change from Leucine to Isoleucine (TTA to <u>A</u>TA in *B. tabaci* and *T. vaporariorum*, CTC to <u>A</u>TC in *R. microplus* and *H. azteca*, CTT to <u>A</u>TT in *C. lectularius*), and two substitutions to change from Leucine to Methionine (<u>A</u>T<u>G</u>).

Further studies are required to accurately document the fitness costs of *kdr*-type mutations on the mite, as well as to determine if the fitness cost associated with L925V is similar for L925M/I or M918L+L925V individuals. Moreover, it must be proven whether this fitness penalty is actually caused by the mutations and not by some other genetic traits being inherited linked to these resistant alleles.

Further factors that condition the prevalence of resistant alleles in a colony

Considering the rapid reversion of resistant mite populations to susceptible when treatment pressure is removed, it is strongly recommended to coordinate efforts to implement a resistance management approach in the context of a *Varroa* IPM programme. The high variability found among USA apiaries in the present study (Chapter 3), together with similar monitoring made in Europe (González-Cabrera et al., 2018; Hernández-Rodríguez et al., 2021), suggests that resistant allele frequencies are also strongly influenced by external factors.

The use of acaricide treatments by beekeepers and the potentially higher biological cost of these alleles are the most noticeable and apparently dominant selective forces (González-Cabrera et al., 2018). Nonetheless, the data collected so far indicate that there might be other selective drivers at play. Our results revealed a considerable high prevalence of the resistant alleles, in a very low rate of *tau*-fluvalinate use scenario among USA beekeepers (Haber et al., 2019). Hence, it is conceivable that there might be other sources of selection pressure keeping resistant alleles at high frequencies in the USA

Varroa population. Similarly, a high incidence of resistant mites has been documented in European apiaries despite the low use of pyrethroid (Hernández-Rodríguez et al., 2021). One possible source is the accumulation of acaricide products in colony matrices like beebread and beeswax. *Tau*-fluvalinate is among the most prevalent and ubiquitous residue detected within colonies beeswax, largely because it is a lipophilic compound and it is sequestered in the beeswax (Bernal et al., 2010; Calatayud-Vernich et al., 2018; Johnson et al., 2010). A recent survey of beeswax collected from USA colonies reported that 70.8% of them had detectable levels of *tau*-fluvalinate (USDA-APHIS, 2020). Furthermore, over a third of all bee bread samples taken from colonies had detectable *tau*-fluvalinate residues (Traynor et al., 2021). Accumulated acaricides in a colony's matrix could exert continuous selection pressure on mite populations, increasing the advantage of having alleles that would otherwise be disadvantageous. This suggests that comb management may have a role in long-term *Varroa* resistance management. By replacing contaminated comb (and contaminated bee bread), beekeepers may help reduce the frequency of resistant mites in their operations over the long-term.

Varroa reproductive biology is also likely to be playing a role in the maintenance and fluctuation of resistance allele frequency in mite populations. *Varroa* mites are highly inbred, as full sibling mating (adelphogamy) is the rule. This, combined with an haplo-diploid sex determination, fosters the formation of homozygotes (Rosenkranz et al., 2010). Such inbreeding by itself scores a more resistant homozygous state in the progeny, even before any selection by acaricide treatment takes place. In the event of uncontrolled or continuous application of pyrethroids, these resistant alleles could easily become fixed in the colony population (Beaurepaire et al., 2017). Without the adoption of a proper resistance management protocol and taking into account the worryingly low rate of hives free of resistant alleles detected in our monitoring (Chapter 3), such a detrimental situation might not be far from happening in several regions.

Integrated Pest Management for better control of *Varroa*

Integrated Pest Management is considered by experts to be the most successful and environmentally friendly approach to dealing with arthropod pests. It integrates the use of chemical insecticides in combination with better cultural and biological techniques, minimising the management impact on the environment (Barzman et al., 2015). To be

effective, an IPM programme requires a well-defined and comprehensive protocol for beekeepers to follow. Firstly, economic threshold (ET) and economic injury level (EIL) thresholds must be identified and defined. The EIL is defined as the lowest population density that will lead to an economic loss for the beekeeper (Stern et al., 1959). The economic threshold (ET), also referred to as the action threshold, is the threshold on which treatment measures should be initiated in order to avoid reaching the EIL. Below these thresholds, a set of preventive techniques will be implemented to keep the mite population beneath the EIL threshold (Stern et al., 1959). Pesticide treatments shall be applied once pest damage exceeds the ET thresholds, following a phased treatment plan according to need (Flint, 2012; Jack and Ellis, 2021).

For now, avoiding *Varroa* parasitism is virtually impossible. The only solution is to keep the mite population below the Economic Injury Level (EIL). If the population of mites were kept in check, so too would be the viral diseases, and honey bees could remain healthy. It is when the *Varroa* population gets out of control that the colony becomes seriously sick and there is a high risk of collapse (Jack and Ellis, 2021).
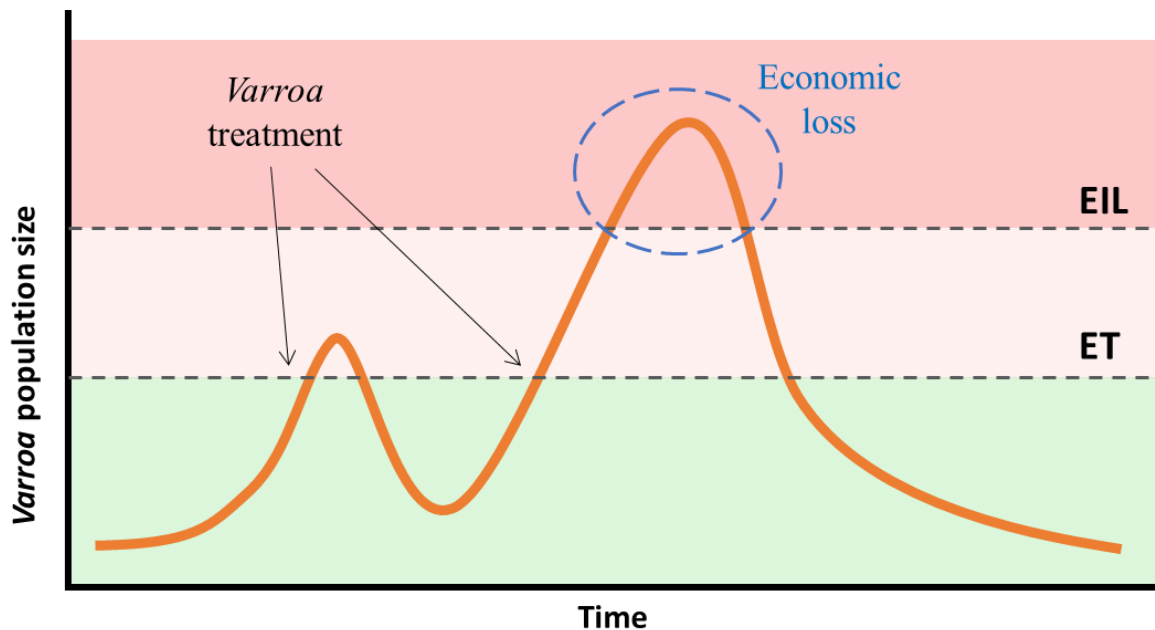
Figure d.1. Graph representing the size of the *Varroa* population in hive over time, showing the Economic Threshold (ET) and Economic Injury Level (EIL) for the mite population size. Above the EIL, the health and productivity of the honey bee colony declines up to the point of an economic loss for the beekeeper. Treatments to control the pest population from reaching the EIL should be initiated when the population size exceeds the TE. Graph modified from Jack and Ellis (2021).

The use of any miticide in apiculture is intended to protect bees but imposes selection pressures that can result in the development of resistance. Worryingly, reports of resistance to the three synthetic active ingredients are on the rise (Elzen et al., 1999a; González-Cabrera et al., 2018; Gracia-Salinas et al., 2006; Hernández-Rodríguez et al., 2021; Lodesani et al., 1995; Maggi et al., 2009; Maggi et al., 2010; Martin, 2004; Milani, 1995, 1999; Miozes-Koch et al., 2000; Pettis, 2004; Rinkevich, 2020; Rodríguez-Dehaibes et al., 2005; Trouiller, 1998). Consequently, *Varroa* control methods must incorporate strategies to minimise resistance development and preserve the utility of the treatments for the long-term, but above all, prevent the emergence of multi-resistant *V. destructor* strains or populations.

It is well known that, in the absence of resistance, pyrethroid miticides are one of the safest and most effective ways of removing mites from a hive. But in those apiaries with a high rate of resistant alleles, the general use of pyrethroid based products would have limited efficacy. These products, however, could still have utility if they are included in an IPM strategy that monitors the frequency of resistant mites and combines pyrethroid-based miticides with others like the organophosphate coumaphos, the amidine amitraz, organic acids, or essential oils, along with correct management approaches.

Managing the development of pesticide resistance is an important component of sustainable pest management that will prolong the lifespan of the few acaricides authorised for *Varroa* control. The monitoring of resistant allele frequencies in mite populations is one of the fundamental pillars in pesticide resistance management. Techniques to detect resistant alleles in the population provide a valuable tool for beekeepers and stakeholders to make decisions on product use and to set up treatment strategies. Deciding the treatment to apply in an apiary is a turning point which can impact both, the dynamics of *Varroa* populations and the honey bee colonies' health. Knowing the expected efficacy of a product beforehand would undoubtedly improve the outcome of *Varroa* control in the short term. In the same way, it would reduce the unnecessary exposure to inefficient treatments and their accumulation in hive matrixes.

Besides, the level of resistance in an apiary's population may fluctuate over a short period of time, for instance depending on the treatment regime or the exposure of mites to acaricide residues from previous treatments (González-Cabrera et al., 2018; Martins and Valle, 2012). Regular monitoring of resistant mutations is therefore essential to assess

changes in populations and to act accordingly. Moreover, regular monitoring will allow for the scheduling of pyrethroid-free periods when those would have been less efficient. It will also allow selective forces to reverse the frequency of resistance mites in the colony. Furthermore, combination and rotation of varroacides based on different modes of action would prevent the fixation of resistant alleles in mite populations (mites resistant to pyrethroids could be controlled by some of the other available treatments, dropping their incidence in the apiary), ensuring the long-term efficacy of chemical and natural acaricides. Having such information would cut down on unnecessary acaricide treatments, thereby minimising the unwanted build-up of residues in bee wax and reducing the likelihood of new resistant mutations developing in a mite population.

In the particular case of pyrethroids, allelic frequency-based tests, such as those used here (Chapters 3 and 4), have been proven to be capable of being implemented as a routine assay in a laboratory and therefore suitable for pesticide resistance management programmes. These methods have been demonstrated to be simple to perform, robust, reliable, and fast for genotyping large numbers of mites individually, hence being able to determine the incidence of pyrethroid resistant and susceptible mites in a given apiary (2018; González-Cabrera et al., 2013; 2016). In addition, they work well with mites collected and preserved without special requirements, which can be shipped at room temperature, making it easier for beekeepers. On one hand, the TaqMan® multiplex assay has been proven highly efficient for 925-allelic discrimination, being more efficient than the preparation of several reactions in a single assay, saving time and materials. The PCR-RFLP developed here, although not accurate enough to differentiate among the resistant alleles, it is quite effective in discriminating susceptible and resistant mites at a fraction of the cost of other methodologies (Chapter 4).

These allelic techniques are particularly useful for early detection of resistance when resistant mites are still at low rates in the population. In fact, they are more powerful than field observations, where the resistance has usually built up to fairly high frequencies by the time a failure in treatment is noticed. Surveys to monitor mutations associated with resistance have resulted in increased management success of pest species such as mosquitoes, aphids, beetles, and ticks (Højland et al., 2015; Lucas et al., 2019; Lynd et al., 2018; MacKenzie et al., 2018; Rosario-Cruz et al., 2009; Willis et al., 2020).

Concerning *Varroa* control within an IPM framework, Jack and Ellis (2021) have recently published a comprehensive review presenting the existing available options and encouraging beekeepers to adopt them. Despite the potential of IPM (Delaplane et al., 2005), the adoption of IPM principles by many beekeepers has unfortunately been unsuccessful, mainly due to insufficient knowledge about *Varroa* population dynamics and deficiencies in training (Whitehead, 2017). Through this thesis, we are contributing to the scientific understanding regarding the mutations that drive pyrethroid resistance in *V. destructor* with the objective of designing an effective management strategy to prevent beekeepers from failing in the control of this destructive pest.

CONCLUSIONS

CONCLUSIONS (EN)

1. The effect of pyrethroids upon the *Vd*VGSC was significantly reduced in the 925-mutated channels, supporting the role of these mutations in the mechanism of resistance to pyrethroids in *V. destructor*.

2. *Tau*-fluvalinate induced a tail current in the wild-type *Vd*VGSC greater than that induced by flumethrin. However, the magnitude of alteration in the activation kinetics was significantly bigger for flumethrin.

3. The interaction of deltamethrin, *tau*-fluvalinate and flumethrin with the *Vd*VGSC alters the channel's gating kinetics by shifting the $V_{50,act}$ to more positive voltages. This variation in the activation properties may indirectly counteract pyrethroid effect on mite VGSC, in contrast to what occurs in insect VGSC.

4. In the absence of the strong selective pressure exerted by pyrethroids, the change of the wild-type Leucine at position 925 of the *Vd*VGSC by Valine, Isoleucine, or Methionine, may be negatively impacting mites' fitness

5. The mutation M918L in the VGSC has been detected for the first time in *V. destructor*. In our study, this mutation was always found in co-occurrence with L925V in mites collected from Spanish apiaries.

6. Phylogenetic analyses of the gene region linked to position 925 of the *Vd*VGSC revealed a single origin for each *kdr*-type mutation. Therefore, their widespread distribution is the outcome of the subsequent distribution of mites carrying these alleles after the mutation events.

7. The phylogenetic reconstruction suggests the occurrence of two different parallel and sequential origins for mutations at position 925 of the *Vd*VGSC. L925M and L925I on one hand, and L925V and M918L on the other. The L925M mutation would be an ancestor of the L925I, which would have arisen in a second mutation event.

8. Our screening results from USA apiaries revealed that both, L925I and L925M are widespread throughout the country, albeit at a variable incidence. Our findings also

evidenced that the persistent reports of *tau*-fluvalinate treatment failures across the USA can be attributed to the prevalence of these mutations in the apiaries.

9. The L925M allele had a lower overall incidence than the L925I in the USA apiaries. Its frequency was significantly reduced overtime.

10. A new diagnostics methodology based on PCR-RFLP have been developed. It is capable of accurately detecting 925-mutant alleles in individual mites and predicting the frequency of resistant mites in a given colony. This methodology, although not precise enough to differentiate among the resistant alleles, is quite effective in discriminating between susceptible and resistant mites at a fraction of the cost of other methodologies, as well as being quite versatile and adaptable to the requirements of most laboratories.

11. The two allelic frequency-based tests used in this thesis, the TaqMan® multiplex and the PCR-RFLP, are simple to perform, robust, reliable, and fast for genotyping large numbers of mites individually. These methods may be implemented as a routine lab test for detecting and determining the incidence of pyrethroid-resistant mites in a given apiary.

CONCLUSIONS (VAL)

1. L'efecte dels piretroides sobre el *Vd*VGSC es va veure significativament reduït en els canals amb la posició 925 mutada, corroborant la implicació d'aquestes mutacions en el mecanisme de resistència als piretroides en *V.destructor*.

2. El *tau*-fluvalinat va induir un corrent de cua en els *Vd*VGSC de tipus salvatge major que la induïda per la flumetrina. D'altra banda, la magnitud de l'alteració de la cinètica d'activació va ser significativament major per a la flumetrina.

3. La interacció de la deltametrina, el *tau*-fluvalinat i la flumetrina amb el *Vd*VGSC altera la cinètica d'activació del canal, desplaçant el $V_{50,act}$ a voltatges més positius. Aquesta variació en l'activació pot contrarestar indirectament l'efecte dels piretroides en els àcars, a diferència del que ocorre en els VGSC dels insectes.

4. En absència de la forta pressió selectiva exercida pels piretroides, el canvi de la leucina en la posició 925 del *Vd*VGSC per la valina, la isoleucina o la metionina, pot tindre un cert impacte negatiu en l'aptitud dels àcars.

5. La mutació M918L en el VGSC s'ha detectat per primera vegada en *V. destructor*. En el nostre estudi, aquesta mutació es va trobar sempre en co-ocurrència amb la L925V en àcars recollits en ruscos espanyols.

6. Els anàlisis filogenètics de la regió gènica vinculada a la posició 925 del *Vd*VGSC van revelar un origen únic per a cada mutació de tipus *kdr*. Per tant, la seua àmplia distribució es deu a la posterior migració dels àcars portadors d'aquests al·lels després dels esdeveniments de mutació.

7. La relació filogenètica suggereix l'aparició de dos orígens diferents, paral·lels i seqüencials, per a les mutacions en la posició 925 del *Vd*VGSC. Amb les mutacions L925M i L925I d'una banda, i L925V i M918L per l'altra. La mutació L925M seria un ancestre de la mutació L925I, que hauria sorgit en un segon esdeveniment de mutació.

8. Els resultats del nostre mostreig en apiaris dels Estats Units van revelar que tant els al·lels L925I com L925M estan repartits per tot el país, encara que amb una

incidència variable. Els nostres resultats també demostren que els informes persistents en els Estats Units de baixa eficàcia en tractaments amb *tau*-fluvalinat poden atribuir-se a la prevalença d'aquestes mutacions en els apiaris.

9. L'al·lel L925M va presentar una incidència global menor que el L925I en els apiaris dels Estats Units. A més, la seua freqüència es va reduir significativament entre els dos anys mostrejats.

10. Hem desenvolupat una nova metodologia de diagnòstic basada en una PCR-RFLP capaç de detectar amb precisió els al·lels mutants per a la posició 925 en àcars individuals i predir la freqüència d'àcars resistents en una colònia determinada. Aquesta metodologia, encara que no és prou precisa com per a diferenciar entre els al·lels resistents, és bastant eficaç per a discriminar entre àcars susceptibles i resistents a una fracció del cost d'altres metodologies, a més de ser prou versàtil i adaptable a les necessitats de qualsevol laboratori.

11. Les dues proves utilitzades en aquesta tesi per a determinar la freqüència al·lèlica, la TaqMan® multiplex i la PCR-RFLP, són senzilles, robustes, fiables i ràpides per a genotipar un gran nombre d'àcars individuals. Aquests mètodes han demostrat ser adequats per a ser implementats com a assaig rutinari de laboratori per a la detecció i determinació de la incidència d'àcars resistents i susceptibles als piretroides en un apiari o rusc.

REFERENCES

Abrol, DP (**2012**) Value of Bee Pollination. In: Pollination Biology: Biodiversity Conservation and Agricultural Production. Springer Netherlands, Dordrecht, pp 185-222. https://doi.org/10.1007/978-94-007-1942-2_7

Afonina, I; Zivarts, M; Kutyavin, I; Lukhtanov, E; Gamper, H; Meyer, RB (**1997**) Efficient priming of PCR with short oligonucleotides conjugated to a minor groove binder. *Nucleic Acids Research* 25:2657-2660. https://doi.org/10.1093/nar/25.13.2657

Aizen, MA; Harder, LD (**2009**) The global stock of domesticated honey bees is growing slower than agricultural demand for pollination. *Current Biology* 19:915-918. https://doi.org/10.1016/j.cub.2009.03.071

Alberti, G; Hänel, H (**1986**) Fine structure of the genital system in the bee parasite, *Varroa jacobsoni* (Gamasida: Dermanyssina) with remarks on spermiogenesis, spermatozoa and capacitation. *Experimental and Applied Acarology* 2:63-104. https://doi.org/10.1007/BF01193355

Aliano, NP; Ellis, MD (**2005**) A strategy for using powdered sugar to reduce varroa populations in honey bee colonies. *Journal of Apicultural Research* 44:54-57. https://doi.org/10.1080/00218839.2005.11101148

Alissandrakis, E; Ilias, A; Tsagkarakou, A (**2017**) Pyrethroid target site resistance in Greek populations of the honey bee parasite *Varroa destructor* (Acari: *Varroidae*). *Journal of Apicultural Research* 56:625-630. https://doi.org/10.1080/00218839.2017.1368822

Almecija, G; Poirot, B; Cochard, P; Suppo, C (**2020**) Inventory of *Varroa destructor* susceptibility to amitraz and *tau*-fluvalinate in France. *Experimental and Applied Acarology* 82:1-16. https://doi.org/10.1007/s10493-020-00535-w

Alon, M; Benting, J; Lueke, B; Ponge, T; Alon, F; Morin, S (**2006**) Multiple origins of pyrethroid resistance in sympatric biotypes of *Bemisia tabaci* (Hemiptera: *Aleyrodidae*). *Insect Biochemistry and Molecular Biology* 36:71-79. https://doi.org/10.1016/j.ibmb.2005.10.007

Amdam, GV; Hartfelder, K; Norberg, K; Hagen, A; Omholt, SW (**2004**) Altered physiology in worker honey bees (Hymenoptera: *Apidae*) infested with the mite *Varroa destructor* (Acari: *Varroidae*): A factor in colony loss during overwintering? *Journal of Economic Entomology* 97:741-747. https://doi.org/10.1093/jee/97.3.741

Amdam, GV; Norberg, K; Hagen, A; Omholt, SW (**2003**) Social exploitation of vitellogenin. *Proceedings of the National Academy of Sciences* 100:1799-1802. https://doi.org/10.1073/pnas.0333979100

Anderson, D, L. (**1994**) Non-reproduction of Varroa jacobsoni in Apis mellifera colonies in Papua New Guinea and Indonesia. *Apidologie* 25:412-421. https://doi.org/10.1051/apido:19940408

Anderson, D; Sukarsih (**1996**) Changed *Varroa jacobsoni* reproduction in *Apis mellifera* colonies in Java. *Apidologie* 27:461-466. https://doi.org/10.1051/apido:19960604

Anderson, DL; Fuchs, S (**1998**) Two genetically distinct populations of *Varroa jacobsoni* with contrasting reproductive abilities on *Apis mellifera*. *Journal of Apicultural Research* 37:69-78. https://doi.org/10.1080/00218839.1998.11100957

Anderson, DL; Trueman, JWH (**2000**) *Varroa jacobsoni* (Acari: *Varroidae*) is more than one species. *Experimental and Applied Acarology* 24:165-189. https://doi.org/10.1023/A:1006456720416

Andino, GK; Gribskov, M; Anderson, DL; Evans, JD; Hunt, GJ (**2016**) Differential gene expression in Varroa jacobsoni mites following a host shift to European honey bees (Apis mellifera). *BMC Genomics* 17:926. https://doi.org/10.1186/s12864-016-3130-3

Annoscia, D; Del Piccolo, F; Covre, F; Nazzi, F (**2015**) Mite infestation during development alters the in-hive behaviour of adult honeybees. *Apidologie* 46:306-314. https://doi.org/10.1007/s13592-014-0323-0

Annoscia, D; Del Piccolo, F; Nazzi, F (**2012**) How does the mite *Varroa destructor* kill the honeybee *Apis mellifera*? Alteration of cuticular hydrcarbons and water loss in infested honeybees. *Journal of Insect Physiology* 58:1548-1555. https://doi.org/10.1016/j.jinsphys.2012.09.008

Anstead, JA; Williamson, MS; Denholm, I (**2005**) Evidence for multiple origins of identical insecticide resistance mutations in the aphid *Myzus persicae*. *Insect Biochemistry and Molecular Biology* 35:249-256. https://doi.org/10.1016/j.ibmb.2004.12.004

Arrese, EL; Soulages, JL (**2010**) Insect fat body: energy, metabolism, and regulation. *Annual Review of Entomology* 55:207-225. https://doi.org/10.1146/annurev-ento-112408-085356

Aznar-Alemany, Ò; Eljarrat, E (**2020**) Introduction to pyrethroid insecticides: Chemical structures, properties, mode of action and use. In: Eljarrat, E (ed) Pyrethroid Insecticides. Springer International Publishing, Cham, pp 1-16. https://doi.org/10.1007/698_2019_435

Bailey, L; Ball, BV; Woods, RD (**1976**) An iridovirus from bees. *Journal of General Virology* 31:459-461. https://doi.org/10.1099/0022-1317-31-3-459

REFERENCES

Bailey, L; Carpenter, J; Woods, R (**1979**) Egypt bee virus and Australian isolates of Kashmir bee virus. *Journal of General Virology* 43:641-647. https://doi.org/10.1099/0022-1317-43-3-641

Bailey, L; Carpenter, J; Woods, R (**1981**) Properties of a filamentous virus of the honey bee (*Apis mellifera*). *Virology* 114:1-7. https://doi.org/10.1016/0042-6822(81)90247-6

Bailey, L; Woods, R (**1977**) Two more small RNA viruses from honey bees and further observations on sacbrood and acute bee-paralysis viruses. *Journal of General Virology* 37:175-182. https://doi.org/10.1099/0022-1317-37-1-175

Bąk, B; Wilde, J; Siuda, M (**2012**) Characteristics of north-eastern population of *Varroa destructor* resistant to synthetic pyrethroids. *Medycyna weterynaryjna* 68:606-603. http://www.medycynawet.edu.pl/231-summary-2012/summary-2012-10/4222-summary-med-weter-68-10-603-606-2012

Ball, B; Allen, M (**1988**) The prevalence of pathogens in honey bee (*Apis mellifera*) colonies infested with the parasitic mite *Varroa jacobsoni*. *Annals of Applied Biology* 113:237-244. https://doi.org/10.1111/j.1744-7348.1988.tb03300.x

Barzman, M; Bàrberi, P; Birch, ANE *et al.* (**2015**) Eight principles of integrated pest management. *Agronomy for Sustainable Development* 35:1199-1215. https://doi.org/10.1007/s13593-015-0327-9

Bass, C; Nikou, D; Donnelly, MJ *et al.* (**2007**) Detection of knockdown resistance (*kdr*) mutations in *Anopheles gambiae*: A comparison of two new high-throughput assays with existing methods. *Malar J* 6:111. https://doi.org/10.1186/1475-2875-6-111

Bass, C; Puinean, AM; Zimmer, CT *et al.* (**2014**) The evolution of insecticide resistance in the peach potato aphid, *Myzus persicae*. *Insect Biochemistry and Molecular Biology* 51:41-51. https://doi.org/10.1016/j.ibmb.2014.05.003

Baxter, J; Eischen, F; Pettis, J; Wilson, W; Shimanuki, H (**1998**) Detection of fluvalinate-resistant Varroa mites in US honey bees. *American bee journal* 138:291. https://doi.org/10.1051/apido:19990102

Baxter, JR; Ellis, MD; Wilson, WT (**2000**) Field evaluation of Apistan and five candidate compounds for parasitic mite control in honey bees. *American bee journal* 140:898-900.

Beaurepaire, A; Piot, N; Doublet, V *et al.* (**2020**) Diversity and global distribution of viruses of the western honey bee, *Apis mellifera*. *Insects* 11. https://doi.org/10.3390/insects11040239

Beaurepaire, AL; Ellis, JD; Krieger, KJ; Moritz, RFA (**2019a**) Association of *Varroa destructor* females in multiply infested cells of the honeybee *Apis mellifera*. *Insect science* 26:128-134. https://doi.org/10.1111/1744-7917.12529

Beaurepaire, AL; Krieger, KJ; Moritz, RFA (**2017**) Seasonal cycle of inbreeding and recombination of the parasitic mite *Varroa destructor* in honeybee colonies and its implications for the selection of acaricide resistance. *Infection, Genetics and Evolution* 50:49-54. https://doi.org/10.1016/j.meegid.2017.02.011

Beaurepaire, AL; Moro, A; Mondet, F; Le Conte, Y; Neumann, P; Locke, B (**2019b**) Population genetics of ectoparasitic mites suggest arms race with honeybee hosts. *Scientific reports* 9:11355. https://doi.org/10.1038/s41598-019-47801-5

Beaurepaire, AL; Truong, TA; Fajardo, AC; Dinh, TQ; Cervancia, C; Moritz, RF (**2015**) Host specificity in the honeybee parasitic mite, *Varroa* spp. in *Apis mellifera* and *Apis cerana*. *PLOS ONE* 10:e0135103. https://doi.org/10.1371/journal.pone.0135103

Becchimanzi, A; Tatè, R; Campbell, EM; Gigliotti, S; Bowman, AS; Pennacchio, F (**2020**) A salivary chitinase of *Varroa destructor* influences host immunity and mite's survival. *PLOS Pathogens* 16:e1009075. https://doi.org/10.1371/journal.ppat.1009075

Beetsma, J (**1994**) The Varroa mite, a devastating parasite of western honeybees and an economic threat to beekeeping. *Outlook on Agriculture* 23:169-175. https://doi.org/10.1177/003072709402300303

Beetsma, J; Boot, W, Jan; Calis, J (**1999**) Invasion behaviour of *Varroa jacobsoni* Oud.: from bees into brood cells. *Apidologie* 30:125-140. https://doi.org/10.1051/apido:19990204

Beetsma, J; Zonneveld, K (**1992**) Observations on the initiation and stimulation of oviposition of the Varroa mite. *Experimental and Applied Acarology* 16:303-312. https://doi.org/10.1007/BF01218572

Bell, JR; Gloor, S; Camazine, SM (**1999**) Biochemical mechanisms of fluvalinate resistance in *Varroa jacobsoni* mites. *American bee journal* 139:308-309.

Benavent-Albarracín, L; Alonso, M; Catalán, J; Urbaneja, A; Davies, TGE; Williamson, MS; González-Cabrera, J (**2020**) Mutations in the voltage-gated sodium channel gene associated with deltamethrin resistance in commercially sourced *Phytoseiulus persimilis*. *Insect Molecular Biology* 29:373-380. https://doi.org/10.1111/imb.12642

Benoit, JB; Yoder, JA; Sammataro, D; Zettler, LW (**2004**) Mycoflora and fungal vector capacity of the parasitic mite *Varroa destructor* (Mesostigmata: *Varroidae*) in honey bee (Hymenoptera: *Apidae*) colonies. *International Journal of Acarology* 30:103-106. https://doi.org/10.1080/01647950408684376

Bernal, J; Garrido-Bailón, E; Del Nozal, MJ *et al.* (**2010**) Overview of pesticide residues in stored pollen and their potential effect on bee colony (*Apis mellifera*) losses in Spain. *Journal of Economic Entomology* 103:1964-1971. https://doi.org/10.1603/EC10235

BIP (**2020**) 2019-2020 honey bee colony losses in the United States: Preliminary results. Bee Informed Partnership, https://beeinformed.org

Blanken, LJ; van Langevelde, F; van Dooremalen, C (**2015**) Interaction between *Varroa destructor* and imidacloprid reduces flight capacity of honeybees. *Proceedings of the Royal Society B: Biological Sciences* 282:20151738. https://doi.org/10.1098/rspb.2015.1738

BOC (**2001**) Boletín Oficial de Canarias - BOC-2001-049-603. http://www.gobiernodecanarias.org/boc/2001/049/003.html

BOC (**2014**) Boletín Oficial de Canarias - BOC-A-2014-086-1889. http://www.gobiernodecanarias.org/boc/2014/086/001.html

Boecking, O; Genersch, E (**2008**) Varroosis – the ongoing crisis in bee keeping. *Journal für Verbraucherschutz und Lebensmittelsicherheit* 3:221-228. https://doi.org/10.1007/s00003-008-0331-y

Boecking, O; Spivak, M (**1999**) Behavioral defenses of honey bees against *Varroa jacobsoni* Oud. *Apidologie* 30:141-158. https://doi.org/10.1051/apido:19990205

Boecking, O; Veromann, E (**2020**) Bee pollination of crops: A natural and cost-free ecological service. In: Smagghe, G, Boecking, O, Maccagnani, B, Mänd, M, Kevan, PG (eds) Entomovectoring for Precision Biocontrol and Enhanced Pollination of Crops. Springer International Publishing, Cham, pp 53-62. https://doi.org/10.1007/978-3-030-18917-4_3

Bogdanov, S; Kilchenmann, V; Imdorf, A (**1998**) Acaricide residues in some bee products. *Journal of apicultural research* 37:57-67. https://doi.org/10.1080/00218839.1998.11100956

Bolli, H; Bogdanov, S; Imdorf, A; Fluri, P (**1993**) Action of formic acid on *Varroa jacobsoni* Oud. and the honeybee (*Apis mellifera* L). *Apidologie*. https://doi.org/10.1051/apido:19930106

Bond, J; Plattner, K; Hunt, K (**2014**) Fruit and tree nuts outlook: economic insight US pollination-services market. https://www.ers.usda.gov/webdocs/outlooks/37059/49131_special-article-september_-pollinator-service-market-4-.pdf?v=6937.9

Bonzini, S; Tremolada, P; Bernardinelli, I; Colombo, M; Vighi, M (**2011**) Predicting pesticide fate in the hive (part 1): experimentally determined τ-fluvalinate residues in bees, honey and wax. *Apidologie* 42:378-390. https://doi.org/10.1007/s13592-011-0011-2

Boot, WJ; Calis, JN; Beetsma, J (**1992**) Differential periods of Varroa mite invasion into worker and drone cells of honey bees. *Experimental and Applied Acarology* 16:295-301. https://doi.org/10.1007/BF01218571

Bordier, C; Suchail, S; Pioz, M *et al.* (**2017**) Stress response in honeybees is associated with changes in task-related physiology and energetic metabolism. *Journal of Insect Physiology* 98:47-54. https://doi.org/10.1016/j.jinsphys.2016.11.013

Bouckaert, RR; Drummond, AJ (**2017**) bModelTest: Bayesian phylogenetic site model averaging and model comparison. *BMC Evolutionary Biology* 17:42. https://doi.org/10.1186/s12862-017-0890-6

Bouckaert, RR; Vaughan, TG; Barido-Sottani, J *et al.* (**2019**) BEAST 2.5: An advanced software platform for Bayesian evolutionary analysis. *PLOS Computational Biology* 15:e1006650. https://doi.org/10.1371/journal.pcbi.1006650

Bourdin, CM; Guérineau, NC; Murillo, L; Quinchard, S; Dong, K; Legros, C (**2015**) Molecular and functional characterization of a novel sodium channel TipE-like auxiliary subunit from the American cockroach *Periplaneta americana*. *Insect Biochemistry and Molecular Biology* 66:136-144. https://doi.org/10.1016/j.ibmb.2015.10.008

Bourdin, CM; Moignot, B; Wang, L *et al.* (**2013**) Intron retention in mRNA encoding ancillary subunit of insect voltage-gated sodium channel modulates channel expression, gating regulation and drug sensitivity. *PLOS ONE* 8:e67290. https://doi.org/10.1371/journal.pone.0067290

Bowen-Walker, PL; Gunn, A (**2001**) The effect of the ectoparasitic mite, *Varroa destructor* on adult worker honeybee (*Apis mellifera*) emergence weights, water, protein, carbohydrate, and lipid levels. *Entomol Exp Appl* 101:207-217. https://doi.org/10.1046/j.1570-7458.2001.00905.x

Božič, J; Valentinčič, T (**1995**) Quantitative analysis of social grooming behavior of the honey bee *Apis mellifera carnica*. *Apidologie* 26:141-147. https://doi.org/10.1051/apido:19950207

REFERENCES

Breeze, TD; Vaissière, BE; Bommarco, R *et al.* (**2014**) Agricultural policies exacerbate honeybee pollination service supply-demand mismatches across Europe. *PLOS ONE* 9:e82996. https://doi.org/10.1371/journal.pone.0082996

Brito, LP; Carrara, L; Freitas, RMd; Lima, JBP; Martins, AJ (**2018**) Levels of resistance to pyrethroid among distinct *kdr* alleles in *Aedes aegypti* laboratory lines and frequency of *kdr* alleles in 27 natural populations from Rio de Janeiro, Brazil. *BioMed Research International* 2018:10. https://doi.org/10.1155/2018/2410819

Brodschneider, R; Gray, A; Adjlane, N *et al.* (**2018**) Multi-country loss rates of honey bee colonies during winter 2016/2017 from the COLOSS survey. *Journal of Apicultural Research* 57:452-457. https://doi.org/10.1080/00218839.2018.1460911

Büchler, R; Berg, S; Le Conte, Y (**2010**) Breeding for resistance to *Varroa destructor* in Europe. *Apidologie* 41:393-408. https://doi.org/10.1051/apido/2010011

Büchler, R; Drescher, W; Tornier, I (**1992**) Grooming behaviour of *Apis cerana*, *Apis mellifera* and *Apis dorsata* and its effect on the parasitic mites *Varroa jacobsoni* and *Tropilaelaps clareae*. *Experimental and Applied Acarology* 16:313-319. https://doi.org/10.1007/BF01218573

Budge, GE; Adams, I; Thwaites, R *et al.* (**2016**) Identifying bacterial predictors of honey bee health. *Journal of invertebrate pathology* 141:41-44. https://doi.org/10.1016/j.jip.2016.11.003

Burgett, M; Daberkow, S; Rucker, R; Thurman, W (**2010**) US pollination markets: Recent changes and historical perspective. *American bee journal*. https://thurmanw.wordpress.ncsu.edu/files/2019/07/pollination-historical-ABJ-2010.pdf

Burritt, NL; Foss, NJ; Neeno-Eckwall, EC *et al.* (**2016**) Sepsis and hemocyte loss in honey bees (*Apis mellifera*) infected with *Serratia marcescens* strain sicaria. *PLOS ONE* 11:e0167752. https://doi.org/10.1371/journal.pone.0167752

Burton, MJ (**2012**) Molecular basis of pyrethroid sensitivity and resistance. University of Nottingham

Burton, MJ; Mellor, IR; Duce, IR; Davies, TGE; Field, LM; Williamson, MS (**2011**) Differential resistance of insect sodium channels with *kdr* mutations to deltamethrin, permethrin and DDT. *Insect Biochemistry and Molecular Biology* 41:723-732. https://doi.org/10.1016/j.ibmb.2011.05.004

Busvine, JR (**1951**) Mechanism of resistance to insecticide in houseflies. *Nature* 168:193-195. https://doi.org/10.1038/168193a0

Busvine, JR (**1953**) Forms of insecticide-resistance in houseflies and body lice. *Nature* 171:118-119. https://doi.org/10.1038/171118a0

Calatayud-Vernich, P; Calatayud, F; Simó, E; Picó, Y (**2017**) Occurrence of pesticide residues in Spanish beeswax. *Science of the Total Environment* 605-606:745-754. https://doi.org/10.1016/j.scitotenv.2017.06.174

Calatayud-Vernich, P; Calatayud, F; Simó, E; Picó, Y (**2018**) Pesticide residues in honey bees, pollen and beeswax: Assessing beehive exposure. *Environmental Pollution* 241:106-114. https://doi.org/10.1016/j.envpol.2018.05.062

Calderón, RA; Fallas, N; Zamora, LG; van Veen, JW; Sánchez, LA (**2009**) Behavior of Varroa mites in worker brood cells of Africanized honey bees. *Experimental and Applied Acarology* 49:329. https://doi.org/10.1007/s10493-009-9266-y

Calderone, NW (**1999**) Evaluation of formic acid and a thymol-based blend of natural products for the fall control of *Varroa jacobsoni* (Acari: *Varroidae*) in colonies of *Apis mellifera* (Hymenoptera: *Apidae*). *Journal of Economic Entomology* 92:253-260. https://doi.org/10.1093/jee/92.2.253

Calderone, NW (**2010**) Evaluation of Mite-Away-II (TM) for fall control of *Varroa destructor* (Acari: *Varroidae*) in colonies of the honey bee *Apis mellifera* (Hymenoptera: *Apidae*) in the northeastern USA. *Experimental and Applied Acarology* 50:123-132. https://doi.org/10.1007/s10493-009-9288-5

Calderone, NW (**2012**) Insect pollinated crops, insect pollinators and US agriculture: Trend analysis of aggregate data for the period 1992–2009. *PLOS ONE* 7:e37235. https://doi.org/10.1371/journal.pone.0037235

Calderone, NW; Lin, S; Kuenen, LPS (**2002**) Differential infestation of honey bee, *Apis mellifera*, worker and queen brood by the parasitic mite *Varroa destructor*. *Apidologie* 33:389-398. https://doi.org/10.1051/apido:2002024

Calderone, NW; Spivak, M (**1995**) Plant extracts for control of the parasitic mite *Varroa jacobsoni* (Acari: *Varroidae*) in colonies of the western honey bee (Hymenoptera: *Apidae*). *Journal of Economic Entomology* 88:1211-1215. https://doi.org/10.1093/jee/88.5.1211

Calis, JNM; Boot, WJ; Beetsma, J; van den Eijnde, JHPM; de Ruijter, A; van der Steen, JJM (**1998**) Control of Varroa by combining trapping in honey bee worker brood with formic acid treatment of the

capped brood outside the colony: putting knowledge on brood cell invasion into practice. *Journal of Apicultural Research* 37:205-215. https://doi.org/10.1080/00218839.1998.11100973

Calis, JNM; Fries, I; Ryrie, SC (**1999**) Population modelling of *Varroa jacobsoni* Oud. *Apidologie* 30:111-124. https://doi.org/10.1051/apido:19990203

Capriotti, N; Mougabure-Cueto, G; Rivera-Pomar, R; Ons, S (**2014**) L925I mutation in the *para*-type sodium channel is associated with pyrethroid resistance in *Triatoma infestans* from the Gran Chaco region. *PLOS Neglected Tropical Diseases* 8:e2659. https://doi.org/10.1371/journal.pntd.0002659

Carletto, J; Martin, T; Vanlerberghe-Masutti, F; Brévault, T (**2010**) Insecticide resistance traits differ among and within host races in *Aphis gossypii*. *Pest Management Science* 66:301-307. https://doi.org/10.1002/ps.1874

Carreck, NL (**2011**) Breeding honey bees for Varroa tolerance. Varroa-still a problem in the 21st century? International Bee Research Association.

Carreck, NL; Ball, BV; Martin, SJ (**2010a**) The epidemiology of cloudy wing virus infections in honey bee colonies in the UK. *Journal of Apicultural Research* 49:66-71. https://doi.org/10.3896/IBRA.1.49.1.09

Carreck, NL; Ball, BV; Martin, SJ (**2010b**) Honey bee colony collapse and changes in viral prevalence associated with *Varroa destructor*. *Journal of Apicultural Research* 49:93-94. https://doi.org/10.3896/IBRA.1.49.1.13

Catterall, WA (**2000**) From ionic currents to molecular mechanisms: the structure and function of voltage-gated sodium channels. *Neuron* 26:13-25. https://doi.org/10.1016/s0896-6273(00)81133-2

Chan, QWT; Chan, MY; Logan, M; Fang, Y; Higo, H; Foster, LJ (**2013**) Honey bee protein atlas at organ-level resolution. *Genome Research* 23:1951-1960. https://doi.org/10.1101/gr.155994.113

Chantawannakul, P; de Guzman, LI; Li, J; Williams, GR (**2016**) Parasites, pathogens, and pests of honeybees in Asia. *Apidologie* 47:301-324. https://doi.org/10.1007/s13592-015-0407-5

Chen, L; Zhong, D; Zhang, D *et al.* (**2010**) Molecular ecology of pyrethroid knockdown resistance in *Culex pipiens* pallens mosquitoes. *PLOS ONE* 5:e11681. https://doi.org/10.1371/journal.pone.0011681

Chen, X; Li, F; Chen, A *et al.* (**2017**) Both point mutations and low expression levels of the nicotinic acetylcholine receptor β1 subunit are associated with imidacloprid resistance in an *Aphis gossypii* (Glover) population from a Bt cotton field in China. *Pesticide Biochemistry and Physiology* 141:1-8. https://doi.org/10.1016/j.pestbp.2016.11.004

Chen, YP; Siede, R (**2007**) Honey Bee Viruses. In: Advances in Virus Research, vol 70. Academic Press, pp 33-80. https://doi.org/10.1016/S0065-3527(07)70002-7

Cifuentes, D; Chynoweth, R; Bielza, P (**2011**) Genetic study of Mediterranean and South American populations of tomato leafminer *Tuta absoluta* (Povolny, 1994) (Lepidoptera: *Gelechiidae*) using ribosomal and mitochondrial markers. *Pest Management Science* 67:1155-1162. https://doi.org/10.1002/ps.2166

Cohen, E (**2013**) Water homeostasis and osmoregulation as targets in the control of insect pests. *Advances in Insect Physiology* 44:1-61. https://doi.org/10.1016/B978-0-12-394389-7.00001-6

Colin, M, E.; Vandame, R; Jourdam, P; Di Pasquale, S (**1997**) Fluvalinate resistance of *Varroa jacobsoni* Oudemans (Acari: *Varroidae*) in Mediterranean apiaries of France. *Apidologie* 28:375-384. https://doi.org/10.1051/apido:19970605

Cook, DC; Thomas, MB; Cunningham, SA; Anderson, DL; De Barro, PJ (**2007**) Predicting the economic impact of an invasive species on an ecosystem service. *Ecological Applications* 17:1832-1840. https://doi.org/10.1890/06-1632.1

Cornara, L; Biagi, M; Xiao, J; Burlando, B (**2017**) Therapeutic properties of bioactive compounds from different honeybee products. *Frontiers in Pharmacology* 8:412. https://doi.org/10.3389/fphar.2017.00412

Cornman, RS; Schatz, MC; Johnston, JS *et al.* (**2010**) Genomic survey of the ectoparasitic mite *Varroa destructor*, a major pest of the honey bee *Apis mellifera*. *BMC Genomics* 11:602. https://doi.org/10.1186/1471-2164-11-602

Crane, E (**1978**) The Varroa mite. *Bee World* 59:164-167. https://www.evacranetrust.org/uploads/document/7d403256314245e8be4c900be16f31430ec9d7fc.pdf

Crane, E (**1999**) The World History of Beekeeping and Honey Hunting. Routledge.

Dahle, B (**2010**) The role of *Varroa destructor* for honey bee colony losses in Norway. *Journal of Apicultural Research* 49:124-125. https://doi.org/10.3896/IBRA.1.49.1.26

Damiani, N; Gende, LB; Bailac, P; Marcangeli, JA; Eguaras, MJ (**2009**) Acaricidal and insecticidal activity of essential oils on *Varroa destructor* (Acari: *Varroidae*) and *Apis mellifera* (Hymenoptera: *Apidae*). *Parasitology research* 106:145-152. https://doi.org/10.1007/s00436-009-1639-y

Davies, TGE; Field, LM; Usherwood, PNR; Williamson, MS (**2007**) DDT, pyrethrins, pyrethroids and insect sodium channels. *IUBMB Life* 59:151-162. https://doi.org/10.1080/15216540701352042

de Guzman, LI; Delfinado-Baker, M (**1996**) A new species of *Varroa* (Acari: *Varroidae*) associated with *Apis koschevnikovi* (*Apidae*: Hymenoptera) in Borneo. *International Journal of Acarology* 22:23-27. https://doi.org/10.1080/01647959608684077

de Guzman, LI; Rinderer, TE; Stelzer, JA (**1997**) DNA evidence of the origin of *Varroa jacobsoni* Oudemans in the Americas. *Biochemical Genetics* 35:327-335. https://doi.org/10.1023/A:1021821821728

de Guzman, LI; Rinderer, TE; Stelzer, JA (**1999**) Occurrence of two genotypes of *Varroa jacobsoni* Oud. in North America. *Apidologie* 30:31-36. https://doi.org/10.1051/apido:19990104

De Jong, D (**1988**) *Varroa jacobsoni* does reproduce in worker cells of *Apis cerana* in South Korea. *Apidologie* 19:241-244. https://doi.org/10.1051/apido:19880303

De Jong, D; De Jong, PH (**1983**) Longevity of africanized honey bees (Hymenoptera: *Apidae*) infested by *Varroa jacobsoni* (Parasitiformes: *Varroidae*). *Journal of Economic Entomology* 76:766-768. https://doi.org/10.1093/jee/76.4.766

De Jong, D; De Jong, PH; Gonçalves, LS (**1982a**) Weight loss and other damage to developing worker honeybees from infestation with *Varroa jacobsoni*. *Journal of Apicultural Research* 21:165-167. https://doi.org/10.1080/00218839.1982.11100535

De Jong, D; Morse, RA; Eickwort, GC (**1982b**) Mite pests of honey bees. *Annual Review of Entomology* 27:229-252. https://doi.org/10.1146/annurev.en.27.010182.001305

De la Rúa, P; Galián, J; Serrano, J; Moritz, RF (**2001**) Genetic structure and distinctness of *Apis mellifera* L. populations from the Canary Islands. *Mol Ecol* 10:1733-1742. https://www.ncbi.nlm.nih.gov/pubmed/11472540

De la Rúa, P; Jaffe, R; Dall'Olio, R; Muñoz, I; Serrano, J (**2009**) Biodiversity, conservation and current threats to European honeybees. *Apidologie* 40:263-284. https://doi.org/10.1051/apido/2009027

De la Rúa, P; Serrano, J; Galián, J (**1998**) Mitochondrial DNA variability in the Canary Islands honeybees (*Apis mellifera* L.). *Molecular Ecology* 7:1543-1547. https://onlinelibrary.wiley.com/doi/abs/10.1046/j.1365-294x.1998.00468.x

de Lillo, E; Di Palma, A; Nuzzaci, G (**2001**) Morphological adaptations of mite chelicerae to different trophic activities (Acari). *Entomologica*. https://doi.org/10.15162/0425-1016/735

de Miranda, JR; Cordoni, G; Budge, G (**2010**) The Acute bee paralysis virus–Kashmir bee virus–Israeli acute paralysis virus complex. *Journal of Invertebrate Pathology* 103:S30-S47. https://doi.org/10.1016/j.jip.2009.06.014

de Miranda, JR; Cornman, RS; Evans, JD; Semberg, E; Haddad, N; Neumann, P; Gauthier, L (**2015**) Genome characterization, prevalence and distribution of a Macula-like virus from *Apis mellifera* and *Varroa destructor*. *Viruses-Basel* 7:3586-3602. https://doi.org/10.3390/v7072789

de Miranda, JR; Genersch, E (**2010**) Deformed wing virus. *Journal of Invertebrate Pathology* 103:S48-S61. https://doi.org/10.1016/j.jip.2009.06.012

Deboutte, W; Beller, L; Yinda, CK; Maes, P; de Graaf, DC; Matthijnssens, J (**2020**) Honey-bee–associated prokaryotic viral communities reveal wide viral diversity and a profound metabolic coding potential. *Proceedings of the National Academy of Sciences* 117:10511-10519. https://doi.org/10.1073/pnas.1921859117

Degrandi-Hoffman, G; Graham, H; Ahumada, F; Smart, M; Ziolkowski, N (**2019**) The economics of honey bee (Hymenoptera: *Apidae*) management and overwintering strategies for colonies used to pollinate almonds. *Journal of Economic Entomology* 112:2524-2533. https://doi.org/10.1093/jee/toz213

Deguines, N; Jono, C; Baude, M; Henry, M; Julliard, R; Fontaine, C (**2014**) Large-scale trade-off between agricultural intensification and crop pollination services. *Frontiers in Ecology and the Environment* 12:212-217. https://doi.org/10.1890/130054

Dekeyser, MA; Downer, RGH (**1994**) Biochemical and physiological targets for miticides. *Pesticide Science* 40:85-101. https://doi.org/10.1002/ps.2780400202

Delaplane, KS; Berry, JA; Skinner, JA; Parkman, JP; Hood, WM (**2005**) Integrated pest management against *Varroa destructor* reduces colony mite levels and delays treatment threshold. *Journal of Apicultural Research* 44:157-162. https://doi.org/10.1080/00218839.2005.11101171

Delaplane, KS; Hood, WM (**1997**) Effects of delayed acaricide treatment in honey bee colonies parasitized by *Varroa jacobsoni* and a late-season treatment threshold for the south-eastern USA. *Journal of Apicultural Research* 36:125-132. https://doi.org/10.1080/00218839.1997.11100938

Delfinado-Baker, M (**1984**) The nymphal stages and male of *Varroa jacobsoni* oudemans a parasite of honey bees. *International Journal of Acarology* 10:75-80. https://doi.org/10.1080/01647958408683356

Delfinado-Baker, M; Aggarwal, K (**1987**) A new Varroa (Acari: *Varroidae*) from the nest of *Apis cerana* (*Apidae*). *International Journal of Acarology* 13:233-237. https://doi.org/10.1080/01647959608684077

Delfinado-Baker, M; Baker, E; Phoon, A (**1989**) Mites (Acari) associated with bees (Apidae) in Asia, with description of a new species. *American bee journal* 129:609-613.

Dempster, J (**1997**) A new version of the Strathclyde Electrophysiology software package running within the Microsoft Windows environment. *Journal of Physiology* 504:P57-P57. http://jp.physoc.org/content/504/P/55P.full.pdf+html

Denholm, I; Rowland, M (**1992**) Tactics for managing pesticide resistance in arthropods: theory and practice. *Annual Review of Entomology* 37:91-112. https://doi.org/10.1146/annurev.en.37.010192.000515

Derst, C; Walther, C; Veh, RW; Wicher, D; Heinemann, SH (**2006**) Four novel sequences in *Drosophila melanogaster* homologous to the auxiliary Para sodium channel subunit TipE. *Biochem Biophys Res Commun* 339:939-948. https://doi.org/10.1016/j.bbrc.2005.11.096

Di Prisco, G; Annoscia, D; Margiotta, M *et al.* (**2016**) A mutualistic symbiosis between a parasitic mite and a pathogenic virus undermines honey bee immunity and health. *Proceedings of the National Academy of Sciences* 113:3203-3208. https://doi.org/10.1073/pnas.1523515113

Di Prisco, G; Pennacchio, F; Caprio, E; Boncristiani, HF, Jr.; Evans, JD; Chen, Y (**2011**) *Varroa destructor* is an effective vector of Israeli acute paralysis virus in the honeybee, *Apis mellifera*. *J Gen Virol* 92:151-155. https://doi.org/10.1099/vir.0.023853-0

Dietemann, V; Beaurepaire, A; Page, P; Yañez, O; Buawangpong, N; Chantawannakul, P; Neumann, P (**2019**) Population genetics of ectoparasitic mites *Varroa* spp. in Eastern and Western honey bees. *Parasitology* 146:1429-1439. https://doi.org/10.1017/S003118201900091X

Dietemann, V; Pflugfelder, J; Anderson, D *et al.* (**2012**) *Varroa destructor*: research avenues towards sustainable control. *Journal of Apicultural Research* 51:125-132. https://doi.org/10.3896/IBRA.1.51.1.15

Dong, K; Du, Y; Rinkevich, F *et al.* (**2014**) Molecular biology of insect sodium channels and pyrethroid resistance. *Insect Biochemistry and Molecular Biology* 50:1-17. https://doi.org/10.1016/j.ibmb.2014.03.012

Dong, K; Scott, JG (**1994**) Linkage of *kdr*-type resistance and the *para*-homologous sodium channel gene in German cockroaches (*Blattella germanica*). *Insect Biochemistry and Molecular Biology* 24:647-654. https://doi.org/10.1016/0965-1748(94)90051-5

Dongol, Y; C. Cardoso, F; Lewis, RJ (**2019**) Spider knottin pharmacology at voltage-gated sodium channels and their potential to modulate pain pathways. *Toxins* 11:626. https://doi.org/10.3390/toxins11110626

Doublet, V; Labarussias, M; de Miranda, JR; Moritz, RFA; Paxton, RJ (**2015**) Bees under stress: sublethal doses of a neonicotinoid pesticide and pathogens interact to elevate honey bee mortality across the life cycle. *Environ Microbiol* 17:969-983. https://doi.org/10.1111/1462-2920.12426

Drescher, W; Schneider, P (**1988**) Effect of the Varroa mite upon the fat body of worker bees and their tolerance of pesticides. Africanized honey bees and bee mites. Chichester, West Sussex, England: E. Horwood, 1988.

Du, Y; Nomura, Y; Liu, Z; Huang, ZY; Dong, K (**2009**) Functional expression of an arachnid sodium channel reveals residues responsible for tetrodotoxin resistance in invertebrate sodium channels. *Journal of Biological Chemistry* 284:33869-33875. https://doi.org/10.1074/jbc.M109.045690

Duay, P; Jong, DD; Engels, W (**2003**) Weight loss in drone pupae (*Apis mellifera*) multiply infested by *Varroa destructor* mites. *Apidologie* 34:61-65. https://doi.org/10.1051/apido:2002052

Dynes, TL; De Roode, JC; Lyons, JI; Berry, JA; Delaplane, KS; Brosi, BJ (**2017**) Fine scale population genetic structure of *Varroa destructor*, an ectoparasitic mite of the honey bee (*Apis mellifera*). *Apidologie* 48:93-101. https://doi.org/10.1007/s13592-016-0453-7

Ebert, D; Fields, PD (**2020**) Host-parasite co-evolution and its genomic signature. *Nature Reviews Genetics* 21:754-768. https://doi.org/10.1038/s41576-020-0269-1

Ebert, TA; Kevan, PG; Bishop, BL; Kevan, SD; Downer, RA (**2007**) Oral toxicity of essential oils and organic acids fed to honey bees (*Apis mellifera*). *Journal of Apicultural Research* 46:220-224. https://doi.org/10.1080/00218839.2007.11101398

Egekwu, NI; Posada, F; Sonenshine, DE; Cook, S (**2018**) Using an in vitro system for maintaining *Varroa destructor* mites on *Apis mellifera* pupae as hosts: Studies of mite longevity and feeding behavior. *Experimental and Applied Acarology*. https://doi.org/10.1007/s10493-018-0236-0

Eguaras, M; Palacio, MA; Faverin, C; Basualdo, M; Del Hoyo, ML; Velis, G; Bedascarrasbure, E (**2003**) Efficacy of formic acid in gel for Varroa control in *Apis mellifera* L.: importance of the dispenser position inside the hive. *Veterinary Parasitology* 111:241-245. https://doi.org/10.1016/S0304-4017(02)00377-1

Eischen, F (**1998**) Trials (and tribulatons) with formic acid for Varroa control. *American bee journal* 138:734-735.

Elliott, M (**1976**) Properties and applications of pyrethroids. *Environmental Health Perspectives* 14:3-13. https://doi.org/10.2307/3428357

Elliott, M (**1977**) Synthetic Pyrethroids. In: Synthetic Pyrethroids, vol 42. ACS Symposium Series, vol 42. American Chemical Society, pp 1-28. https://doi.org/10.1021/bk-1977-0042.ch001

Elliott, M (**1989**) The pyrethroids: Early discovery, recent advances and the future. *Pesticide Science* 27:337-351. https://doi.org/10.1002/ps.2780270403

Elliott, M; Farnham, AW; Janes, NF; Needham, PH; Pulman, DA (**1973a**) Potent pyrethroid insecticides from modified cyclopropane acids. *Nature* 244:456-457. https://doi.org/10.1038/244456a0

Elliott, M; Farnham, AW; Janes, NF; Needham, PH; Pulman, DA; Stevenson, JH (**1973b**) A photostable pyrethroid. *Nature* 246:169-170. https://doi.org/10.1038/246169a0

Elliott, M; Janes, NF (**1978**) Synthetic pyrethroids – a new class of insecticide. *Chemical Society Reviews* 7:473-505. https://doi.org/10.1039/CS9780700473

Ellis, JD; Evans, JD; Pettis, J (**2010**) Colony losses, managed colony population decline, and Colony Collapse Disorder in the United States. *Journal of Apicultural Research* 49:134-136. https://doi.org/10.3896/IBRA.1.49.1.30

Ellis, M; Nelson, R; Simonds, C (**1988**) A comparison of the fluvalinate and ether roll methods of sampling for Varroa mites in honey bee colonies. *American bee journal* 128:262-263.

Elzen, PJ; Baxter, JR; Spivak, M; Wilson, WT (**1999a**) Amitraz resistance in Varroa: New discovery in North America. *American bee journal* 139:362-362.

Elzen, PJ; Baxter, JR; Spivak, M; Wilson, WT (**2000**) Control of *Varroa jacobsoni* Oud. resistant to fluvalinate and amitraz using coumaphos. *Apidologie* 31:437-441. https://doi.org/10.1051/apido:2000134

Elzen, PJ; Eischen, FA; Baxter, JB; Pettis, J; Elzen, GW; Wilson, WT (**1998**) Fluvalinate resistance in *Varroa jacobsoni* from several geographic locations. *American bee journal* 138:674-676.

Elzen, PJ; Eischen, FA; Baxter, JR; Elzen, GW; Wilson, WT (**1999b**) Detection of resistance in US *Varroa jacobsoni* Oud. (Mesostigmata: *Varroidae*) to the acaricide fluvalinate. *Apidologie* 30:13-17. https://doi.org/10.1051/apido:19990102

EPA (**1975**) DTT: A review of scientific and economic aspects of the decision to ban its use as a pesticide. https://www.nal.usda.gov/exhibits/speccoll/items/show/2236

Erban, T; Sopko, B; Kadlikova, K; Talacko, P; Harant, K (**2019**) *Varroa destructor* parasitism has a greater effect on proteome changes than the deformed wing virus and activates TGF-β signaling pathways. *Scientific reports* 9:9400. https://doi.org/10.1038/s41598-019-45764-1

Evans, JD; Cook, SC (**2018**) Genetics and physiology of Varroa mites. *Current Opinion in Insect Science* 26:130-135. https://doi.org/10.1016/j.cois.2018.02.005

Evans, JD; Schwarz, RS; Chen, YP *et al.* (**2013**) Standard methods for molecular research in *Apis mellifera*. *Journal of Apicultural Research* 52:1-54. https://doi.org/10.3896/IBRA.1.52.4.11

Fakhimzadeh, K; Ellis, JD; Hayes, JW (**2011**) Physical control of Varroa mites (*Varroa destructor*): the effects of various dust materials on Varroa mite fall from adult honey bees (*Apis mellifera*) *in vitro*. *Journal of Apicultural Research* 50:203-211. https://doi.org/10.3896/IBRA.1.50.3.04

Farjamfar, M; Saboori, A; González-Cabrera, J; Hernández Rodríguez, CS (**2018**) Genetic variability and pyrethroid susceptibility of the parasitic honey bee mite *Varroa destructor* (Acari: *Varroidae*) in Iran. *Experimental and Applied Acarology* 76:139-148. https://doi.org/10.1007/s10493-018-0296-1

Feldman, DH; Lossin, C (**2014**) The Nav channel bench series: Plasmid preparation. *MethodsX* 1:6-11. https://doi.org/10.1016/j.mex.2014.01.002

Feng, G; Deak, P; Chopra, M; Hall, LM (**1995**) Cloning and functional analysis of TipE, a novel membrane protein that enhances Drosophila *para* sodium channel function. *Cell* 82:1001-1011. https://doi.org/10.1016/0092-8674(95)90279-1

ffrench-Constant, RH; Devonshire, AL (**1987**) A multiple homogenizer for rapid sample preparation in immunoassays and electrophoresis. *Biochemical Genetics* 25:493-499. https://doi.org/10.1007/BF00554351

ffrench-Constant, RH; Williamson, MS; Davies, TGE; Bass, C (**2016**) Ion channels as insecticide targets. *Journal of Neurogenetics* 30:163-177. https://doi.org/10.1080/01677063.2016.1229781

Field, LM; Emyr Davies, TG; O'Reilly, AO; Williamson, MS; Wallace, BA (**2017**) Voltage-gated sodium channels as targets for pyrethroid insecticides. *European Biophysics Journal* 46:675-679. https://doi.org/10.1007/s00249-016-1195-1

Finley, J; Camazine, S; Frazier, M (**1996**) The epidemic of honey bee colony losses during the 1995-1996 season. *American bee journal* 136:805-808.

Flint, ML (**2012**) IPM in Practice, 2nd Edition: Principles and Methods of Integrated Pest Management. University of California Agriculture and Natural Resources.

Fontaine, S; Caddoux, L; Brazier, C; Bertho, C; Bertolla, P; Micoud, A; Roy, L (**2011**) Uncommon associations in target resistance among French populations of *Myzus persicae* from oilseed rape crops. *Pest Management Science* 67:881-885. https://doi.org/10.1002/ps.2224

Francis, RM; Nielsen, SL; Kryger, P (**2013**) Varroa-Virus interaction in collapsing honey bee colonies. *PLOS ONE* 8:e57540. https://doi.org/10.1371/journal.pone.0057540

Free, JB (**1993**) Insect pollination of crops. vol Ed. 2. Academic press.

Frey, E; Rosenkranz, P (**2014**) Autumn invasion rates of *Varroa destructor* (Mesostigmata: *Varroidae*) into honey bee (Hymenoptera: *Apidae*) colonies and the resulting increase in mite populations. *Journal of Economic Entomology* 107:508-515. https://doi.org/10.1603/EC13381

Frey, E; Schnell, H; Rosenkranz, P (**2011**) Invasion of *Varroa destructor* mites into mite-free honey bee colonies under the controlled conditions of a military training area. *Journal of Apicultural Research* 50:138-144. https://doi.org/10.3896/IBRA.1.50.2.05

Fries, I; Rosenkranz, P (**1996**) Number of reproductive cycles of Varroa jacobsoni in honey-bee (Apis mellifera) colonies. *Experimental & Applied Acarology* 20:103-112. https://doi.org/10.1007/BF00051156

Fuchs, S; Langenbach, K (**1989**) Density-dependent reproduction of *Varroa jacobsoni* Oud. and impact on population growth. In: Cavalloro, R (ed) Present status of varroatosis in Europe and progress in the Varroa mite control, Luxembourg. Commission of the European communities, pp 125-130. https://op.europa.eu/en/publication-detail/-/publication/aa02d54a-65bf-4c8b-823a-67068534499a

Fujiyuki, T; Ohka, S; Takeuchi, H; Ono, M; Nomoto, A; Kubo, T (**2006**) Prevalence and phylogeny of Kakugo virus, a novel insect picorna-like virus that infects the honeybee (*Apis mellifera* L.), under various colony conditions. *Journal of Virology* 80:11528-11538. https://doi.org/10.1128/JVI.00754-06

Furutani, K; Kurachi, Y (**2012**) Heterologous expression systems and analyses of ion channels. In: Okada, Y (ed) Patch Clamp Techniques: From Beginning to Advanced Protocols. Springer Japan, Tokyo, pp 353-370. https://doi.org/10.1007/978-4-431-53993-3_23

Gajendiran, A; Abraham, J (**2018**) An overview of pyrethroid insecticides. *Frontiers in Biology* 13:79-90. https://doi.org/10.1007/s11515-018-1489-z

Gajic, B; Radulovic, Z; Stevanovic, J; Kulisic, Z; Vucicevic, M; Simeunovic, P; Stanimirovic, Z (**2013**) Variability of the honey bee mite *Varroa destructor* in Serbia, based on mtDNA analysis. *Experimental and Applied Acarology* 61:97-105. https://doi.org/10.1007/s10493-013-9683-9

Gallai, N; Salles, J-M; Settele, J; Vaissière, BE (**2009**) Economic valuation of the vulnerability of world agriculture confronted with pollinator decline. *Ecological Economics* 68:810-821. http://doi.org/10.1016/j.ecolecon.2008.06.014

Gammon, DW; Brown, MA; Casida, JE (**1981**) Two classes of pyrethroid action in the cockroach. *Pesticide Biochemistry and Physiology* 15:181-191. https://doi.org/10.1016/0048-3575(81)90084-5

Garrido, C; Rosenkranz, P; Paxton, RJ; Gonçalves, LS (**2003**) Temporal changes in *Varroa destructor* fertility and haplotype in Brazil. *Apidologie* 34:535-541. https://doi.org/10.1051/apido:2003041

Gauthier, L; Cornman, S; Hartmann, U; Cousserans, F; Evans, JD; De Miranda, JR; Neumann, P (**2015**) The *Apis mellifera* filamentous virus genome. *Viruses* 7:3798-3815. https://doi.org/10.3390/v7072798

Gauthier, L; Tentcheva, D; Tournaire, M; Dainat, B; Cousserans, F; Colin, ME; Bergoin, M (**2007**) Viral load estimation in asymptomatic honey bee colonies using the quantitative RT-PCR technique. *Apidologie* 38:426-435. https://doi.org/10.1051/apido:2007026

Gauthier, N; Clouet, C; Perrakis, A; Kapantaidaki, D; Peterschmitt, M; Tsagkarakou, A (**2014**) Genetic structure of *Bemisia tabaci* Med populations from home-range countries, inferred by nuclear and cytoplasmic markers: impact on the distribution of the insecticide resistance genes. *Pest Management Science* 70:1477-1491. https://doi.org/10.1002/ps.3733

REFERENCES

Geffre, AC; Gernat, T; Harwood, GP *et al.* (**2020**) Honey bee virus causes context-dependent changes in host social behavior. *Proceedings of the National Academy of Sciences* 117:10406-10413. https://doi.org/10.1073/pnas.2002268117

Genersch, E (**2010**) Honey bee pathology: current threats to honey bees and beekeeping. *Applied Microbiology and Biotechnology* 87:87-97. https://doi.org/10.1007/s00253-010-2573-8

Gisder, S; Aumeier, P; Genersch, E (**2009**) Deformed wing virus: replication and viral load in mites (*Varroa destructor*). *Journal of General Virology* 90:463-467. https://doi.org/10.1099/vir.0.005579-0

Gisder, S; Genersch, E (**2017**) Viruses of commercialized insect pollinators. *Journal of Invertebrate Pathology* 147:51-59. https://doi.org/10.1016/j.jip.2016.07.010

Glynne-Jones, A (**2001**) Pyrethrum. *Pesticide Outlook* 12:195-198. https://doi.org/10.1039/B108601B

González-Cabrera, J; Bumann, H; Rodríguez-Vargas, S *et al.* (**2018**) A single mutation is driving resistance to pyrethroids in European populations of the parasitic mite, *Varroa destructor*. *Journal of Pest Science* 91:1137-1144. https://doi.org/10.1007/s10340-018-0968-y

González-Cabrera, J; Davies, TGE; Field, LM; Kennedy, PJ; Williamson, MS (**2013**) An amino acid substitution (L925V) associated with resistance to pyrethroids in *Varroa destructor*. *PLOS ONE* 8:e82941. https://doi.org/10.1371/journal.pone.0082941

González-Cabrera, J; Rodríguez-Vargas, S; Davies, TGE *et al.* (**2016**) Novel Mutations in the voltage-gated sodium channel of pyrethroid-resistant *Varroa destructor* populations from the Southeastern USA. *Plos One* 11:e0155332. http://www.ncbi.nlm.nih.gov/pubmed/27191597

Goodwin, M; Scarrow, S; Taylor, M (**2006**) Supply of and demand for pollination hives in New Zealand. A briefing paper prepared for the Strategic Pollination Group. https://businessdocbox.com/Agriculture/73480992-Supply-of-and-demand-for-pollination-hives-in-new-zealand.html

Gosselin-Badaroudine, P; Chahine, M (**2017**) Biophysical characterization of the *Varroa destructor* Nav1 sodium channel and its affinity for *tau*-fluvalinate insecticide. *FASEB Journal*. https://doi.org/10.1096/fj.201601338R

Gosselin-Badaroudine, P; Moreau, A; Delemotte, L *et al.* (**2015**) Characterization of the honeybee AmNav1 channel and tools to assess the toxicity of insecticides. *Scientific reports* 5:12475. https://doi.org/10.1038/srep12475

Goulson, D; Nicholls, E; Botías, C; Rotheray, EL (**2015**) Bee declines driven by combined stress from parasites, pesticides, and lack of flowers. *Science* 347:1255957. https://doi.org/10.1126/science.1255957

Gracia-Salinas, MJ; Ferrer-Dufol, M; Latorre-Castro, E; Monero-Manera, C; Castillo-Hernández, JA; Lucientes-Curd, J; Peribáñez-López, MA (**2006**) Detection of fluvalinate resistance in *Varroa destructor* in Spanish apiaries. *Journal of Apicultural Research* 45:101-105. https://doi.org/10.1080/00218839.2006.11101326

Greatti, M; Milani, N; Nazzi, F (**1992**) Reinfestation of an acaricide-treated apiary by *Varroa jacobsoni* Oud. *Experimental and Applied Acarology* 16:279-286. https://doi.org/10.1007/BF01218569

Grozinger, CM; Flenniken, ML (**2019**) Bee viruses: Ecology, pathogenicity, and impacts. *Annual Review of Entomology* 64:205-226. https://doi.org/10.1146/annurev-ento-011118-111942

Guan, B; Chen, X; Zhang, H (**2013**) Two-Electrode Voltage Clamp. In: Gamper, N (ed) Ion Channels: Methods and Protocols. Humana Press, Totowa, NJ, pp 79-89. https://doi.org/10.1007/978-1-62703-351-0_6

Guengerich, FP (**2020**) A history of the roles of cytochrome P450 enzymes in the toxicity of drugs. *Toxicological Research*:1-23. https://doi.org/10.1007/s43188-020-00056-z

Gunjima, K; Sato, K (**1992**) Oral toxicities of some pyrethroids to the housefly, *Musca domestica* L.(Diptera:*Muscidae*). *Applied Entomology and Zoology* 27:319-324. https://doi.org/10.1303/aez.27.319

Guzmán-Novoa, E; Eccles, L; Calvete, Y; McGowan, J; Kelly, PG; Correa-Benítez, A (**2010**) *Varroa destructor* is the main culprit for the death and reduced populations of overwintered honey bee (*Apis mellifera*) colonies in Ontario, Canada. *Apidologie* 41:443-450. https://doi.org/10.1051/apido/2009076

Guzman-Novoa, E; Emsen, B; Unger, P; Espinosa-Montaño, LG; Petukhova, T (**2012**) Genotypic variability and relationships between mite infestation levels, mite damage, grooming intensity, and removal of *Varroa destructor* mites in selected strains of worker honey bees (*Apis mellifera* L.). *Journal of Invertebrate Pathology* 110:314-320. https://doi.org/10.1016/j.jip.2012.03.020

Haber, AI; Steinhauer, NA; vanEngelsdorp, D (**2019**) Use of chemical and nonchemical methods for the control of *Varroa destructor* (Acari: *Varroidae*) and associated winter colony losses in U.S. beekeeping operations. *Journal of Economic Entomology* 112:1509-1525. https://doi.org/10.1093/jee/toz088

240

Haddi, K; Berger, M; Bielza, P *et al.* (**2012**) Identification of mutations associated with pyrethroid resistance in the voltage-gated sodium channel of the tomato leaf miner (*Tuta absoluta*). *Insect Biochemistry and Molecular Biology* 42:506-513. https://doi.org/10.1016/j.ibmb.2012.03.008

Hafi, A; Millist, N; Morey, K; Caley, P; Buetre, B (**2012**) A benefit-cost framework for responding to an incursion of *Varroa destructor*. Australian Bureau of Agricultural and Resource Economics and Sciences, https://www.awe.gov.au/abares/research-topics/biosecurity/biosecurity-economics/benefit-cost-framework-responding-varroa

Harris, JW; Harbo, JR (**2000**) Changes in reproduction of *Varroa destructor* after honey bee queens were exchanged between resistant and susceptible colonies. *Apidologie* 31:689-699. https://doi.org/10.1051/apido:2000153

Häußermann, CK; Giacobino, A; Munz, R; Ziegelmann, B; Palacio, MA; Rosenkranz, P (**2020**) Reproductive parameters of female *Varroa destructor* and the impact of mating in worker brood of *Apis mellifera*. *Apidologie* 51:342-355. https://doi.org/10.1007/s13592-019-00713-9

Häußermann, CK; Ziegelmann, B; Bergmann, P; Rosenkranz, P (**2015**) Male mites (*Varroa destructor*) perceive the female sex pheromone with the sensory pit organ on the front leg tarsi. *Apidologie* 46:771-778. https://doi.org/10.1007/s13592-015-0367-9

Häußermann, CK; Ziegelmann, B; Rosenkranz, P (**2016**) Spermatozoa capacitation in female *Varroa destructor* and its influence on the timing and success of female reproduction. *Experimental and Applied Acarology* 69:371-387. https://doi.org/10.1007/s10493-016-0051-4

Hernández-Rodríguez, CS; Marín, Ó; Calatayud, F *et al.* (**2021**) Large-scale monitoring of resistance to coumaphos, amitraz, and pyrethroids in *Varroa destructor*. *Insects* 12:27. https://doi.org/10.3390/insects12010027

Higes, M; Martín-Hernández, R; Hernández-Rodríguez, CS; González-Cabrera, J (**2020**) Assessing the resistance to acaricides in *Varroa destructor* from several Spanish locations. *Parasitology research* 119:3595-3601. https://doi.org/10.1007/s00436-020-06879-x

Hillesheim, E; Ritter, W; Bassand, D (**1996**) First data on resistance mechanisms of *Varroa jacobsoni* (Oud.) against tau-fluvalinate. *Experimental and Applied Acarology* 20:283-296. https://doi.org/10.1007/BF00052878

Højland, DH; Nauen, R; Foster, SP; Williamson, MS; Kristensen, M (**2015**) Incidence, spread and mechanisms of pyrethroid resistance in european populations of the cabbage stem flea beetle, *Psylliodes chrysocephala* L. (Coleoptera: *Chrysomelidae*). *PLOS ONE* 10:e0146045. https://doi.org/10.1371/journal.pone.0146045

Houck, M; OConnor, B (**1991**) Ecological and evolutionary significance of phoresy in the Astigmata. *Annual Review of Entomology* 36:611-636. https://doi.org/10.1146/annurev.en.36.010191.003143

Huang, Z-Y; Robinson, GE (**1996**) Regulation of honey bee division of labor by colony age demography. *Behav Ecol Sociobiol* 39:147-158. https://doi.org/10.1007/s002650050276

Hubert, J; Nesvorna, M; Kamler, M; Kopecky, J; Tyl, J; Titera, D; Stara, J (**2014**) Point mutations in the sodium channel gene conferring *tau*-fluvalinate resistance in *Varroa destructor*. *Pest Management Science* 70:889-894. https://doi.org/10.1002/ps.3679

Hung, K-LJ; Kingston, JM; Albrecht, M; Holway, DA; Kohn, JR (**2018**) The worldwide importance of honey bees as pollinators in natural habitats. *Proceedings of the Royal Society B: Biological Sciences* 285:20172140. https://doi.org/10.1098/rspb.2017.2140

Hunt, G; Given, JK; Tsuruda, JM; Andino, GK (**2016**) Breeding mite-biting bees to control Varroa. vol 8. https://www.beeculture.com/breeding-mite-biting-bees-to-control-varroa/

Ifantidis, M (**1983**) Ontogenesis of the mite *Varroa jacobsoni* in worker and drone honeybee brood cells. *Journal of Apicultural Research* 22:200-206. https://doi.org/10.1080/00218839.1983.11100588

Ifantidis, MD (**1988**) Some aspects of the process of *Varroa jacobsoni* mite entrance into honey bee (*Apis mellifera*) brood cells. *Apidologie* 19:387-396. https://doi.org/10.1051/apido:19880406

Ilias, A; Vontas, J; Tsagkarakou, A (**2014**) Global distribution and origin of target site insecticide resistance mutations in *Tetranychus urticae*. *Insect Biochemistry and Molecular Biology* 48:17-28. https://doi.org/10.1016/j.ibmb.2014.02.006

Imdorf, A; Bogdanov, S; Ochoa, R, Ibáñez; Calderone, N, W. (**1999**) Use of essential oils for the control of *Varroa jacobsoni* Oud. in honey bee colonies. *Apidologie* 30:209-228. https://doi.org/10.1051/apido:19990210

Iwasaki, JM; Barratt, BIP; Lord, JM; Mercer, AR; Dickinson, KJM (**2015**) The New Zealand experience of Varroa invasion highlights research opportunities for Australia. *Ambio* 44:694-704. https://doi.org/10.1007/s13280-015-0679-z

REFERENCES

Jack, CJ; Ellis, JD (**2021**) Integrated pest management control of *Varroa destructor* (Acari: *Varroidae*), the most damaging pest of (*Apis mellifera* L. (Hymenoptera: *Apidae*)) colonies. *Journal of Insect Science* 21:6. https://doi.org/10.1093/jisesa/ieab058

Jiménez, JJ; Bernal, JL; del Nozal, MJ; Martín, MT (**2005**) Residues of organic contaminants in beeswax. *European Journal of Lipid Science and Technology* 107:896-902. https://doi.org/10.1002/ejlt.200500284

Johnson, RM; Ellis, MD; Mullin, CA; Frazier, M (**2010**) Pesticides and honey bee toxicity – USA. *Apidologie* 41:312-331. https://doi.org/10.1051/apido/2010018

Johnson, RM; Wen, Z; Schuler, MA; Berenbaum, MR (**2006**) Mediation of pyrethroid insecticide toxicity to honey bees (Hymenoptera: *Apidae*) by cytochrome P450 monooxygenases. *Journal of economic entomology* 99:1046-1050. https://doi.org/10.1603/0022-0493-99.4.1046

Jouraku, A; Kuwazaki, S; Iida, H *et al.* (**2019**) T929I and K1774N mutation pair and M918L single mutation identified in the voltage-gated sodium channel gene of pyrethroid-resistant *Thrips tabaci* (Thysanoptera: *Thripidae*) in Japan. *Pesticide Biochemistry and Physiology* 158:77-87. https://doi.org/10.1016/j.pestbp.2019.04.012

Kachel, HS; Patel, RN; Franzyk, H; Mellor, IR (**2016**) Block of nicotinic acetylcholine receptors by philanthotoxins is strongly dependent on their subunit composition. *Scientific reports* 6:38116. https://doi.org/10.1038/srep38116

Kaleta, C; Schäuble, S; Rinas, U; Schuster, S (**2013**) Metabolic costs of amino acid and protein production in *Escherichia coli*. *Biotechnology Journal* 8:1105-1114. https://doi.org/10.1002/biot.201200267

Kamler, M; Nesvorna, M; Stara, J; Erban, T; Hubert, J (**2016**) Comparison of *tau*-fluvalinate, acrinathrin, and amitraz effects on susceptible and resistant populations of *Varroa destructor* in a vial test. *Experimental and Applied Acarology* 69:1-9. https://doi.org/10.1007/s10493-016-0023-8

Kanbar, G; Engels, W (**2004**) Visualisation by vital staining with trypan blue of wounds punctured by *Varroa destructor* mites in pupae of the honey bee (*Apis mellifera*). *Apidologie* 35:25-29. https://doi.org/10.1051/apido:2003057

Kanbar, G; Engels, W (**2005**) Communal use of integumental wounds in honey bee (*Apis mellifera*) pupae multiply infested by the ectoparasitic mite *Varroa destructor*. Genet Mol Res 4:465-472. https://geneticsmr.com/articles/190

Kapantaidaki, DE; Sadikoglou, E; Tsakireli, D *et al.* (**2018**) Insecticide resistance in *Trialeurodes vaporariorum* populations and novel diagnostics for *kdr* mutations. *Pest Management Science* 74:59-69. https://doi.org/10.1002/ps.4674

Karatolos, N; Gorman, K; Williamson, MS; Denholm, I (**2012**) Mutations in the sodium channel associated with pyrethroid resistance in the greenhouse whitefly, *Trialeurodes vaporariorum*. *Pest Management Science* 68:834-838. https://doi.org/10.1002/ps.2334

Katsavou, E; Vlogiannitis, S; Karp-Tatham, E *et al.* (**2020**) Identification and geographical distribution of pyrethroid resistance mutations in the poultry red mite *Dermanyssus gallinae*. *Pest Management Science* 76:125-133. https://doi.org/10.1002/ps.5582

Katsuda, Y (**1975**) LTD.(patent for fluvalinate development). Sumitomo Chemical Co Patent,

Katsuda, Y (**2012**) Progress and Future of Pyrethroids. In: Matsuo, N, Mori, T (eds) Pyrethroids: From chrysanthemum to modern industrial insecticide. Springer Berlin Heidelberg, Berlin, Heidelberg, pp 1-30. https://doi.org/10.1007/128_2011_252

Kearse, M; Moir, R; Wilson, A *et al.* (**2012**) Geneious Basic: an integrated and extendable desktop software platform for the organization and analysis of sequence data. *Bioinformatics (Oxford, England)* 28:1647-1649. https://doi.org/10.1093/bioinformatics/bts199

Kelley, LA; Mezulis, S; Yates, CM; Wass, MN; Sternberg, MJE (**2015**) The Phyre2 web portal for protein modeling, prediction and analysis. *Nature Protocols* 10:845-858. https://doi.org/10.1038/nprot.2015.053

Kelomey, AE; Paraiso, A; Sina, H; Legout, H; Garnery, L; Baba-Moussa, L (**2017**) Genetic characterization of the honeybee ectoparasitic mite *Varroa destructor* from Benin (West Africa) using mitochondrial and microsatellite markers. *Experimental and Applied Acarology* 72:61-67. https://doi.org/10.1007/s10493-017-0141-y

Khambay, BPS; Jewess, PJ (**2005**) 6.1 - Pyrethroids. In: Gilbert, LI (ed) Comprehensive Molecular Insect Science. Elsevier, Amsterdam, pp 1-29. https://doi.org/10.1016/B0-44-451924-6/00075-2

Kim, W; Lee, M; Han, S *et al.* (**2009**) A geographical polymorphism in a Voltage-Gated Sodium Channel gene in the mite, *Varroa destructor*, from Korea. *Korean Journal of Apiculture* 24:159-165.

Klatt, BK; Holzschuh, A; Westphal, C; Clough, Y; Smit, I; Pawelzik, E; Tscharntke, T (**2014**) Bee pollination improves crop quality, shelf life and commercial value. *Proceedings of the Royal Society B: Biological Sciences* 281. https://doi.org/10.1098/rspb.2013.2440

Klein, A-M; Vaissière, BE; Cane, JH; Steffan-Dewenter, I; Cunningham, SA; Kremen, C; Tscharntke, T (**2007**) Importance of pollinators in changing landscapes for world crops. *Proceedings of the Royal Society B: Biological Sciences* 274:303-313. https://doi.org/10.1098/rspb.2006.3721

Kliot, A; Ghanim, M (**2012**) Fitness costs associated with insecticide resistance. *Pest Management Science* 68:1431-1437. https://doi.org/10.1002/ps.3395

Koç, N; İnak, E; Jonckheere, W; Van Leeuwen, T (**2021**) Genetic analysis and screening of pyrethroid resistance mutations in *Varroa destructor* populations from Turkey. *Experimental and Applied Acarology*. https://doi.org/10.1007/s10493-021-00626-2

Koeniger, G; Koeniger, N; Anderson, DL; Lekprayoon, C; Tingek, S (**2002**) Mites from debris and sealed brood cells of *Apis dorsata* colonies in Sabah (Borneo) Malaysia, including a new haplotype of *Varroa jacobsoni*. *Apidologie* 33:15-24. https://doi.org/10.1051/apido:2001005

Kostaropoulos, I; Papadopoulos, AI; Metaxakis, A; Boukouvala, E; Papadopoulou-Mourkidou, E (**2001**) Glutathione S-transferase in the defence against pyrethroids in insects. *Insect Biochemistry and Molecular Biology* 31. https://doi.org/10.1016/S0965-1748(00)00123-5

Kralj, J; Fuchs, S (**2006**) Parasitic *Varroa destructor* mites influence flight duration and homing ability of infested *Apis mellifera* foragers. *Apidologie* 37:577-587. https://doi.org/10.1051/apido:2006040

Kremen, C; Williams, NM; Thorp, RW (**2002**) Crop pollination from native bees at risk from agricultural intensification. *Proceedings of the National Academy of Sciences* 99:16812-16816. https://doi.org/10.1073/pnas.262413599

Kuenen, L; Calderone, N (**1997**) Transfers of Varroa mites from newly emerged bees: Preferences for age- and function-specific adult bees (Hymenoptera: *Apidae*). *Journal of Insect Behavior* 10:213-228. https://doi.org/10.1007/BF02765554

Kulhanek, K; Steinhauer, N; Rennich, K *et al.* (**2017**) A national survey of managed honey bee 2015–2016 annual colony losses in the USA. *Journal of Apicultural Research* 56:328-340. https://doi.org/10.1080/00218839.2017.1344496

Lee, SH; Gao, J-R; Sup Yoon, K *et al.* (**2003**) Sodium channel mutations associated with knockdown resistance in the human head louse, *Pediculus capitis* (De Geer). *Pesticide Biochemistry and Physiology* 75:79-91. https://doi.org/10.1016/S0048-3575(03)00018-X

Lee, SH; Smith, TJ; Knipple, DC; Soderlund, DM (**1999**) Mutations in the house fly Vssc1 sodium channel gene associated with super-*kdr* resistance abolish the pyrethroid sensitivity of Vssc1/tipE sodium channels expressed in *Xenopus oocytes*. *Insect Biochemistry and Molecular Biology* 29:185-194. https://doi.org/10.1016/S0965-1748(98)00122-2

Leoncini, I; Crauser, D; Robinson, GE; Le Conte, Y (**2004a**) Worker-worker inhibition of honey bee behavioural development independent of queen and brood. *Insectes Sociaux* 51:392-394. https://doi.org/10.1007/s00040-004-0757-x

Leoncini, I; Le Conte, Y; Costagliola, G *et al.* (**2004b**) Regulation of behavioral maturation by a primer pheromone produced by adult worker honey bees. *Proceedings of the National Academy of Sciences* 101:17559-17564. https://doi.org/10.1073/pnas.0407652101

Letunic, I; Bork, P (**2019**) Interactive Tree Of Life (iTOL) v4: recent updates and new developments. *Nucleic Acids Research* 47:W256-W259. https://doi.org/10.1093/nar/gkz239

Levin, S; Galbraith, D; Sela, N; Erez, T; Grozinger, CM; Chejanovsky, N (**2017**) Presence of Apis Rhabdovirus-1 in Populations of Pollinators and Their Parasites from Two Continents. *Frontiers in Microbiology* 8:2482. https://doi.org/10.3389/fmicb.2017.02482

Levin, S; Sela, N; Erez, T; Nestel, D; Pettis, J; Neumann, P; Chejanovsky, N (**2019**) New viruses from the ectoparasite mite *Varroa destructor* infesting *Apis mellifera* and *Apis cerana*. *Viruses* 11. https://doi.org/10.3390/v11020094

Li, AY; Cook, SC; Sonenshine, DE *et al.* (**2019a**) Insights into the feeding behaviors and biomechanics of Varroa destructor mites on honey bee pupae using electropenetrography and histology. *Journal of Insect Physiology* 119:103950. https://doi.org/10.1016/j.jinsphys.2019.103950

Li, C (**2021**) Understanding, Conservation, and Protection of Precious Natural Resources: Bees. In: Environmental and Natural Resources Engineering. Springer, pp 1-51.

Li, J; Waterhouse, RM; Zdobnov, EM (**2011**) A remarkably stable TipE gene cluster: evolution of insect *Para* sodium channel auxiliary subunits. *BMC Evolutionary Biology* 11:337. https://doi.org/10.1186/1471-2148-11-337

REFERENCES

Li, JL; Cornman, RS; Evans, JD *et al.* (**2014**) Systemic spread and propagation of a plant-pathogenic virus in European honeybees, *Apis mellifera*. *mBio* 5:e00898-00813. https://doi.org/10.1128/mBio.00898-13

Li, W; Wang, C; Huang, ZY; Chen, Y; Han, R (**2019b**) Reproduction of distinct *Varroa destructor* genotypes on honey bee worker brood. *Insects* 10. https://doi.org/10.3390/insects10110372

Liman, ER; Tytgat, J; Hess, P (**1992**) Subunit stoichiometry of a mammalian K+ channel determined by construction of multimeric cDNAs. *Neuron* 9:861-871. https://doi.org/10.1016/0896-6273(92)90239-a

Lin, Z; Qin, Y; Page, P *et al.* (**2018**) Reproduction of parasitic mites *Varroa destructor* in original and new honeybee hosts. *Ecology and Evolution* 8:2135-2145. https://doi.org/10.1002/ece3.3802

Lipiński, Z; Szubstarski, J; Szubstarska, D (**2007**) Detection of the high risk pyrethroid resistant *Varroa destructor* mites in apiaries of the Warmia-Mazury province in Poland. *Wiad Parazytol* 53:245-249.

Liu, Z; Tan, J; Huang, ZY; Dong, K (**2006**) Effect of a fluvalinate-resistance-associated sodium channel mutation from varroa mites on cockroach sodium channel sensitivity to fluvalinate, a pyrethroid insecticide. *Insect Biochem Mol Biol* 36:885-889. https://doi.org/10.1016/j.ibmb.2006.08.006

Locke, B; Semberg, E; Forsgren, E; de Miranda, JR (**2017**) Persistence of subclinical deformed wing virus infections in honeybees following Varroa mite removal and a bee population turnover. *PLOS ONE* 12:e0180910. https://doi.org/10.1371/journal.pone.0180910

Locke, B; Thaduri, S; Stephan, JG *et al.* (**2021**) Adapted tolerance to virus infections in four geographically distinct *Varroa destructor*-resistant honeybee populations. *Scientific reports* 11:12359. https://doi.org/10.1038/s41598-021-91686-2

Locke, M (**1980**) The cell biology of fat body development. In: Locke, M, Smith, DS (eds) Insect Biology in the Future. Academic Press, pp 227-252. https://doi.org/10.1016/B978-0-12-454340-9.50015-X

Lodesani, M; Colombo, M; Spreafico, M (**1995**) Ineffectiveness of Apistan® treatment against the mite *Varroa jacobsoni* Oud in several districts of Lombardy (Italy). *Apidologie* 26:67-72. https://doi.org/10.1051/apido:19950109

Lodesani, M; Costa, C; Serra, G; Colombo, R; Sabatini, AG (**2008**) Acaricide residues in beeswax after conversion to organic beekeeping methods. *Apidologie* 39:324-333. https://doi.org/10.1051/apido:2008012

Loglio, G; Plebani, G (**1992**) Valutazione dell'efficacia dell'Apistan. *Apic Mod* 83:95-98.

Lombet, A; Mourre, C; Lazdunski, M (**1988**) Interaction of insecticides of the pyrethroid family with specific binding sites on the voltage-dependent sodium channel from mammalian brain. *Brain research* 459:44-53. https://doi.org/10.1016/0006-8993(88)90284-3

Lucas, ER; Rockett, KA; Lynd, A *et al.* (**2019**) A high throughput multi-locus insecticide resistance marker panel for tracking resistance emergence and spread in *Anopheles gambiae*. *Scientific reports* 9:13335. https://doi.org/10.1038/s41598-019-49892-6

Lynd, A; Oruni, A; Van't Hof, AE *et al.* (**2018**) Insecticide resistance in *Anopheles gambiae* from the northern Democratic Republic of Congo, with extreme *knockdown* resistance (*kdr*) mutation frequencies revealed by a new diagnostic assay. *Malar J* 17:412. https://doi.org/10.1186/s12936-018-2561-5

Macedo, P; Ellis, M; Siegfried, B (**2002**) Detection and quantincation of fluvalinate resistance in Varroa mites in Nebraska. *American bee journal* 142:523-526.

MacKenzie, TDB; Arju, I; Poirier, R; Singh, M (**2018**) A genetic survey of pyrethroid insecticide resistance in aphids in New Brunswick, Canada, with particular emphasis on aphids as vectors of Potato virus Y. *J Econ Entomol* 111:1361-1368. https://doi.org/10.1093/jee/toy035

Maggi, MD; Ruffinengo, SR; Damiani, N; Sardella, NH; Eguaras, MJ (**2009**) First detection of *Varroa destructor* resistance to coumaphos in Argentina. *Experimental and Applied Acarology* 47:317-320. https://doi.org/10.1007/s10493-008-9216-0

Maggi, MD; Ruffinengo, SR; Negri, P; Eguaras, MJ (**2010**) Resistance phenomena to amitraz from populations of the ectoparasitic mite *Varroa destructor* of Argentina. *Parasitology research* 107:1189-1192. https://doi.org/10.1007/s00436-010-1986-8

Major, KM; Weston, DP; Lydy, MJ; Wellborn, GA; Poynton, HC (**2018**) Unintentional exposure to terrestrial pesticides drives widespread and predictable evolution of resistance in freshwater crustaceans. *Evolutionary Applications* 11:748-761. https://doi.org/10.1111/eva.12584

Martin, SJ (**1994**) Ontogenesis of the mite *Varroa jacobsoni* Oud. in worker brood of the honeybee *Apis mellifera* L. under natural conditions. *Experimental and Applied Acarology* 18:87-100. https://doi.org/10.1007/BF00055033

Martin, SJ (**1998**) A population model for the ectoparasitic mite *Varroa jacobsoni* in honey bee (*Apis mellifera*) colonies. *Ecological Modelling* 109:267-281. https://doi.org/10.1016/S0304-3800(98)00059-3

Martin, SJ (**2004**) Acaricide (pyrethroid) resistance in *Varroa destructor. Bee World* 85:67-69. https://doi.org/10.1080/0005772X.2004.11099632

Martin, SJ; Highfield, AC; Brettell, L *et al.* (**2012**) Global honey bee viral landscape altered by a parasitic mite. *Science* 336:1304-1306. https://doi.org/10.1126/science.1220941

Martins, AJ; Valle, D (**2012**) The pyrethroid knockdown resistance. In: Soloneski, DS (ed) Insecticides - Basic and Other Applications. IntechOpen, pp 17 - 38. https://doi.org/10.5772/30588

Martins, JR; Nunes, FMF; Simões, ZLP; Bitondi, MMG (**2008**) A honeybee storage protein gene, hex 70a, expressed in developing gonads and nutritionally regulated in adult fat body. *Journal of Insect Physiology* 54:867-877. https://doi.org/10.1016/j.jinsphys.2008.03.009

Matsuo, N (**2019**) Discovery and development of pyrethroid insecticides. *Proc Jpn Acad Ser B Phys Biol Sci* 95:378-400. https://doi.org/10.2183/pjab.95.027

McGregor, SE (**1976**) Insect pollination of cultivated crop plants. https://www.ars.usda.gov/ARSUserFiles/20220500/OnlinePollinationHandbook.pdf

McMahon, DP; Furst, MA; Caspar, J; Theodorou, P; Brown, MJF; Paxton, RJ (**2015**) A sting in the spit: widespread cross-infection of multiple RNA viruses across wild and managed bees. *J Anim Ecol* 84:615-624. https://doi.org/10.1111/1365-2656.12345

McMenamin, AJ; Flenniken, ML (**2018**) Recently identified bee viruses and their impact on bee pollinators. *Current Opinion in Insect Science* 26:120-129. https://doi.org/10.1016/j.cois.2018.02.009

McMenamin, AJ; Genersch, E (**2015**) Honey bee colony losses and associated viruses. *Current Opinion in Insect Science* 8:121-129. https://doi.org/10.1016/j.cois.2015.01.015

Milani, N (**1993**) Possible presence of fluvalinate-resistant strains of *Varroa jacobsoni* in northern Italy. New perspectives on Varroa. In: International Bee Research Association, Prague. Proceedings of the International Meeting, Cardiff, United Kingdom, p p. 87.

Milani, N (**1995**) The resistance of *Varroa jacobsoni* Oud to pyrethroids: a laboratory assay. *Apidologie* 26:415-429. https://doi.org/10.1051/apido:19950507

Milani, N (**1999**) The resistance of *Varroa jacobsoni* Oud. to acaricides. *Apidologie* 30:229-234. https://doi.org/10.1051/apido:19990211

Milani, N; Della Vedova, G (**2002**) Decline in the proportion of mites resistant to fluvalinate in a population of *Varroa destructor* not treated with pyrethroids. *Apidologie* 33:417-422. https://doi.org/10.1051/apido:2002028

Millán-Leiva, A; Marín, Ó; Christmon, K; van Engelsdorp, D; González-Cabrera, J (**2021a**) Mutations associated with pyrethroid resistance in Varroa mite, a parasite of honey bees, are widespread across the USA. *Pest Management Science* n/a. https://doi.org/10.1002/ps.6366

Millán-Leiva, A; Marín, Ó; Rúa, PDl *et al.* (**2021b**) Mutations associated with pyrethroid resistance in the honey bee parasite *Varroa destructor* evolved as a series of parallel and sequential events. *Journal of Pest Science*:1-13. https://doi.org/10.1007/s10340-020-01321-8

Miozes-Koch, R; Slabezki, Y; Efrat, H; Kalev, H; Kamer, Y; Yakobson; Dag, A (**2000**) First detection in Israel of fluvalinate resistance in the Varroa mite using bioassay and biochemical methods. *Experimental and Applied Acarology* 24:35-43. https://doi.org/10.1023/a:1006379114942

Mitton, GA; Quintana, S; Mendoza, Y; Eguaras, M; Maggi, MD; Ruffinengo, SR (**2021**) L925V mutation in voltage-gated sodium channel of *Varroa destructor* populations from Argentina and Uruguay, with different degree of susceptibility to pyrethroids. *International Journal of Acarology* 47:374-380. https://doi.org/10.1080/01647954.2021.1914158

Mizrahi, A; Lensky, Y (**2013**) Bee products: properties, applications, and apitherapy. Springer Science & Business Media.

Morais, MM; Francoy, TM; Pereira, RA; De Jong, D; Gonçalves, LS (**2009**) Africanized honey bees are efficient at detecting, uncapping and removing dead brood. *Genet Mol Res* 8:718-724. https://doi.org/10.4238/vol8-2kerr020

Morgan, JAT; Corley, SW; Jackson, LA; Lew-Tabor, AE; Moolhuijzen, PM; Jonsson, NN (**2009**) Identification of a mutation in the *para*-sodium channel gene of the cattle tick *Rhipicephalus* (*Boophilus*) *microplus* associated with resistance to synthetic pyrethroid acaricides. *International Journal for Parasitology* 39:775-779. https://doi.org/10.1016/j.ijpara.2008.12.006

Morin, S; Williamson, MS; Goodson, SJ; Brown, JK; Tabashnik, BE; Dennehy, TJ (**2002**) Mutations in the *Bemisia tabaci* para sodium channel gene associated with resistance to a pyrethroid plus

REFERENCES

organophosphate mixture. *Insect Biochemistry and Molecular Biology* 32:1781-1791. https://doi.org/10.1016/S0965-1748(02)00137-6

Mozes-Koch, R; Slabezki, Y; Efrat, H; Kalev, H; Kamer, Y; Yakobson, BA; Dag, A (**2000**) First detection in Israel of fluvalinate resistance in the Varroa mite using bioassay and biochemical methods. *Experimental and Applied Acarology* 24:35-43. https://doi.org/10.1023/A:1006379114942

Muñoz, I; Cepero, A; Pinto, MA; Martín-Hernández, R; Higes, M; De la Rúa, P (**2014**) Presence of *Nosema ceranae* associated with honeybee queen introductions. *Infection, Genetics and Evolution* 23:161-168. https://doi.org/10.1016/j.meegid.2014.02.008

Muñoz, I; Garrido-Bailón, E; Martín-Hernández, R; Meana, A; Higes, M; De la Rúa, P (**2008**) Genetic profile of *Varroa destructor* infesting *Apis mellifera* iberiensis colonies. *Journal of Apicultural Research* 47:310-313. https://doi.org/10.1080/00218839.2008.11101480

Muñoz, I; Pinto, MA; De la Rúa, P (**2013**) Temporal changes in mitochondrial diversity highlights contrasting population events in Macaronesian honey bees. *Apidologie* 44:295-305. https://doi.org/10.1007/s13592-012-0179-0

Musa-Aziz, R; Boron, WF; Parker, MD (**2010**) Using fluorometry and ion-sensitive microelectrodes to study the functional expression of heterologously-expressed ion channels and transporters in *Xenopus oocytes*. *Methods* 51:134-145. https://doi.org/10.1016/j.ymeth.2009.12.012

Mutinelli, F (**2016**) Veterinary medicinal products to control *Varroa destructor* in honey bee colonies (*Apis mellifera*) and related EU legislation – an update. *Journal of Apicultural Research* 55:78-88. https://doi.org/10.1080/00218839.2016.1172694

Nakayama, I; Koh-Ichiaketa, N; Suzuki, Y; Kato, T; Yoshioka, H (**1979**) Chemistry, absolute structures and biological aspect of the most active isomers of fenvalerate and other recent pyrethroids. In: Synthesis of pesticides chemical structure and biological activity natural products with biological activity. Elsevier, pp 174-181.

Nasuti, C; Cantalamessa, F; Falcioni, G; Gabbianelli, R (**2003**) Different effects of Type I and Type II pyrethroids on erythrocyte plasma membrane properties and enzymatic activity in rats. *Toxicology* 191:233-244. https://doi.org/10.1016/s0300-483x(03)00207-5

National Research Council (**2007**) Status of pollinators in North America. The National Academies Press, Washington, DC. https://doi.org/10.17226/11761

Navajas, M; Anderson, DL; de Guzman, LI; Huang, ZY; Clement, J; Zhou, T; Le Conte, Y (**2010**) New Asian types of *Varroa destructor*: a potential new threat for world apiculture. *Apidologie* 41:181-193. https://doi.org/10.1051/apido/2009068

Nazzi, F; Brown, SP; Annoscia, D *et al.* (**2012**) Synergistic parasite-pathogen interactions mediated by host immunity can drive the collapse of honeybee colonies. *PLOS Pathogens* 8:e1002735. https://doi.org/10.1371/journal.ppat.1002735

Nee, S (**1989**) Antagonistic co-evolution and the evolution of genotypic randomization. *Journal of Theoretical Biology* 140:499-518. https://doi.org/10.1016/s0022-5193(89)80111-0

Neumann, P; Carreck, NL (**2010**) Honey bee colony losses. *Journal of Apicultural Research* 49:1-6. https://doi.org/10.3896/IBRA.1.49.1.01

Nilsen, K-A; Ihle, KE; Frederick, K; Fondrk, MK; Smedal, B; Hartfelder, K; Amdam, GV (**2011**) Insulin-like peptide genes in honey bee fat body respond differently to manipulation of social behavioral physiology. *Journal of Experimental Biology* 214:1488-1497. https://doi.org/10.1242/jeb.050393

O'Reilly, AO; Khambay, BPS; Williamson, MS; Field, LM; Wallace, BA; Davies, TGE (**2006**) Modelling insecticide-binding sites in the voltage-gated sodium channel. *Biochemical Journal* 396:255-263. https://doi.org/10.1042/BJ20051925

O'Reilly, AO; Williamson, MS; González-Cabrera, J; Turberg, A; Field, LM; Wallace, BA; Davies, TGE (**2014**) Predictive 3D modelling of the interactions of pyrethroids with the voltage-gated sodium channels of ticks and mites. *Pest Management Science* 70:369-377. https://doi.org/10.1002/ps.3561

Octaviano-Salvadé, CE; Leher, CE; De Jong, D; Pinto, PM; Delgado-Cañedo, A; Boldo, JT (**2017**) A scientific note on genetic profile of the mite *Varroa destructor* infesting apiaries in Rio Grande do Sul state, Brazil. *Apidologie* 48:621-622. https://doi.org/10.1007/s13592-017-0504-8

Ogihara, MH; Kobayashi, E; Morimoto, N; Yoshiyama, M; Kimura, K (**2021**) Molecular analysis of voltage-gated sodium channels to assess τ-fluvalinate resistance in Japanese populations of *Varroa destructor* (Acari: *Varroidae*). *Applied Entomology and Zoology* 56:277-284. https://doi.org/10.1007/s13355-020-00717-3

Ohno, N; Fujimoto, K; Okuno, Y *et al.* (**1976**) 2-arylalkanoates, a new group of synthetic pyrethroid esters not containing cyclopropanecarboxylates. *Pesticide Science* 7:241-246. https://doi.org/10.1002/ps.2780070306

Oldroyd, BP (**1999**) Coevolution while you wait: *Varroa jacobsoni*, a new parasite of western honeybees. *Trends Ecol Evol* 14:312-315. https://doi.org/10.1016/s0169-5347(99)01613-4

Oldroyd, BP (**2007**) What's killing American honey bees? *PLOS Biology* 5:e168. https://doi.org/10.1371/journal.pbio.0050168

Oliveira, EE; Du, Y; Nomura, Y; Dong, K (**2013**) A residue in the transmembrane segment 6 of domain I in insect and mammalian sodium channels regulate differential sensitivities to pyrethroid insecticides. *Neurotoxicology* 38:42-50. https://doi.org/10.1016/j.neuro.2013.06.001

Olivier, V; Blanchard, P; Chaouch, S *et al.* (**2008**) Molecular characterisation and phylogenetic analysis of Chronic bee paralysis virus, a honey bee virus. *Virus Res* 132:59-68. https://doi.org/10.1016/j.virusres.2007.10.014

Ongus, JR; Peters, D; Bonmatin, JM; Bengsch, E; Vlak, JM; van Oers, MM (**2004**) Complete sequence of a picorna-like virus of the genus Iflavirus replicating in the mite *Varroa destructor*. *Journal of General Virology* 85:3747-3755. https://doi.org/10.1099/vir.0.80470-0

Oppenoorth, F (**1985**) Biochemistry and genetics of insecticide resistance. *Comprehensive Insect Physiology Biochemistry and Pharmacology: Insect Control* 12:731-733. https://doi.org/10.1016/0048-3575(84)90088-9

Orantes-Bermejo, FJ; Pajuelo, AG; Megías, MM; Fernández-Píñar, CT (**2010**) Pesticide residues in beeswax and beebread samples collected from honey bee colonies (*Apis mellifera* L.) in Spain. Possible implications for bee losses. *Journal of Apicultural Research* 49:243-250. https://doi.org/10.3896/IBRA.1.49.3.03

Otis, GW; Kralj, J (**2001**) Parasitic brood mites not present in North America.

Oudemans, AC (**1904**) On a new genus and species of parasitic acari. https://repository.naturalis.nl/pub/508650

Page, P; Lin, Z; Buawangpong, N *et al.* (**2016**) Social apoptosis in honey bee superorganisms. *Scientific reports* 6:27210. https://doi.org/10.1038/srep27210

Panini, M; Dradi, D; Marani, G; Butturini, A; Mazzoni, E (**2014**) Detecting the presence of target-site resistance to neonicotinoids and pyrethroids in Italian populations of *Myzus persicae*. *Pest Management Science* 70:931-938. https://doi.org/10.1002/ps.3630

Panini, M; Reguzzi, MC; Chiesa, O; Cominelli, F; Lupi, D; Moores, G; Mazzoni, E (**2019**) Pyrethroid resistance in Italian populations of the mite *Varroa destructor*: a focus on the Lombardy region. *Bulletin of Insectology* 72:227 - 232. http://www.bulletinofinsectology.org/pdfarticles/vol72-2019-227-232panini.pdf

Paterson, S; Vogwill, T; Buckling, A *et al.* (**2010**) Antagonistic coevolution accelerates molecular evolution. *Nature* 464:275-278. https://doi.org/10.1038/nature08798

Pauron, D; Barhanin, J; Amichot, M; Pralavorio, M; Berge, JB; Lazdunski, M (**1989**) Pyrethroid receptor in the insect sodium channel: alteration of its properties in pyrethroid-resistant flies. *Biochemistry* 28:1673-1677. https://doi.org/10.1021/bi00430a037

Peck, DT; Seeley, TD (**2019**) Mite bombs or robber lures? The roles of drifting and robbing in *Varroa destructor* transmission from collapsing honey bee colonies to their neighbors. *PLOS ONE* 14:e0218392. https://doi.org/10.1371/journal.pone.0218392

Peck, DT; Smith, ML; Seeley, TD (**2016**) *Varroa destructor* mites can nimbly climb from flowers onto foraging honey bees. *PLOS ONE* 11:e0167798. https://doi.org/10.1371/journal.pone.0167798

Peng, Y-S; Fang, Y; Xu, S; Ge, L (**1987**) The resistance mechanism of the Asian honey bee, *Apis cerana* Fabr., to an ectoparasitic mite, *Varroa jacobsoni* Oudemans. *Journal of Invertebrate Pathology* 49:54-60. https://doi.org/10.1016/0022-2011(87)90125-X

Perry, CJ; Søvik, E; Myerscough, MR; Barron, AB (**2015**) Rapid behavioral maturation accelerates failure of stressed honey bee colonies. *Proceedings of the National Academy of Sciences* 112:3427-3432. https://doi.org/10.1073/pnas.1422089112

Pettis, JS (**2004**) A scientific note on *Varroa destructor* resistance to coumaphos in the United States. *Apidologie* 35:91-92. https://doi.org/10.1051/apido:2003060

Pietropaoli, M; Formato, G (**2019**) Acaricide efficacy and honey bee toxicity of three new formic acid-based products to control *Varroa destructor*. *Journal of Apicultural Research* 58:824-830. https://doi.org/10.1080/00218839.2019.1656788

REFERENCES

Pinto, J; Lynd, A; Vicente, JL *et al.* (**2007**) Multiple origins of knockdown resistance mutations in the Afrotropical mosquito vector *Anopheles gambiae*. *PLOS ONE* 2:e1243. https://doi.org/10.1371/journal.pone.0001243

Posada-Florez, F; Childers, AK; Heerman, MC *et al.* (**2019**) Deformed wing virus type A, a major honey bee pathogen, is vectored by the mite Varroa destructor in a non-propagative manner. *Scientific reports* 9:12445. https://doi.org/10.1038/s41598-019-47447-3

Potts, SG; Imperatriz-Fonseca, V; Ngo, HT *et al.* (**2016**) Safeguarding pollinators and their values to human well-being. *Nature* 540:220-229. https://doi.org/10.1038/nature20588

Potts, SG; Roberts, SPM; Dean, R *et al.* (**2010**) Declines of managed honey bees and beekeepers in Europe. *J Apicult Res* 49:15-22.

Pritchard, DJ (**2016**) Grooming by honey bees as a component of Varroa resistant behavior. *Journal of Apicultural Research* 55:38-48. https://doi.org/10.1080/00218839.2016.1196016

Rambaut, A; Drummond, AJ; Xie, D; Baele, G; Suchard, MA (**2018**) Posterior summarization in bayesian phylogenetics using Tracer 1.7. *Systematic Biology* 67:901-904. https://doi.org/10.1093/sysbio/syy032

Ramsey, S; Gulbronson, CJ; Mowery, J; Ochoa, R; vanEngelsdorp, D; Bauchan, G (**2018**) A multi-microscopy approach to discover the feeding site and host tissue consumed by *Varroa destructor* on host honey bees. *Microscopy and Microanalysis* 24:1258-1259. https://doi.org/10.1017/S1431927618006773

Ramsey, SD; Ochoa, R; Bauchan, G *et al.* (**2019**) *Varroa destructor* feeds primarily on honey bee fat body tissue and not hemolymph. *Proceedings of the National Academy of Sciences* 116:1792-1801. https://doi.org/10.1073/pnas.1818371116

Rath, W (**1999**) Co-adaptation of *Apis cerana* Fabr. and *Varroa jacobsoni* Oud. *Apidologie* 30:97-110. https://doi.org/10.1051/apido:19990202

Ratnieks, FLW; Carreck, NL (**2010**) Clarity on Honey Bee Collapse? *Science* 327:152-153. https://doi.org/10.1126/science.1185563

Ray, DE; Forshaw, PJ (**2000**) Pyrethroid insecticides: poisoning syndromes, synergies, and therapy. *Journal of Toxicology: Clinical Toxicology* 38:95-101. https://doi.org/10.1081/clt-100100922

Reeves, G; Cutler, H (**2005**) Future directions for the Australian honey bee industry. https://honeybee.org.au/pdf/CIE_FINAL_REPORT.pdf

Rehm, S; Ritter, W (**1989**) Succession and time of development of male and female offspring of *Varroa jacobsoni* in the worker brood. Paper presented at the Working Group in the Apicultural Institutes in Western Germany, Freiburg, https://www.apidologie.org/articles/apido/pdf/1989/06/Apidologie_0044-8435_1989_20_6_ART0005.pdf

Remnant, EJ; Shi, M; Buchmann, G; Blacquière, T; Holmes, EC; Beekman, M; Ashe, A (**2017**) A diverse range of novel RNA viruses in geographically distinct honey bee populations. *Journal of Virology* 91. https://doi.org/10.1128/jvi.00158-17

Richards, EH; Jones, B; Bowman, A (**2011**) Salivary secretions from the honeybee mite, *Varroa destructor*: effects on insect haemocytes and preliminary biochemical characterization. *Parasitology* 138:602-608. https://doi.org/10.1017/s0031182011000072

Richter, A; Steuber, S (**2010**) Antiparasitica. *Lehrbuch der Pharmakologie und Toxikologie* 3.

Rinderer, T; De Guzman, L; Sylvester, HA (**2004**) Re-examination of the accuracy of a detergent solution for varroa mite detection. *American bee journal* 144:560-562.

Rinderer, TE; Harris, JW; Hunt, GJ; De Guzman, LI (**2010**) Breeding for resistance to *Varroa destructor* in North America. *Apidologie* 41:409-424. https://doi.org/10.1051/apido/2010015

Rinkevich, FD (**2020**) Detection of amitraz resistance and reduced treatment efficacy in the Varroa Mite, *Varroa destructor*, within commercial beekeeping operations. *PLOS ONE* 15:e0227264. https://doi.org/10.1371/journal.pone.0227264

Rinkevich, FD; Du, Y; Dong, K (**2013**) Diversity and convergence of sodium channel mutations involved in resistance to pyrethroids. *Pesticide biochemistry and physiology* 106:93-100. https://doi.org/10.1016/j.pestbp.2013.02.007

Rinkevich, FD; Hedtke, SM; Leichter, CA *et al.* (**2012a**) Multiple origins of *kdr-type* resistance in the house fly, *Musca domestica*. *PLOS ONE* 7:e52761. https://doi.org/10.1371/journal.pone.0052761

Rinkevich, FD; Su, C; Lazo, TA; Hawthorne, DJ; Tingey, WM; Naimov, S; Scott, JG (**2012b**) Multiple evolutionary origins of knockdown resistance (*kdr*) in pyrethroid-resistant Colorado potato beetle, *Leptinotarsa decemlineata*. *Pesticide Biochemistry and Physiology* 104:192-200. https://doi.org/10.1016/j.pestbp.2012.08.001

Riveron, JM; Irving, H; Ndula, M; Barnes, KG; Ibrahim, SS; Paine, MJ; Wondji, CS (**2013**) Directionally selected cytochrome P450 alleles are driving the spread of pyrethroid resistance in the major malaria vector *Anopheles funestus*. *Proceedings of the National Academy of Sciences* 110. https://doi.org/10.1073/pnas.1216705110

Roberts, JMK; Anderson, DL; Durr, PA (**2017**) Absence of deformed wing virus and *Varroa destructor* in Australia provides unique perspectives on honeybee viral landscapes and colony losses. *Scientific reports* 7:6925. https://www.ncbi.nlm.nih.gov/pubmed/28761114

Roberts, JMK; Anderson, DL; Tay, WT (**2015**) Multiple host shifts by the emerging honeybee parasite, *Varroa jacobsoni*. *Molecular Ecology* 24:2379-2391. https://doi.org/10.1111/mec.13185

Roberts, JMK; Simbiken, N; Dale, C; Armstrong, J; Anderson, DL (**2020**) Tolerance of honey bees to Varroa mite in the absence of Deformed wing virus. *Viruses* 12. https://doi.org/10.3390/v12050575

Robinson, GE (**1987**) Regulation of honey bee age polyethism by juvenile hormone. *Behav Ecol Sociobiol* 20:329-338. https://doi.org/10.1007/BF00300679

Rodríguez-Dehaibes, SR; Otero-Colina, G; Sedas, VP; Jiménez, JAV (**2005**) Resistance to amitraz and flumethrin in *Varroa destructor* populations from Veracruz, Mexico. *J Apicult Res* 44:124-125.

Rosario-Cruz, R; Guerrero, FD; Miller, RJ *et al.* (**2009**) Molecular survey of pyrethroid resistance mechanisms in Mexican field populations of *Rhipicephalus* (*Boophilus*) *microplus*. *Parasitology research* 105:1145-1153. https://doi.org/10.1007/s00436-009-1539-1

Rosenkranz, P; Aumeier, P; Ziegelmann, B (**2010**) Biology and control of *Varroa destructor*. *J Invertebr Pathol* 103 Suppl 1:S96-119. https://doi.org/10.1016/j.jip.2009.07.016

Ross, MK (**2011**) Pyrethroids. In: Nriagu, JO (ed) Encyclopedia of Environmental Health. Elsevier, Burlington, pp 702-708. https://doi.org/10.1016/B978-0-444-52272-6.00608-5

Rossignol, D (**1988**) Reduction in number of nerve membrane sodium channels in pyrethroid resistant house flies. *Pesticide Biochemistry and Physiology* 32:146-152. https://doi.org/10.1016/0048-3575(88)90007-7

Roth, MA; Wilson, JM; Tignor, KR; Gross, AD (**2020**) Biology and management of *Varroa destructor* (Mesostigmata: *Varroidae*) in *Apis mellifera* (Hymenoptera: *Apidae*) colonies. *Journal of Integrated Pest Management* 11. https://doi.org/10.1093/jipm/pmz036

Rozas, J; Ferrer-Mata, A; Sánchez-DelBarrio, JC; Guirao-Rico, S; Librado, P; Ramos-Onsins, SE; Sánchez-Gracia, A (**2017**) DnaSP 6: DNA sequence polymorphism analysis of large data sets. *Molecular Biology and Evolution* 34:3299-3302. https://doi.org/10.1093/molbev/msx248

Rucker, RR; Thurman, WN; Burgett, M (**2012**) Honey bee pollination markets and the internalization of reciprocal benefits. *American Journal of Agricultural Economics* 94:956-977. https://doi.org/10.1093/ajae/aas031

Rucker, RR; Thurman, WN; Burgett, M (**2019**) Colony collapse and the consequences of bee disease: market adaptation to environmental change. *Journal of the Association of Environmental and Resource Economists* 6:927-960. https://doi.org/10.1086/704360

Ruttner, F; Ritter, W (**1980**) The spread of *Varroa jacobsoni* into Europe–in retrospect. *Allgemeine Deutsche Imkerzeitung* 14:130-134.

Sakai, T; Okada, I (**1973**) Present beekeeping in Japan. *Gleanings in bee culture*.

Sammataro, D; Gerson, U; Needham, G (**2000**) Parasitic mites of honey bees: Life history, implications, and impact. *Annual Review of Entomology* 45:519-548. https://doi.org/10.1146/annurev.ento.45.1.519

Sammataro, D; Untalan, P; Guerrero, F; Finley, J (**2005**) The resistance of Varroa mites (Acari : *Varroidae*) to acaricides and the presence of esterase. *International Journal of Acarology* 31:67-74. https://doi.org/10.1080/01647950508684419

Samnegård, U; Hambäck, PA; Smith, HG (**2019**) Pollination treatment affects fruit set and modifies marketable and storable fruit quality of commercial apples. *Royal Society Open Science* 6:190326. https://doi.org/10.1098/rsos.190326

Sanders, HJ; Taff, AW (**1954**) Staff-industry collaborative report allethrin. *Industrial & Engineering Chemistry* 46:414-426. https://doi.org/10.1021/ie50531a018

Santillán-Galicia, MT; Ball, BV; Clark, SJ; Alderson, PG (**2010**) Transmission of Deformed wing virus and Slow paralysis virus to adult bees (*Apis mellifera* L.) by *Varroa destructor*. *Journal of Apicultural Research* 49:141-148. https://doi.org/10.3896/IBRA.1.49.2.01

Santillán-Galicia, MT; Ball, BV; Clark, SJ; Alderson, PG (**2014**) Slow bee paralysis virus and its transmission in honey bee pupae by *Varroa destructor*. *Journal of Apicultural Research* 53:146-154. https://doi.org/10.3896/IBRA.1.53.1.16

Schäfer, MO; Cardaio, I; Cilia, G *et al.* (**2019**) How to slow the global spread of small hive beetles, Aethina tumida. *Biological Invasions* 21:1451-1459. https://doi.org/10.1007/s10530-019-01917-x

Schechter, MS; Green, N; LaForge, F (**1949**) Constituents of pyrethrum flowers. XXIII. Cinerolone and the synthesis of related cyclopentenolones. *Journal of the American Chemical Society* 71:3165-3173. https://doi.org/10.1021/ja01177a065

Schmidt, JO (**1997**) Bee products. In: Bee Products. Springer, pp 15-26.

Seeley, TD (**1989**) The Honey Bee Colony as a Superorganism. *American Scientist* 77:546-553. https://doi.org/10.2307/27856005

Shen, M; Cui, L; Ostiguy, N; Cox-Foster, D (**2005a**) Intricate transmission routes and interactions between picorna-like viruses (Kashmir bee virus and Sacbrood virus) with the honeybee host and the parasitic Varroa mite. *Journal of General Virology* 86:2281-2289. https://doi.org/10.1099/vir.0.80824-0

Shen, M; Yang, X; Cox-Foster, D; Cui, L (**2005b**) The role of Varroa mites in infections of Kashmir bee virus (KBV) and Deformed wing virus (DWV) in honey bees. *Virology* 342:141-149. https://doi.org/10.1016/j.virol.2005.07.012

Shimanuki, H; Calderone, N; Knox, D (**1994**) Parasitic mite syndrome: the symptoms. *American bee journal*.

Shin, TM; Smith, RD; Toro, L; Goldin, AL (**1998**) [29] High-level expression and detection of ion channels in *Xenopus oocytes*. In: Methods in Enzymology, vol 293. Academic Press, pp 529-556. https://doi.org/10.1016/S0076-6879(98)93032-4

Simone-Finstrom, M; Li-Byarlay, H; Huang, MH; Strand, MK; Rueppell, O; Tarpy, DR (**2016**) Migratory management and environmental conditions affect lifespan and oxidative stress in honey bees. *Scientific reports* 6:32023. https://doi.org/10.1038/srep32023

Smith, TJ; Lee, SH; Ingles, PJ; Knipple, DC; Soderlund, DM (**1997**) The L1014F point mutation in the house fly Vssc1 sodium channel confers knockdown resistance to pyrethroids. *Insect Biochemistry and Molecular Biology* 27:807-812. https://doi.org/10.1016/s0965-1748(97)00065-9

Soderlund, DM (**2005**) 5.1 - Sodium Channels. In: Gilbert, LI (ed) Comprehensive Molecular Insect Science. Elsevier, Amsterdam, pp 1-24. https://doi.org/10.1016/B0-44-451924-6/00068-5

Soderlund, DM; Clark, JM; Sheets, LP *et al.* (**2002**) Mechanisms of pyrethroid neurotoxicity: implications for cumulative risk assessment. *Toxicology* 171:3-59. https://doi.org/10.1016/S0300-483X(01)00569-8

Soderlund, DM; Hessney, CW; Helmuth, DW (**1983**) Pharmacokinetics of cis-and trans-substituted pyrethroids in the American cockroach. *Pesticide Biochemistry and Physiology* 20:161-168. https://doi.org/10.1016/0048-3575(79)90092-0

Solignac, M; Cornuet, JM; Vautrin, D *et al.* (**2005**) The invasive Korea and Japan types of *Varroa destructor*, ectoparasitic mites of the Western honeybee (*Apis mellifera*), are two partly isolated clones. *Proceedings of the Royal Society B: Biological Sciences* 272:411-419. https://doi.org/10.1098/rspb.2004.2853

Solignac, M; Vautrin, D; Pizzo, A; Navajas, M; Le Conte, Y; Cornuet, J-M (**2003**) Characterization of microsatellite markers for the apicultural pest *Varroa destructor* (Acari: *Varroidae*) and its relatives. *Molecular Ecology Notes* 3:556-559. https://doi.org/10.1046/j.1471-8286.2003.00510.x

Song, W; Liu, Z; Tan, J; Nomura, Y; Dong, K (**2004**) RNA editing generates tissue-specific sodium channels with distinct gating properties. *Journal of Biological Chemistry* 279:32554-32561. https://doi.org/10.1074/jbc.M402392200

Southwick, EE; Southwick, JL (**1992**) Estimating the economic value of honey bees (Hymenoptera: *Apidae*) as agricultural pollinators in the United States. *Journal of Economic Entomology* 85:621-633. https://doi.org/10.1093/jee/85.3.621

Sparks, TC; Nauen, R (**2015**) IRAC: Mode of action classification and insecticide resistance management. *Pesticide Biochemistry and Physiology* 121:122-128. https://doi.org/10.1016/j.pestbp.2014.11.014

Standley, DM; Katoh, K (**2013**) MAFFT multiple sequence alignment software version 7: Improvements in performance and usability. *Molecular Biology and Evolution* 30:772-780. https://doi.org/10.1093/molbev/mst010

Stanimirović, Z; Glavinić, U; Ristanić, M; Aleksić, N; Jovanović, N; Vejnović, B; Stevanović, J (**2019**) Looking for the causes of and solutions to the issue of honey bee colony losses. *Acta Veterinaria-Beograd* 69:1-31. https://doi.org/10.2478/acve-2019-0001

Stara, J; Pekar, S; Nesvorna, M *et al.* (**2019a**) Detection of *tau*-fluvalinate resistance in the mite *Varroa destructor* based on the comparison of vial test and PCR–RFLP of *kdr* mutation in sodium channel gene. *Experimental and Applied Acarology* 77:161-171. https://doi.org/10.1007/s10493-019-00353-9

Stara, J; Pekar, S; Nesvorna, M; Kamler, M; Doskocil, I; Hubert, J (**2019b**) Spatio-temporal dynamics of *Varroa destructor* resistance to *tau*-fluvalinate in Czechia, associated with L925V sodium channel point mutation. *Pest Management Science* 75:1287-1294. https://doi.org/10.1002/ps.5242

Staveley, JP; Law, SA; Fairbrother, A; Menzie, CA (**2014**) A causal analysis of observed declines in managed honey bees (*Apis mellifera*). *Human and Ecological Risk Assessment* 20:566-591. https://doi.org/10.1080/10807039.2013.831263

Steinhauer, N; Kulhanek, K; Antunez, K; Human, H; Chantawannakul, P; Chauzat, MP; vanEngelsdorp, D (**2018**) Drivers of colony losses. *Current Opinion in Insect Science* 26:142-148. https://doi.org/10.1016/j.cois.2018.02.004

Steinhauer, N; vanEngelsdorp, D; Saegerman, C (**2021**) Prioritizing changes in management practices associated with reduced winter honey bee colony losses for US beekeepers. *Science of The Total Environment* 753:141629. https://doi.org/10.1016/j.scitotenv.2020.141629

Stell, I (**2012**) Understanding bee anatomy: a full colour guide. Catford Press.

Stern, V; Smith, R; van den Bosch, R; Hagen, K (**1959**) The integration of chemical and biological control of the spotted alfalfa aphid: the integrated control concept. *Hilgardia* 29:81-101. https://doi.org/10.3733/hilg.v29n02p081

Stevenson, M; Benard, H; Bolger, P; Morris, R (**2005**) Spatial epidemiology of the Asian honey bee mite (*Varroa destructor*) in the North Island of New Zealand. *Preventive veterinary medicine* 71:241-252. https://doi.org/10.1016/j.prevetmed.2005.07.007

Sumpter, DJT; Martin, SJ (**2004**) The dynamics of virus epidemics in Varroa-infested honey bee colonies. *J Anim Ecol* 73:51-63. https://doi.org/10.1111/j.1365-2656.2004.00776.x

Sun, H; Tong, KP; Kasai, S; Scott, JG (**2016**) Overcoming super-*knock down* resistance (super-*kdr*) mediated resistance: multi-halogenated benzyl pyrethroids are more toxic to super-*kdr* than *kdr* house flies. *Insect Molecular Biology* 25:126-137. https://doi.org/10.1111/imb.12206

Sun, W; Shahrajabian, MH; Cheng, Q (**2020**) Pyrethrum an organic and natural pesticide. *Journal of Biological and Environmental Sciences* 14:41-44.

Tan, J; Liu, Z; Nomura, Y; Goldin, AL; Dong, K (**2002**) Alternative splicing of an insect sodium channel gene generates pharmacologically distinct sodium channels. *Journal of Neuroscience* 22:5300-5309. https://doi.org/10.1523/JNEUROSCI.22-13-05300.2002

Tatebayashi, H; Narahashi, T (**1994**) Differential mechanism of action of the pyrethroid tetramethrin on tetrodotoxin-sensitive and tetrodotoxin-resistant sodium channels. *Journal of Pharmacology and Experimental Therapeutics* 270:595-603. https://jpet.aspetjournals.org/content/270/2/595.long

Techer, MA; Rane, RV; Grau, ML *et al.* (**2019**) Divergent evolutionary trajectories following speciation in two ectoparasitic honey bee mites. *Communications Biology* 2:357. https://doi.org/10.1038/s42003-019-0606-0

Thaduri, S; Stephan, JG; de Miranda, JR; Locke, B (**2019**) Disentangling host-parasite-pathogen interactions in a Varroa-resistant honeybee population reveals virus tolerance as an independent, naturally adapted survival mechanism. *Scientific reports* 9:6221. https://doi.org/10.1038/s41598-019-42741-6

Thompson, AJ; Verdin, PS; Burton, MJ *et al.* (**2020**) The effects of knock-down resistance mutations and alternative splicing on voltage-gated sodium channels in *Musca domestica* and *Drosophila melanogaster*. *Insect Biochemistry and Molecular Biology* 122:103388. https://doi.org/10.1016/j.ibmb.2020.103388

Thompson, HM; Brown, MA; Ball, RF; Bew, MH (**2002**) First report of *Varroa destructor* resistance to pyrethroids in the UK. *Apidologie* 33:357-366. https://doi.org/10.1051/apido:2002027

Thrall, PH; Laine, AL; Ravensdale, M; Nemri, A; Dodds, PN; Barrett, LG; Burdon, JJ (**2012**) Rapid genetic change underpins antagonistic coevolution in a natural host-pathogen metapopulation. *Ecology Letters* 15:425-435. https://doi.org/10.1111/j.1461-0248.2012.01749.x

Toth, AL; Robinson, GE (**2005**) Worker nutrition and division of labour in honeybees. *Animal Behaviour* 69:427-435. https://doi.org/10.1016/j.anbehav.2004.03.017

Traynor, KS; Mondet, F; de Miranda, JR *et al.* (**2020**) *Varroa destructor*: a complex parasite, crippling honey bees worldwide. *Trends in Parasitology* 36:592-606. https://doi.org/10.1016/j.pt.2020.04.004

Traynor, KS; Rennich, K; Forsgren, E *et al.* (**2016**) Multiyear survey targeting disease incidence in US honey bees. *Apidologie* 47:325-347. https://doi.org/10.1007/s13592-016-0431-0

Traynor, KS; Tosi, S; Rennich, K *et al.* (**2021**) Pesticides in Honey Bee Colonies: establishing a baseline for real world exposure over seven years in the USA. *Environmental Pollution*:116566. https://doi.org/10.1016/j.envpol.2021.116566

REFERENCES

Trouiller, J (**1998**) Monitoring Varroa jacobsoni resistance to pyrethroids in western Europe. *Apidologie* 29:537-546. https://doi.org/10.1051/apido:19980606

Tseng, TT; McMahon, AM; Johnson, VT; Mangubat, EZ; Zahm, RJ; Pacold, ME; Jakobsson, E (**2007**) Sodium channel auxiliary subunits. *Journal of Molecular Microbiology and Biotechnology* 12:249-262. https://doi.org/10.1159/000099646

Ujihara, K (**2019**) The history of extensive structural modifications of pyrethroids. *J Pestic Sci* 44:215-224. https://doi.org/10.1584/jpestics.D19-102

Ulbricht, W (**2005**) Sodium Channel Inactivation: Molecular Determinants and Modulation. *Physiological Reviews* 85:1271-1301. https://doi.org/10.1152/physrev.00024.2004

Umpiérrez, ML; Santos, E; González, A; Rossini, C (**2011**) Plant essential oils as potential control agents of varroatosis. *Phytochemistry Reviews* 10:227-244. https://doi.org/10.1007/s11101-010-9182-0

Underwood, RM; Currie, RW (**2003**) The effects of temperature and dose of formic acid on treatment efficacy against *Varroa destructor* (Acari: *Varroidae*), a parasite of *Apis mellifera* (Hymenoptera: *Apidae*). *Experimental and Applied Acarology* 29:303. https://doi.org/10.1023/A:1025892906393

Untergasser, A; Cutcutache, I; Koressaar, T; Ye, J; Faircloth, BC; Remm, M; Rozen, SG (**2012**) Primer3-new capabilities and interfaces. *Nucleic Acids Research* 40:e115-e115. https://doi.org/10.1093/nar/gks596

USDA-APHIS (**2020**) National honey bee survey wax pesticide sampling report. Accessed August 2020 https://research.beeinformed.org/state_reports/pesticides_wax/

USDA-NASS (**2020**) Honey bee colonies. https://usda.library.cornell.edu/concern/publications/rn301137d?locale=en

Usherwood, PN; Davies, TG; Mellor, IR *et al.* (**2007**) Mutations in DIIS5 and the DIIS4-S5 linker of *Drosophila melanogaster* sodium channel define binding domains for pyrethroids and DDT. *FEBS Letters* 581:5485-5492. https://doi.org/10.1016/j.febslet.2007.10.057

Vais, H; Atkinson, S; Eldursi, N; Devonshire, AL; Williamson, MS; Usherwood, PNR (**2000a**) A single amino acid change makes a rat neuronal sodium channel highly sensitive to pyrethroid insecticides. *FEBS Letters* 470:135-138. https://doi.org/10.1016/S0014-5793(00)01305-3

Vais, H; Atkinson, S; Pluteanu, F; Goodson, SJ; Devonshire, AL; Williamson, MS; Usherwood, PNR (**2003**) Mutations of the *para* sodium channel of *Drosophila melanogaster* identify putative binding sites for pyrethroids. *Molecular Pharmacology* 64:914-922. https://doi.org/10.1124/mol.64.4.914

Vais, H; Williamson, MS; Devonshire, AL; Usherwood, PNR (**2001**) The molecular interactions of pyrethroid insecticides with insect and mammalian sodium channels. *Pest Management Science* 57:877-888. https://doi.org/10.1002/ps.392

Vais, H; Williamson, MS; Goodson, SJ; Devonshire, AL; Warmke, JW; Usherwood, PN; Cohen, CJ (**2000b**) Activation of Drosophila sodium channels promotes modification by deltamethrin. Reductions in affinity caused by knock-down resistance mutations. *J Gen Physiol* 115:305-318. https://doi.org/10.1085/jgp.115.3.305

van Dooremalen, C; Cornelissen, B; Poleij-Hok-Ahin, C; Blacquière, T (**2018**) Single and interactive effects of *Varroa destructor*, *Nosema* spp., and imidacloprid on honey bee colonies (*Apis mellifera*). *Ecosphere* 9:e02378. https://doi.org/10.1002/ecs2.2378

van Dooremalen, C; Gerritsen, L; Cornelissen, B; van der Steen, JJ; van Langevelde, F; Blacquiere, T (**2012**) Winter survival of individual honey bees and honey bee colonies depends on level of *Varroa destructor* infestation. *PLOS ONE* 7:e36285. https://doi.org/10.1371/journal.pone.0036285

van Dooremalen, C; Stam, E; Gerritsen, L; Cornelissen, B; van der Steen, J; van Langevelde, F; Blacquière, T (**2013**) Interactive effect of reduced pollen availability and *Varroa destructor* infestation limits growth and protein content of young honey bees. *Journal of Insect Physiology* 59:487-493. https://doi.org/10.1016/j.jinsphys.2013.02.006

Vandame, R; Colin, M; Belzunces, LP; Jourdan, P (**1995**) Résistance de Varroa au fluvalinate. *Carnets du CARI*:5-11.

vanEngelsdorp, D; Evans, JD; Saegerman, C *et al.* (**2009**) Colony collapse disorder: a descriptive study. *PLOS ONE* 4:e6481. https://doi.org/10.1371/journal.pone.0006481

vanEngelsdorp, D; Hayes, J, Jr.; Underwood, RM; Pettis, J (**2008**) A survey of honey bee Colony losses in the US, fall 2007 to spring 2008. *PLOS ONE* 3:e4071. https://doi.org/10.1371/journal.pone.0004071

vanEngelsdorp, D; Meixner, MD (**2010**) A historical review of managed honey bee populations in Europe and the United States and the factors that may affect them. *Journal of Invertebrate Pathology* 103 Suppl 1:S80-95. https://doi.org/10.1016/j.jip.2009.06.011

vanEngelsdorp, D; Underwood, R; Caron, D; Hayes, J (**2007**) An estimate of managed colony losses in the winter of 2006 - 2007: A report commissioned by the apiary inspectors of America. *American bee journal*. https://bee-health.extension.org/wp-content/uploads/2019/08/AnEstimateofManagedColonyLossesintheWinterof2006-2007.pdf

Venkatachalan, SP; Bushman, JD; Mercado, JL; Sancar, F; Christopherson, KR; Boileau, AJ (**2007**) Optimized expression vector for ion channel studies in *Xenopus oocytes* and mammalian cells using alfalfa mosaic virus. *Pflugers Archiv - European Journal of Physiology* 454:155-163. https://doi.org/10.1007/s00424-006-0183-1

Verschoyle, RD; Aldridge, WN (**1980**) Structure-activity relationships of some pyrethroids in rats. *Archives of Toxicology* 45:325-329. https://doi.org/10.1007/bf00293813

Voorhies, EC; Galbraith, JK; Todd, FE (**1933**) Economic aspects of the bee industry. vol B555. Agricultural Experiment Station, Berkeley, Calif. https://doi.org/10.5962/bhl.title.61191

Wallberg, A; Han, F; Wellhagen, G *et al.* (**2014**) A worldwide survey of genome sequence variation provides insight into the evolutionary history of the honeybee *Apis mellifera*. *Nature Genetics* 46:1081-1088. https://doi.org/10.1038/ng.3077

Walsh, PS; Metzger, DA; Higuchi, R (**1991**) Chelex 100 as a medium for simple extraction of DNA for PCR-based typing from forensic material. *Biotechniques* 10:506-513. https://doi.org/10.2144/000114018

Wang, K; Bai, J; Zhao, J; Su, S; Liu, L; Han, Z; Chen, M (**2020**) Super-*kdr* mutation M918L and multiple cytochrome P450s associated with the resistance of *Rhopalosiphum padi* to pyrethroid. *Pest Management Science* 76:2809-2817. https://doi.org/10.1002/ps.5829

Wang, L; Du, Y; Nomura, Y; Dong, K (**2015**) Distinct modulating effects of TipE-homologs 2-4 on Drosophila sodium channel splice variants. *Insect Biochemistry and Molecular Biology* 60:24-32. https://doi.org/10.1016/j.ibmb.2015.02.006

Wang, L; Nomura, Y; Du, Y; Dong, K (**2013**) Differential effects of TipE and a TipE-homologous protein on modulation of gating properties of sodium channels from Drosophila melanogaster. *PLOS ONE* 8:e67551. https://doi.org/10.1371/journal.pone.0067551

Wang, R; Huang, ZY; Dong, K (**2003**) Molecular characterization of an arachnid sodium channel gene from the varroa mite (*Varroa destructor*). *Insect Biochem Mol Biol* 33:733-739. http://www.sciencedirect.com/science/article/B6T79-48TM9R9-1/2/9c1214a985a842bf152991407c84d370

Wang, RW; Liu, ZQ; Dong, K; Elzen, PJ; Pettis, J; Huang, ZY (**2002**) Association of novel mutations in a sodium channel gene with fluvalinate resistance in the mite, *Varroa destructor*. *Journal of Apicultural Research* 41:17-25. https://doi.org/10.1080/00218839.2002.11101064

Warmke, JW; Reenan, RA; Wang, P *et al.* (**1997**) Functional expression of Drosophila *para* sodium channels: modulation by the membrane protein tipE and toxin pharmacology. *The Journal of General Physiology* 110:119-133. https://doi.org/10.1085/jgp.110.2.119

Watkins, M (**1997**) Resistance and its relevance to beekeeping. *Bee World* 78:15-22. https://doi.org/10.1080/0005772X.1997.11099327

Wegener, J; Ruhnke, H; Scheller, K; Mispagel, S; Knollmann, U; Kamp, G; Bienefeld, K (**2016**) Pathogenesis of varroosis at the level of the honey bee (*Apis mellifera*) colony. *Journal of Insect Physiology* 91-92:1-9. https://doi.org/10.1016/j.jinsphys.2016.06.004

Wenner, AM; Bushing, WW (**1996**) Varroa mite spread in the United States. *Bee culture* 124:341 - 343. https://www.beesource.com/threads/varroa-mite-spread-in-the-united-states.365462/

Weston, DP; Poynton, HC; Wellborn, GA; Lydy, MJ; Blalock, BJ; Sepulveda, MS; Colbourne, JK (**2013**) Multiple origins of pyrethroid insecticide resistance across the species complex of a nontarget aquatic crustacean, *Hyalella azteca*. *Proceedings of the National Academy of Sciences*:201302023. https://doi.org/10.1073/pnas.1302023110

White, GF (**1913**) Sacbrood, a disease of bees. vol 169. US Government Printing Office.

White, PS; Morran, L; de Roode, J (**2017**) Phoresy. *Current Biology* 27:R578-R580. https://doi.org/10.1016/j.cub.2017.03.073

Whitehead, HR (**2017**) Varroa mite management among small-scale beekeepers: Characterizing factors that affect IPM adoption, and exploring drone brood removal as an IPM tool. The Ohio State University

Wilfert, L; Long, G; Leggett, HC; Schmid-Hempel, P; Butlin, R; Martin, SJM; Boots, M (**2016**) Deformed wing virus is a recent global epidemic in honeybees driven by Varroa mites. *Science* 351:594-597. https://doi.org/10.1126/science.aac9976

Williamson, MS; Denholm, I; Bell, CA; Devonshire, AL (**1993**) Knockdown resistance (*kdr*) to DDT and pyrethroid insecticides maps to a sodium channel gene locus in the housefly (*Musca domestica*). *Molecular and General Genetics MGG* 240:17-22. https://doi.org/10.1007/BF00276878

Williamson, MS; Martinez-Torres, D; Hick, CA; Devonshire, AL (**1996**) Identification of mutations in the housefly *para*-type sodium channel gene associated with knockdown resistance (*kdr*) to pyrethroid insecticides. *Molecular and General Genetics MGG* 252:51-60. https://doi.org/10.1007/BF02173204

Willis, CE; Foster, SP; Zimmer, CT *et al.* (**2020**) Investigating the status of pyrethroid resistance in UK populations of the cabbage stem flea beetle (*Psylliodes chrysocephala*). *Crop Protection* 138:105316. https://doi.org/10.1016/j.cropro.2020.105316

Winston, ML (**1991**) The biology of the honey bee. harvard university press.

Wu, M; Adesanya, AW; Morales, MA; Walsh, DB; Lavine, LC; Lavine, MD; Zhu, F (**2018**) Multiple acaricide resistance and underlying mechanisms in *Tetranychus urticae* on hops. *Journal of Pest Science* 92:543-555. https://doi.org/10.1007/s10340-018-1050-5

Wu, S; Nomura, Y; Du, Y; Zhorov, BS; Dong, K (**2017**) Molecular basis of selective resistance of the bumblebee BiNav1 sodium channel to *tau*-fluvalinate. *Proceedings of the National Academy of Sciences*. https://doi.org/10.1073/pnas.1711699114

Xie, X; Huang, ZY; Zeng, Z (**2016**) Why do Varroa mites prefer nurse bees? *Scientific reports* 6:28228. https://www.ncbi.nlm.nih.gov/pubmed/27302644

Yan, R; Zhou, Q; Xu, Z; Zhu, G; Dong, K; Zhorov, BS; Chen, M (**2020**) Three sodium channel mutations from *Aedes albopictus* confer resistance to Type I, but not Type II pyrethroids. *Insect Biochemistry and Molecular Biology* 123:103411. https://doi.org/10.1016/j.ibmb.2020.103411

Yang, X; Cox-Foster, D (**2007**) Effects of parasitization by *Varroa destructor* on survivorship and physiological traits of *Apis mellifera* in correlation with viral incidence and microbial challenge. *Parasitology* 134:405-412. https://doi.org/10.1017/s0031182006000710

Yañez, O; Piot, N; Dalmon, A *et al.* (**2020**) Bee viruses: Routes of infection in Hymenoptera. *Frontiers in Microbiology* 11. https://doi.org/10.3389/fmicb.2020.00943

Yates, CM; Filippis, I; Kelley, LA; Sternberg, MJE (**2014**) SuSPect: Enhanced prediction of single amino acid variant (SAV) phenotype using network features. *Journal of Molecular Biology* 426:2692-2701. https://doi.org/10.1016/j.jmb.2014.04.026

Yoon, KS; Kwon, DH; Strycharz, JP; Hollingsworth, CS; Lee, SH; Clark, JM (**2008**) Biochemical and molecular analysis of deltamethrin resistance in the common bed bug (Hemiptera: *Cimicidae*). *Journal of Medical Entomology* 45:1092-1101. https://doi.org/10.1603/0022-2585(2008)45[1092:bamaod]2.0.co;2

Zanni, V; Değirmenci, L; Annoscia, D; Scheiner, R; Nazzi, F (**2018**) The reduced brood nursing by mite-infested honey bees depends on their accelerated behavioral maturation. *Journal of Insect Physiology* 109:47-54. https://doi.org/10.1016/j.jinsphys.2018.06.006

Ziegelmann, B; Lindenmayer, A; Steidle, J; Rosenkranz, P (**2013**) The mating behavior of *Varroa destructor* is triggered by a female sex pheromone. *Apidologie* 44:314-323. https://doi.org/10.1007/s13592-013-0198-5

Zuo, Y; Peng, X; Wang, K; Lin, F; Li, Y; Chen, M (**2016**) Expression patterns, mutation detection and RNA interference of *Rhopalosiphum padi* voltage-gated sodium channel genes. *Scientific reports* 6:30166. https://doi.org/10.1038/srep30166

ANNEX

Supplementary Table Si.1. Taxonomic classification of *V. destructor* and *A. mellifera*.

Scientific classification		
Kingdom	Animalia	
Phylum	Arthropoda	
Subphylum	Chelicerata	Hexapoda
Class	Arachnida	Insecta
Subclass	Acari (Mites and Ticks)	Pterygota
Superorder	Parasitiformes	Hymenopterida
Order	Mesostigmata	Hymenoptera
Suborder	Dermanyssina	Apocrita
Superfamily	*Dermanyssoidea*	*Apoidea*
Family	*Varroidae*	*Apidae*
Genus	*Varroa*	*Apis*
Species	 ***V. destructor*** Anderson & Trueman, 2000	 ***A. mellifera*** Linnaeus, 1758

Supplementary Table S1.1. Primers used in the present work.

Primer Name	Sequence	Binding site	Objective
3_UTR4m_R	GAATACTCAAGCTAGCCTCGAGGCGG	pGH19	Amplification
5_UTR4_F	GATGTGCTGCAAGGCGATTAAGTTGGG	pGH19	Amplification
620_iF_Vd	TTGGAGATCTCGATACCGCGCACGC	*Vd*VGSC_intron	Sequencing, amplification
653_F_Vd	CCGAAACAATATTCACGACG	*Vd*VGSC_CDS	Sequencing, amplification
708_iF_Vd	CTGCCAGTGCGTCAACTAGTTGTCT	*Vd*VGSC_intron	Sequencing, amplification
753_R_Vd	CCATGGATCCCCAAGATATG	*Vd*VGSC_CDS	Sequencing, amplification
925_iF_Vd	GCTTCTACCGTATTTTGCTGTCT	*Vd*VGSC_intron	Sequencing, amplification
1273-iF_Vd	AAGCCGCCATTGTTACCAGA	*Vd*VGSC_intron	Sequencing, amplification
1356_F_Vd	CAATCTGATTCTCGCCATTG	*Vd*VGSC_CDS	Sequencing, amplification
1371_F_Vd	TGATTCTCGCCATTGTCGCAATGTCA	*Vd*VGSC_CDS	Sequencing, amplification
1406_F_Vd	CGCGCCGAAGAAGAAGCCGAAGAGG	*Vd*VGSC_CDS	Sequencing, amplification
1457_R_Vd	AATCGCATAGCCTCTTCCAA	*Vd*VGSC_CDS	Sequencing, amplification
1481_iF_Vd	TCTTTCTCCCTCCCTCCCTC	*Vd*VGSC_intron	Sequencing, amplification
1497_iR_Vd	GGAGGGAGGGAGAAAGAGTC	*Vd*VGSC_intron	Sequencing, amplification
1542_iF_Vd	TTCTCTCTGACACATTGCCGC	*Vd*VGSC_intron	Sequencing, amplification
1830_iF_Vd	TTTCCTTCGTTGGCTCATTGTAG	*Vd*VGSC_intron	Sequencing, amplification
1973-iR_Vd	GCTGTTGTTACCGTGGAGCA	*Vd*VGSC_intron	Sequencing, amplification
2043_F_Vd	CGTAGACGCTCAGGAACACC	*Vd*VGSC_CDS	Sequencing, amplification
2150_R_Vd	TGCTGCAAATTGGAGTAGAGA	*Vd*VGSC_CDS	Sequencing, amplification
2441_iR_Vd	TTTGTAAGGCCGTGGCGATGGTGGC	*Vd*VGSC_CDS	Sequencing, amplification
2452_iR_Vd	TTATTCGGACGGTGTCGGTG	*Vd*VGSC_intron	Sequencing, amplification
2491_iR_Vd	GCGATGGTGGCTTTCTCCCTCTATC	*Vd*VGSC_intron	Sequencing, amplification
2502_iR_Vd	TTTGTAAGGCCGTGGCGATGGTGGC	*Vd*VGSC_intron	Sequencing, amplification
2751_F_Vd	TTTCTTCACCGCTACCTTCG	*Vd*VGSC_CDS	Sequencing, amplification
2843_R_Vd	TCAAATATATTCCACCCTTCTTT	*Vd*VGSC_CDS	Sequencing, amplification
2945_F_Vd	CCAAGTCATGGCCAACGTTG	*Vd*VGSC_CDS	Sequencing, amplification
3074_R_Vd	CCGAAAAGTTGCATGCCCAT	*Vd*VGSC_CDS	Sequencing, amplification
3088_R_Vd	CGAGATAGTTCTTGCCGAAAAG	*Vd*VGSC_CDS	Sequencing, amplification
3120_F_Vd	GCCGCGCTGGAATTTCTTAG	*Vd*VGSC_CDS	Sequencing, amplification
3304_R_Vd	GCAACAGGGCCAAAAAGAGG	*Vd*VGSC_CDS	Sequencing, amplification
3317_R_Vd	AACGAAGAGAGCAACAGGGC	*Vd*VGSC_CDS	Sequencing, amplification
3448_F_Vd	GGTAAACAGCGCAACCAGAT	*Vd*VGSC_CDS	Sequencing, amplification
3476_R_Vd	TGATCCGAGATCTGGTTGCG	*Vd*VGSC_CDS	Sequencing, amplification
3556_R_Vd	GCGTGGGGCTATCCTTCTTA	*Vd*VGSC_CDS	Sequencing, amplification
4143_R_Vd	TGCAGGCAGAGAAACGGTTGCGTCG	*Vd*VGSC_CDS	Sequencing, amplification
4146_F_Vd	CGCAGAAGGAAAAGAAACG	*Vd*VGSC_CDS	Sequencing, amplification
4190_R_Vd	TCAGCCCCTACATCACTACCACCAG	*Vd*VGSC_CDS	Sequencing, amplification
4256_R_Vd	TCAGGGATGATGAGGTCAGA	*Vd*VGSC_CDS	Sequencing, amplification
4846_F_Vd	GGCAGATTCTACCACTGCGT	*Vd*VGSC_CDS	Sequencing, amplification
4949_R_Vd	GGGTTTTTCCAGGTAAAGTTGTT	*Vd*VGSC_CDS	Sequencing, amplification
5560_F_Vd	CTTTCGATCCTTGGCACAGT	*Vd*VGSC_CDS	Sequencing, amplification
5650_R_Vd	CAACCTTAACGACGCGTACA	*Vd*VGSC_CDS	Sequencing, amplification
6251_F_Vd	AGTACAAGCTGATCGCGCTG	*Vd*VGSC_CDS	Sequencing, amplification
6357_R_Vd	ATGACCCTTACGAGCGAAGA	*Vd*VGSC_CDS	Sequencing, amplification
Vdpara_L925IF	GGCAAGACGATAGGAGCTATAGGTAACCTG	*Vd*VGSC_CDS	Site-directed mutagenesis

<div align="right">(Cont.)</div>

(Cont.)

Vdpara_L925IR	CAGGTTACCTATAGCTCCTATCGTCTTGCC	*Vd*VGSC_CDS	Site-directed mutagenesis
Vdpara_L925MF	GGCAAGACGATAGGAGCTATGGGTAACCTG	*Vd*VGSC_CDS	Site-directed mutagenesis
Vdpara_L925MR	CAGGTTACCCATAGCTCCTATCGTCTTGCC	*Vd*VGSC_CDS	Site-directed mutagenesis
Vdpara_L925VF	GGCAAGACGATAGGAGCTGTGGGTAACCTG	*Vd*VGSC_CDS	Site-directed mutagenesis
Vdpara_L925VR	CAGGTTACCCACAGCTCCTATCGTCTTGCC	*Vd*VGSC_CDS	Site-directed mutagenesis
Vd_TM_L925V_F	CCAAGTCATGGCCAACGTT	*Vd*VGSC_CDS	TaqMan
Vd_TM_L925V_R	AAGATGATAATTCCCAACACAAAGG	*Vd*VGSC_CDS	TaqMan

Supplementary Table S1.2. Gating properties for activation and steady-state inactivation from the for the wild-type *Vd*VGSC analysed in this work and the *V. destructor* sodium channel constructs published to date in previous studies by Du *et al.* (2009) and Gosselin-Badaroudine and Chahine (2017). Values are expressed as mean ± SEM (mV), indicated if different. V_{50} is the voltage for half-maximal activation or inactivation ($V_{50, act}$ and $V_{50, inact}$, respectively), k is the slope factor (k_{act} for activation and k_{inact} for inactivation), and n is the number of oocytes tested.

		Activation	**Inactivation**
wild-type	V_{50} (mV)	**-18.39** ± 0.2507	**-31.04** ± 0.1265
	k (mV)	5.05 ± 0.2181	4.873 ± 0.1102
	n	26	28
VdNav1 (Du et al., 2009)	V_{50} (mV)	-18.23 ± 3.33 (SD)	-29.16 ± 1.72 (SD)
	k (mV)	3.58 ± 0.57 (SD)	4.98 ± 0.57 (SD)
	n	5	5
VdNav1a (Du et al., 2009)	V_{50} (mV)	-19.78 ± 2.85 (SD)	-30.58 ±2.08 (SD)
	k (mV)	2.97 ± 0.69 (SD)	4.47 ± 0.31 (SD)
	n	15	15
VdNav1 (Gosselin-Badaroudine and Chahine, 2017)	V_{50} (mV)	–7.9 ± 1.1	–28.2 ± 0.5
	k (mV)		
	n	19	14
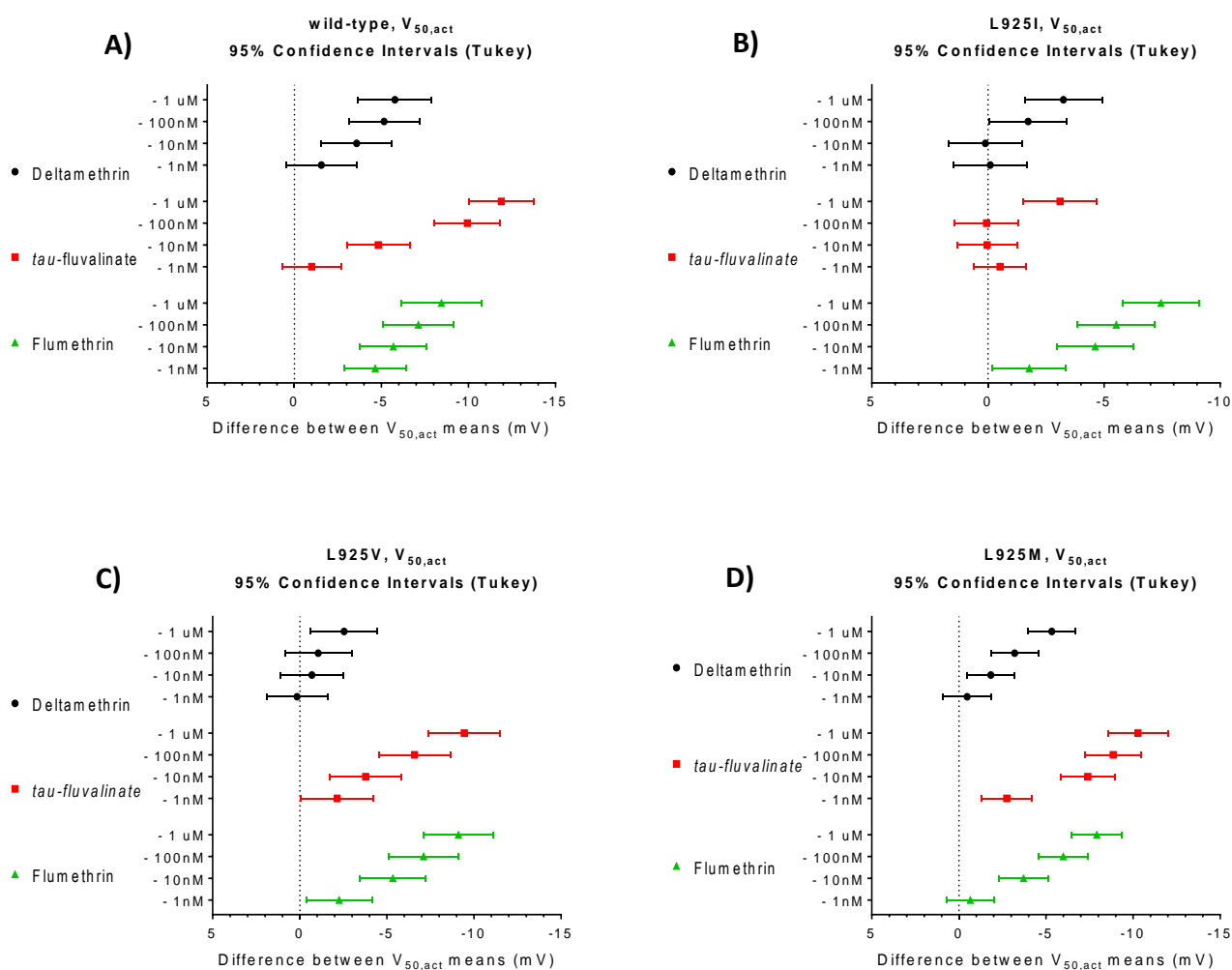
Supplementary Figure S1.1. Pyrethroid effect upon the $V_{50,act}$ of the *Vd*VGSC wild-type (A), L925I (B), L925V (C) and L925M (D) mutations. Data are shown as the mean difference for, and 95% confidence intervals, between the $V_{50,act}$ values obtained from the same oocytes non-exposed and exposed to increasing pyrethroid concentrations. Legend: Black (dots) for deltamethrin; red (squares) for *tau*-fluvalinate; and green (triangles) for flumethrin.
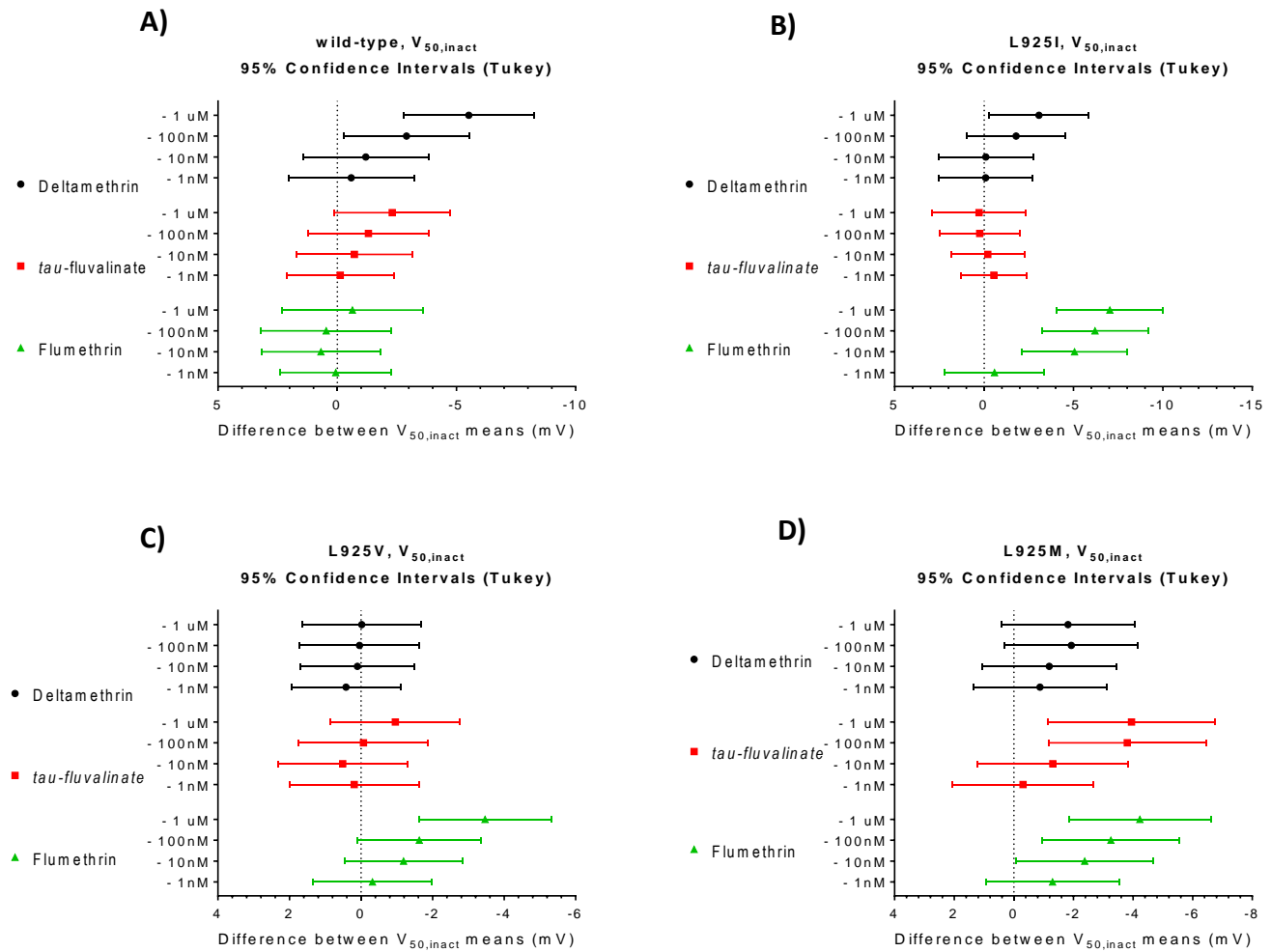
Supplementary Figure S1.2. Pyrethroid effect upon the $V_{50,inact}$ of the *Vd*VGSC wild-type (A), L925I (B), L925V (C) and L925M (D) mutations. Data are shown as the mean difference for, and 95% confidence intervals, between the $V_{50,inact}$ values obtained from the same oocytes non-exposed and exposed to increasing pyrethroid concentrations. Legend: Black (dots) for deltamethrin; red (squares) for *tau*-fluvalinate; and green (triangles) for flumethrin.

Pyrethroid effect upon K_{act}
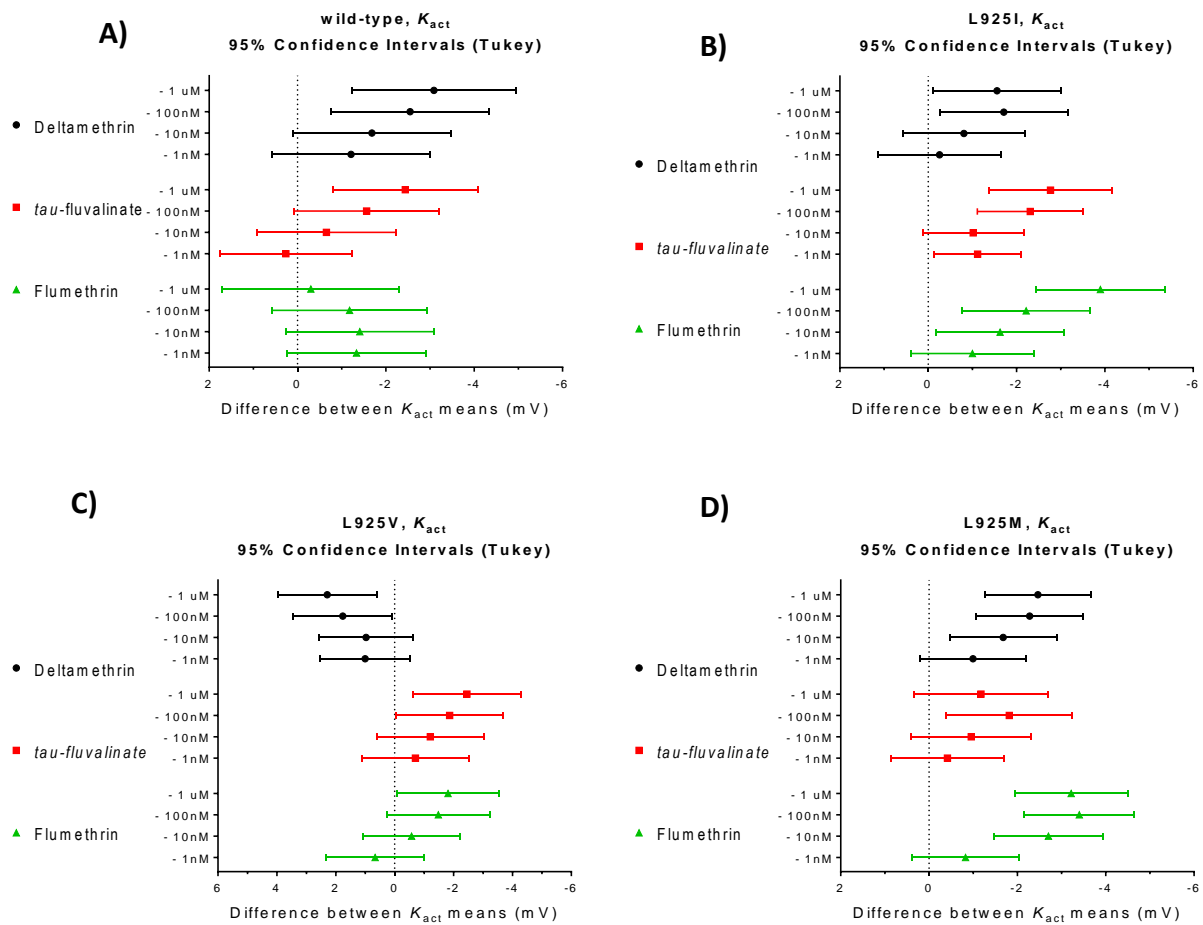
Supplementary Figure S1.3. Pyrethroid effect upon the k_{act} of the VdVGSC wild-type (A), L925I (B), L925V (C) and L925M (D) mutations. Data are shown as the mean difference for, and 95% confidence intervals, between the k_{act} values obtained from the same oocytes non-exposed and exposed to increasing pyrethroid concentrations. Legend: Black (dots) for deltamethrin; red (squares) for *tau*-fluvalinate; and green (triangles) for flumethrin.

Pyrethroid effect upon K_{inact}
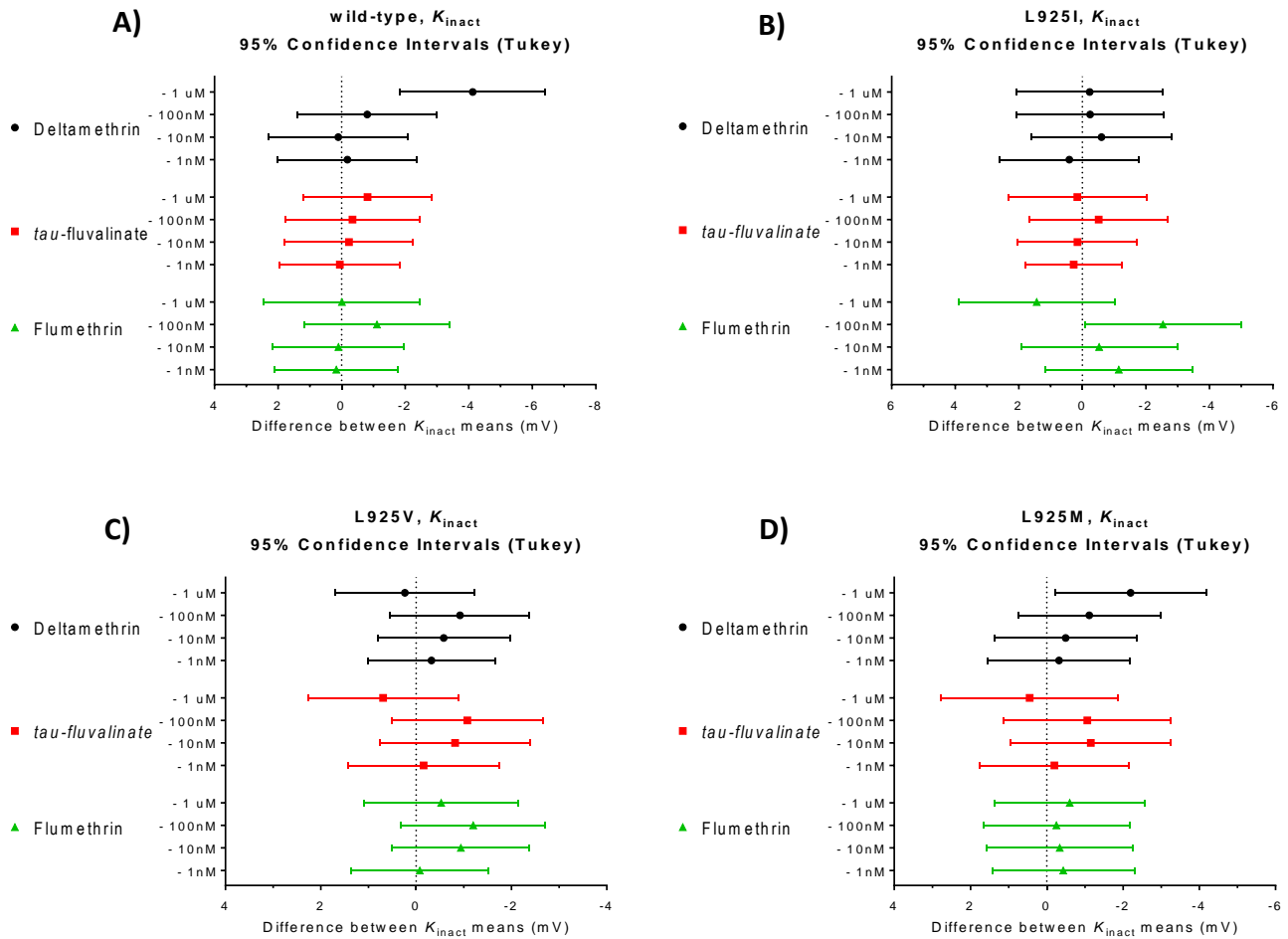
Supplementary Figure S1.4. Pyrethroid effect upon the k_{inact} of the VdVGSC wild-type (A), L925I (B), L925V (C) and L925M (D) mutations. Data are shown as the mean difference for, and 95% confidence intervals, between the k_{inact} values obtained from the same oocytes non-exposed and exposed to increasing pyrethroid concentrations. Legend: Black (dots) for deltamethrin; red (squares) for tau-fluvalinate; and green (triangles) for flumethrin.

Supplementary Figure S.1.5 (on next page). Prediction of the effect on protein function of amino acid differences between the *V. destructor* sodium channel contructs analysed by TEVC to date (wild-type channels, L925). Prediction was made by the SuSPect method (Yates et al., 2014) using the *Vd*VGSC construct of this work (sequence 3) as reference. Sequence 1 and 2 corresponds to the *Vd*Nav constructions made by Du *et al.* (2009) (AY259834.1) and Gosselin-Badaroudine and Chahine (2017), respectively. Numbers above the amino acid sequence indicates the residue in the *Vd*VGSC protein (numbered after the *Vd*VGSC amino acid sequence, AY259834.1). The mutational analysis graph represents the predicted effect of mutations at a particular position in the sequence. Coloured bars indicate the probability that a mutation to the corresponding residue will have some effect on function of the protein or on the phenotype of the organism, ranging from red (higher effect) to dark blue (neutral change). The tallest the bar, the highest likelihood that mutation affects the protein function. See Fig. 1.1 and Table 1.1 for more info. Figure on next page.
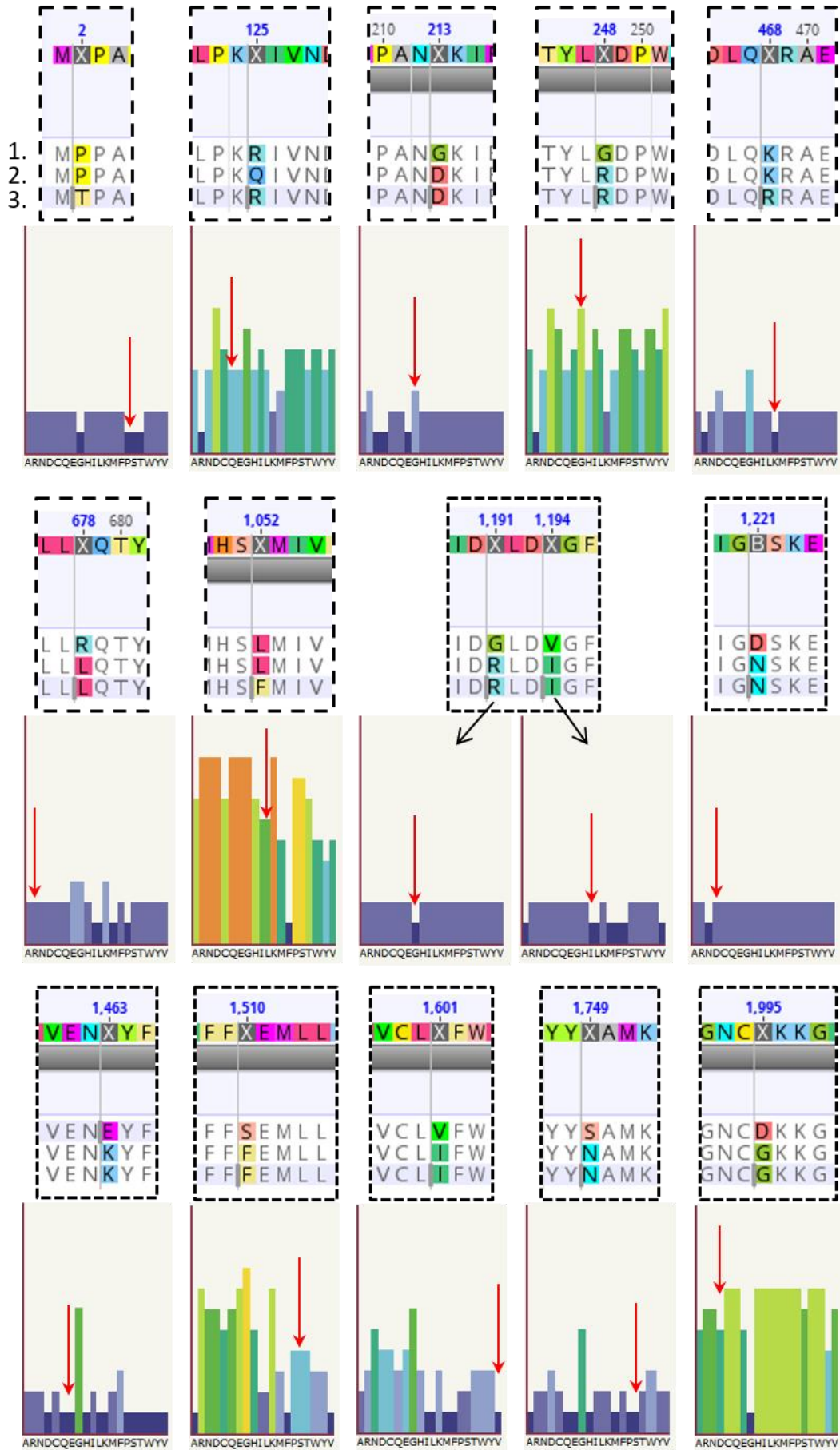
Supplementary Table S2.1. Sample mite representatives for each location. Sample codes of mites sequenced in this study with their corresponding haplotype, country and location when known, the collection year and *kdr*-type alleles for positions 925 and 918.

Haplotype	Sample	Country	Location	*kdr*-type alleles	Collection year
Hap1	US680c_L	USA	Colorado	925 L/L (wt)	2016
Hap2	ESCN-CR10_L	Spain	La Palma, Canarias	925 L/L (wt)	2010
Hap3	ESMC71_6E_L	Spain	Murcia	925 L/L (wt)	2017
	US738_L	USA	Pennsylvania	925 L/L (wt)	2017
Hap4	ESCN-H814_V	Spain	El Hierro, Canarias	925 V/V	2017
Hap5	ENG2A7_V	England	Peterborough	925 V/V	2013
Hap6	ESCV7b5_L	Spain	Valencia	925 L/L (wt)	2017
Hap7, Hap8	US612c_M	USA	Wisconsin	925 M/M	2016
Hap79	US722_I	USA	Idaho	925 I/I	2017
Hap9	US612a_L	USA	Wisconsin	925 L/L (wt)	2016
	US630a_L	USA	Pennsylvania	925 L/L (wt)	2016
	US685d_L	USA	Utah	925 L/L (wt)	2016
Hap9, Hap10	ENG19F5_L	England	Harpenden	925 L/L (wt)	2013
Hap9, Hap48	SCTB1_L	Scotland		925 L/L (wt)	2013
Hap10	CNA10_L	China		925 L/L (wt)	2014
	ES208D1_L	Spain		925 L/L (wt)	2013
	ES208F1_L	Spain		925 L/L (wt)	2013
	ES68G9_L	Spain		925 L/L (wt)	2013
	ESCV7b4_L	Spain	Valencia	925 L/L (wt)	2017
	ESCV7c3_L	Spain	Valencia	925 L/L (wt)	2017
	ESCV7c4_L	Spain	Valencia	925 L/L (wt)	2017
	ESCV7c7_L	Spain	Valencia	925 L/L (wt)	2017
	ESCV7d46_L	Spain	Valencia	925 L/L (wt)	2017
	ESCV7d48_L	Spain	Valencia	925 L/L (wt)	2017
	ESCV9_081_L	Spain	Valencia	925 L/L (wt)	2019
	ESCV9_131_L	Spain	Valencia	925 L/L (wt)	2019
	ESCV9_193_L	Spain	Alicante	925 L/L (wt)	2019
	ESCV9_301_L	Spain	Valencia	925 L/L (wt)	2019
	ESMC70_1_L	Spain	Murcia	925 L/L (wt)	2017
	ESMC70_12_L	Spain	Murcia	925 L/L (wt)	2017
	ESMC79_9_L	Spain	Murcia	925 L/L (wt)	2017
	FR135A9_L	France		925 L/L (wt)	2014
	FR9A1_L	France	Puy-de-Dôme	925 L/L (wt)	2019
	FR9A3_L	France	Puy-de-Dôme	925 L/L (wt)	2019
	GRC4_6_L	Greece	Attiki	925 L/L (wt)	2015
	GRC4_8_L	Greece	Attiki	925 L/L (wt)	2015
	GRC9_3_L	Greece	Cyprus	925 L/L (wt)	2015
	KC152655.2 (Hubert et al., 2014)	Czech Republic		925 L/L (wt)	2010

(Cont.)

(Cont.)

	US636b_L	USA	Delaware	925 L/L (wt)	2016
	US636c_L	USA	Delaware	925 L/L (wt)	2016
	US680a_L	USA	Colorado	925 L/L (wt)	2016
	US704_L	USA	Rhode Island	925 L/L (wt)	2017
	US708_L	USA	Washington	925 L/L (wt)	2017
	US713_L	USA	Missouri	925 L/L (wt)	2017
	US716_L	USA	Missouri	925 L/L (wt)	2017
	US726_L	USA	Maryland	925 L/L (wt)	2017
	US727_L	USA	Maryland	925 L/L (wt)	2017
	US730_L	USA	West Virginia	925 L/L (wt)	2017
	US735_L	USA	Pennsylvania	925 L/L (wt)	2017
	US742_L	USA	Ohio	925 L/L (wt)	2017
	US753_L	USA	Kansas	925 L/L (wt)	2017
Hap10, Hap48	AT159B1_L	Austria		925 L/L (wt)	2014
	AT159C1_L	Austria		925 L/L (wt)	2014
	ENG8B5_L	England	Peterborough	925 L/L (wt)	2013
	SCTE1_L	Scotland		925 L/L (wt)	2013
Hap11	ESCV9_141_L	Spain	Valencia	925 L/L (wt)	2019
Hap12	GRC5_4_I	Greece	Peloponnisos	925 I/I	2015
Hap13	ESCV9_112_V	Spain	Valencia	925 V/V	2019
Hap14, Hap15	ESCV8_123_V_918L	Spain	Alicante	918 L/L + 925 V/V	2018
Hap16	ESMC63_5C_V	Spain	Murcia	925 V/V	2017
Hap17	ESCV9_291_V_918L	Spain	Alicante	918 L/L + 925 V/V	2019
Hap18	GRC8_3_L	Greece	Crete	925 L/L (wt)	2015
	GRC9_2_L	Greece	Cyprus	925 L/L (wt)	2015
Hap19, Hap20	US664a_I	USA	Illinois	925 I/I	2016
Hap21, Hap22	US682d_M	USA	Wisconsin	925 M/M	2016
Hap23	ESCV9_041_V_918L	Spain	Castellón	918 L/L + 925 V/V	2019
	ESCV9_302_V_918L	Spain	Valencia	918 L/L + 925 V/V	2019
Hap23, Hap24	ESCV8_221_V_918L	Spain	Valencia	918 L/L + 925 V/V	2018
	ESCV8_243_V_918L	Spain	Alicante	918 L/L + 925 V/V	2018
Hap24, Hap65	ESCV8_242_V_918L	Spain	Alicante	918 L/L + 925 V/V	2018
Hap25	US701_M	USA	Rhode Island	925 M/M	2017
Hap26, Hap27	US632d_I	USA	California	925 I/I	2016
Hap26, Hap69	GRC5_7_I	Greece	Peloponnisos	925 I/I	2015
Hap28	GRC5_3_L	Greece	Peloponnisos	925 L/L (wt)	2015
Hap29	GRC8_14_I	Greece	Crete	925 I/I	2015
	US632a_I	USA	California	925 I/I	2016
	US637e_I	USA	Delaware	925 I/I	2016
	US684a_I	USA	Utah	925 I/I	2016
	US703_I	USA	Rhode Island	925 I/I	2017

(Cont.)

(Cont.)

	US710_I	USA	Oregon	925 I/I	2017
	US717_I	USA	North Dakota	925 I/I	2017
	US718_I	USA	North Dakota	925 I/I	2017
	US721_I	USA	Idaho	925 I/I	2017
	US733_I	USA	Wisconsin	925 I/I	2017
Hap29, Hap30	GRC3_11_I	Greece	Crete	925 I/I	2015
	US651c_I	USA	North Dakota	925 I/I	2016
	US662b_I	USA	Illinois	925 I/I	2016
	US662c_I	USA	Illinois	925 I/I	2016
	US732_I	USA	Wisconsin	925 I/I	2017
Hap31, Hap32	GRC3_20_I	Greece	Crete	925 I/I	2015
Hap33	US737_L	USA	Pennsylvania	925 L/L (wt)	2017
Hap34	ESCN-Fr02_M	Spain	El Hierro, Canarias	925 M/M	2011
Hap35	ESCV9_292_L	Spain	Alicante	925 L/L (wt)	2019
Hap36, Hap37	US684c_I	USA	Utah	925 I/I	2016
Hap38	ESCV9_192_L	Spain	Alicante	925 L/L (wt)	2019
	IRN5_L (Farjamfar *et al.*, 2018)	Iran	Kelachay	925 L/L (wt)	2016
	US697c_L	USA	California	925 L/L (wt)	2016
	US765_L	USA	Virginia	925 L/L (wt)	2017
Hap39	ESCN-PU122_V	Spain	La Palma, Canarias	925 V/V	2017
Hap40	ESCV7c8_L	Spain	Valencia	925 L/L (wt)	2017
Hap41	ESCV9_293_L	Spain	Alicante	925 L/L (wt)	2019
Hap42	GRC5_6_V	Greece	Peloponnisos	925 V/V	2015
Hap43, Hap44	ESCN-H82_M	Spain	El Hierro, Canarias	925 M/M	2008
Hap45	ESCV9_253_L	Spain	Valencia	925 L/L (wt)	2019
Hap46	ESMC63_5G_L	Spain	Murcia	925 L/L (wt)	2017
Hap47	US691b_L	USA	Nevada	925 L/L (wt)	2016
Hap49	US696d_M	USA	Florida	925 M/M	2016
	US697a_M	USA	California	925 M/M	2016
	US697b_M	USA	California	925 M/M	2016
	US711_M	USA	Oregon	925 M/M	2017
	US739_M	USA	Ohio	925 M/M	2017
	US764_M	USA	Virginia	925 M/M	2017
Hap49, Hap60	US619f_M	USA	Alabama	925 M/M	2016
Hap50	ESCN-BB111_L	Spain	La Palma, Canarias	925 V/V	2016
Hap51	ESCN-VM111_V	Spain	La Palma, Canarias	925 V/V	2017
Hap52	ESCV9_261_V_918L	Spain	Alicante	918 L/L + 925 V/V	2019
Hap53	IRN8_L (Farjamfar *et al.*, 2018)	Iran	Sari	925 L/L (wt)	2016
	US747_L	USA	Missouri	925 L/L (wt)	2017
	US748_L	USA	Missouri	925 L/L (wt)	2017

(Cont.)

(Cont.)

Hap54	ESCN-Fr05_M	Spain	El Hierro, Canarias	925 M/M	2011
	ESCV9_033_L	Spain	Castellón	925 L/L (wt)	2019
Hap55	ESMC71_6C_L	Spain	Murcia	925 L/L (wt)	2017
	US674b_L	USA	Minnesota	925 L/L (wt)	2016
Hap56	US635d_L	USA	Delaware	925 L/L (wt)	2016
	ENG8C5_V	England	Peterborough	925 V/V	2013
	ENG8D6_V	England	Peterborough	925 V/V	2013
	ES208A1_V	Spain		925 V/V	2013
	ES208C1_V	Spain		925 V/V	2013
	ES208E1_V	Spain		925 V/V	2013
	ESCN-LL111_V	Spain	La Palma, Canarias	925 V/V	2017
	ESCN-SC2242_V	Spain	La Palma, Canarias	925 V/V	2017
	ESCV7c2_V	Spain	Valencia	925 V/V	2017
	FR135B9_V	France		925 V/V	2014
Hap57	FR135F9_V	France		925 V/V	2014
	FR7N03_V	France	Maine et Loire	925 V/V	2017
	FR7N16_V	France	Maine et Loire	925 V/V	2017
	GRC3_19_V	Greece	Crete	925 V/V	2015
	GRC8_8_V	Greece	Crete	925 V/V	2015
	KC152656.2 (Hubert et al., 2014)	Czech Republic		925 V/V	2010
	SCTA1_V	Scotland		925 V/V	2013
	WLS123D_V	Wales	Cornwall	925 V/V	2014
	WLS123E_V	Wales	Cornwall	925 V/V	2014
Hap58	ESCV9_241_V	Spain	Valencia	925 V/V	2019
Hap59	FR7N15_V	France		925 V/V	2017
Hap61, Hap62	US719_M	USA	North Dakota	925 M/M	2017
Hap63	FR7N06_V	France		925 V/V	2017
Hap64	US634c_L	USA	Michigan	925 L/L (wt)	2016
Hap66, Hap67	US672a_M	USA	Texas	925 M/M	2016
Hap68	US694a_M	USA	Connecticut	925 M/M	2016
Hap70, Hap71	GRC8_5_I	Greece	Crete	925 I/I	2015
Hap72	ESMC79_11_L	Spain	Murcia	925 L/L (wt)	2017
Hap73	ESCV9_201_V_918L	Spain	Alicante	918 L/L + 925 V/V	2019
Hap74, Hap75	GRC5_2_I	Greece	Peloponnisos	925 I/I	2015
Hap76	ESCV8_152_V_918L	Spain	Valencia	918 L/L + 925 V/V	2018
	BE62F3_V	Belgium		925 V/V	2013
Hap77, Hap78	BE62G3_V	Belgium		925 V/V	2013
	SCTC1_V	Scotland		925 V/V	2013

Supplementary Table S2.2. Accession number of the sequences corresponding to the haplotypes for the *V. destructor* VGSC gene region sequenced in this work. The (wt) refers to the wild-type allele.

| Haplotype	918 allele	925 allele	Accession number
Hap1_925L	Methionine (wt)	Leucine (wt)	MT859428
Hap2_925L	Methionine (wt)	Leucine (wt)	MT859429
Hap3_925L	Methionine (wt)	Leucine (wt)	MT859430
Hap4_925V	Methionine (wt)	Valine	MT859431
Hap5_925V	Methionine (wt)	Valine	MT859432
Hap6_925L	Methionine (wt)	Leucine (wt)	MT859433
Hap7_925M	Methionine (wt)	Methionine	MT859434
Hap8_925M	Methionine (wt)	Methionine	MT859435
Hap9_925L	Methionine (wt)	Leucine (wt)	MT859436
Hap10_925L	Methionine (wt)	Leucine (wt)	MT859437
Hap11_925L	Methionine (wt)	Leucine (wt)	MT859438
Hap12_925I	Methionine (wt)	Isoleucine	MT859439
Hap13_925V	Methionine (wt)	Valine	MT859440
Hap14_925V_918L	Leucine	Valine	MT859441
Hap15_925V_918L	Leucine	Valine	MT859442
Hap16_925V	Methionine (wt)	Valine	MT859443
Hap17_925V_918L	Leucine	Valine	MT859444
Hap18_925L	Methionine (wt)	Leucine (wt)	MT859445
Hap19_925I	Methionine (wt)	Isoleucine	MT859446
Hap20_925I	Methionine (wt)	Isoleucine	MT859447
Hap21_925M	Methionine (wt)	Methionine	MT859448
Hap22_925M	Methionine (wt)	Methionine	MT859449
Hap23_925V_918L	Leucine	Valine	MT859450
Hap24_925V_918L	Leucine	Valine	MT859451
Hap25_925M	Methionine (wt)	Methionine	MT859452
Hap26_925I	Methionine (wt)	Isoleucine	MT859453
Hap27_925I	Methionine (wt)	Isoleucine	MT859454
Hap28_925L	Methionine (wt)	Leucine (wt)	MT859455
Hap29_925I	Methionine (wt)	Isoleucine	MT859456
Hap30_925I	Methionine (wt)	Isoleucine	MT859457
Hap31_925I	Methionine (wt)	Isoleucine	MT859458
Hap32_925I	Methionine (wt)	Isoleucine	MT859459
Hap33_925L	Methionine (wt)	Leucine (wt)	MT859460
Hap34_925M	Methionine (wt)	Methionine	MT859461
Hap35_925L	Methionine (wt)	Leucine (wt)	MT859462
Hap36_925I	Methionine (wt)	Isoleucine	MT859463
Hap37_925I	Methionine (wt)	Isoleucine	MT859464
Hap38_925L	Methionine (wt)	Leucine (wt)	MT859465
Hap39_925V	Methionine (wt)	Valine	MT859466
Hap40_925L	Methionine (wt)	Leucine (wt)	MT859467
Hap41_925L	Methionine (wt)	Leucine (wt)	MT859468
Hap42_925V	Methionine (wt)	Valine	MT859469
Hap43_925M	Methionine (wt)	Methionine	MT859470
Hap44_925M	Methionine (wt)	Methionine	MT859471
Hap45_925L	Methionine (wt)	Leucine (wt)	MT859472
Hap46_925L	Methionine (wt)	Leucine (wt)	MT859473
Hap47_925L	Methionine (wt)	Leucine (wt)	MT859474

(Cont.)

Hap48_925L	Methionine (wt)	Leucine (wt)	MT859475
Hap49_925M	Methionine (wt)	Methionine	MT859476
Hap50_925L	Methionine (wt)	Leucine (wt)	MT859477
Hap51_925V	Methionine (wt)	Valine	MT859478
Hap52_925V_918L	Leucine	Valine	MT859479
Hap53_925L	Methionine (wt)	Leucine (wt)	MT859480
Hap54_925M	Methionine (wt)	Methionine	MT859481
Hap55_925L	Methionine (wt)	Leucine (wt)	MT859482
Hap56_925L	Methionine (wt)	Leucine (wt)	MT859483
Hap57_925V	Methionine (wt)	Valine	MT859484
Hap58_925V	Methionine (wt)	Valine	MT859485
Hap59_925V	Methionine (wt)	Valine	MT859486
Hap60_925M	Methionine (wt)	Methionine	MT859487
Hap61_925M	Methionine (wt)	Methionine	MT859488
Hap62_925M	Methionine (wt)	Methionine	MT859489
Hap63_925V	Methionine (wt)	Valine	MT859490
Hap64_925L	Methionine (wt)	Leucine (wt)	MT859491
Hap65_925V_918L	Leucine	Valine	MT859492
Hap66_925M	Methionine (wt)	Methionine	MT859493
Hap67_925M	Methionine (wt)	Methionine	MT859494
Hap68_925M	Methionine (wt)	Methionine	MT859495
Hap69_925I	Methionine (wt)	Isoleucine	MT859496
Hap70_925I	Methionine (wt)	Isoleucine	MT859497
Hap71_925I	Methionine (wt)	Isoleucine	MT859498
Hap72_925L	Methionine (wt)	Leucine (wt)	MT859499
Hap73_925V_918L	Leucine	Valine	MT859500
Hap74_925I	Methionine (wt)	Isoleucine	MT859501
Hap75_925I	Methionine (wt)	Isoleucine	MT859502
Hap76_925V_918L	Leucine	Valine	MT859503
Hap77_925V	Methionine (wt)	Valine	MT859504
Hap78_925V	Methionine (wt)	Valine	MT859505
Hap79_925I	Methionine (wt)	Isoleucine	MT859506

Supplementary Table S2.3. Identity table (link) and heatmap representation of pairwise distance of the haplotypes found in this work. Values of the table are shown in percentages. Table is displayed as a heatmap, with the lowest value (98.4 %) in yellow and the highest in dark red (99.9%). Heatmap representation figure was generated by Heatmapper web service with values expressed as Euclidean distances (http://www.heatmapper.ca).

Data on the following link:

https://static-content.springer.com/esm/art%3A10.1007%2Fs10340-020-01321-8/MediaObjects/10340_2020_1321_MOESM4_ESM.xlsx
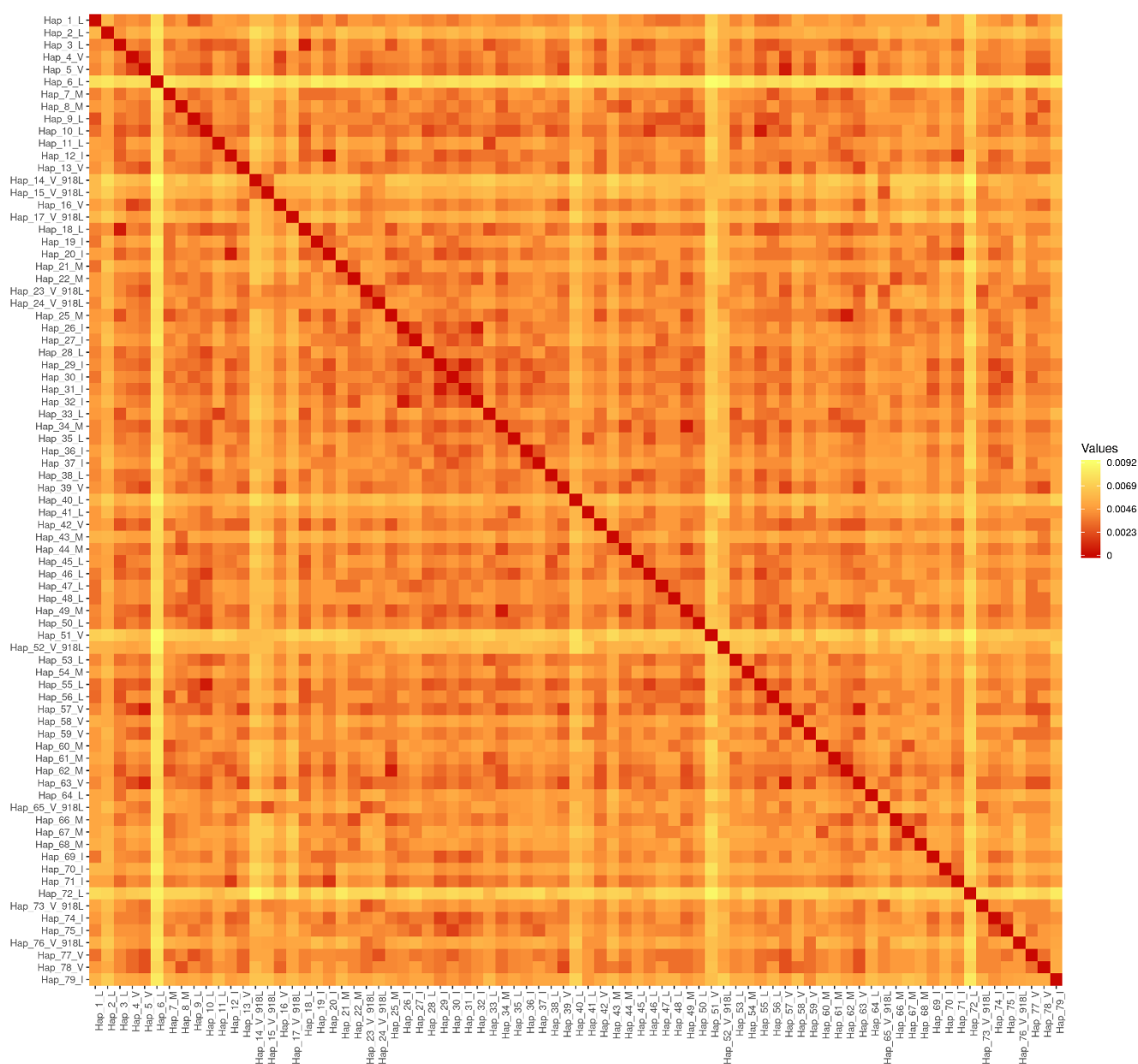
Supplementary Table S3.1. *Varroa destructor* 925 allele data obtained for each sampled apiary in absolute and normalized values. L: wild-type L925, I: mutant L925I and M: mutant L925M. L/L: Homozygous for the wild-type allele L925, L/I: Heterozygous for L925/I925, L/M: Heterozygous for L925/M925, I/I: Homozygous for the resistant allele I925, M/M: Homozygous for the resistant allele M925, I/M: Heterozygous for I925/M925.

Data on the following link:

https://onlinelibrary.wiley.com/action/downloadSupplement?doi=10.1002%2Fps.6366 &file=ps6366-sup-0001-TableS1.xlsx

Supplementary Table S3.2. Frequencies of genotype for the 925 position in the VGSC of *V. destructor* grouped by State for years 2016 and 2017, and the predicted phenotype for them. The colour of the headings relates to the colour code on maps (Fig. 3.5).

State	year	Genotype						Phenotype	
		% L/L	% L/I	% L/M	% I/I	% M/M	% I/M	Susceptible	Resistant
Alabama	2016	65.18	0.89	11.61	12.50	8.93	0.89	77.68	22.32
	2017	72.92	4.17	4.17	2.08	16.67	0.00	81.25	18.75
Arizona	2017	89.13	2.17	6.52	0.00	2.17	0.00	97.83	2.17
Arkansas	2017	70.97	3.23	3.23	9.68	12.90	0.00	77.42	22.58
California	2016	12.90	3.23	0.00	64.52	19.35	0.00	16.13	83.87
	2017	22.58	6.45	6.45	51.61	9.68	3.23	35.48	64.52
Colorado	2016	60.42	8.33	10.42	8.33	6.25	6.25	79.17	20.83
	2017	0.00	0.00	3.13	71.88	21.88	3.13	3.13	96.88
Connecticut	2016	36.00	4.00	5.33	28.00	16.00	10.67	45.33	54.67
	2017	87.50	0.00	0.00	6.25	6.25	0.00	87.50	12.50
Delaware	2016	56.25	6.25	4.17	22.92	10.42	0.00	66.67	33.33
	2017	6.67	0.00	6.67	26.67	53.33	6.67	13.33	86.67
Florida	2016	43.75	3.13	15.63	0.00	34.38	3.13	62.50	37.50
	2017	31.25	0.00	21.88	3.13	40.63	3.13	53.13	46.88
Georgia	2016	12.90	0.00	3.23	38.71	38.71	6.45	16.13	83.87
	2017	21.88	0.00	0.00	40.63	28.13	9.38	21.88	78.13
Hawaii	2016	95.74	0.00	2.13	0.00	2.13	0.00	97.87	2.13
Idaho	2017	21.28	8.51	0.00	61.70	2.13	6.38	29.79	70.21
Illinois	2016	67.74	5.16	3.87	12.26	8.39	2.58	76.77	23.23
Indiana	2016	75.00	4.17	2.08	12.50	6.25	0.00	81.25	18.75
	2017	37.50	12.50	0.00	25.00	21.88	3.13	50.00	50.00
Iowa	2016	31.25	6.25	9.38	28.13	21.88	3.13	46.88	53.13
	2017	45.16	9.68	3.23	19.35	22.58	0.00	58.06	41.94
Kansas	2017	76.60	8.51	0.00	6.38	2.13	6.38	85.11	14.89
Kentucky	2016	70.91	5.45	0.00	10.91	11.82	0.91	76.36	23.64
	2017	87.50	0.00	6.25	6.25	0.00	0.00	93.75	6.25
Louisiana	2016	18.75	3.13	0.00	75.00	3.13	0.00	21.88	78.13
Maine	2017	29.03	16.13	0.00	41.94	12.90	0.00	45.16	54.84
Maryland	2016	50.00	12.50	0.00	6.25	31.25	0.00	62.50	37.50
	2017	46.88	6.25	6.25	31.25	3.13	6.25	59.38	40.63
Massachusetts	2016	37.50	0.00	9.38	15.63	31.25	6.25	46.88	53.13
	2017	29.03	3.23	9.68	38.71	16.13	3.23	41.94	58.06
Michigan	2016	50.00	6.25	3.13	28.13	9.38	3.13	59.38	40.63
	2017	26.56	1.56	6.25	21.88	40.63	3.13	34.38	65.63
Minnesota	2016	47.87	8.51	7.45	13.83	15.96	6.38	63.83	36.17
	2017	45.83	2.08	0.00	35.42	10.42	6.25	47.92	52.08
Mississippi	2016	65.63	3.13	6.25	6.25	18.75	0.00	75.00	25.00

(Cont.)

(Cont.)

	2017	93.75	0.00	0.00	0.00	6.25	0.00	93.75	6.25
Missouri	**2017**	64.06	7.81	9.38	4.69	10.94	3.13	81.25	18.75
Montana	**2017**	28.13	0.00	3.13	25.00	28.13	15.63	31.25	68.75
Nebraska	**2016**	18.75	18.75	6.25	50.00	6.25	0.00	43.75	56.25
	2017	46.81	6.38	4.26	31.91	8.51	2.13	57.45	42.55
Nevada	**2016**	49.09	12.73	5.45	18.18	5.45	9.09	67.27	32.73
	2017	43.48	13.04	6.52	23.91	4.35	8.70	63.04	36.96
New Hampshire	**2017**	6.25	0.00	0.00	87.50	6.25	0.00	6.25	93.75
New Jersey	**2016**	41.05	5.79	6.32	19.47	18.42	8.95	53.16	46.84
New Mexico	**2016**	25.00	0.00	0.00	31.25	25.00	18.75	25.00	75.00
	2017	78.13	6.25	3.13	6.25	6.25	0.00	87.50	12.50
New York	**2016**	43.52	2.78	6.48	15.74	24.07	7.41	52.78	47.22
	2017	34.38	12.50	3.13	43.75	6.25	0.00	50.00	50.00
North Carolina	**2017**	71.43	0.00	0.00	12.70	15.87	0.00	71.43	28.57
North Dakota	**2016**	25.81	8.60	4.30	31.18	21.51	8.60	38.71	61.29
	2017	21.88	0.00	0.00	71.88	6.25	0.00	21.88	78.13
Ohio	**2017**	51.56	4.69	6.25	15.63	18.75	3.13	62.50	37.50
Oregon	**2017**	12.50	6.25	2.08	56.25	14.58	8.33	20.83	79.17
Pennsylvania	**2016**	70.13	5.19	3.90	6.49	10.39	3.90	79.22	20.78
	2017	35.48	3.23	0.00	45.16	12.90	3.23	38.71	61.29
Puerto Rico	**2017**	100.0	0.00	0.00	0.00	0.00	0.00	100.00	0.00
Rhode Island	**2017**	53.13	12.50	0.00	28.13	6.25	0.00	65.63	34.38
South Carolina	**2017**	19.35	3.23	3.23	48.39	22.58	3.23	25.81	74.19
South Dakota	**2016**	33.33	4.76	1.59	31.75	12.70	15.87	39.68	60.32
	2017	60.87	10.87	4.35	17.39	6.52	0.00	76.09	23.91
Tennessee	**2017**	76.25	2.50	0.00	11.25	5.00	5.00	78.75	21.25
Texas	**2016**	54.17	14.58	2.08	22.92	2.08	4.17	70.83	29.17
	2017	50.00	6.25	3.13	12.50	25.00	3.13	59.38	40.63
Utah	**2016**	18.75	6.25	4.17	33.33	22.92	14.58	29.17	70.83
	2017	9.38	21.88	6.25	40.63	9.38	12.50	37.50	62.50
Vermont	**2017**	71.88	6.25	3.13	9.38	6.25	3.13	81.25	18.75
Virginia	**2017**	84.78	2.17	0.00	4.35	8.70	0.00	86.96	13.04
Washington	**2017**	28.13	3.13	12.50	15.63	37.50	3.13	43.75	56.25
West Virginia	**2016**	84.38	0.00	6.25	3.13	6.25	0.00	90.63	9.38
	2017	75.00	5.00	3.75	12.50	3.75	0.00	83.75	16.25
Wisconsin	**2016**	38.10	4.76	7.14	19.05	17.86	13.10	50.00	50.00
	2017	19.15	6.38	2.13	46.81	14.89	10.64	27.66	72.34
Overall US	**2016**	49.24	5.50	5.35	19.49	14.65	5.77	60.09	39.91
	2017	50.26	5.17	3.63	24.44	13.17	3.33	59.06	40.94

Supplementary Table S3.3. Genotype and predicted phenotype for the 925 mutation of the VGSC of *V. destructor* of mites from the eleven apiaries (A to K) sampled in the consecutive years, 2016 and 2017. Data is shown as number of mites found for each genotype and the predicted phenotype for pyrethroid resistance. See figure 3.7 for graphical representation of this data.

Apiary code	year	Genotype						Phenotype	
		L/L	L/I	L/M	I/I	M/M	I/M	Susceptible	Resistant
A	2016	11	1	2	1	0	1	14	2
	2017	0	0	1	9	6	0	1	15
B	2016	6	0	1	3	5	1	7	9
	2017	14	0	0	1	1	0	14	2
C	2016	16	0	0	0	0	0	16	0
	2017	9	2	0	3	2	0	11	5
D	2016	16	0	0	0	0	0	16	0
	2017	15	0	1	0	0	0	16	0
E	2016	3	3	3	3	2	1	9	6
	2017	9	1	0	5	1	0	10	6
F	2016	12	1	0	1	1	1	13	3
	2017	5	0	0	6	2	3	5	11
G	2016	14	0	0	0	1	1	14	2
	2017	5	0	0	7	3	0	5	10
H	2016	11	1	1	0	2	0	13	2
	2017	6	1	0	7	1	1	7	9
I	2016	2	0	0	9	4	1	2	14
	2017	0	3	1	7	2	3	4	12
J	2016	9	0	1	2	3	1	10	6
	2017	1	2	0	10	1	2	3	13
K	2016	1	1	2	2	0	2	4	4
	2017	2	0	1	4	5	3	3	12

ARTICLES PUBLISHED

DURING THE THESIS

ORIGINAL PAPER

Mutations associated with pyrethroid resistance in the honey bee parasite *Varroa destructor* evolved as a series of parallel and sequential events

Anabel Millán-Leiva[1] · Óscar Marín[1] · Pilar De la Rúa[2] · Irene Muñoz[2] · Anastasia Tsagkarakou[3] · Heather Eversol[4] · Krisztina Christmon[4] · Dennis vanEngelsdorp[4] · Joel González-Cabrera[1]

Abstract

Managed honey bees have suffered severe seasonal losses for most of the past 30 years, while at the same time there is a growing need for food crop pollination. Parasitism by *Varroa destructor* plays a key role in explaining these losses as this parasite directly damages honey bees by feeding on them and by vectoring an array of viruses while doing so. Pyrethroids like *tau*-fluvalinate and flumethrin are among the few acaricides that may control Varroa mites in honey bee colonies. However, their intensive use has led to the evolution of resistance in many locations. Knockdown resistance (*kdr*-type) in *Varroa destructor* is associated with point mutations that change the amino acid at position 925 in the *para*-type voltage-gated sodium channel (VGSC) from leucine to valine, methionine or isoleucine. In order to assess the evolution of resistant mutations, we genotyped a region of the VGSC from *V. destructor* samples collected worldwide. Our phylogenetic analysis supports the hypothesis of independent origin for resistant alleles in Europe and the USA, and a close relation between L925M and L925I alleles. Our data also suggest that uncontrolled trading of parasitised honey bees might be an important route for spreading resistant alleles overseas. The substitution M918L, associated with pyrethroid resistance in other species, is reported here for the first time in *V. destructor*, in conjunction with L925V in mites from Spain. The implications of these evolutionary and dispersal processes for Varroa mite management are discussed.

Keywords Honey bee · VGSC · Acaricide · Mutation · Pesticide resistance · *Tau*-fluvalinate · Flumethrin

Key Message

- Phylogenetic analyses revealed a single origin for each *kdr*-type mutation at position 925 of the *V. destructor* VGSC.
- The mutation M918L of the VGSC has been detected for the first time in *V. destructor*.
- Understanding the evolutionary history of pyrethroid-resistant alleles in *V. destructor* and its impact in the current geographical distribution will contribute to design more finely tuned management strategies.

Introduction

Parasitism of honey bees by *Varroa destructor* Anderson and Trueman (Acari: *Varroidae*) is one of the major concerns in modern apiculture. This highly specialised, obligate

[1] Institute BIOTECMED, Department of Genetics, Universitat de València, Valencia, Spain

[2] Departamento de Zoología y Antropología Física, Facultad de Veterinaria, Universidad de Murcia, Murcia, Spain

[3] Hellenic Agricultural Organisation - "DEMETER", Institute of Olive Tree, Subtropical Crops and Viticulture, Heraklion, Greece

[4] Department of Entomology, University of Maryland, College Park, MD 20742, USA

 Springer

Research Article

Mutations associated with pyrethroid resistance in Varroa mite, a parasite of honey bees, are widespread across the United States

Anabel Millán-Leiva,[a] Óscar Marín,[a] Krisztina Christmon,[b] Dennis vanEngelsdorp[b] and Joel González-Cabrera[a*]

Abstract

BACKGROUND: Managed honey bees are key pollinators of many crops and play an essential role in the United States food production. For more than ten years, beekeepers in the United States have been reporting high rates of colony losses. One of the drivers of these losses is the parasitic mite *Varroa destructor*. Maintaining healthy honey bee colonies in the United States is dependent on a successful control of this mite. The pyrethroid *tau*-fluvalinate (Apistan®) was among the first synthetic varroacides registered in the United States. With over 20 years of use, mites resistant to Apistan® have emerged, and so it is unsurprising that treatment failures have been reported. Resistance to *tau*-fluvalinate in US mite populations is associated with point mutations at position 925 of the voltage-gated sodium channel.

RESULTS: Here, we have generated a distribution map of pyrethroid resistance alleles in Varroa samples collected from US apiaries in 2016 and 2017, using a high throughput allelic discrimination assay based on TaqMan®. Our results evidence that *knockdown resistance* (*kdr*)-type mutations are widely distributed in Varroa populations across the country showing high variability among apiaries. We used these data to predict the phenotype of the mites in the case of treatments with pyrethroids.

CONCLUSION: We highlight the relevance of monitoring the resistance in mite populations to achieve an efficient control of this pest. We also put forward the benefits of implementing this methodology to provide data for designing pest management programs aiming to control Varroa.
© 2021 Society of Chemical Industry

Supporting information may be found in the online version of this article.

Keywords: *Varroa destructor*; colony losses; pyrethroid resistance; pest management; TaqMan; genotyping

1 INTRODUCTION

Beekeepers in the United States have noted higher than acceptable annual colony losses in the past 14 years.[1,2] Prior to 2006, colony losses in the United States were estimated to average 5–10% each year,[3] but they significantly increased to average around 39% annually in the last ten years.[1] These losses are recoverable by replacing colonies, but this effort costs beekeepers millions of US dollars per year, in terms of increased labor and resource costs.[3–6] These high levels of losses are a concern for US beekeepers, the farmers that rely on beekeepers to provide bees for pollination, and the consumers who benefit from the diversity of food products that honey bee pollination facilitates.[6–9]

Beekeepers and researchers seem to agree that there are different factors, some of them interacting synergistically, that affect the bee health.[10–13] Of these factors, there is mounting evidence that the largest single driver of colony losses is the parasite *Varroa destructor* Anderson and Trueman (Acari: *Varroidae*) and the viruses this mite vectors.[10,13–24] The mite *V. destructor* is an obligated ectoparasite which feeds on the fat body of immature and adult honey bees[23] weakening bees by reducing their hosts immune response, changing their physiology, and shortening their lifespan.[25–30] Varroa shows an extraordinary capacity for vectoring honey bee viruses, which in turn cause colonies to crash suddenly.[11,13] Currently, Varroa causes more economic damage than all other bee diseases.[9,11]

Since untreated colonies experience a rapid reduction in health, regular treatment against Varroa mite have become an essential part of bee management for US beekeepers. The use of synthetic varroacides like the formamidine amitraz, the organophosphate coumaphos, and the pyrethroids flumethrin and *tau*-fluvalinate have long been in beekeepers 'toolbox'.[8,31] Although there are other non-synthetic acaricides and management techniques available, synthetic miticides are often the preferred choice because, when effective, they remove mites rapidly, do not cause obvious damage to bee populations, and are relatively cheap and easy to use.[5,31–33]

* Correspondence to: J González-Cabrera, Department of Genetics, Institute BIOTECMED, Universitat de València, Burjassot 46100, Spain. E-mail: joel.gonzalez@uv.es

a Department of Genetics, Institute BIOTECMED, Universitat de València, Burjassot, Spain

b Department of Entomology, University of Maryland, College Park, MD, USA

RAPID COMMUNICATION

CrossMark

New PCR–RFLP diagnostics methodology for detecting *Varroa destructor* resistant to synthetic pyrethroids

Anabel Millán-Leiva[1] · Carmen Sara Hernández-Rodríguez[1] · Joel González-Cabrera[1]

Abstract

A significant share of the current seasonal losses of honey bee colonies can be attributed to the ectoparasitic mite *Varroa destructor*. Its direct feeding behaviour and virus vectoring decimate the colony until collapse if there is no effective control management in place. The synthetic pyrethroids such as tau-fluvalinate and flumethrin were intensively used to control the mite until multiple cases of resistance were reported since the early 1990s. Previous studies have shown that there are three different mutations at amino acid position 925 (L925V, I and M) of the *V. destructor* voltage-gated sodium channel associated with the resistance to these compounds. Here, we report the development of a new PCR–RFLP methodology to discriminate between susceptible and pyrethroid-resistant *Varroa destructor* mites. This is a DNA-based assay that proved to be as accurate and robust as the previously reported TaqMan®-based high-throughput genotyping assays but significantly cheaper and more accessible to low-resourced laboratories. It is also easier to identify resistant mites using the new assay. The beekeeping community will surely welcome this new technology since there are very few effective acaricides to deal with the mite. They are aware that pyrethroids can be very effective in absence of resistance so having the possibility to use them as alternative to other compounds as part of an integrated management strategy would be of great help for long-term controlling of the parasite.

Keywords Varroa mite · Acaricides · Target-site resistance · Voltage-Gated Sodium Channel (VGSC)

Key message

- A new PCR–RFLP-based methodology has been designed to discriminate between susceptible and pyrethroid-resistant *Varroa destructor* mites.
- The new methodology shows several advantages over other previously described high-throughput allelic discrimination assays. It is significantly cheaper, easier to perform and more accessible to low-resourced laboratories. It is also more straightforward assigning susceptible or resistant phenotypes to a given sample.

✉ Joel González-Cabrera
joel.gonzalez@uv.es

[1] ERI BIOTECMED, Department of Genetics, Universitat de València, Valencia, Spain

Introduction

The ectoparasitic mite *Varroa destructor* Anderson and Trueman is a serious threat for the health of the Western honey bee (*Apis mellifera* L.). It feeds directly on immature and adult bees but also vectors a wide array of viruses that decimate the population (Chen and Siede 2007). A parasitized colony usually collapses in 2–3 years in absence of an effective management of the parasite (Rosenkranz et al. 2010).

As it is almost impossible to prevent the parasitism, controlling the mite is a key priority for beekeepers. There are several approaches available to remove the mites from the hives, but beekeepers rely widely in a few number of synthetic miticides, mainly because they are effective, easy to use and usually require less manpower than other cultural or mechanical methodologies (Rosenkranz et al. 2010). The pyrethroids such as tau-fluvalinate and flumethrin have been among the most intensively used miticides resulting in the selection of resistance in many locations (Milani 1995; Elzen et al. 1998, 2000; Mozes-Koch et al. 2000; Thompson

🖄 Springer

285

Identification of new viral variants specific to the honey bee mite *Varroa destructor*

Salvador Herrero[1] · Anabel Millán-Leiva[1] · Sandra Coll[1] ·
Rosa M. González-Martínez[1] · Stefano Parenti[1] · Joel González-Cabrera[1]

Abstract

Large-scale colony losses among managed Western honey bees have become a serious threat to the beekeeping industry in the last decade. Multiple factors contribute to these losses, but the impact of *Varroa destructor* parasitism is by far the most important, along with the contribution of some pathogenic viruses vectored by the mite. So far, more than 20 viruses have been identified infecting the honey bee, most of them RNA viruses. They may be maintained either as covert infections or causing severe symptomatic infections, compromising the viability of the colony. In silico analysis of available transcriptomic data obtained from mites collected in the USA and Europe, as well as additional investigation with new samples collected locally, allowed the description of three RNA viruses, two of them variants of the previously described VDV-2 and VDV-3 and the other a new species reported here for the first time. Our results showed that these viruses were widespread among samples and that they were present in the mites as well as in the bees but with differences in the relative abundance and prevalence. However, we have obtained strong evidence showing that these three viruses were able to replicate in the mite, but not in the bee, suggesting that they are selectively infecting the mite. This opens the door to future applications that may help controlling the mite through biological control approaches.

✉ Salvador Herrero
salvador.herrero@uv.es

✉ Joel González-Cabrera
joel.gonzalez@uv.es

[1] ERI BIOTECMED, Department of Genetics, Universitat de València, Valencia, Spain

toxins

MDPI

Article

Reduced Membrane-Bound Alkaline Phosphatase Does Not Affect Binding of Vip3Aa in a *Heliothis virescens* Resistant Colony

Daniel Pinos [1], Maissa Chakroun [1,†], Anabel Millán-Leiva [1], Juan Luis Jurat-Fuentes [2], Denis J. Wright [3], Patricia Hernández-Martínez [1] and Juan Ferré [1,*]

[1] Department of Genetics, Instituto de Biotecnología y Biomedicina (BIOTECMED), Universitat de València, 46100 Burjassot, Spain; daniel.pinos@uv.es (D.P.); chakrounmaissa7@gmail.com (M.C.); anabel.millan@uv.es (A.M.-L.); patricia.hernandez@uv.es (P.H.-M.)

[2] Department of Entomology and Plant Pathology, University of Tennessee, Knoxville, TN 37996, USA; jurat@utk.edu

[3] Department of Life Sciences, Imperial College London, Silwood Park Campus, Ascot, Berks SL5 7PY, UK; d.wright@imperial.ac.uk

* Correspondence: juan.ferre@uv.es

† Current address: Centre de Biotechnologie de Sfax, Sfax, Tunisia.

check for updates

Abstract: The Vip3Aa insecticidal protein from *Bacillus thuringiensis* (Bt) is produced by specific transgenic corn and cotton varieties for efficient control of target lepidopteran pests. The main threat to this technology is the evolution of resistance in targeted insect pests and understanding the mechanistic basis of resistance is crucial to deploy the most appropriate strategies for resistance management. In this work, we tested whether alteration of membrane receptors in the insect midgut might explain the >2000-fold Vip3Aa resistance phenotype in a laboratory-selected colony of *Heliothis virescens* (Vip-Sel). Binding of ^{125}I-labeled Vip3Aa to brush border membrane vesicles (BBMV) from 3rd instar larvae from Vip-Sel was not significantly different from binding in the reference susceptible colony. Interestingly, BBMV from Vip-Sel larvae showed dramatically reduced levels of membrane-bound alkaline phosphatase (mALP) activity, which was further confirmed by a strong downregulation of the membrane-bound alkaline phosphatase 1 (*HvmALP1*) gene. However, the involvement of HvmALP1 as a receptor for the Vip3Aa protein was not supported by results from ligand blotting and viability assays with insect cells expressing *HvmALP1*.

Keywords: *Bacillus thuringiensis*; insecticidal proteins; insect resistance; tobacco budworm

Key Contribution: The biochemical characterization of a Vip3Aa-resistant colony of *H. virescens* shows that binding to receptors in the midgut is not affected and discards the role of mALP as a Vip3Aa receptor. This study suggests that Vip3A resistance may occur through mechanisms other than those commonly found for Cry proteins.

1. Introduction

The polyphagous pest *Heliothis virescens* (L.) (Lepidoptera: Noctuidae) is well known for producing substantial economic losses, particularly in cotton production, due to its ability to evolve resistance to different synthetic control products such as methyl parathion or pyrethroids [1,2]. As an alternative approach, genetically modified crops expressing Cry and Vip3A insecticidal protein genes from *Bacillus thuringiensis* (Bt crops) were introduced in 1996 for the control of this and other pests. However,